Robust Detection of A Moving Chipless RFID Tag

Meriam Anushani Bibile

BSc. In Engineering Physics (1st Class Honours) University of Colombo
MSc. In Mobile, Personal & Satellite Communication, University of Westminster, UK

A thesis submitted in total fulfilment of the requirements for the degree of
Doctor of Philosophy

Department of Electrical and Computer Systems Engineering
Monash University

June 2019

Copyright notice

Abstract

At present the demand for chipless RFID tag is gaining maximum interest in the global market. The chipless RFID tag can be attached to a mobile object such as a product on a conveyor belt, an item dropping into a shopping trolley basket, a human or an animal in which the information is more difficult to detect than in the case where the tag is attached to a stationary object. The detection process is a challenging phase of the chipless RFID system. In this research a new aspect of the chipless RFID tag detection which is detecting the tag while it is in motion is addressed in real world environment. The main goal is to achieve an unperturbed reading of the mobile chipless RFID tag. An empirical model based on experimental data of a moving tag is developed. A novel adaptive-wavelet based detection technique is developed and is validated with experimental data on the moving tag detection using a single reader antenna. One of the main aims of this research is to commercialize the chipless RFID system. Therefore the detection will expand from a single antenna to an array of antennas as a larger reading range is expected for a reasonable moving tag detection. The developed detection algorithm is to be further fine-tuned for a chipless RFID reader with an array of antennas. Furthermore, a detailed study is proposed to analyse the parameters giving rise to erroneous frequency signatures of the chipless tags in motion. Another major challenge aroused through these experiments is the tracking of the moving chipless RFID tag and its direction of movement. This is to be overcome using the received signal power strength (RSS) of the reader antennas which will give rise to a new optimization algorithm for a chipless RFID system. In a chipless RFID system, the signal received by the reader antenna comprises of the backscattered signal from the chipless RFID tag located in the reader area, reflections from background objects (clutter) and noise. Due to this, false positives and false negatives are a problem in chipless RFID systems since the resultant decisions depend crucially on those results. A detection error rate and sensitivity

analysis is proposed using a repeatability and reproducibility test and coloured noise, to check the reliability and robustness of the reader and the detection algorithm respectively. The detection algorithm is further fine-tuned to reduce the false negatives and false positives of the chipless RFID system and is implemented in a new generation vector modulator reader with an improved reading range using an array antenna. This will give rise to a robust detection of a moving chipless RFID tag which could be used for industry applications. The completed chipless RFID system is installed in a smart shopping trolley to detect different items. This is a breakthrough in the field of chipless RFID and gives a high opportunity for the commercialization of the chipless tag.

Declaration

This thesis contains no material which has been accepted for the award of any other degree or diploma at any university or equivalent institution and that, to the best of my knowledge and belief, this thesis contains no material previously published or written by another person, except where due reference is made in the text of the thesis.

Signature: ……

Print Name: …Meriam Anushani Bibile….

Date: …27-06-2019….

List of Publications

Journal papers

1. M.A.Bibile and N.C. Karmakar, "Moving Chipless RFID Tag detection using Adaptive Wavelet Based Detection Algorithm", *IEEE Transactions on Antennas and Propagation,* 2018

2. Meriam Anushani Bibile, Grishma Khadka, Larry M. Arjomondi and Nemai C. Karmakar, "Analysis of Artifacts on Chipless RFID Backscatter Tag Signals for Real World Implementation", *IEEE Access*, 2019

3. M.A.Bibile and N.C. Karmakar, "A novel- adaptive wavelet based detection for chipless RFID system", *AIRCC Signal & Image Processing: An International Journal (SIPIJ),* Mar 2017

Conference papers

4. M.A.Bibile and N.C. Karmakar, "Detection performance of a chipless RFID tag in motion", *IEEE International Microwave and RF Conference (IMaRC)*, 2016. , Delhi, India, Dec 26 – 29, 2016.

5. M.A.Bibile and N.C. Karmakar, "A novel- adaptive wavelet based detection for chipless RFID system", *Fourth International Conference on Signal and Image Processing (*SIGL), Geneva, Switzerland, Mar. 25 – 26, 2017. and *Computer Science Conference*

Proceedings in Computer Science & Information Technology (CS & IT) series, Geneva, Switzerland, Mar. 25 – 26, 2017.

6. M.A.Bibile and N.C. Karmakar, "Detection Error Rate Analysis using Coloured Noise for Moving Chipless RFID Tag", *IEEE Australian Microwave Sysmposium (AMS)*, 2018, Brisbane, Australia, Feb 6-8, 2018

Articles

7. M.A.Bibile, S.Shresta and N. C. Karmakar, "C*hipless RFID",* Access Science / McGraw Hill Encyclopedia of Science & Technology, Article ID YB150720, Feb 2017.

8. M.A.Bibile, S.Shresta and N.C. Karmakar, "Tag ID generation and detection of Chipless RFID system"*, FERMAT(Forum for Electromagnetic Research Methods and Application Technology), Volume 21, Article 3, May-Jun., 2017*

Acknowledgement

I would like to express my sincere gratitude to my supervisor, Associate Professor Nemai Chandra Karmakar, for his valuable suggestions and continuous guidance throughout the development of this research work. His directions helped me in improving the quality of my research work, research papers as well as this thesis. I sincerely appreciate his dedication, enthusiasm, understanding, knowledge and encouragement at all times.

I would like to acknowledge the financial support from the Australian Research Council (ARC) Linkage Project grant LP130101044, titled, "Discreet Reading of Printable Multi-bit Chipless RFID Tags on Polymer Banknotes" to conduct my PhD research work. Financial support from Monash University in the form of Monash Graduate Scholarship (MGS) in the later stage of the research is also acknowledged. I would like to acknowledge the services provided by Monash University in terms of access to internet, scholarly articles, necessary software, fabrication machine and measurement laboratory are also duly acknowledged.

I am grateful to Dr. Md. Shakil Bhuiyan for his valuable suggestions and thought-provoking discussions, particularly at the first stages of my research. I would also like to thank my senior researchers and friends Dr. Prasanna Kalansuriya, Dr. Emran Md Amin, Dr. Chamath Divarathne, Dr. Mohammad Zomorrodi, Dr. Jhantu Saha, Dr. Ms. Rubayet E-Azim, Dr. Shuvashis Dey, Mr. Wan Wan Mohd Zamri, Mr. Muhsiul Hassan for their cordial supports at different times of the research. Special thanks to my colleagues who were working side to side with me Ms. Sika Shresta, Mr. Mazyar Forouzandeh, Mr. Larry Arjourmandi, Ms. Fatemeh Babeian, Mr. Grishma Khadhka, Mr. Shahriar Hassan, Mr. Tharindu Aththauda, and Mr. Jiewei. Sincere thanks for the valuable suggestions and help extended by Dr. Shamsul Amin at the final stages of my research work.

My special gratitude is extended to all the staff and the postgraduate students in the Department of Electrical and Computer Systems Engineering (ECSE) at Monash University for offering me their fullest cooperation.

Lastly, I wish to acknowledge the endless encouragement, support and sacrifice of my family members, (husband and two daughters) especially my husband for giving me a free mind by taking the responsibility of the kids during crucial times and my daughters for being with me in the lab spending late nights. I would like to dedicate my thesis to my family and also my parents who are the main inspirations behind all the hard work during my PhD candidature from the far end and finally thank God for being my strength till the end.

Dedicated to my beloved Husband

Rajindra

And two daughters

Geeshani & Devduni

Table of Contents

1 Introduction 1
1.1 Chipped/Chipless RFID 1
1.2 Research aims 6
1.3 Research contributions 7
1.4 Thesis outline 11

2 Detection of Chipless RFID Tag ID 15
2.1 Introduction 15
2.2 Review on Chipless RFID detection and localisation techniques 15
2.2.1 Decoding and de-noising techniques 15
2.2.2 Localisation techniques 19
2.3 Gaps and New research Directions in Chipless RFID system 20

3 Chipless RFID Tag in motion 22
3.1 Introduction 22
3.2 Theory 23
3.3 Experiments on static motion 26
3.3.1 Patch resonant tag with horn antenna 26
3.3.2 Experiment using two waveguide antennas and U-slot tag 33
3.3.3 Experiment using single and two SWB antennas and 4-bit tag for moving tag detection 35
3.3.4 Detection of chipless tag response while the tag is in vertical motion using horn antenna 39
3.4 Conclusions 44

4 Adaptive wavelet based detection algorithm for Chipless RFID system 45
4.1 Introduction 45
4.2 System model and design 46
4.2.1 Experimental model 46
4.2.2 Wavelet design 48
4.2.3 Flowchart for detection algorithm 49
4.3 Results 50
4.4 Analysis 52
4.5 Conclusions 53

5 Chipless RFID tag detection with stepped movement using improved adaptive wavelet based detection algorithm 55
5.1 Introduction 55
5.2 Chipless RFID system 57
5.2.1 Working principle of a chipless RFID tag 57
5.2.2 Chipless RFID tag in motion 58
5.2.3 Reader antenna 59
..... 60
5.2.4 Chipless RFID tag 60
5.2.5 Experimental setup 61
5.3 Improved adaptive wavelet based detection algorithm 62
5.4 Measurement results and analysis 68
5.5 Conclusion 75

6 Implementation of detection algorithm for single antenna reader system 76
6.1 Introduction 76
6.2 Reader architecture 78
6.3 Implementation of the detection algorithm in the microcontroller 81
6.3.1 Implementation of the detection algorithm 81
6.3.2 Testing patch antennas and detection of copper tags using VNA 81
6.3.3 Characterization of clutter and detection of printed tag using VNA 84
6.4 Simulation of clutters and detection in CST 91
6.4.1 Simulated results for a 4-bit circular tag using single aperture coupled antenna 91
6.4.2 Detection of the simulated results using new detection algorithm 93
6.4.3 Introducing clutter in CST simulation environment 95
6.5 New detection algorithm for the detection of printed tags using VNA 99
6.5.1 Application of printed chipless RFID tags 99
6.5.2 New detection algorithm on measured results using VNA 100
6.6 Applying the detection algorithm for tag at different distances 102
6.6 Comparison of VNA results and chipless RFID reader results 104
6.6.1 Experimental results using VNA for printed tag (3 bits) 104
6.6.2 Experimental results using Modular reader for printed tag (3 bits) 106
6.6.3 Experiment using VNA with copper tag (5 bits) 107
6.6.4 Experiment using modular reader with copper tag (5 bits) 108
6.7 Conclusion 109

7 Detection error rate and sensitivity analysis of a chipless RFID system 111
7.1 Introduction 111
7.2 Detection error rate Analysis using coloured noise 112
7.2.1 Coloured noise 112
7.2.2 Experimental design and results 112
7.2.3 Analysis of results 114
7.3 Sensitivity analysis using gage R & R study 116
7.3.1 Sample preparation 116
7.3.2 Detector and test preparation 118
7.3.3 Results and analysis 119
7.4 Conclusion 120

8 Application of detection algorithm for moving tag detection with improved reading range using array antenna 121
8.1 Introduction 121
8.2 Detection of chipless RFID tag in movement 123
8.2.1 Analysis on the number of data sets captured by reader depending on the antenna beamwidth covering the shopping trolley 123
8.2.2 Experiment with two big horn antennas and hexagonal tag, S21 measurement using VNA 125
8.2.3 Passive microwave circuit design and simulation for moving tag 130
8.2.4 Simulation of a chipless RFID tag covered with a material layer 132
8.2.5 Doppler Effect while reading the tag in vertical movement 137
8.3 Detection with different items held in hand with the tag 139
8.4 Effect of attaching the tag to different materials 142
8.5 Detection of tag on different items using Vector Modular Reader 144
8.5.1 Detection of different tag IDs using 4 x 4 array antenna with VMR 144
8.5.2 Detection of Tagged Items using Single patch antenna with VMR 147
8.6 Conclusion 155

9 Smart trolley project using chipless RFID system 157
9.1 Introduction 157
9.2 Individual item detection on the move 160
9.2.1 Calibration of material effects 162
9.2.2 Detection of tagged items 167
9.3 Tagged object dynamics and direction of movement 170
9.4 Detection of tag in a dynamic environment 173
9.5 Conclusion 174

10 Conclusion 176

10.1 Fulfilling the goals of the thesis 176
10.2 Limitations of the proposed system 178
10.3 Future improvements and applications 180

Appendix A 182

References 184

List of Figures

Figure 1.1 - Chipless RFID System 1
Figure 1.2 - Data exchange between an RFID reader and a tag 2
Figure 1.3 - Chipless RFID system with reader and tag 3
Figure 1.4 - Attributes to be taken into consideration when designing a chipless RFID tag 3
Figure 1.5 – Research aims 6
Figure 1.6 – Proposed research 8
Figure 1.7 – Thesis outline linked with original contributions and outcomes in prestigious outlets 13

Figure 2.1 - Flow chart of the moving average filtering technique [17] 16
Figure 2.2 - Flow chart of the signal processing using Hilbert Transform [18] 17

Figure 3.1 – An RFID scenario with tagged items on a moving conveyor belt (top view) [27] 23
Figure 3.2 – Chipless RFID system model for moving tag analysis 24
Figure 3.3 – Top view of the moving tag 26
Figure 3.4 - Radiation pattern of Horn antenna 27
Figure 3.5 - Experimental set up to measure the radiation pattern 27
Figure 3.6 – (a) Rectangular patch tag, (b) RCS of the rectangular patch resonant tag 28
Figure 3.7 - Experimental setup used for moving tag detection 28
Figure 3.8 - Flowchart explaining the collection of data and the post processing of the data for moving tag detection 29
Figure 3.9 - S11 Magnitude vs. Frequency of the patch resonant tag, moving the tag in positive direction from 0cm to +3.5cm 31
Figure 3.10 - Magnitude S11 error vs. the distance 31
Figure 3.11 - Relative phase vs. distance at f = 7.851GHz, comparison between the experimental relative phase and calculated values of relative phase of the moving tags 32
Figure 3.12 – (a) U-Slot resonant tag, (b) RCS of the slot resonant tag 33
Figure 3.13 – Radiation pattern of Waveguide Antenna 33
Figure 3.14 - Experimental set up for U slot resonant tag using two waveguides as transmitter and receiver 34
Figure 3.15 – (a) S11 magnitude vs. Frequency (GHz) (b) Angle (degrees) vs. Frequency (GHz) 34
Figure 3.16 - Error in amplitude variation at the resonant frequencies using waveguide experimental results 35
Figure 3.17 – Front view and back view of SWB antenna with a patch height of 0.5 mm [30] 36
Figure 3.18 – Radiation pattern of the SWB antenna with a patch height of 0.5 mm [30] 36
Figure 3.19 - (a) Experiment using single SWB for horizontal movement of the tag, (b) Experiment using 2 SWB antennas for vertical movement of the tag, (c) Experiment using two SWB antennas for the horizontal movement of the tag. 37
Figure 3.20 - S21 Magnitude vs. Frequency for experiment using 2 SWB antennas 37
Figure 3.21 - S21 Magnitude vs. Frequency for experiment using 2 SWB antennas 38
Figure 3.22 - Error in amplitude variation at the resonant frequencies using super wide band antenna experimental results 38
Figure 3.23 - Horn antenna with dimensions 24 x 14 cm and working in the frequency range of 0-18 GHz 40

Figure 3.24 - Testing the tag response in step vertical motion using horn antenna and hexagonal tag 40
Figure 3.25 - Antenna and background S11 41
Figure 3.26 - The tag response at the reference level of 0 cm, 4 cm away from the phase centre of the antenna. 41
Figure 3.27 - Phase variation while the tag is in vertical motion 42
Figure 3.28 – S11 Magnitude in dB vs frequency for the tag movement from 0 to 8 cm 42
Figure 3.29 - The magnitude variation and the frequency shifts occurred at each resonance while the tag is in vertical motion from 0 to 8 cm 42
Figure 3.30 - Detected signals after applying algorithm 43

Figure 4.1 – Chipless RFID system 46
Figure 4.2 - S11 Magnitude (dB) vs. frequency of the 5-bit resonant tag 47
Figure 4.3 – Novel wavelet design 48
Figure 4.4 – Flowchart of the new detection algorithm 49
Figure 4.5 - Placing hand on top of the tag at 7 cm distance giving attenuation to the signal received at the VNA 50
Figure 4.6 - Measured results (a) of the original tag at 1.5 cm above the patch antenna, (b) with hand placed above the tag at a distance of 7 cm, (c) with copper plate placed on top of the tag at a distance of 7 cm, (d) by placing the tag at the corner of the patch antenna. 50
Figure 4.7 – Wavelet coefficients of the detected signals after applying the developed algorithm. (a) Original tag detection (b) Hand on top of tag (c) Copper plate on top of tag (d) Tag moved to the corner of antenna 51

Figure 5.1 – Chipless RFID system with reader and tag 57
Figure 5.2 - Moving chipless RFID tag detection 58
Figure 5.3 - Top view of the moving tag in reader antennas radiation pattern (zone) 58
Figure 5.4 – 3 dB look angle 59
Figure 5.5 - Radiation pattern of the antenna measured in lab 59
Figure 5.6 – S11 of the horn antenna used in experiment between 8-12GHz 60
Figure 5.7 - Taconic 4-bit patch resonant tag 60
Figure 5.8 – S11 (dB) magnitude of the 4-bit patch resonant tag at its minimum distance. The resonant frequencies are located at 8.4, 9.4, 10.5 and 11.6 GHz 61
Figure 5.9– Experimental setup using horn antenna, 4-bit Taconic chipless RFID tag and VNA 61
Figure 5.10 – Flowchart of the procedure for the moving tag experiment 63
Figure 5.11 - Continuous Wavelet Transform (CWT) algorithm 64
Figure 5.12– Adaptive mother wavelet 65
Figure 5.13 - Condition band set for the decoding of the frequency ID 66
Figure 5.14 – Flowchart for detection 67
Figure 5.15 - Background subtracted S11 Magnitude (in dB) vs. Frequency (in GHz) while the tag is moved in the positive direction (+d) from 0cm mid position to +7 cm by varying the distance in 0.5 cm steps 68
Figure 5.16 - Background subtracted S11 Magnitude (in dB) vs. Frequency (in GHz) while the tag is moved in the negative direction (-d) from 0cm mid position to -7cm by varying the distance in 0.5cm steps 69
Figure 5.17 – Magnitude variation at each bit resonance with movement in dB relative to the result when the tag is in mid position at d=0cm 69

Figure 5.18 – Frequency shift at each bit resonance with movement of the tag in both positive and negative directions 70
Figure 5.19 - The variation in both amplitude and frequency at each bit resonance in both positive and negative directions 71
Figure 5.20 - Detected frequency ID at 0cm 71
Figure 5.21 – Detected frequency ID at +7cm 72
Figure 5.22 – Detected frequency ID at -7cm 72
Figure 5.23 – Variation in calculated wavelet coefficient for each bit resonance with distance 74
Figure 5.24 – The variation of coefficient for bit 2. The mean value is shown by the red solid line and one standard deviation around the mean value is shown by the black dashed lines 74

Figure 6.1 – Block diagram of the single-antenna chipless RFID front end [3] 76
Figure 6.2 – (a) 4- bit printed tag on flexible material PET, (b) 9 – bit Copper tag, (c) ACMPA 77
Figure 6.3 – Detailed block diagram of the chipless RFID reader [3] 78
Figure 6.4- Digital Section of the Desktop Reader with PIC32MZ microcontroller 79
Figure 6.5- ICD3 serial programmer used to program PIC microcontroller 79
Figure 6.6 - Using MPLAB X IDE software to program the pic microcontroller, the inset figure on the left shows the single reader antenna 80
Figure 6.7 - Patch antenna loaded with the printed tag at 1cm 80
Figure 6.8 - Testing setup 81
Figure 6.9 – patch antennas used for testing 82
Figure 6.10 – Tags tested for detection 82
Figure 6.11- S11 magnitude (dB) vs frequency comparison of patch antennas used for testing 83
Figure 6.12 - Tag responses of Tag 1 -‘AM05’ and Tag 2 – ‘a41’ using VNA 83
Figure 6.13– Detected tag ID using the implemented algorithm 84
Figure 6.14– S11 Magnitude (dB) vs. Frequency for Ant 2 (patch antenna 2) 84
Figure 6.15 – Patch antenna loaded with the printed tag at 1cm 85
Figure 6.16 – Measured result for printed tag using VNA without any clutter object 85
Figure 6.17 – Detection of the frequency ID without any clutter object 86
Figure 6.18 - Tag with wooden block placed at different positions 87
Figure 6.19 – Received signal of tag with wooden block at different distances 87
Figure 6.20 – Detected frequency ID while the wooden block is at different distances from the tag 88
Figure 6.21- Tag with rectangular Cu plate placed at different positions 88
Figure 6.22 – Received signal of tag with copper plate at different distances 89
Figure 6.23– Detected frequency ID with copper plate at different distances from tag 89
Figure 6.24 – Tag with hand with gold ring at different positions 90
Figure 6.25 – Received signal with hand with gold ring placed near tag at different distances 90
Figure 6.26 – Detected frequency ID for tag with hand with gold ring placed as clutter object 91
Figure 6.27 – 4-bit circular tag used for simulation 92
Figure 6.28 – CST simulation with patch antenna 92
Figure 6.29 – RCS of the 4-bit circular tag 92
Figure 6.30 – Detected signal of the 4-bit tag at 2cm from the antenna 93
Figure 6.31 – New adopted wavelet pattern 94
Figure 6.32 - Detected after the baseline removal 94
Figure 6.33 - Detected signal after wavelet transform 95
Figure 6.34 –Simulation setup in CST with clutter object 95

Figure 6.35 – S11 Magnitude (dB) vs. Frequency (GHz) for tag detection with clutter objects placed at very near distance....96
Figure 6.36 – S11 Magnitude (dB) vs. Frequency (GHz) without any clutter....96
Figure 6.37- Outputs obtained by placing copper object and bio tissue....97
Figure 6.38– Detected frequency IDs from the cluttered signals....98
Figure 6.39 – Banknote reader set up....99
Figure 6.40 – Printed tags on PET....99
Figure 6.41 – Measured results of the two 2-bit tags using the ACMPA used for banknote project..100
Figure 6.42 – Applying detection algorithm on measured results for printed tags (a) Detected signal of 4-bit tag giving the threshold coefficients (b) Detection of Tag 1 giving tag ID '0101' (c) Detection of Tag 2 giving tag ID '1010'....100
Figure 6.43 - (a) The measured result of 'SC4_RC2_bc4' using Horn antenna (b) Detected signal using the detection algorithm giving the output as '1111'....101
Figure 6.44– Received signal using VNA for the printed tag at different distances....102
Figure 6.45 – Detected tag IDs after applying the detection algorithm for tag at 1.5 cm above the patch antenna to 6 cm above patch antenna....103
Figure 6.46 – Detected tag IDs after applying the detection algorithm for tag at 7 cm above the patch antenna to 8.5 cm above patch antenna....104
Figure 6.47– (a) Printed tag on PET flexible material (b) Copper tag on Taconic (c) Patch antenna (d) Experimental setup for printed tag test using VNA....104
Figure 6.48 – (a) The blue line plot is the VNA s11 result for the antenna only. The foam was also placed in order to get the complete background data before placing the tag. (b) The red line plot is the s11 result when the tag was placed above the antenna on the foam where the foam has a thickness of 1cm....105
Figure 6.49 – Detected signal after applying the algorithm....105
Figure 6.50 – (a) The blue line plot shows the s11 result when the tag is placed above the antenna using vector subtraction (b) The red line plot shows the s11 result for the tag by looking only at the magnitude subtraction these plots are obtained using Matlab with saved VNA data....106
Figure 6.51 - (a) The blue line plot is the VNA s11 result for the antenna only. The foam was also placed in order to get the complete background data before placing the tag. (b) The red line plot is the s11 result when the tag was placed above the antenna on the foam where the foam has a thickness of 1cm....107
Figure 6.52 – Experimental setup for copper tag test using VNA....107
Figure 6.53 - Detection using the modular reader. (a) The blue line plot shows the background data (antenna + foam + noise). (b) The red line plot shows the received signal from the system when the tag was placed above the antenna on the foam. (c) The yellow line plot shows the subtraction of the signals (a) & (b) which gives the tag data to which the detection algorithm is applied to retrieve the tag ID....108
Figure 6.54 - (a) The blue line plot is the VNA s11 result. (b) The red line plot is the s11 result when the tag was placed above the antenna on the foam where the foam has a thickness of 1cm. 108

Figure 7.1 – Experimental set up using two horn antennas and hexagonal tag to measure S21 of the vertical movement of the tag....113
Figure 7.2 - Vertical movement of tag at 30cm from horn antenna set up....113
Figure 7.3 - Original sample tag used for test, the marked resonator gives frequency signature FS1 116

Figure 7.4 – The relevant resonators are shorted to obtain required tag frequency (a) 4 resonators giving frequency signature FS2 for Tag A (b) 4 resonators giving frequency signature FS3 for Tag B 116
Figure 7.5- (a) Tag C having only one frequency signature FS1 (b) Reflector used for Tag D 117
Figure 7.6– Sample used for Gage R&R test 117
Figure 7.7- Modular Detector designed by MMARS team to be evaluated by the gage R&R test. 118
Figure 7.8- Correct placement of sample tags on reader antenna 118

Figure 8.1 - Block diagram of a single-antenna scalar chipless RFID reader: a) Conventional architecture, b) Enabled with vector modulator unit [3] 121
Figure 8.2 – (a) 4 x 4 patch array antenna with improved reading range (b) single patch antenna structure [4] 122
Figure 8.3 – Data capturing while the chipless tag is in vertical movement 123
Figure 8.4 – (a) The experimental setup with two big horn antennas (0-18GHz) for S21 measurement using VNA (b) The hexagonal tag of 18-bits working in the range of 3-10GHz 125
Figure 8.5 - RCS of the hexagonal tag with 18-bits. CST simulation results for two different tag IDs as shown in dotted black line and red line plot. The highlighted bits from 4-6GHz is focused in this experiment 126
Figure 8.6 – Vertical movement of tag at 15 cm from Horn antenna set up 127
Figure 8.7- Vertical movement of tag at 20 cm from Horn antenna set up 127
Figure 8.8 - Vertical movement of tag at 25 cm from Horn antenna set up 128
Figure 8.9 - Vertical movement of tag at 30 cm from Horn antenna set up 128
Figure 8.10– 4-bit circular ring tag 130
Figure 8.11– 4-bit tag response when the line widths are 0.4, 0.5, 0.5, 0.5, 0.4 mm respectively giving frequency signature at 3.7 GHz, 4.1 GHz, 4.6 GHz and 5.2 GHz 130
Figure 8.12 – 4-bit tag response when the line widths are reduced from 12 to 7.4 mm giving 4 bits within 4 to 7 GHz range. 131
Figure 8.13 - 4-bit tag response when the line widths are reduced from 10 to 6 mm giving 4 bits within 4 to 8 GHz range. 131
Figure 8.14– 4-bit circular ring tag with stubs to generate different tag IDs 132
Figure 8.15 – The different tag ID responses 0101, 1011 and 1101 132
Figure 8.16 – 4-bit circular ring tag 133
Figure 8.17 – RCS of the 4-bit circular ring tag 133
Figure 8.18 – Tag covered with paper layer 133
Figure 8.19 – Simulation result when the paper thickness is varied from 1 to 100 µm 134
Figure 8.20 – Tag covered with BOPP layer 134
Figure 8.21– Simulation result when BOPP layer thickness is varied from 100 to 500 µm 134
Figure 8.22 - Simulation result when BOPP layer thickness is varied from 1µm to 100µm 135
Figure 8.23 – 4 bit square patch tag with ground plane 135
Figure 8.24– Square patch tag RCS 136
Figure 8.25 – Square patch tag with BOPP layer 136
Figure 8.26 - Simulation results when BOPP layer thickness is varied from 1 to 100 µm 136
Figure 8.27 – Simulation results when paper layer thickness is varied from 1µm to 100µm 137
Figure 8.28 - Experimental Setup to measure the Doppler effects 138
Figure 8.29 – Hexagonal tag held with Right hand in dropping position 140
Figure 8.30– Hexagonal tag result from 4-6 GHz (3- bits) 140
Figure 8.31– Hexagonal tag result from 4-6 GHz (3- bits) 140

Figure 8.32 – Hand with ring and key tag.....141
Figure 8.33– S11 magnitude vs. frequency hand with ring and keys 141
Figure 8.34– Hand with Ring, Keys, Watch and Tag 141
Figure 8.35– (a) Hand with Ring, Keys, Watch and Tag (b) S11 magnitude vs. frequency results ...142
Figure 8.36 - Detection of chipless RFID tag attached to different items coke can, water bottle and cereal box using 4x4 patch array antenna. 143
Figure 8.37 - Detection of chipless RFID tag attached to different items coke can, water bottle and cereal box using 4x4 patch array antenna. 144
Figure 8.38 - The background signal and the backscatter signal without any tag……..……..…145
Figure 8.39 - Tag signature measured using VMR for tag 1100…….……146
Figure 8.40 - Detected tag ID 1100 after applying the detection algorithm ……..……146
Figure 8.41 - Tag signature measured using VMR for tag 1011…….146
Figure 8.42 - Detected tag ID 1011 after applying the detection algorithm ……..……147
Figure 8.43 - 4-bit circular patch copper tag design with ground plane…...……..……147
Figure 8.44 - Coke can as the tagged item ……...……..……148
Figure 8.45 - Coke can without the tag placed at 5, 10 and 15 cm ……...……..……149
Figure 8.46 - Coke can with tag ID 1111 at 5, 10 and 15 cm ……..……..……150
Figure 8.47 - Comparison of results with tag attached to coke can ……..……150
Figure 8.48 - Result with cereal box only…….……..……151
Figure 8.49 - Tag and cereal box result ……152
Figure 8.50 - Comparison of results with cereal box ……152
Figure 8.51 - Tagged milk carton detection using single patch antenna …….....152
Figure 8.52 - Milk carton only ……...153
Figure 8.53 - Results of tag with milk carton ……..……..……154
Figure 8.54 - Comparison of results ……..……154

Figure 9.1 – UHF RFID based smart trolley system [34] 157
Figure 9.2 – Proposed smart shopping trolley 158
Figure 9.3 – Shopping trolley with VMR and 4 x 4 patch array antennas installed for detection of items.....159
Figure 9.4 – Detection in a dynamic environment.....159
Figure 9.5 – S11 Measurement of tag 1000 in Smart shopping trolley 160
Figure 9.6– Tag 1000 detection with array antenna using VMR.....161
Figure 9.7- Calibration only antenna with environment 161
Figure 9.8– Placing metal plate in front of antenna.....162
Figure 9.9– (a) Metal plate in front of antenna (b) Metal plate with tag 1000 attached 162
Figure 9.10 – Tag 1000 on metal plate 163
Figure 9.11 – Small thin cardboard in front of the antenna 163
Figure 9.12 – Cardboard only placed in front of array antenna.....164
Figure 9.13 - Cardboard with tag 1000 at 30cm 164
Figure 9.14 – Cardboard with two tags of 1000 165
Figure 9.15 – Small cardboard box with tag 1111 attached.....165
Figure 9.16 – Cardboard box with 2 tags of tag ID 1000 166
Figure 9.17 – Cardboard box with 8 tags of tag ID 1111 166
Figure 9.18 – Cereal box in front of the system.....167
Figure 9.19 – Cereal box only with array antenna ……167
Figure 9.20 – Empty cereal box with tag 1000……1678

Figure 9.21 – Coke can only detected as 0000 169
Figure 9.22 – Tag 1111 attached to the coke can detected as 1111 169
Figure 9.23 - Chipless RFID reader system for Smart Trolley Project 170
Figure 9.24 – Flowchart for the detection of tagged items in the smart shopping trolley with direction of movementCheck for bits within the condition band for each bit frequency 172
Figure 9.25 – Antenna configuration for the detection of the direction of movement 173
Figure 9.26 – Measurement results with clutter 173
Figure 9.27 - Wavelet coefficients of the detected signals after applying the detection algorithm 174

List of Tables

4.1 Wavelet coefficients for tag detection ……...……52

5.1 Detected tag ID and wavelet coefficients ……..73

6.1 Details of the dimensions of the clutter object and the distance from tag and antenna 96

6.2 Clutter object position and its material properties …….97

7.1 RMSE amplitude variation in dB at the specific frequency points ……...…..114

7.2 Change in probability of detection and detection error rate with increased distance from 15 – 30 cm……..…….....115

7.3 Detection error rate and signal to noise ratio at different distances in simulation……...…115

7.4 Grouping of samples for the test ……...……...……...117

7.5 Results of gage R & R test performed in MMARS lab ……...…...119

8.1 Calculation of data captures during the free dropping of the tag …...…….…..…..125

8.2 Important parameters related to the tag, horn antenna and VNA ……..…….126

8.3 Wavelet coefficient and detected tag ID when the tag is at 20 cm ……...……...128

8.4 Wavelet coefficient and detected tag ID when the tag is at 30 cm ……...……...129

8.5 Experimental parameters and set up…….…….……...……138

8.6 Analysis of Doppler spread ……..139

1 Introduction

Chipless RFID technology is continuously developing and is at the edge of its application phase. The chipless RFID technology can be widely applied in many applications including item level tagging and tracking, infrastructure health monitoring and sensing, protecting food & drug counterfeiting, airline luggage tracking, animal identification, environment monitoring and inventory control [1]. In the recent past the chipless tag design and identification has been the main focus among researchers. The focus of the research is to identify a chipless RFID tag in motion and to further develop a robust detection algorithm to detect a tagged item while in movement. The thesis represents an adaptive wavelet-based detection algorithm [2] for the robust detection of chipless RFID tags in motion. The implementation of the algorithm in a single antenna reader and a vector modulator reader [3] with an array antenna [4] is presented to validate the robustness of the detection algorithm for chipless RFID tagged items in motion.

1.1 Chipped/Chipless RFID

The chipped RFID tag consists of an antenna and an application specific integrated circuit (ASIC) chip. The RFID reader consists of a transmitter, a receiver, a baseband processor, a circulator and an antenna. The operation of a chipped RFID tag is illustrated in Figure 1.1. A RFID interrogating signal is transmitted by the RFID reader and the tag sends back a modulated backscatter signal by switching its input impedance between two states. At each impedance it gives a certain radar cross section (RCS), usually high and low.

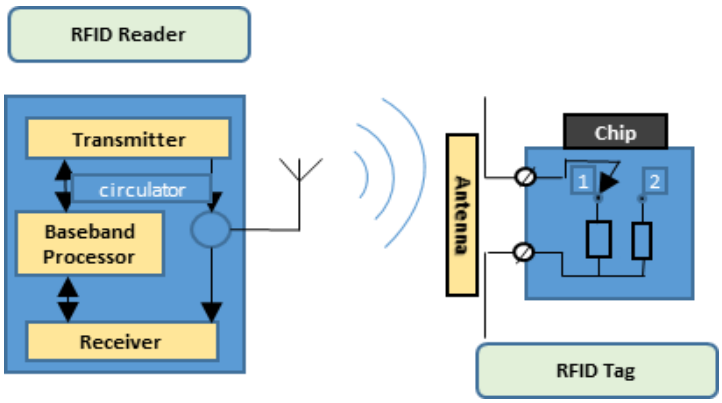

Figure 1.1 - Chipped RFID System

Figure 1.2 shows the time domain data transmission between a RFID reader and a tag. The data uplink consists of a continuous wave and a set of queries and the downlink shows the tag response. The backscattered signal from a loaded antenna can be divided into two parts. The first part is called the "structural mode" and is due to currents induced on the antenna when it is terminated with the complex conjugate impedance. The second part is called the "antenna mode" and is caused by the mismatch between the antenna impedance and the load impedance. The author of [5] notes down that the power of the modulated backscattered signal received by the RFID reader depends not only on the tag RCS but also on relative phases of the reflected field components. The main bottleneck of the chipped RFID tag in mass deployment is the cost of the ASIC. Unless the cost of the chipped tag is reduced to small cent the commercial applications becomes a limiting factor. Therefore, researchers developed a new tag without the ASIC, a new class of RFID called the chipless RFID tag. The tag is void of intelligence hence all processing burden is bestowed on the reader.

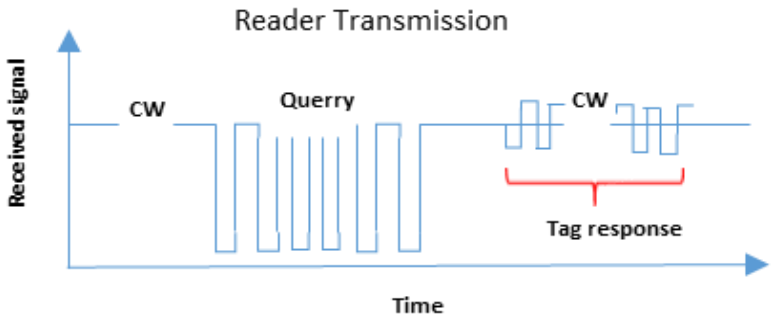

Figure 1.2 - Data exchange between an RFID reader and a tag

A typical chipless RFID technology also deals with a reader and a tag. The chipless RFID system differs to the chipped RFID system in many ways. The main difference is the absence of a microchip in a chipless system also it does not use any hand shaking protocol or modulation techniques. The reader sends the interrogation signal to the tag and the tag encodes the tag ID and sends it back to the reader for identification. Figure 1.3 illustrates the operating principle of a backscattering chipless RFID tag.

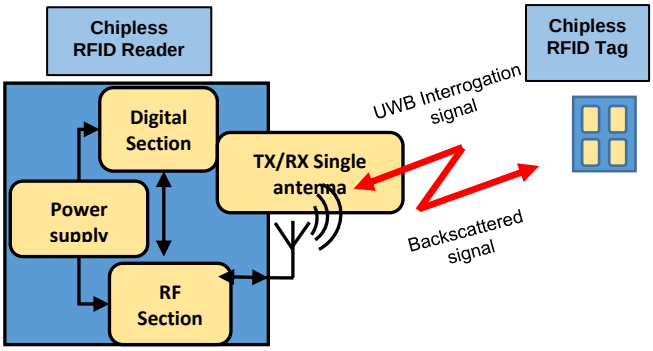

Figure 1.3 - Chipless RFID system with reader and tag

The reader interrogates the tag with an ultra-wide band (UWB) envelop of constant amplitude. The tag returns a backscattering signal of a very low amplitude with a data stream which is the identification data. The RCS of a chipless RFID tag is the strength or ability to reflect a signal in the direction of the receiver. The RCS of a tag is given by equation [6] (1.1).

$$\sigma_{tag} = \frac{\lambda^2 G_{tag}^2}{2\pi} \qquad (1.1)$$

where, λ is the wavelength of operating frequency and G_{tag} is the gain of the tag antenna.

There have been great amounts of work done [7-9] on chipless RFID tag and antenna designing during the recent years. Most of them still remain as prototypes and there are only very few commercially available. From the articles it can be seen that the following attributes are taken into consideration when designing the tag and the antenna.

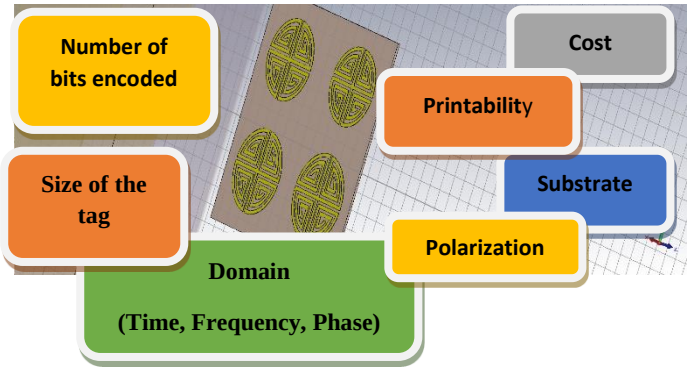

Figure 1.4 - Attributes to be taken into consideration when designing a chipless RFID tag

Researchers have been able to increase the efficiency of the tag and antenna design starting from Balbin's phase encoded chipless RFID transponder published in 2009 [10] to Sumi's high bit encoding chipless RFID tag using E-shaped microstrip resonators published in 2015 [11] from the selected articles for this review.

Reading of the chipless RFID tag requires either a frequency domain measurement, measurement of the amplitude or the phase of the transmission coefficient of the tag that can be used for decoding data. In many of the experiments carried out in the laboratory, a vector network analyser (VNA) has been used for this purpose. Since the VNA is not a conventional reading technique and is an expensive piece of equipment three generations of chipless RFID tag readers are reported in 2012 [12]. The work is done in Monash, Microwave, Antenna, RFID and Sensor (MMARS) Laboratory at Monash University.

The reader extracts the scattered signal and decodes the tag ID. This is an ongoing challenge as the detection procedure for a chipless RFID tag has more complexities compared to a conventional RFID tag. The signal collides with other scatterers or tags which gives a 'clutter' signal with interference.

Reading of the chipless RFID tag requires either a frequency domain measurement, measurement of the amplitude or the phase of the transmission coefficient of the tag that can be used for decoding data. In many of the experiments carried out in the laboratory, a VNA has been used for this purpose. Since the VNA is not a conventional reading technique and is an expensive piece of equipment three generations of chipless RFID tag readers are reported in articles published in 2012 [12].

In Chapter 2, a number of detection techniques are discussed which have been applied to achieve an accurate result of its tag ID. Tag localization is the next research problem which has been addressed. Many commercial applications need identification as well as tracking items. This has lead researchers explore into this area of finding the accurate location of the chipless RFID tags [13].

There have been great amounts of work done on chipless RFID tag and antenna designing during the recent years. Most of them still remain as prototypes and there are only very few commercially available. From the journal articles and conference papers published so far it can be seen that the number of bits

encoded, size of the tag, substrate, polarization, printability, domain (time, frequency, and phase) and the cost are the main attributes taken into consideration when designing a tag and an antenna [14].

Advancement of affordable customer level chipless RFID tags owing to simplified technology and low manufacturing cost has contributed to chipless RFID market growth over the past few years [14]. Some of the chipless technologies include chemical-based tags, magnetism-based tags, surface acoustic wave (SAW) based tags and capacitively tuned split micro strip resonators [15]. However, only SAW tags for non-stop road tolling and acoustomagnetic tags for error prevention in healthcare are available in the application market.

Despite the 'hot' trend in chipless RFID among academics and practitioners, it can be clearly seen that it has a long journey to accomplish to thrive the global market. Along the years the chipless RFID technology has matured and large number of tags and antenna design can be seen [16]. Comparatively the detection and localisation of the chipless tag needs more development to attract the business organisations.

On the point of applications, it is still at a childhood state. Whereas many industries are keeping an eye on its developments in regard to their identified industrial problems. Some of the industries where chipless RFID can be applied are environmental monitoring, retail, building management, construction, animal detection, aviation, fabric and clothing, food safety warranties, health, library services, logistics and supply chain management, mining and Counterfeiting Money.

1.2 Research aims

The aim of this research is to evaluate the robust detection of the chipless RFID system by investigating the detection of moving tags, development of robust detection algorithms and by testing the system performance on these conditions. The research problems are:

1. Direct detection of moving chipless RFID tags - Need new detection schemes.
2. How to improve the detection range of a chipless RFID system for a moving tag?
3. How to incorporate fabrication errors into the detection problem and combat them?
4. Why the received signal is heavily distorted? - How to reduce errors using de-noising techniques.

To address the research questions the following aims of the research are set.

1. Robust detection of a moving chipless RFID tag.
2. Experimental / Empirical model for moving tag detection and a robust detection algorithm for moving tag detection to be implemented in hardware.
3. Reducing false negatives/ false positives of the system.

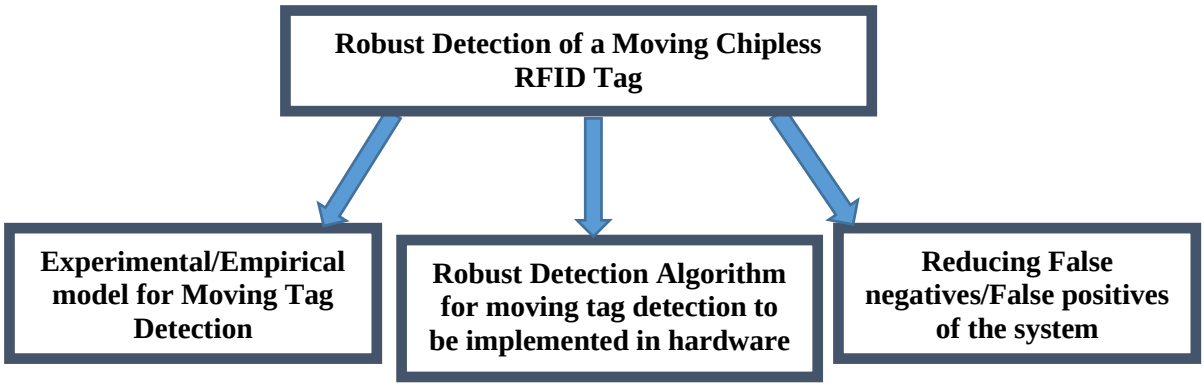

Figure 1.5 – Research aims

The research aims are shown in Figure 1.5.

One of the main aims of this research is to commercialize the chipless RFID system, therefore the detection should be performed using the developed low cost chipless RFID reader at MMARS

Laboratory of Monash University. Therefore, a robust detection algorithm is needed which can be used in a moving tag environment. Also, the detection will expand from a single antenna to an array of antennas as a larger reading range is expected for a reasonable moving tag detection. So, a novel detection technique is to be developed for a chipless RFID single reader antenna.

Once the detection is complete, the detection of a chipless tag using the chipless RFID reader system needs to be tested for its reliability and repeatability. By the performance of a sensitivity analysis on the parameters of variability of a chipless RFID system giving rise to false negatives and false positives during fabrication and printing an algorithm is to be developed to reduce the errors of the system.

1.3 Research contributions

As shown in Figure 1.6, for the fulfilment of the thesis goals the following original contributions are made.

1. A novel empirical model approach is presented to detect a moving tag.
2. A novel detection algorithm is developed using wavelet transform to detect a moving tag in an improved reading range.
3. Real time application of detection algorithm for moving tag detection with improved reading range using array antenna.
4. Sensitivity analysis studying the readability and repeatability of the chipless RFID reader and the robustness of the detection algorithm.
5. The algorithms are successfully implemented in a smart shopping trolley mounted reader.

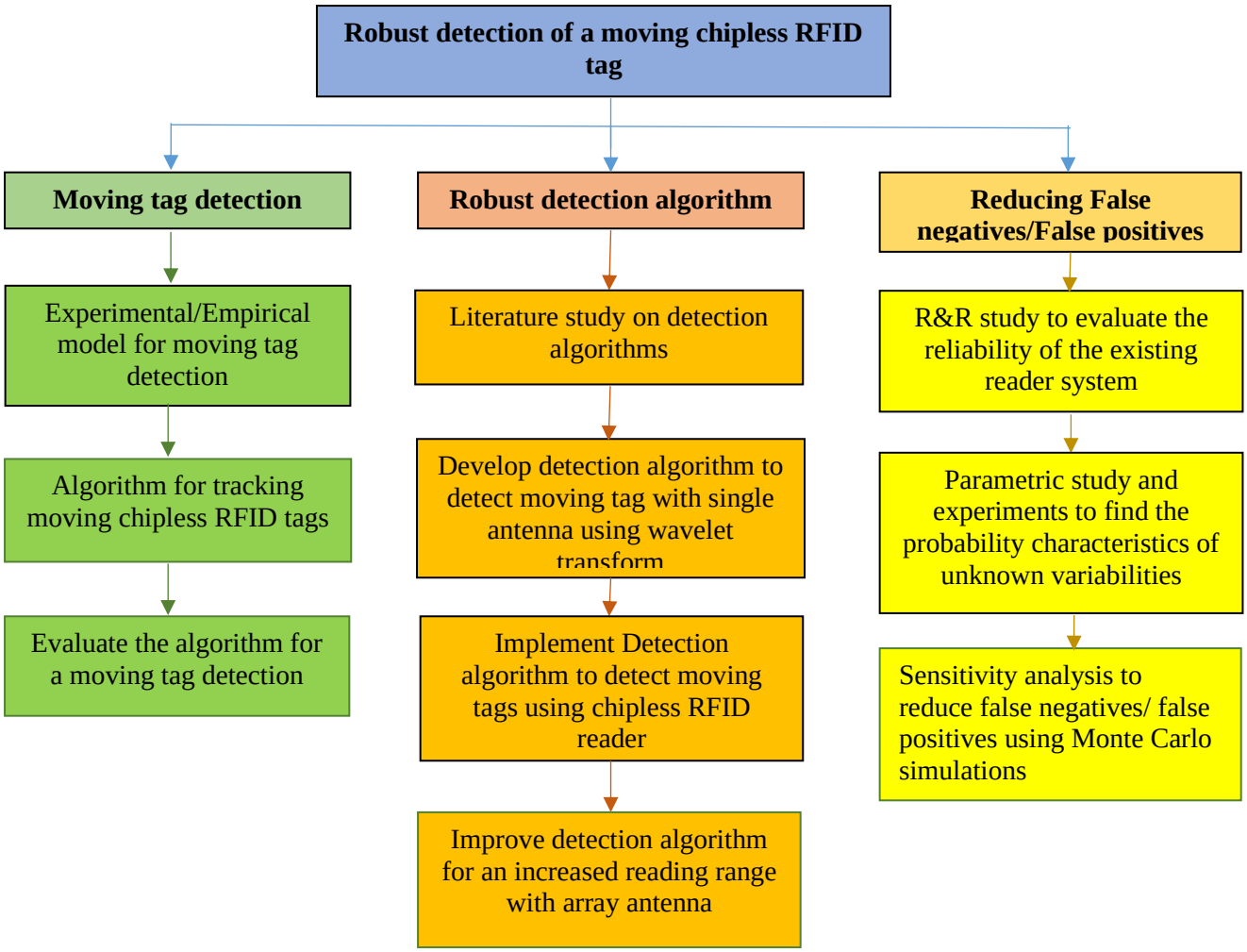

Figure 1.6 – Proposed research

In the following the proposed research that form the main body the thesis is presented.

- **Moving Tag detection**

In Chapter 3, preliminary research has been mainly carried out in experiments on moving tag detection using different antennas to study the effect of the move on the received signal and a repeatability and reliability (R&R) study to evaluate the reliability of the existing reader system.

Through the preliminary experiments for a moving tag the parameters that can be affected and the factors that are important during moving tag detection are identified. One of the limitations in the performed experiment was that the readings were taken at stationary positions. Thus, the real time movement of the tag is not presented. As stated in Chapter 2, even in the literature that presents the

moving of a chipped tag, real-time movement is not considered. A new experimental model has been proposed in this research to detect the tag ID while it is in motion. Through this experiment tracking the moving chipless RFID tag and its effect on detection of the frequency signature has been the major challenge. This has been overcome using the novel detection algorithm which has given rise to a new optimization algorithm for a chipless RFID system with movement.

- **Robust detection algorithm**

In the literature review the developed detection techniques were studied and a clear understanding of the requirements for a chipless RFID system tag identification is highlighted in Chapter 2. As reported, none of the advanced detection algorithms have been implemented in the current reader system. It is proposed to develop a detection algorithm for the present firmware with a single reader antenna. For this purpose, continuous wavelet transform given in equation 1.2 and windowing techniques will be explored, and performance will be evaluated. The starting position and the size of the window are two important parameters for this approach as unwanted clutter can be easily added if it has wrong estimation.

$$CWT\ {}_{x}^{\psi}(\tau,\ s) = \Psi_{x}^{\psi}(\tau,\ s) = \frac{1}{\sqrt{|s|}}\int x(t).\ \psi^{*}\left(\frac{t-\tau}{s}\right)dt \qquad (1.2)$$

Translation (Location of the window)

Scale

Mother wavelet

Another limitation factor that was found through the preliminary research was the half- power beamwidth (HPBW) of the reader antenna. The reader (the vector network analyser) was able to detect the tag only when the latter was located within the antenna beam. Therefore, the moving distance was limited to a maximum of -7cm to +7cm. If it is a moving belt application still, it is applicable as the speed can be controlled so that the object can be detected within the reading zone. But for different applications this will be a limitation factor. Currently research is being carried out to extend the reading range through the use of array antenna. The detection algorithm is then proposed to enhance and to be applied to the chipless RFID system with array antenna. Different detection schemes have been

evaluated to arrive at the best scheme for the system. From previous research it is clear that the backscattered signal carrying the information is very weak and will be further distorted by added noise.

Further tests are performed for the movement of the tag in different environments such as in the anechoic chamber and indoor environments.

- **Detection of False negatives/ False positives**

The research problem of false negatives and false positives has been explored in the preliminary research. The R&R test has given an idea of the acceptability of the chipless RFID system. This has been performed without the implementation of any advanced detection technique and has been proven better performance after implementation of the proposed detection algorithms. The parameters which can be related to the false negatives and false positive readings has been studied. It is difficult to find the probability density functions of all these parameters as the fabrication process and printing process is highly complexed. The complexity of the tag design and the printing conditions are more likely to contribute towards the false readings. It is proposed to find the probability characteristics of the highly affecting parameters (conductivity of the ink, viscosity of the ink, line width and gap widths of the printed tags) by experimentally finding the variability of the tag responses due to the variations of those parameters. Given that the noise is Additive White Gaussian Noise (AWGN), the present method of detection shows good performance. However, due to the noise introduced by fabrication errors, the total noise affecting the signal would not essentially possess a white spectrum as in AWGN. The mean, the magnitude of the variance, would give us a sense how much jitter or 'noise' is in the signal. A sensitivity analysis has been performed using Monte Carlo simulations. This has helped to arrive at a new probabilistic model for the total noise of a chipless RFID system. Finally, the system has been integrated with the proposed detection algorithms and tested for robust detection of stationary and moving chipless RFID tag detection.

In conclusion the thesis had made significant contributions in the signal processing of the chipless RFID technology. The logical flow graph with the original contributions and the research outcomes in prestigious outlets are shown in Figure 1.7. The following section presents the thesis outlines.

1.4 Thesis outline

Chapter 1: Introduction

An introduction to chipped and chipless RFID systems, an overview on detection of static and moving objects using chipless RFID technology and the research aims are presented. Then the original contributions of the research were listed followed by an outline of the chapters.

Chapter 2: Detection of chipless RFID tag ID

This chapter gives a detailed review of chipless RFID tag detection and localization. Namely, moving average technique, Hilbert transform (HT), signal space representation, maximum likelihood technique and continuous wavelet transform used for the detection are presented. It gives a brief review on localisation techniques. The gaps and new research directions are also presented.

Chapter 3: Chipless RFID tag in motion

This chapter presents experiments and results on tag movement. First the important parameters related to the backscattered signal of the tag are discussed. Experiments have been performed using different antennas and different chipless RFID tags. The motion of the tag in horizontal and vertical directions are analysed using experimental results and are presented in detail in this chapter.

Chapter 4: Adaptive wavelet-based technique for chipless RFID tag detection

A novel wavelet-based detection technique has been presented in this chapter. The application of this algorithm is tested on simulated results. Simulation under dynamic environments and their results are also presented in this chapter.

Chapter 5: Further improvement of detection algorithm for moving tag detection

The developed adaptive wavelet-based detection algorithm has been improved and tested on the results obtained in chipless RFID tag stepped motion. The wavelet suitable for the variations observed while the tag is in movement in magnitude and phase are considered in this chapter.

Chapter 6: Implementation of detection algorithm for single antenna reader system

The implementation of the developed detection algorithm has been presented in this chapter. Different tag readings using the reader system is analysed using the adaptive wavelet-based detection algorithm in order to detect the correct frequency identification of the chipless RFID tag.

Chapter 7: Detection error rate and sensitivity analysis of a chipless RFID system

A detection error rate analysis has been performed to check the robustness of the proposed detection algorithm for a higher number of data sets. Coloured noise has been introduced as the perfect match for the noise experienced in a real environment of a moving tag. The analysis is performed using Matlab programming. A sensitivity analysis is also performed and presented in this chapter. It is to study the readability and repeatability of the chipless RFID reader with the applied detection algorithm. An attribute agreement analysis is produced in this chapter.

Chapter 8: Application of detection algorithm for moving tag detection with improved reading range using array antenna

An improved detection algorithm for array antenna is presented in this chapter. Real time tag movement and its performances were evaluated using the improved vector modulator reader system. Programming and downloading the detection algorithm into the microcontroller using C++ programming and then further detected results are presented in this chapter.

Chapter 9: Smart shopping trolley project with chipless RFID system

The complete chipless RFID system is practically implemented in a smart shopping trolley in this chapter. The successful detection of tagged items dropped into and out of the trolley is presented. The direction of the tagged item is also detected and displayed in a user interface.

Chapter 10: Conclusion

Chapter 10 reiterate the research objectives and its successful achievements. Also, future directions of the research and possible applications are presented.

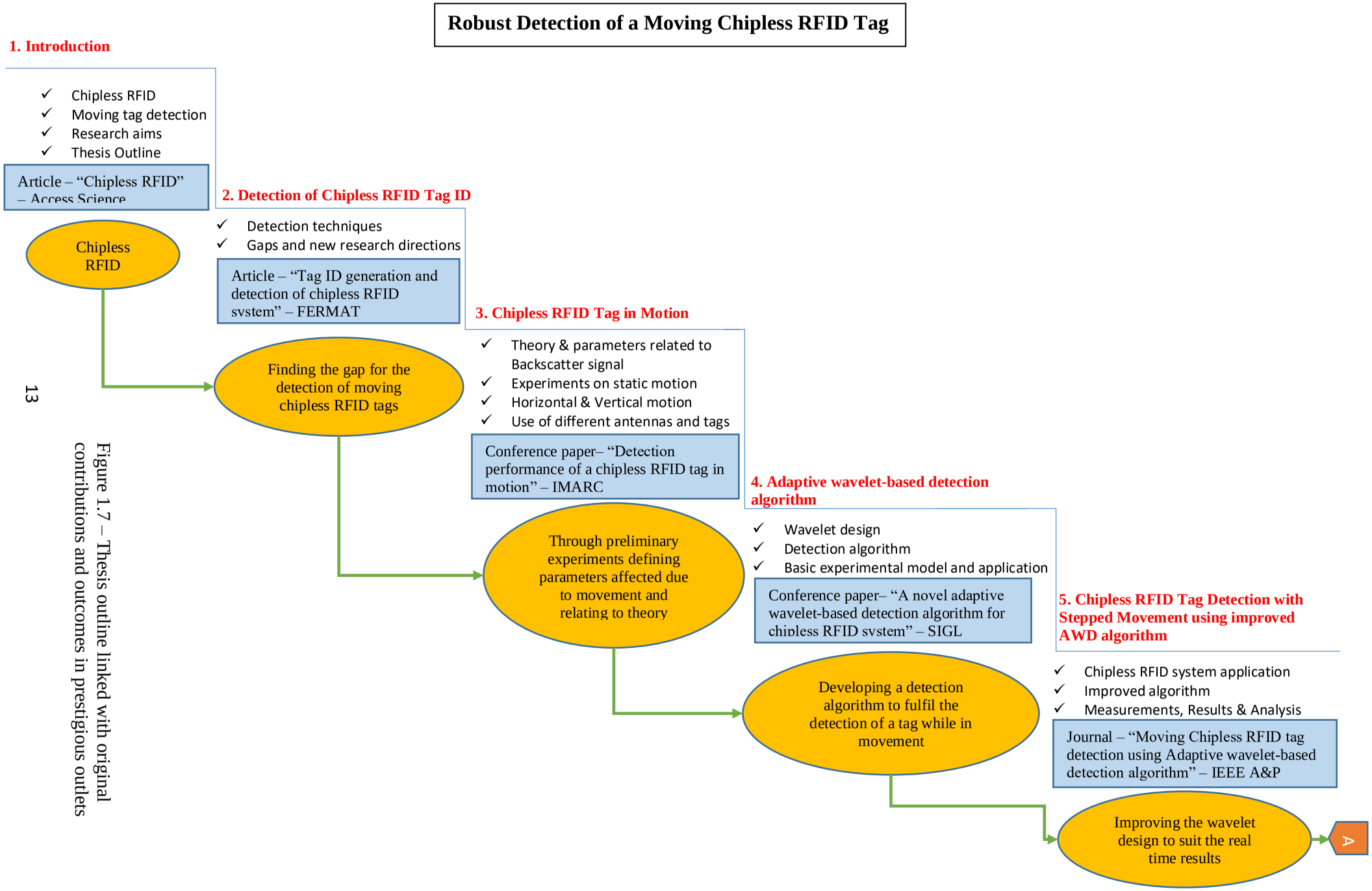

Figure 1.7 – Thesis outline linked with original contributions and outcomes in prestigious outlets

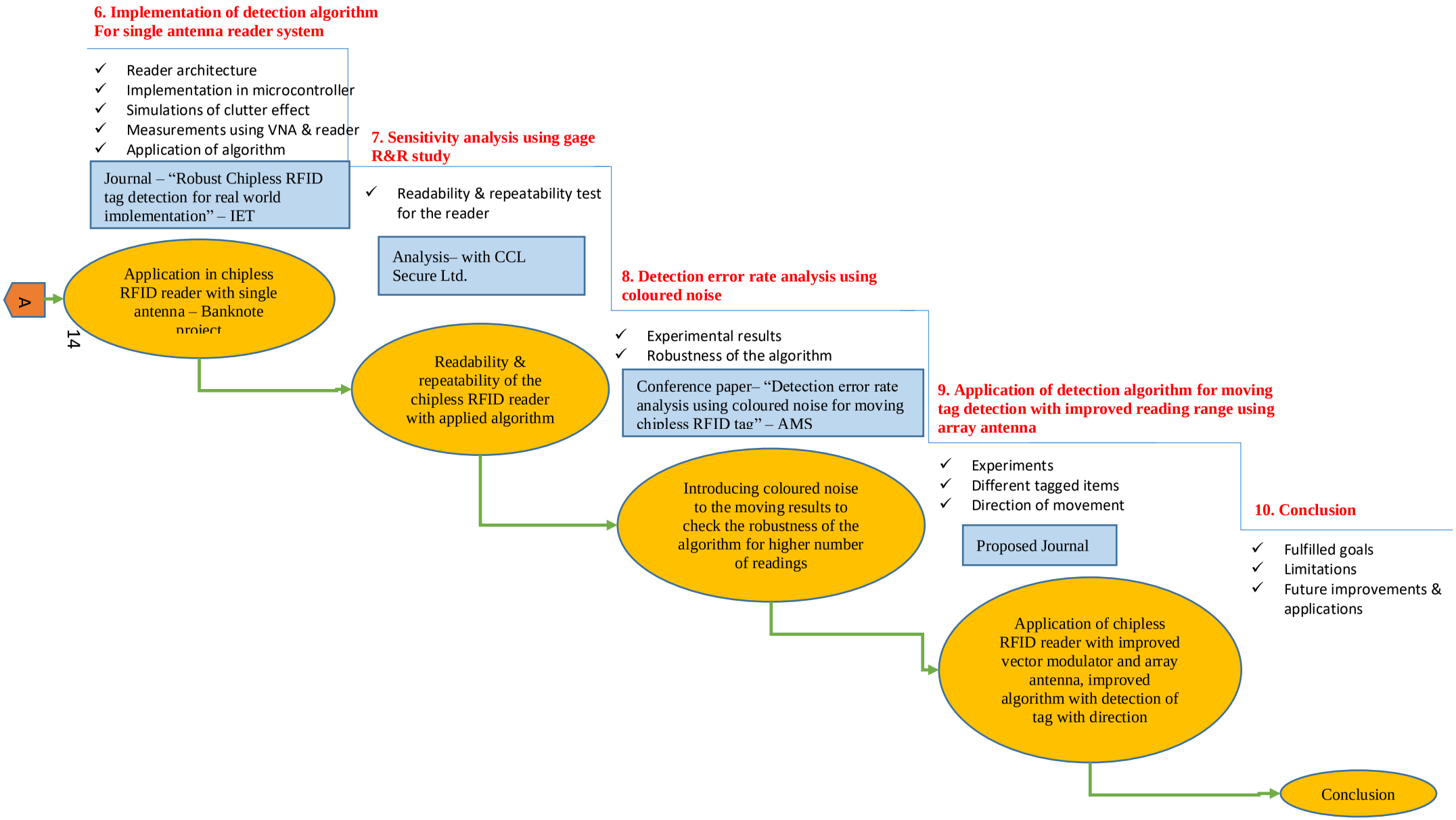
6. Implementation of detection algorithm
For single antenna reader system
✓ Reader architecture
✓ Implementation in microcontroller
✓ Simulations of clutter effect
✓ Measurements using VNA & reader
✓ Application of algorithm
Journal – "Robust Chipless RFID tag detection for real world implementation" – IET
7. Sensitivity analysis using gage R&R study
✓ Readability & repeatability test for the reader
Analysis– with CCL Secure Ltd.
8. Detection error rate analysis using coloured noise
✓ Experimental results
✓ Robustness of the algorithm
Conference paper– "Detection error rate analysis using coloured noise for moving chipless RFID tag" – AMS
9. Application of detection algorithm for moving tag detection with improved reading range using array antenna
✓ Experiments
✓ Different tagged items
✓ Direction of movement
Proposed Journal
10. Conclusion
✓ Fulfilled goals
✓ Limitations
✓ Future improvements & applications
A
Application in chipless RFID reader with single antenna – Banknote project
Readability & repeatability of the chipless RFID reader with applied algorithm
Introducing coloured noise to the moving results to check the robustness of the algorithm for higher number of readings
Application of chipless RFID reader with improved vector modulator and array antenna, improved algorithm with detection of tag with direction
Conclusion

2 Detection of Chipless RFID Tag ID

2.1 Introduction

The chipless RFID reader extracts the backscattered signal and decodes the tag ID. This is an ongoing challenge as the detection procedure for a chipless RFID tag has more complexities compared to a conventional RFID tag. The signal collides with other scatterers or tags which gives a 'clutter' signal with interference. Number of detection techniques have been applied to achieve an accurate result of its tag ID. This chapter reviews different detection and denoising techniques of the chipless RFID tags followed by localisation of the tag. There are not many algorithms and signal processing of the tag detection on the move.

The chapter is organised as follows. Section 2 reviews different detection techniques for stationary chipless tags that are reported in open literature. Section 3 reviews the localisation techniques. Section 4 presents the research gap in moving tag detection and proposed adaptive wavelet based moving tag detection. Section 5 concludes the chapter.

2.2 Review on Chipless RFID detection and localisation techniques

This section presents a literature review on the detection techniques used to decode the tag ID of a chipless RFID tag, de-noising techniques used for noise reduction and the localisation techniques used to locate the tag in the field of chipless RFID.

2.2.1 Decoding and de-noising techniques

The basic detection technique used in [1] is based on comparing the received data with threshold values obtained by calibration. This approach therefore has a major drawback as it does not possess the flexibility and adaptability required in the detection process to address errors due to a dynamic environment. In [17] two types of techniques namely (i) Moving Average technique, (ii) Hilbert

Transform (HT), has been used in frequency domain-based reader development and Fast Fourier Transform (FFT) has been used in time domain based reader development.

The received signal at the reader contains the unique spectral signature with the desired attenuation and phase jumps of the tag. In the Gen-1 reader developed in a gain/phase detector is used to distinguish the difference in magnitude and phase of the received signal and the transmitted signal which is used as the reference signal. The waveform is used to analyse the data, and this can be deteriorated due to different sources of noises leading to errors in the detection. Moving average technique is a simple de-noising technique which removes noises by acting as a low pass filter.

Hence a research gap is found to detect, denoise and localise a chipless RFID tag on the move. The proposed technique is a novel adaptive wavelet transform technique. The technique can successfully decode a moving tag and can also provide direction of movement and localisation. Therefore, the proposed technique has huge industrial potentials in many emerging applications such as luggage tagging and sorts on conveyer belts in airports and smart shopping trolleys in shopping centres.

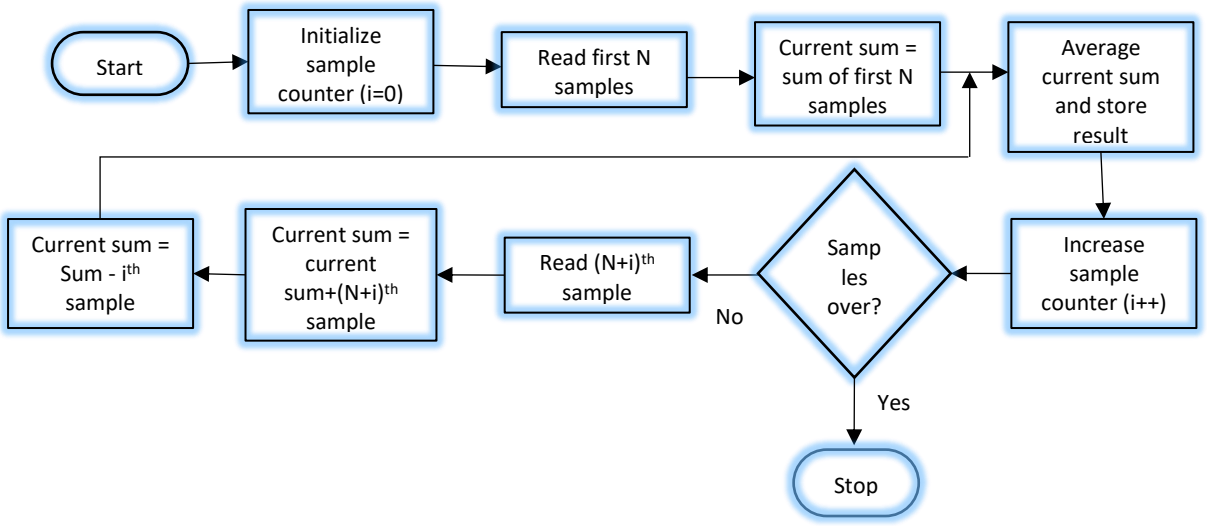

Figure 2.1 - Flow chart of the moving average filtering technique [17]

The flow chart of the moving average filtering technique used in [17] is shown in Figure 2.1. It has been observed that a smoothened waveform is resulted after using this filtering technique. An 11 samples averaging moving average filtering has been successfully implemented on a low-cost mid-range

microcontroller having low processing power capabilities. The calibration of data has not been eliminated in this technique which gives the same drawback to this technique as in [1].

Hilbert transform is a complex analytical signal processing technique. This technique has been used in [18] to reconstruct the frequency signatures of the chipless tags. The flow chart of the signal processing of the HT used in [18] is shown in Figure 2.2. A chirp signal is used as the interrogation signal in the Gen-2 reader development in [18].

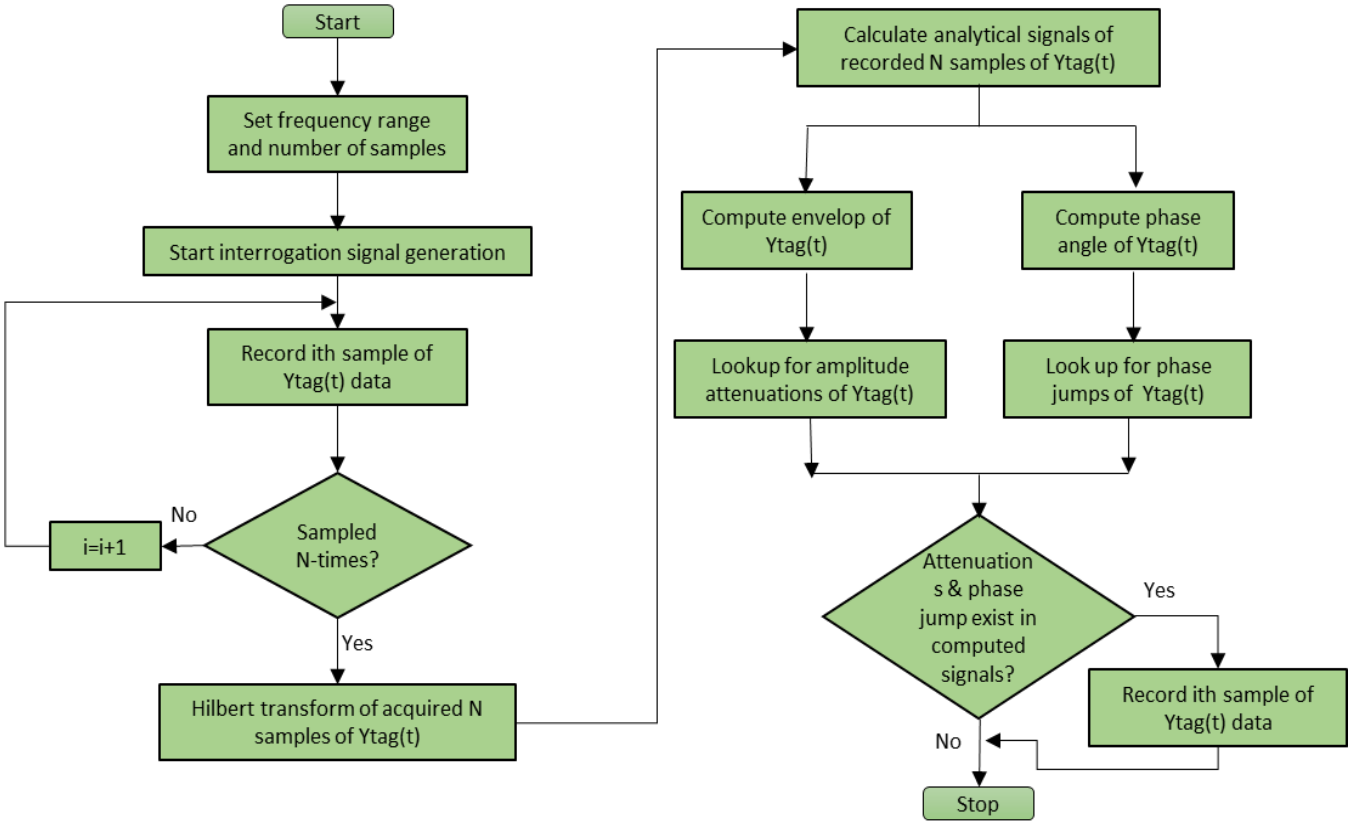

Figure 2.2 - Flow chart of the signal processing using Hilbert Transform [18]

It has been experimentally proven that HT provides the extraction of the amplitude and phase functions of the frequency signature. Author points out the limitation on high speed tag reading due to the signal processing method and highlights that the phase response is less affected by the interference caused by the system set up and surrounding noises.

The signal space representation of chipless RFID tags presented in [19] uses an efficient mathematical model to decode information in a chipless RFID tag. It has been reported that reader designs presented

in [12] and [18] can be improved by the new detection algorithm to overcome the detection errors. It represents 2^b possible tag frequency signatures of a b-bit tag in a signal space and the detection is based on minimum distance detection. The analysis is performed in the frequency domain. The frequency signatures are represented by a matrix which is composed of orthonormal column vectors and a singular value matrix. For the design a 3-bit chipless RFID spiral resonator based on co-planar waveguide theory (CPW) based tag [20] is used and it consists of two monopole antennas at 2.2-6.5 GHz. Each spiral resonator works as notch filter at 2.42, 2.66 and 2.96 GHz. It has been designed and simulated using CST and practically measured using the VNA. The magnitude and phase of S_{21} parameter (in dB) against frequency is studied. The constellation of signal points are plotted with a basis function. It can be seen that as the number of bits increase this method will face limitations and also the distance is very limited.

The authors in [21] clearly explains the approach of wavelet transform in the time-frequency analysis of the backscattered signal of the tag. The Morlet wavelet has been used as the mother wavelet in this application. It gives the turn on times and the resonant frequencies of the signal and the wavelet coefficients provide significant information of the tag. It emphasises the fact that the original signal can be decomposed into multiple frequency bands and each component can be analysed independently, which is beneficial in analysing the backscattered signal from a chipless RFID tag. The limitation of this method is that it has low frequency resolution for high density of data.

Matrix pencil method (MPM) and Short time MPM (STMPM) are two more detection techniques that has been applied for chipless RFID systems [22]. These two techniques are applied in time domain and are mentioned as accurate detection techniques in extracting the CNR of the response. Detection is performed by extracting the poles and residues from the backscattered signal using the Matrix Pencil Algorithm. An advantage of this technique is that it does not use calibration of tags and also by increasing the filtering parameter in STMPM the poles with lower energy can be recognized in the presence of the high energy poles which is significant over wavelet decomposition for detection of chipless RFID tags.

A Maximum Likelihood (ML) based tag detection technique and Trellis decoding technique has been developed in [23]. The detection error rate is compared with bit by bit detection and it has been found that ML detection has the best performance. It also reports that the computational complexity is higher in ML detection technique than Trellis detection technique. These techniques have been simulated only using Matlab, so implementation in firmware would be a future challenge.

From the above review of various detection techniques of the chipless RFID tag, it can be concluded that much work is needed in the field of the moving chipless RFID tags. In the following section the localisation techniques of the chipless RFID tag is presented.

2.2.2 Localisation techniques

Further research has been performed into the localisation of the chipless RFID tag which has paved the way for the application of the chipless RFID system in the industry. In [24] the localisation issue has been addressed by analysing the backscattered signal of the tag in time domain and thus applying a UWB-IR ranging technique. The distance to the tag from the antenna is calculated using the round trip time of flight data obtained through this technique. The ID of the tag is not obtained in this research, but it has been stated that the time domain RCS can be used to detect the ID of the chipless RFID tag. One drawback of this localisation technique is that the presence of multiple tags will make it difficult to obtain the RTOF for a single tag as overlapping of signals may occur.

A space-time-frequency anti-collision algorithm for identifying and localising of chipless RFID tags is presented in [25]. This technique is applied for localisation of multiple multi-bit tags in the reader zone. The accurate values of turn on time of the tag and its ID is found by applying STMPM to the time domain response. The accurate turn on times are depicted in a space-frequency diagram. By employing narrow-frequency pencil method to the frequency domain of early time response, the accurate values of round trip time of the scattering centres are obtained. A sliding frequency window is moved along the frequency axis which is used to find the distance from the tags to the antenna. This technique is applied

for a low number of bits and using three horn antennas placed in a circle 120^0 apart from each other. The measurements are taken using the vector network analyser.

2.3 Gaps and New research Directions in Chipless RFID system

The chipless RFID technology has been developed in its journey and is at edge of its commercialisation. The tag and antenna designing had been the major concerns in the past years and the importance of identification/detection techniques has aroused in the recent past. Through the literature review the successful detection algorithms and their drawbacks were highlighted. It is clearly seen that the techniques have not yet been implemented in the firmware and would be an important aspect of future research in chipless RFID. Thus, improvement to present techniques or a novel detection technique for the desired chipless RFID reader system would be appropriate.

Also, the above implementation would give rise to find the robustness of the chipless RFID system to present to the industry. The present measurements have been mainly taken using the Vector Network Analyser. Therefore, testing with the firmware likely give rise to errors in its backscattered signal. There can be many parameters contributing to the total noise in the received signal which can be due to imperfections in fabrication, printing and depending on the surrounding environment. The author proposes a sensitivity analysis to the chipless RFID system by performing a suitable method of testing false negative and false positive readings under different conditions. Leading to a novel probabilistic model for the noise of the chipless RFID system.

To the author's best knowledge, detection of the chipless RFID tag while in motion has not been reported to date. In literature multiple tag detection and localization techniques have been discussed which are based on stationary chipless RFID tags. The literature on active RFID tags shows the importance and demonstrates the localisation capability of moving tags. The moving chipless RFID tag detection is therefore a novel approach which will help to evaluate the reliability of the chipless RFID system and will give a broader marketing aspect to its applications. The detection of a moving tag is significant when introducing the system to the industry. Some of the applications that has the necessity

are namely, product manufacturing process, airport baggage handling, sorting of post which uses conveyor belts; human movement, animal detection, environment sensing and smart shopping trolley.

The smart shopping trolley project was supported by the industry partner CCC Secure Ltd. Under the Australian Research Council Linkage Project Grant # LP130101044, titled, “Discrete reading of printable multi-bit chipless RFID tags on polymer banknotes”. The smart shopping trolley project developed is presented in Chapter 9. The proposed method is a novel adaptive wavelet based moving tag detection technology, the technique is evaluated in various experimental set up and environmental conditions. After getting satisfactory performance, finally the novel technique is used in a chipless RFID based smart shopping trolley in a laboratory environment.

3 Chipless RFID Tag in motion

3.1 Introduction

This chapter proposes a novel approach towards chipless RFID tags in motion. The main aim in chipless tag detection is to obtain the unperturbed frequency signature of the tag. The detection is done by using horn antennas. The chipless RFID tags were selected so that their frequency ID falls within the frequency range of the horn antenna. The tag is moved within the half power beam width (HPBW) of the antenna. Either the amplitude or the phase of the reflection coefficient of the tag loaded antenna can be used for the decoding of the frequency signatures of the tags being read. Signal processing using MATLAB validate the received signals obtained to the original data of the tag. A novel detection of a chipless RFID tag in motion is proposed. The performance is evaluated through experiment and measured using vector network analyser. An error analysis is conducted on the experimental results to study the variation of magnitude, frequency and phase due to the movement of a chipless RFID tag. The relative phase variation due to movement of the tag is calculated and compared using measured and numerical results. Based on the error analysis the confidence levels for reading the tags in motion is defined. As far as the tag signature has not been disappeared from the reading range it has the same confidence level for the detection of its tag ID. This opens a new avenue towards developing detection algorithms and decoding techniques when the chipless RFID tag is in motion. Using this data, it also opens the doors for the localization of moving chipless RFID tags and prediction of the tagged objects moving trajectory modelling in the future.

Firstly, the operations of the chipped and the chipless RFID tags are compared to analyse the impact of the received signal for the chipless RFID tag detection. A system for determining chipped RFID tag movement is disclosed in [26]. The system includes an RFID reader that is configured to detect an RFID tag's motion by comparing backscattered signals received from the tag. The detection is performed by transmitting a plurality of RF signals from the RFID reader to the RFID tag and at least two modulated

backscattered signals are received from the tag in response. The back scattered signals are then compared to one another by calculating a return signal strength indicator (RSSI) for each signal and also calculating the phase angle of each backscattered signal. Also, it calculates the velocity of the tag relative to the antenna.

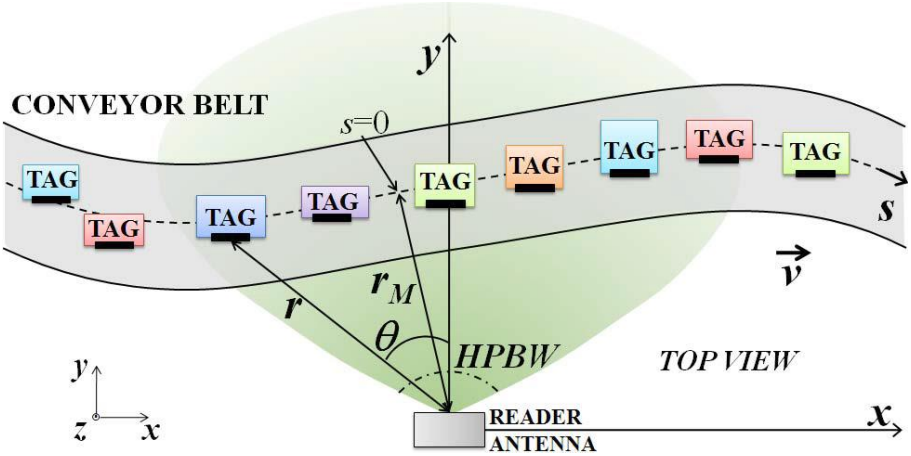

Figure 3.1 – An RFID scenario with tagged items on a moving conveyor belt (top view) [27]

Some of the localization techniques for Active RFID tags in motion are discussed in [27]. In this paper it gives an understanding of the tag backscatter loss due to tag location. Also, it explains three techniques based on the phase difference of arrival (PDOA) namely: (a) Time Domain PDOA, (b) Frequency Domain PDOA and (c) Spatial Domain PDOA.

This chapter is organized as follows. Section 2 discusses the theory behind a chipless RFID tag in motion and moves into the important parameters related to the backscattered signal. Section 3 presents the experimental design. Section 4 shows the experimental results and error analysis. Section 5 concludes this chapter.

3.2 Theory

The main challenge in moving chipless RFID tags is that the backscattered signal is not a modulated time domain signal as in a chipped RFID tag. Therefore, the backscattered signal of a moving chipless RFID tag needs to be studied in order to come to a conclusion where the tag is detectable while in

motion. In real time movement the tagged object can be moved in different directions as shown in Figure 3.2. A tagged object that is moving in Horizontal motion is considered in these experiments. The geometrical and system parameters are considered in relative to a translational motion.

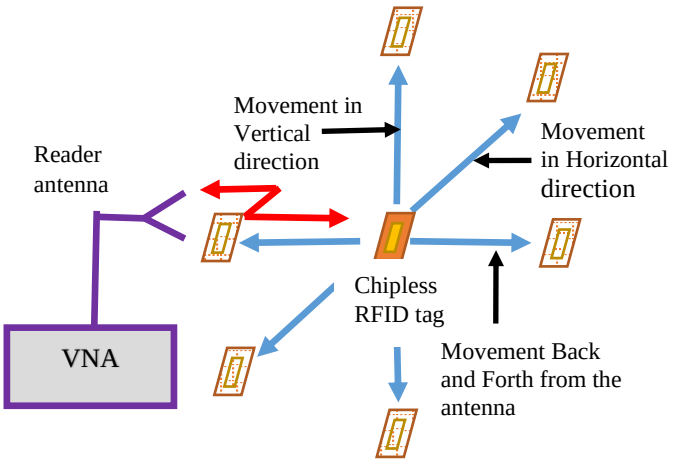

Figure 3.2 – Chipless RFID system model for moving tag analysis

The important parameters related to the backscattered signal of a Chipless RFID tag are as follows. In this work we focus on the magnitude of S_{11} (in dB) output of the reflected signal at the tag loaded antenna which is given by equation (3.1).

$$S_{11} = 20 \log |\Gamma| \quad \text{(dB)} \qquad (3.1)$$

where Γ is the voltage reflection coefficient.

The tag backscatter loss varies with the power incident on the tag (which varies with the tag location) because the input impedance of the antenna is power dependent. This can be explained as the Poynting vector which represents the directional power flux density vector (the rate of power transfer per unit area) of an electromagnetic field and is given by:

$$\vec{P} = \vec{E} \times \vec{H} \qquad (3.2)$$

where $\vec{E}$ is the Electric field intensity vector and $\vec{H}$ is the Magnetic field intensity vector. The Input impedance of the antenna is given by:

$$Z_{in} = \frac{P}{I^2} \qquad (3.3)$$

where P is the power density amplitude and I is the current. Therefore, the input impedance of the antenna is power dependent since the power varies with the varying $\vec{E}$ and $\vec{H}$ fields due to the movement of the tag, the reflection coefficient is given by:

$$\Gamma = \frac{Z_{in} - Z_0}{Z_{in} + Z_0} \tag{3.4}$$

where Z_0 is the load impedance. Γ is a function with the input impedance. This explains any variation in the S_{11} of the received signal, at the input port of the tag loaded antenna contains the frequency signature of the tag.

The distance between the tag and antenna is another parameter that changes when the tag is in motion. This changes the phase of the backscattered signal of the tag. When the tag moves, multiple replies are activated by the reader interrogations and in any propagation environment, the phase of the received tag signal can be written as [27]:

$$\varphi_{rn} = \varphi_{prop} + \varphi_{offset} + \varphi_{BS} \tag{3.5}$$

where φ_{prop} is the phase accumulated due to the electromagnetic wave propagation, φ_{offset} is the phase offset which includes the phases of cables and other reader components and φ_{BS} denotes the backscatter phase of the tag modulation. In free space, the electromagnetic phase field wave propagation is proportional to the distance travelled. Hence, φ_{prop} can be written as:

$$\varphi_{prop} = -2kR \tag{3.6}$$

where $k = \frac{2\pi f}{c}$ is the wave phase constant and *R* is the distance from the antenna to the tag. Therefore, the relative phase $\varphi_{rel}$is given by,

$$\varphi_{rel} = \varphi_{rn} - \varphi_{r1,\ \ n=1,\ldots\ldots N} \tag{3.7}$$

The relative phase can be calculated using the experimental phase data.

3.3 Experiments on static motion

3.3.1 Patch resonant tag with horn antenna

In real time movement the tagged object can be moved in different directions. A tagged object that is moving in the horizontal direction has been considered in these experiments. The geometrical and system parameters are considered in relative to a translational motion. The top view of the horizontal displacements $\pm d$ of the tagged object is shown in Figure 3.3. The chipless tag on the object follows a straight line motion in direction d, of the object. The origin of the spatial coordinate ($d = 0$) is assumed to be coincident at minimum distance R_{min} from the reader antenna.

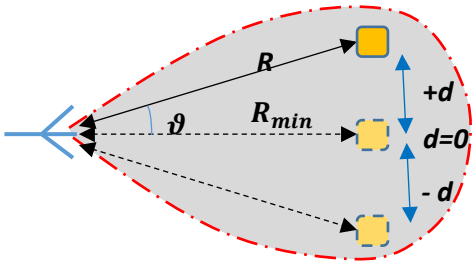

Figure 3.3 – Top view of the moving tag

where R_{min}- Minimum distance from reader to tag

R- Direct distance from reader to tag

$\pm d$- The horizontal distance from mid position

The direct distance (R) and phase angle (θ) can be given by,

$$R = \sqrt{d^2 + R_{min}^2} \tag{3.8}$$

$$\vartheta = \tan^{-1}\frac{d}{R_{min}} \tag{3.9}$$

The perpendicular distance between the reader antenna and the tag was kept constant at a given distance. The instantaneous measurements of the magnitude and the phase of the tag were measured at different positions using the vector network analyser (VNA).

3.3.1.1 Reader Antenna

The radiation pattern of the horn antenna used for the experiment was measured in Monash University anechoic chamber as shown in Figure 3.4. The main lobe half power beam width (HPBW) of the horn antenna is 40^0. It shows an operational bandwidth of 7-14 GHz.

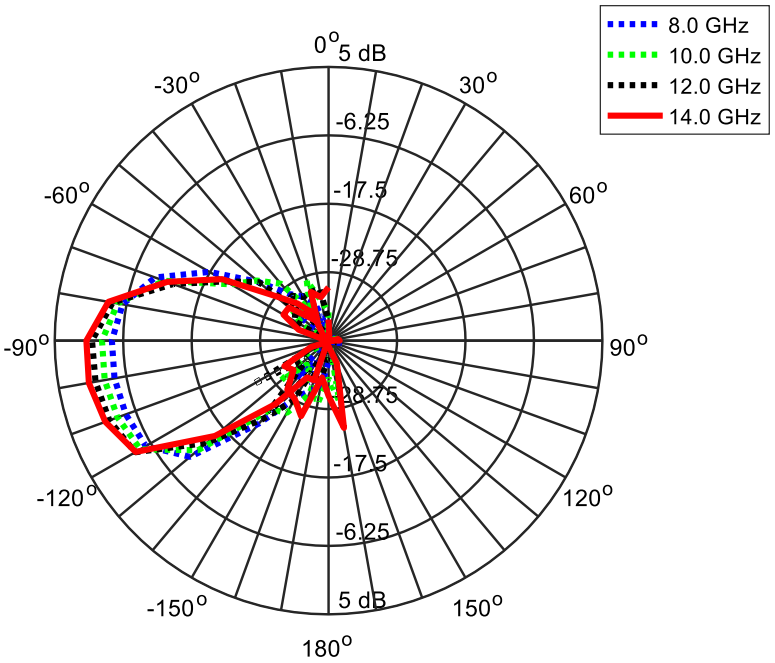

Figure 3.4 - Radiation pattern of Horn antenna

Figure 3.5 - Experimental set up to measure the radiation pattern

3.3.1.2 Chipless RFID tag

This experiment was performed using a 4-bit rectangular patch resonant tag as shown in Figure 3.6 (a). The RCS of the tag is as shown in Figure 3.6 (b). The tag is polarized in the y direction and the frequency signatures are at 7.8, 8.3, 8.8 and 9.2 GHz respectively.

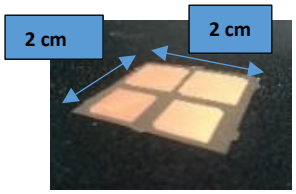

(a)

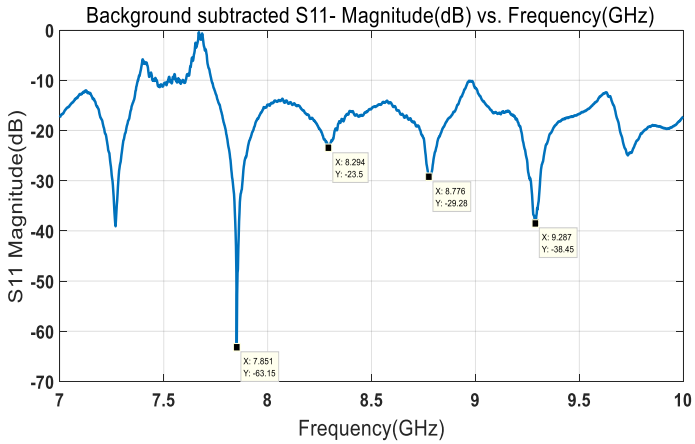

(b)

Figure 3.6 – (a) Rectangular patch tag, (b) RCS of the rectangular patch resonant tag

The background subtracted S11 of the chipless RFID tag at d = 0 mm which is at its minimum distance (R_{min}) is shown in Figure 3.5. This is considered as the reference plot for the comparison with movement.

3.3.1.3 System

In this experiment the horn antenna was used for transmitting and receiving the signal. The patch resonant tag was loaded, and the magnitude and phase measurements were collected using the vector network analyser. The tag was placed 10 cm away from the antenna and was displaced within the HPBW of the antenna. The displacement was in d = ±5 mm steps in positive and negative directions from the reference point at d = 0 mm. The frequency was varied between 7 – 10 GHz in this instance. The experimental set up for the horn antenna in the MMARS lab environment is shown in Figure 3.7.

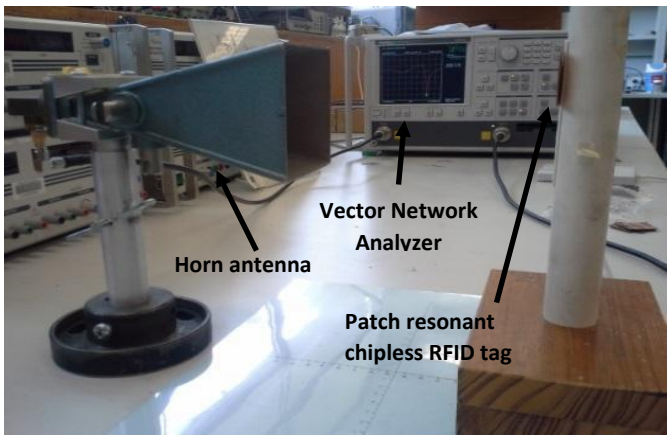

Figure 3.7 - Experimental setup used for moving tag detection

3.3.1.4 Post processing

The flowchart shown in Figure 3.8 explains the collecting of data and the post processing of the experiment. The experimental data are measured and stored in the VNA. The distance *R* from the tag to the antenna is varied and 16 different positions are considered for measurement. The collected results are then processed in Matlab. The main idea was to compare the results and retrieve the original frequency signature of the tag so that a moving chipless RFID tag can be detected without any misinterpretation.

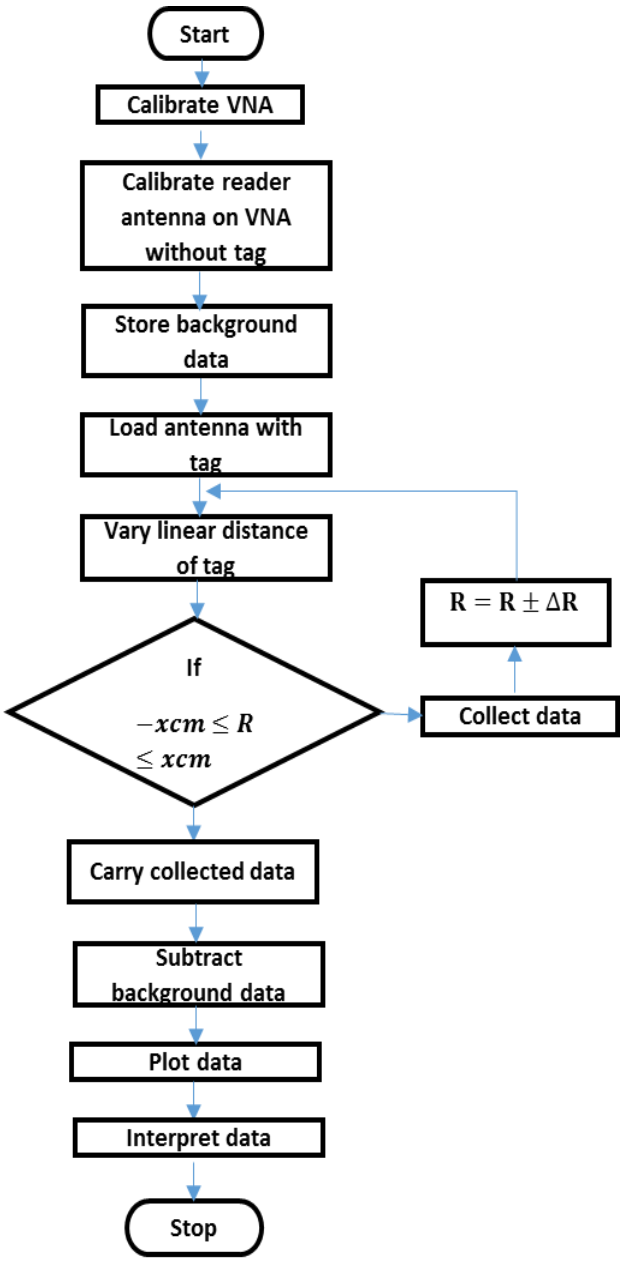

Figure 3.8 - Flowchart explaining the collection of data and the post processing of the data for moving tag detection

3.3.1.5 Results and analysis

By performing the experiment explained in section 3.3 the measurements were stored using the VNA. The plotted results in Matlab are shown in Figure 3.9. This shows the variation in the magnitude of S_{11} while the chipless RFID tag is in motion.

It can be seen that at the resonance with the maximum depth at 7.85 GHz, the amplitude shift is more significant than the other resonant frequencies. The S_{11} value is increasing as the tag is moving away from the antenna. In this case the distance R is increasing from its reference point at R_{min} as moving in the positive and negative directions. The frequency shift is comparatively less and is in opposite directions while moving away from the midpoint.

Analysing the data, the variation of the S_{11} magnitude related to the distance travelled by the chipless tag is plotted in Figure 3.10. When the tag is moving between $d = \pm 2\ cm$ the frequency variation is between +0.034 and -0.037 GHz. Moving towards $d = +3.5\ cm$ there is a slight increase in the frequency shift by 0.06 GHz and when $d = -3.5\ cm$ there is no change. Comparatively the amplitude shift is varying positively from +4.74 dB to +38.81 dB in magnitude.

We can see that the change in the magnitude of the S_{11} is not linear. The maximum distance the tag can be moved while within the beamwidth can be calculated and lies between +3.64 cm and -3.64 cm range. This shows that a moving tag ID detection will be dependent on the beamwidth of the relevant antenna used for the detection. Also, the tag frequency response is unperturbed within the beamwidth of the antenna.

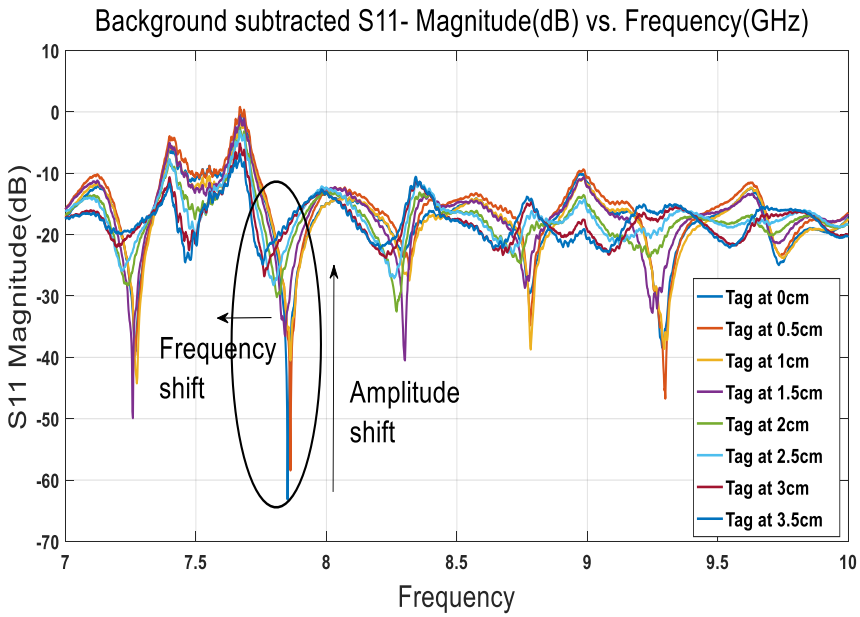

Figure 3.9 - S11 Magnitude vs. Frequency of the patch resonant tag, moving the tag in positive direction from 0cm to +3.5cm

Further research with the speed of the moving tag with improved reading range would give a broader idea to the performance of the moving tag detection.

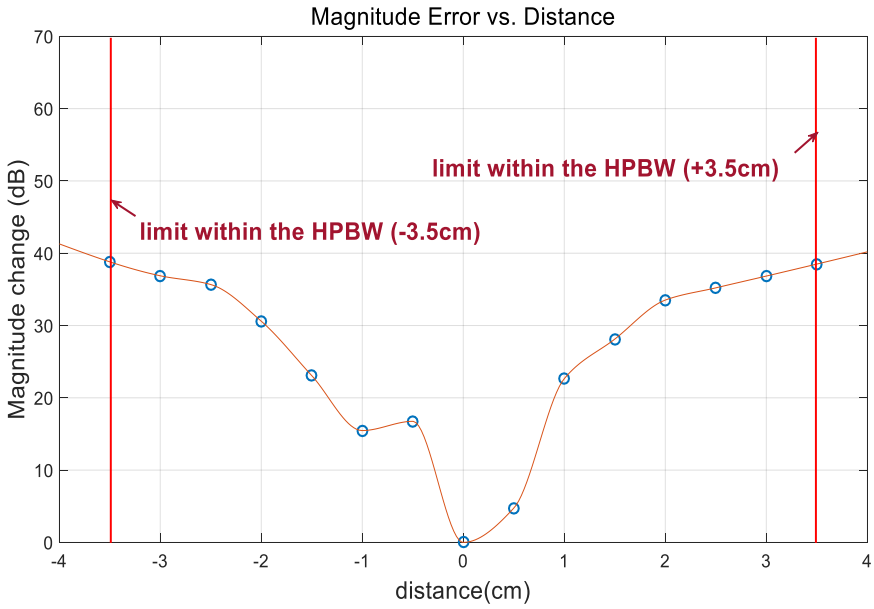

Figure 3.10 - Magnitude S11 error vs. the distance

Using equation (3.8) and (3.9) the relative phase plot is shown in Figure 3.11 for the numerical data and experimental data using the horn antenna. According to the plot using predetermined phase angles of the tag in different positions the exact location of the tag can be verified.

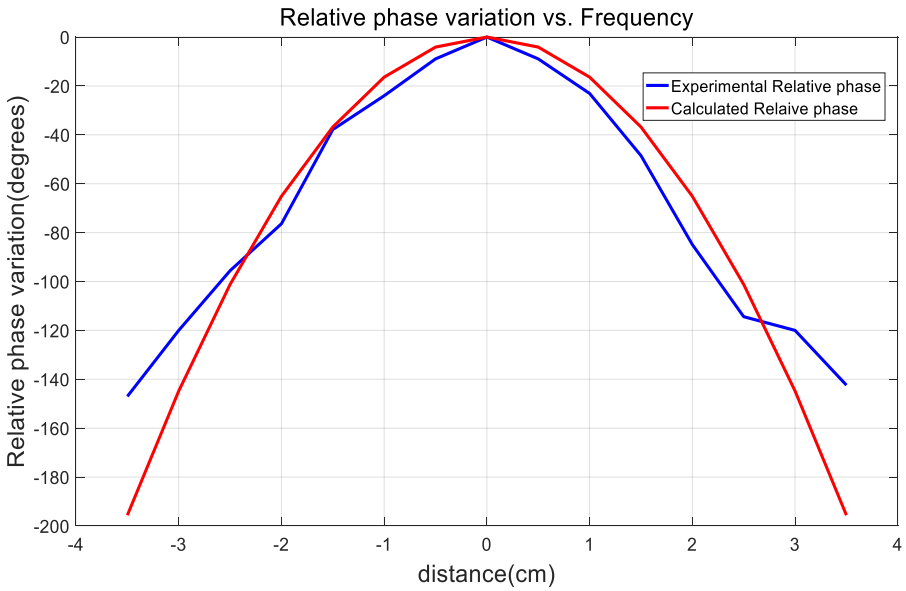

Figure 3.11 - Relative phase vs. distance at f = 7.851GHz, comparison between the experimental relative phase and calculated values of relative phase of the moving tags

The results obtained for the amplitude shift and the slight frequency shift opens a new avenue to the extracting of the frequency ID when a tagged object is in motion. Most of the detection algorithms written for chipless RFID tag detection uses a threshold-based detection technique for decoding the ID. Therefore, these results set a clear picture to determine a “condition band” for the detection of tags in motion. For a given chipless RFID system the used reader antenna and the type of tag being used will be known priori. So, for any chipless RFID system the “condition band” can be predefined so that the detection made easy. This approach will be further investigated in developing a novel detection algorithm for moving tag detection.

3.3.2 Experiment using two waveguide antennas and U-slot tag

This experiment was performed using a U-shaped slot tag which gives 4 different frequency signatures. The dimensions of the tag are shown in Figure 3.12 (a).

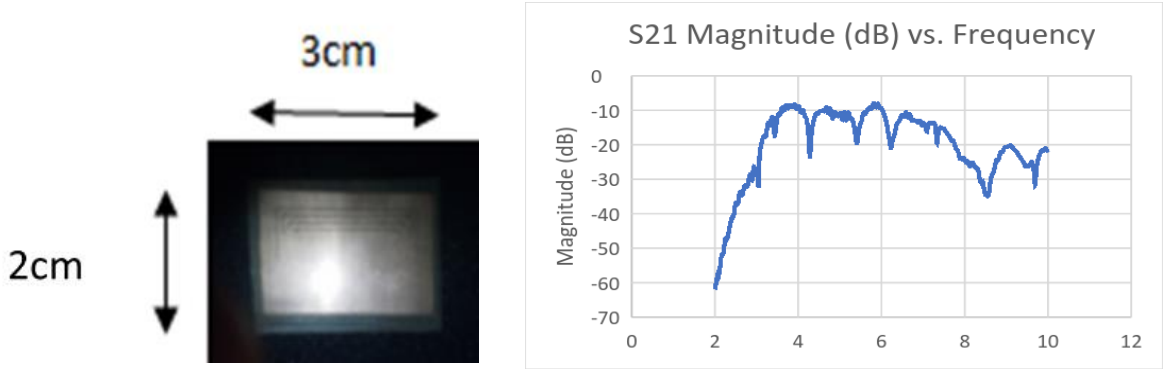

(a) (b)

Figure 3.12 – (a) U-Slot resonant tag, (b) RCS of the slot resonant tag

The RCS of the tag was measured using the Vector Network Analyser and is shown in Figure 3.12 (b). According to Figure 3.12 (b) the 4 bits are at frequencies 3.6, 4.34, 5.02, 6.24 GHz respectively.

For this experiment a waveguide antenna available in MMARS Lab was used to measure the backscattered signal from the chipless tag. The radiation pattern of the waveguide is shown in Figure 3.13 which was experimentally verified and plotted using Matlab.

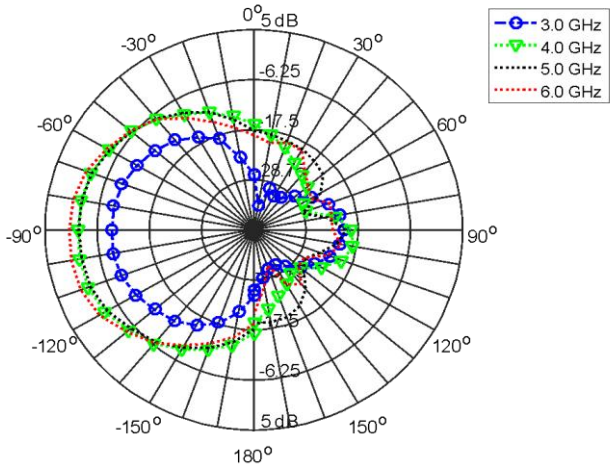

Figure 3.13 – Radiation pattern of Waveguide Antenna

Two waveguides were used for transmitting and receiving the signal. The slot resonant tag was used, and the magnitude and phase measurements were collected using the Vector Network Analyser. The distance between the two reader antennas were kept constant at 10 cm. The tag was placed in between at a minimum distance of 5 cm as shown in Figures 3.14. The instantaneous measurements of the phase and magnitude of the tag was taken at different positions varying from -30 mm to +30 mm range which falls within the 3 dB beamwidth of the antenna. The frequency was varied from 2 – 7 GHz as the S_{11} parameters of the waveguides showed its best performance between the above mentioned frequency range.

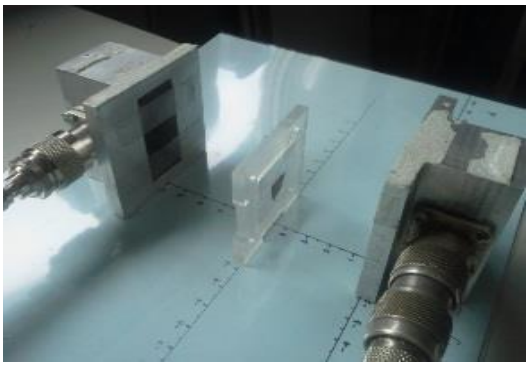

Figure 3.14 - Experimental set up for U slot resonant tag using two waveguides as transmitter and receiver

3.3.2.1 Results and analysis

As before the data is stored in the VNA and processed in Matlab. Results of S11 vs. frequency at different positions were plotted using Matlab. The results are shown in Figures 3.16 (a) and (b) which shows the measured S11 magnitude in dB and the phase change with frequency respectively. The maximum change due to the movement of the tag in magnitude and phase is highlighted in a circle in

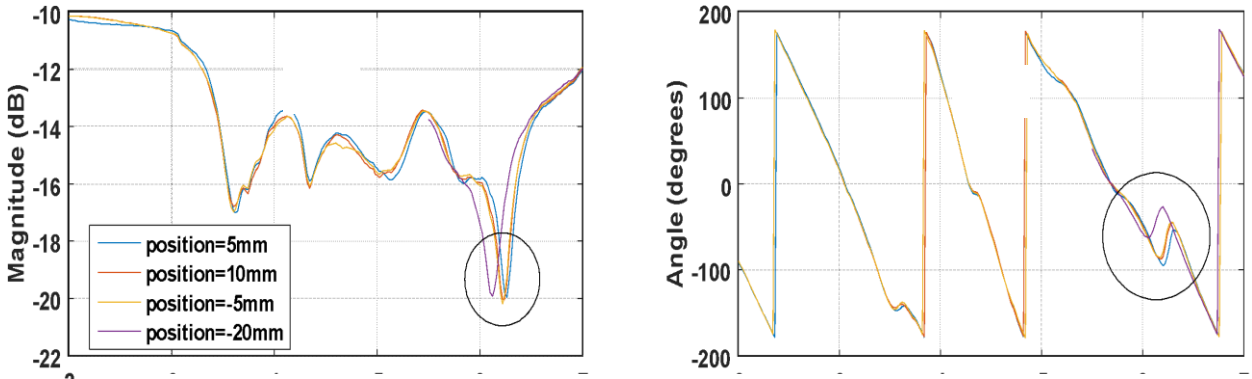

Figure 3.15 – (a) S11 magnitude vs. Frequency (GHz) (b) Angle (degrees) vs. Frequency (GHz)

both figures. As seen in Figure 3.15 when the tag is moved between -30 mm and +30 mm both magnitude and phase shifts are present.

The movement of the tag can be in different applications. The movement considered in the above experiments were in linear motion. The variables related to the movement of tag were discussed in Section 3.1. The main observation through all the experiments using different tags and different antennas was the variation in the amplitude of the detected signal. The error analysis for the amplitude variation is shown in Figure 3.16.

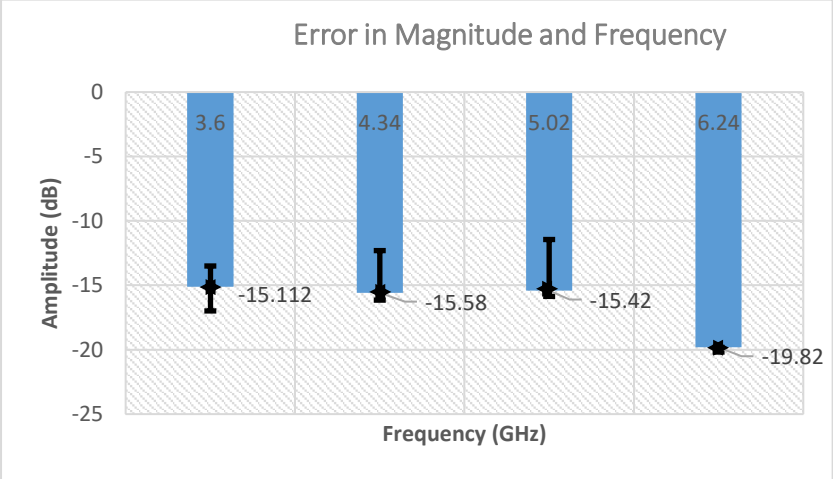

Figure 3.16 - Error in amplitude variation at the resonant frequencies using waveguide experimental results

The correct frequency responses and its amplitude is given as a bar chart and the results for the slot resonant tag using the waveguides are represented in Figure 3.16. As shown in Figure 3.16 the amplitude is shifted giving positive and negative errors in its magnitude values. The positive error is maximum at 5.02 GHz and the variation is 4 dB. At the most significant bit frequency 6.24 GHz it only shows a negative variation in its amplitude. The frequency variation was also calculated for these experimental results and was found that it varies between -0.02 GHz to +0.02 GHz which cannot be distinguished in the error graph.

3.3.3 Experiment using single and two SWB antennas and 4-bit tag for moving tag detection

As shown in Figure 3.17 two super wide band antennas (SWB) with a patch height of 0.5 mm and a 4-bit tag design was used for this experiment. The antennas were placed with a 5 cm gap and the tag was placed in between to obtain the best response. Observing the radiation pattern of the SWB which gives an omni-directional pattern as shown in Figure 3.18 the experiment was carried out in both directions horizontal and vertical tag movement.

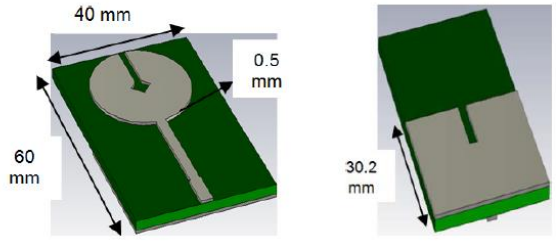

(a) Front View (b) Back View

Figure 3.17 – Front view and back view of SWB antenna with a patch height of 0.5 mm [30]

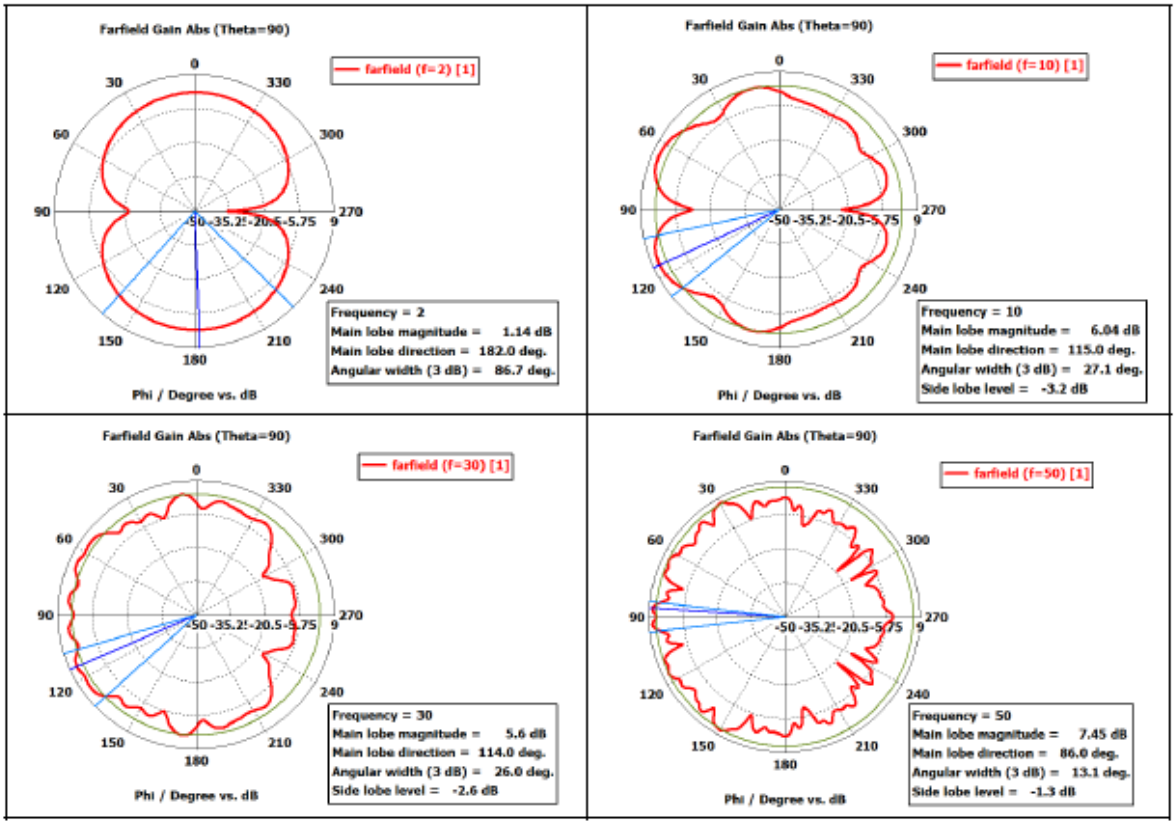

Figure 3.18 – Radiation pattern of the SWB antenna with a patch height of 0.5 mm [30]

The tag was placed at 5cm as shown in Figure 3.19. The vertical and horizontal movement of the tag was experimented using the Agilent Vector Network Analyser.

(a)

(b)

(c)

Figure 3.19 - (a) Experiment using single SWB for horizontal movement of the tag, (b) Experiment using 2 SWB antennas for vertical movement of the tag, (c) Experiment using two SWB antennas for the horizontal movement of the tag

3.3.3.1 Results and analysis

The collected data of the above experiments were plotted using Matlab and is shown in Figure 3.20.

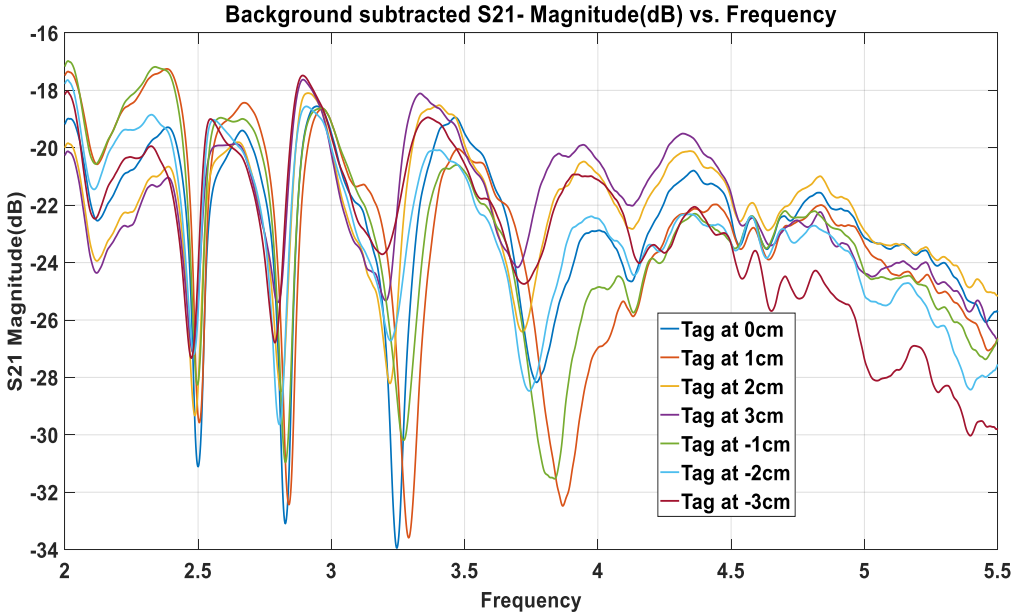

Figure 3.20 - S21 Magnitude vs. Frequency for experiment using 2 SWB antennas

The S11 measurements were taken using the Agilent VNA for the moving tag using single antenna.

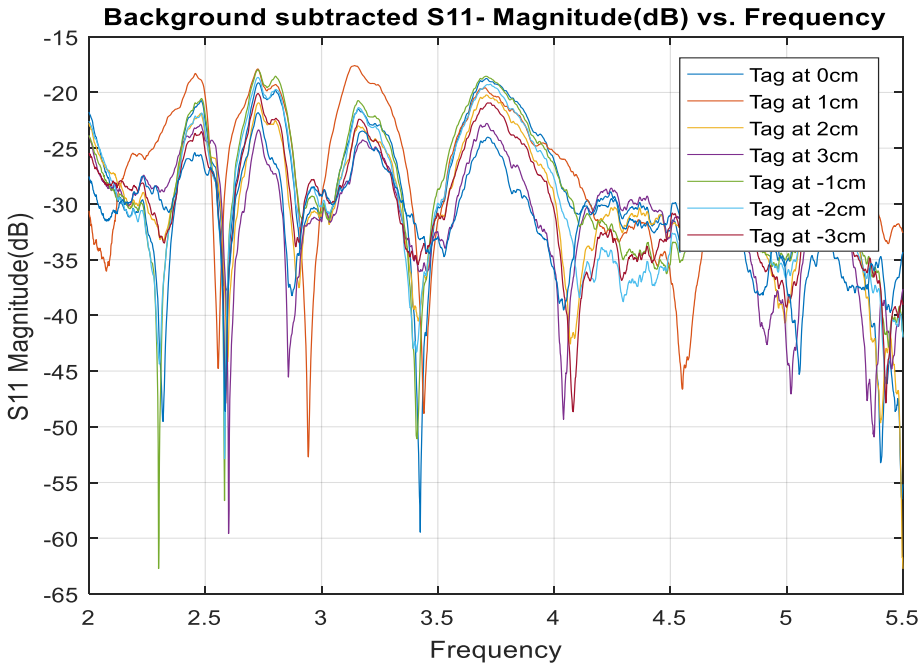

Figure 3.21 - S21 Magnitude vs. Frequency for experiment using 2 SWB antennas

In Figure 3.22 it gives similar results as in the earlier experiment. The amplitude variation is larger compared to the waveguide results, but the frequency shift is still negligible.

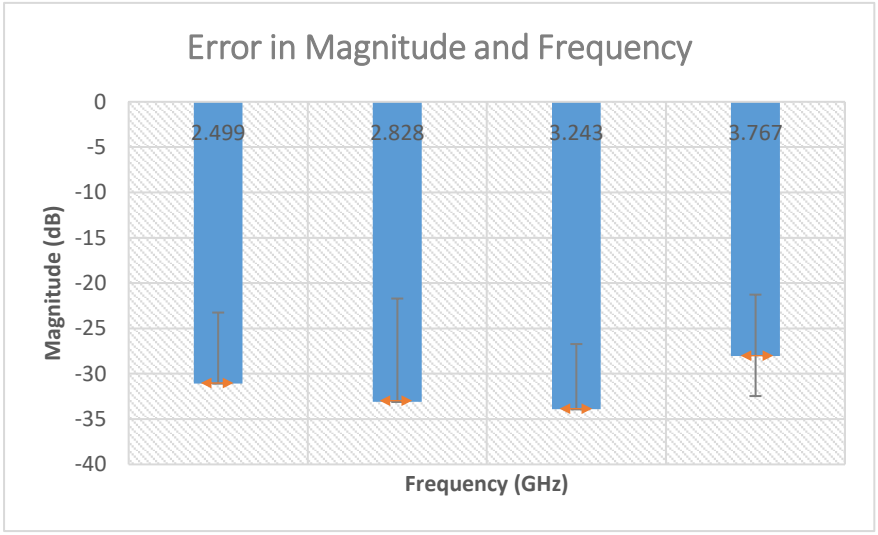

Figure 3.22 - Error in amplitude variation at the resonant frequencies using super wide band antenna experimental results

There can be several factors and reasons behind the amplitude shift observed through these experiments. Some of them were identified as:

1. Reader antenna half power beam width (HPBW)
2. Tag RCS pattern
3. Distance between the tag and antenna

The effect of reader antenna half power beam width is a known factor as the tag should be within its reading zone to detect the absolute response of the tag. If the tag is partially or outside its reading zone the response would show errors in some bits or would not be due to the chipless tag. Therefore, the HPBW of the antenna is a limitation to perform a good movement of the tag. Hence it is proposed in this research to develop detection algorithms for an array scan antenna which would give a broader reading zone. However, an UWB scan array antenna development is a non-trivial task and out of the scope of the PhD thesis.

3.3.4 Detection of chipless tag response while the tag is in vertical motion using horn antenna

Horn antenna shown in Figure 3.23 with dimensions of 24 cmx14 cm and working in the frequency range of 0-18 GHz wss used for this experiment. The tag used for this experiment was a hexagonal copper tag [29] with its tag signature falling between the frequency range of the chosen horn antenna. The motive of this experiment was to increase the reading zone by using this horn antenna having a larger HPBW. The length of the antenna which is 28cm was taken as the dropping distance/ vertical distance of the tag and the tag response was measured using the VNA. The fall of the tag was tested under gravity. The change in the signal is visually identifiable from the VNA as it passes the antenna. Since the signal cannot be captured from the VNA as a snapshot at the right location the tag was fixed to a moveable plastic jig and the measurements were taken at different tag locations. The tag positioned at the middle of the antenna was taken as the reference point (0 cm) and the tag was moved vertically in positive and negative directions as shown in Figure 3.24.

The tag used for this experiment is the Hexagonal shape copper tag with a dimension of 8 x 8 cm shown in Figure 3.35. The results were taken at different positions from the middle level 0 cm, 2 cm, 4 cm, 6 cm and 8 cm distance. Looking at 4-bits in the 4-6 GHz range we can see the variation during the vertical movement.

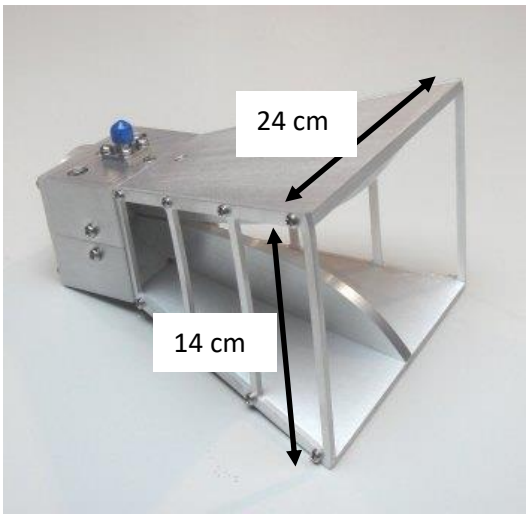

Figure 3.23 - Horn antenna with dimensions 24 x 14 cm and working in the frequency range of 0-18 GHz

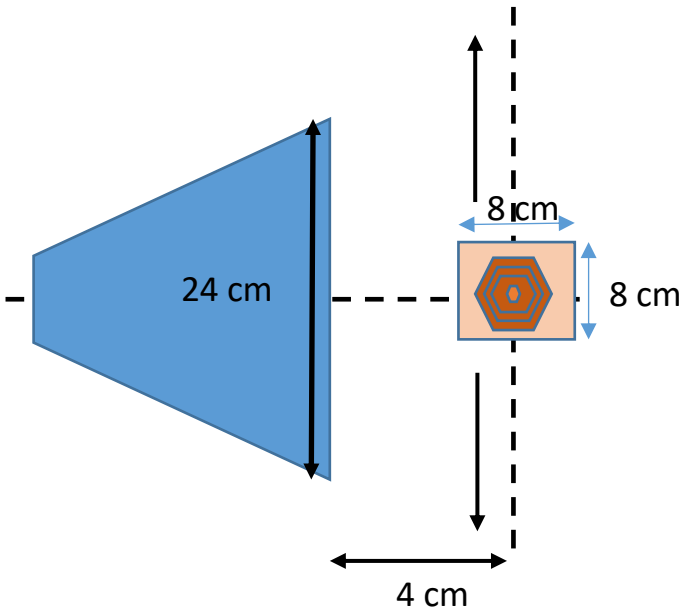

Figure 3.24 - Testing the tag response in step vertical motion using horn antenna and hexagonal tag

The antenna S11 and the background data including the stand for the tag vs. frequency is shown in Figure 3.25.

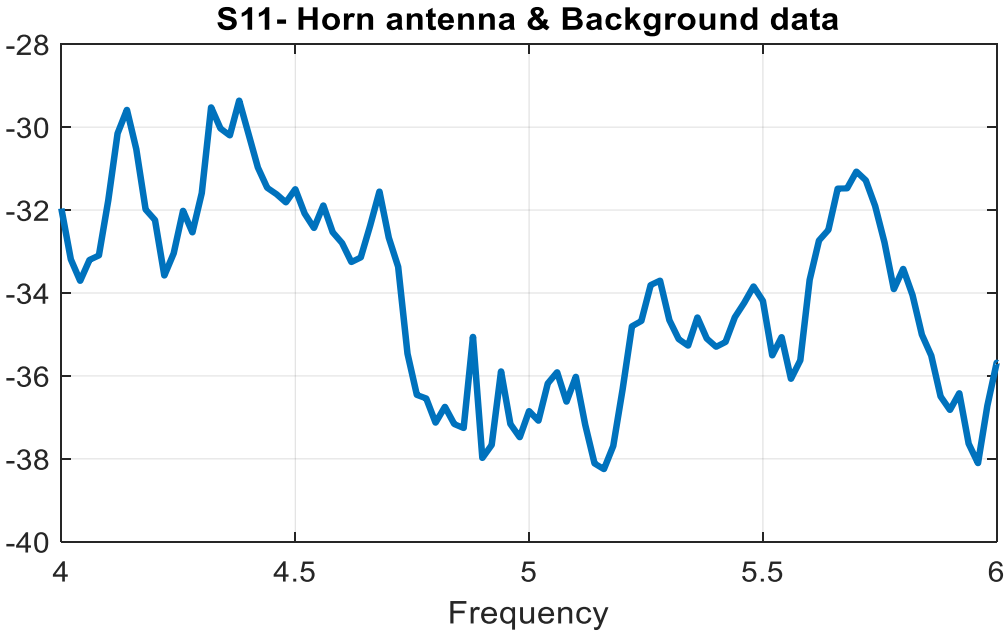

Figure 3.25 - Antenna and background S11

The tag response when the tag was held at the reference level of 0 cm is shown in Figure 3.26. According to Figure 3.26, the S11 magnitude level of the nulls have shifted from -30 dB level to approximately to -65 dB level with the movement. A frequency shift is also visible in the range of 200 MHz.

The phase change is also shown in Figure 3.27. The variations in magnitude and frequency are plotted in Figure 3.28. The blue vertical lines show the magnitude variation occurred during the movement at each bit positions and the horizontal red lines shows the frequency shift occurred at each resonance.

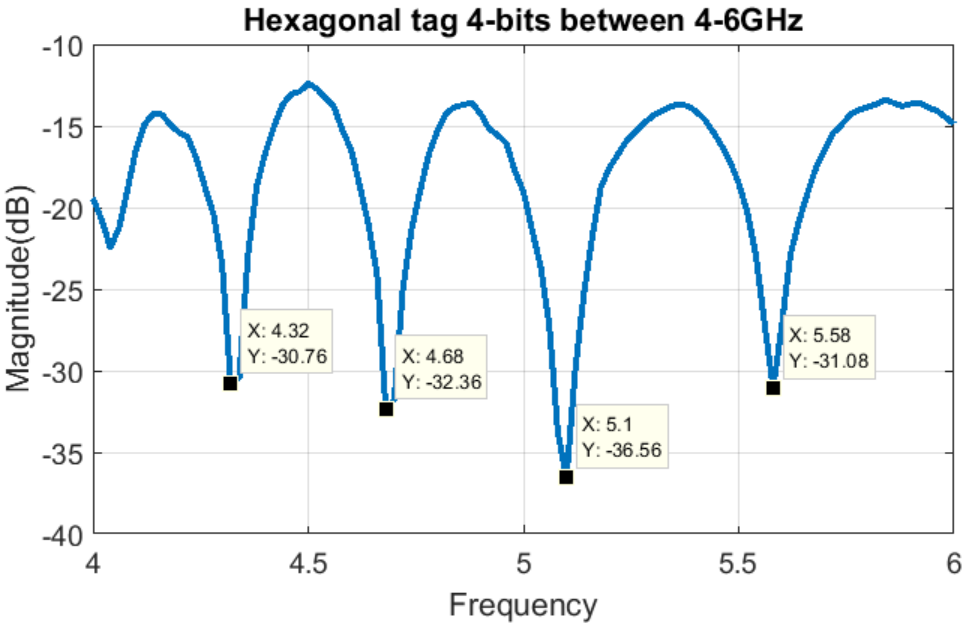

Figure 3.26 - The tag response at the reference level of 0cm, 4cm away from the phase centre of the antenna.

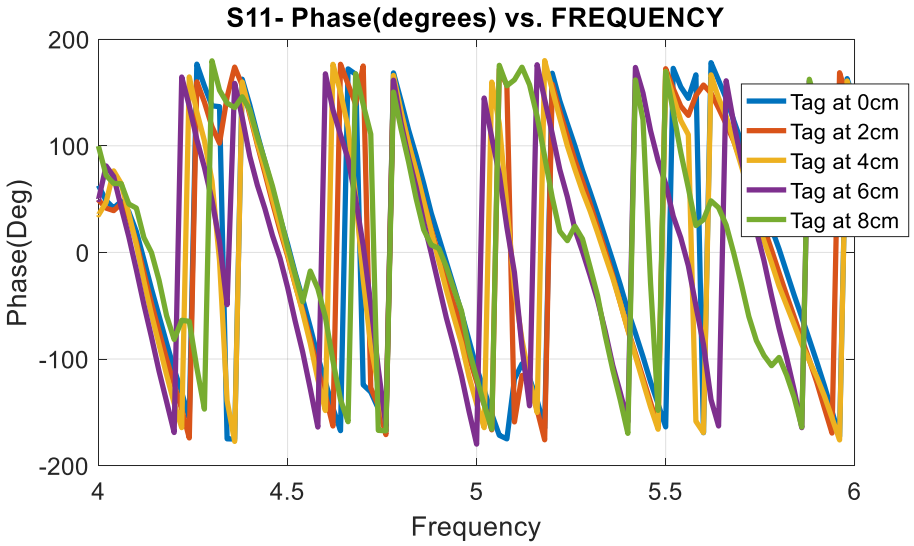

Figure 3.27 - Phase variation while the tag is in vertical motion

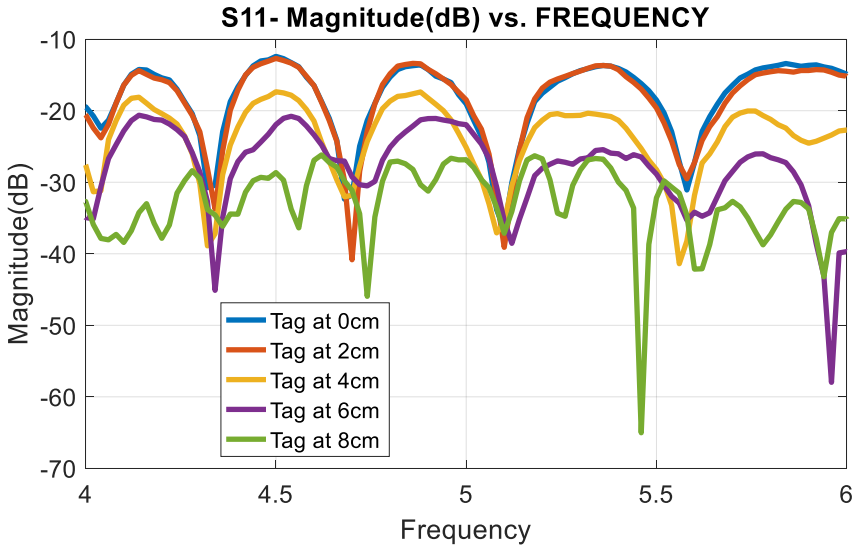

Figure 3.28 – S11 Magnitude in dB vs frequency for the tag movement from 0 to 8 cm

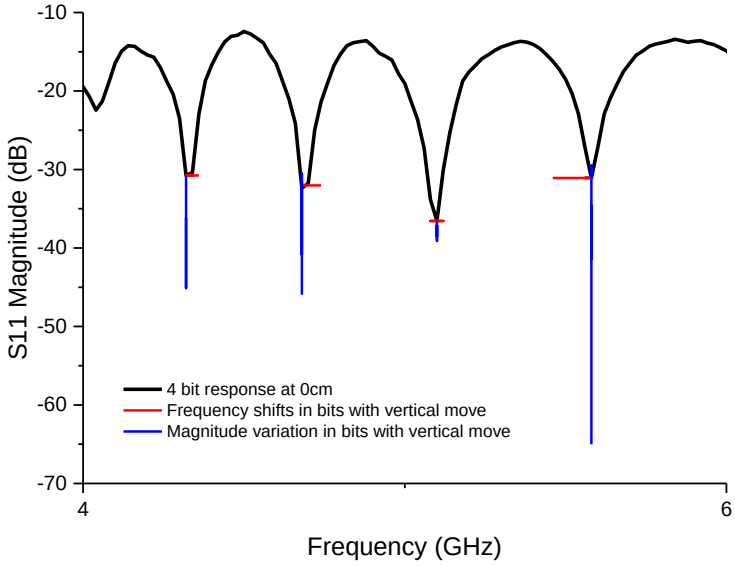

Figure 3.29 – The magnitude variation and the frequency shifts occurred at each resonance while the tag is in vertical motion from 0cm to 8cm.

The detection algorithm was applied on the results and Figure 3.30 shows the detected signals and the detected frequency ID for each position.

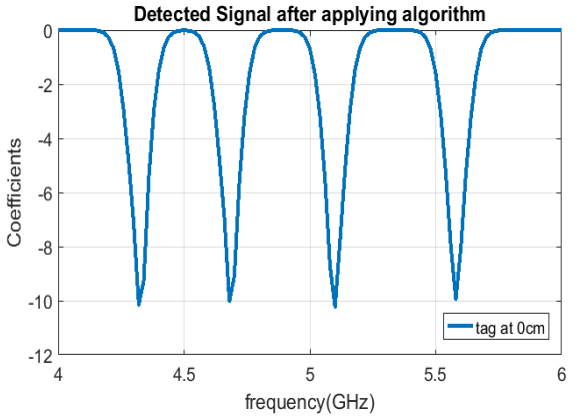

Coeff_nulls = -10.1521 -10.0305 -10.2372 -9.9457

Locs_nulls_GHz = 4.3400 4.7000 5.1000 5.5800

Freq_ID = 1111

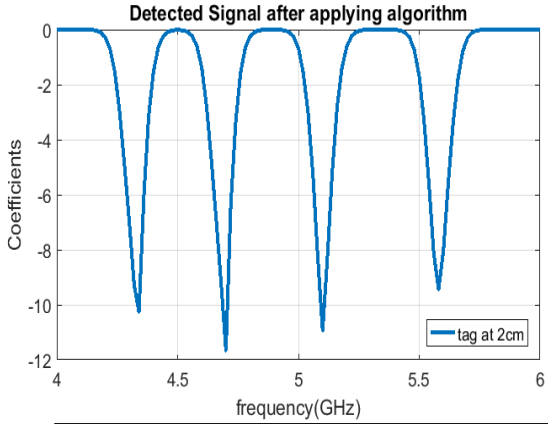

Coeff_nulls = -10.2646 -11.6670 -10.9484 -9.4468

Locs_nulls_GHz = 4.3400 4.7000 5.1000 5.5800

Freq_ID = 1111

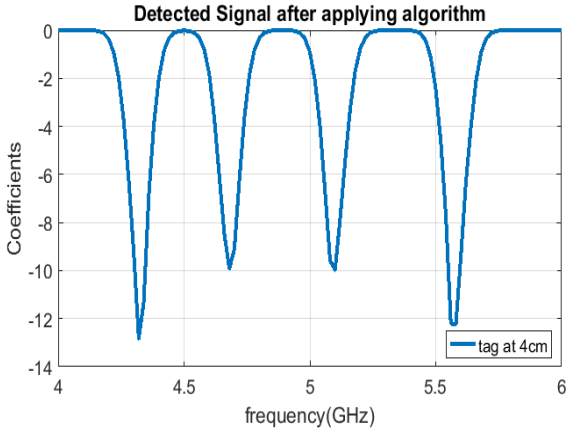

Coeff_nulls = -12.8355 -9.9276 -9.9736 -12.2294

Locs_nulls_GHz = 4.3400 4.7000 5.1000 5.5800

Freq_ID = 1111

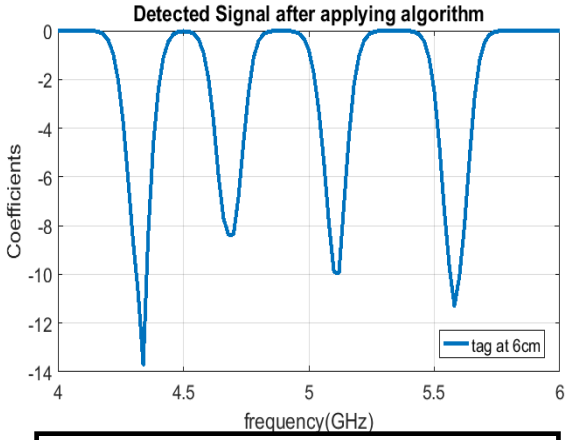

Coeff_nulls = -13.7198 -8.3830 -9.9452 -11.2959

Locs_nulls_GHz = 4.3400 4.7000 5.1000 5.5800

Freq_ID = 1111

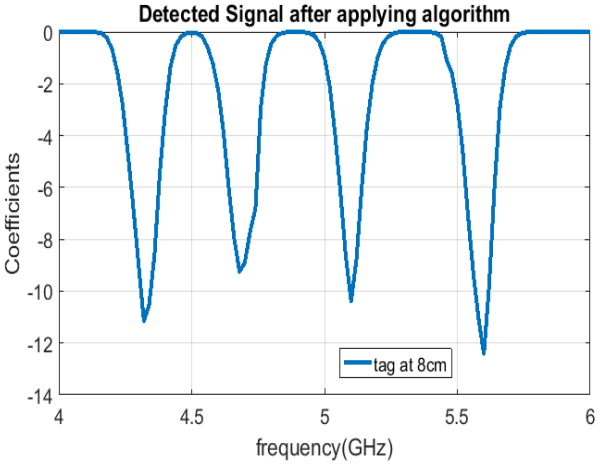

Coeff_nulls = -11.1613 -9.2448 -10.3982 -12.4285

Locs_nulls_GHz = 4.3400 4.7000 5.1000 5.5800

Freq_ID = 1111

Figure 3.30 – Detected signal after applying algorithm when the tag is at 0cm level

3.4 Conclusions

These experiments reveal an approach and method to detect the movement of a chipless RFID tag. It gives an exposure to the parameters that are affected by a moving chipless RFID tag and also gives an estimation to the robustness of its tag ID.

- The tag was vertically dropped under free gravitational acceleration and the change in the VNA signal was observed. During the fall the change in the signal is visually seen but holding the signal exactly at its best position is not possible using the VNA.
- Therefore, the tag response was measured in step motion by changing the height of the tag. The tag placed at the center of the antenna where the best result could be observed was taken as the reference level 0 cm. The vertical distance was then changed from 0 cm to 8 cm towards the ground.
- From the measured results a variation in the magnitude and a slight frequency shift can be observed.
- Applying the detection algorithm still the correct tag ID can be detected under these differences.

The S_{11} magnitude shifts show that given the predetermined magnitudes at the relevant resonant frequencies, a confident band for the determination of the frequency ID can be set using these results for a moving chipless RFID tag. Also, this leads to a research pathway for the improvement of the reading range which is essential as the variation in magnitude and phase increases as it moves beyond the beamwidth of the given antenna. The experiments also confirm that the frequencies stay mostly unperturbed thus giving the ability to detect the tag ID without much difficulty.

The comparison between the relative phases for numerical data and experiments data shows that without the effect of the phase due to backscattering and offset, the tag position can be distinguished. Using this data, the localization of the moving chipless RFID tag is made easy. It is clear that as seen the tag RCS is dependent on the distance and these experiments confirm that even when the chipless tag is in motion the tag location and its frequency ID can be detected.

4 Adaptive wavelet-based detection algorithm for Chipless RFID system

4.1 Introduction

The chipless RFID reader extracts the backscattered signal and decodes the tag ID. This is an ongoing challenge, as the detection procedure for a chipless RFID tag has more complexities compared to a conventional RFID tag. The signal collides with other scatterers or tags which give a ‘clutter' signal with interference. A number of detection techniques have been applied to achieve an accurate result of the tag ID.

The basic detection technique is based on comparing the received data with threshold values obtained by calibration. It is; therefore, a basic approach and it does not possess the flexibility and adaptability required in the detection process to address errors due to a dynamic environment. Different types of detection algorithms and decoding techniques have been revealed in the past few years.

Moving average technique is a simple de-noising technique which removes noises by acting as a low pass filter. An 11-sample averaging moving average filtering has been successfully implemented on a low-cost mid-range microcontroller having low processing power capabilities, and a smoothened waveform is resulted after using this filtering technique [17]. Hilbert transform (HT) is a complex analytical signal processing technique. This technique has been used to reconstruct the frequency signatures of the chipless tags. It has been experimentally proven that HT provides the extraction of the amplitude and phase functions of the frequency signature.

The signal space representation of chipless RFID tags uses an efficient mathematical model to decode information in a chipless RFID tag [18]. The frequency signatures are represented by a matrix which is composed of orthonormal column vectors and a singular value matrix. The constellation of signal points are plotted with a basis function. It can be seen that as the number of bits increase this method will face limitations. Matrix pencil method (MPM) and Short time matrix principle method (STMPM) [23] are

two more detection techniques that have been applied for chipless RFID systems. These two techniques are applied in the time domain and are mentioned as accurate detection techniques in extracting the carrier to noise ratio (CNR) of the response. Detection is performed by extracting the poles and residues from the backscattered signal using the Matrix Pencil Algorithm. A Maximum Likelihood (ML) based tag detection technique and Trellis decoding technique has been developed where detection error rate is compared with the bit to bit detection [27]. It has been found that ML detection has the best performance. It also reports that the computational complexity is higher in ML detection technique than Trellis detection technique.

The main aim of this chapter is to give a detailed explanation of the developed detection algorithm which can be practically applied in firmware. As many of the above algorithms are highly complexed in implementing in the chipless RFID reader. Also, most of them have the limitation in the number of bits that can be detected. In this work, we have developed a novel wavelet-based detection technique which suits the chipless RFID received signal to detect the frequency ID of the chipless RFID tag.

4.2 System model and design

In this section the system model of the chipless RFID system used in this analysis is discussed. A description of the backscattered signal is also given, and the backscattered signal of the used tag is analysed using simulation results obtained through CST microwave studio. The chipless RFID system is shown in Figure 4.1.

4.2.1 Experimental model

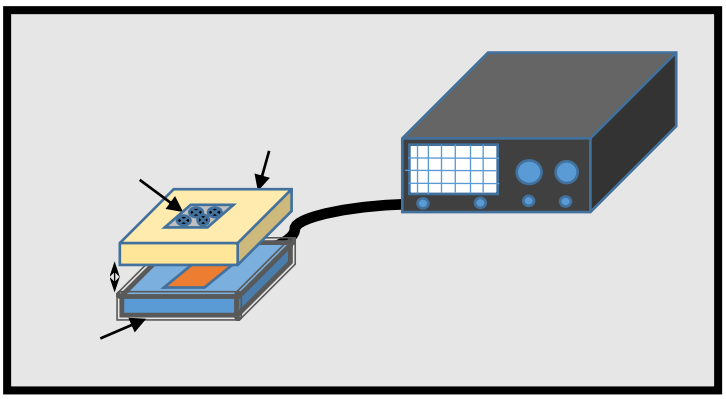

Figure 4.1 – Chipless RFID system

The experiment is performed using a 5-bit chipless RFID tag with spiral resonator design [5]. Each resonator has its own resonance frequency and has a diameter of 5mm. The tag with 5 bits has a dimension of 2 cm × 2 cm. The tag design is not presented in this paper to due to the confidentiality of the tag design. The tag RCS is shown in Figure 4.2. A patch antenna is used for the measurements, and the reading is taken by loading the antenna with a tag using vector network analyzer (VNA) as shown in Figure 4.1. The tag is loaded above the patch antenna and is placed on a piece of foam with 1cm thickness.

Backscattered signals from chipless RFID tags are very weak, and the detection process at the RFID reader is extremely susceptible to noise. This is because the information is represented as analog variations as opposed to a modulated digital stream of data as in conventional wireless communication of information where error correction schemes can be used to detect the presence of errors and discard erroneous data packets.

According to Figure 4.2, the resonant frequencies of the tag are located at 4.15, 4.70, 5.37, 6.10 and 6.95 GHz respectively. The other local maxima detected in the signal are due to the amplitude spectrum of the background and antenna S11 parameter in dB. These spurious peaks need to be carefully filtered out to detect the correct frequency signature of the chipless RFID tag.

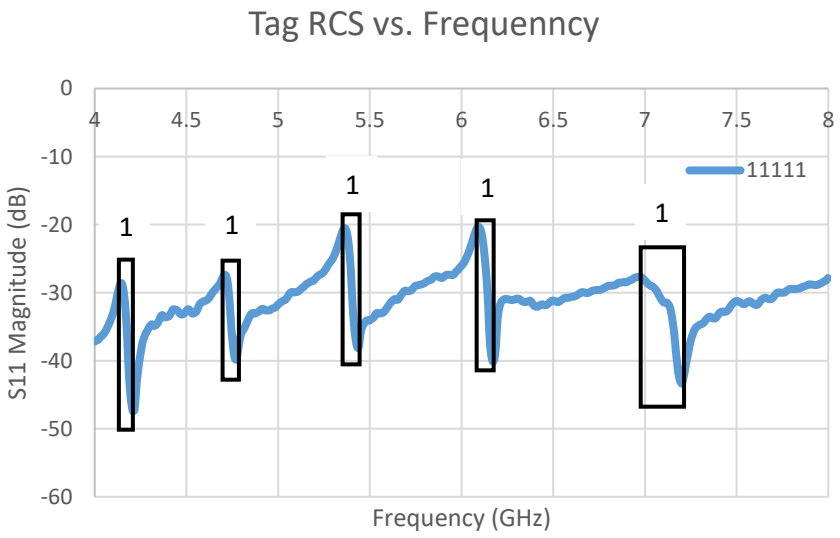

Figure 4.2 - S11 Magnitude (dB) vs. frequency of the 5-bit resonant tag

4.2.2 Wavelet design

In this study, a novel wavelet is adopted to detect the peaks of the backscattered signal. It is based on the Gaussian function which is given by equation (4.1).

$$f(x) = a \times e^{\frac{-(x-b)^2}{2c^2}} \tag{4.1}$$

where a is the height, b is the position and c is the width of the wavelet. The values a, b and c are adjusted to maximise the detection.

The novel wavelet design is shown in Figure 4.3. The width of the wavelet is adaptive according to the number of bits in the tag. In Figure 4.3, the width of the wavelet has been taken as 250 MHz giving a wider bandwidth to the wavelet. Further for the detection of the results this has been changed to 100 MHz giving better resolution of the detected bits. This is an advantage of this algorithm as higher number of bits can be detected with better resolution.

The detected signal is compared with the wavelet, and a coefficient is defined to represent how closely correlated the wavelet is with each part of the signal. The larger the coefficient is in absolute value, the more the similarity appears. The wavelet is shifted until it covers the whole signal bandwidth. The threshold coefficient is defined after performing the experiment for the tag with bit '11111' number of times under different environmental changes. By the variation in the detected signal under different circumstances a minimum and maximum coefficients are set giving rise to a 'confident band' for detection.

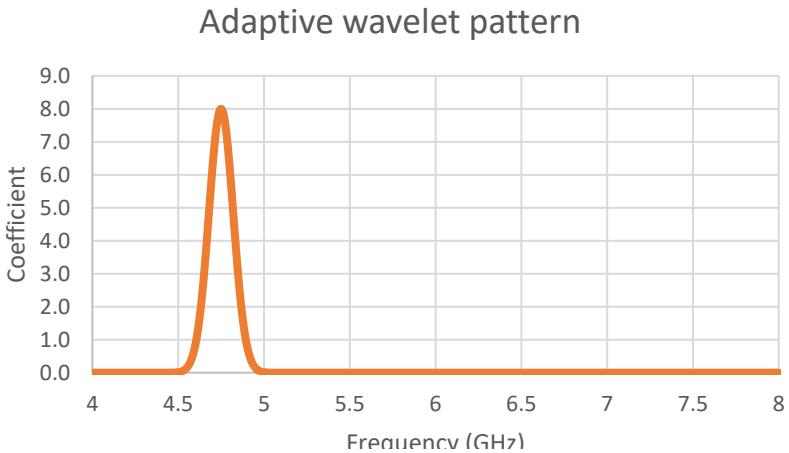

Figure 4.3 – Novel wavelet design

4.2.3 Flowchart for detection algorithm

The flowchart given in Figure 4.4, shows the steps of the developed algorithm and how it is applied to the received signal. First the measured results using VNA are loaded into Matlab. The post processing is performed using Matlab programming software. The program can be directly downloaded to the microcontroller of the frequency domain reader developed by the MMARS Laboratory which will be implemented in the next step of this research. A baseline removal is performed on the first results to remove the nulls of the antenna S11 parameter (in dB) vs frequency. Then the wavelet is defined and is integrated with the resulting signal. The tag ID is decoded based on the condition band defined for the detection.

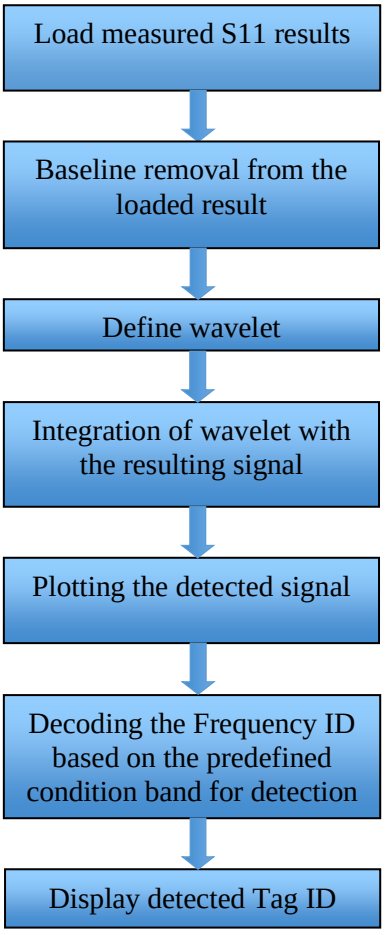

Figure 4.4 – Flowchart of the new detection algorithm

Experiments have been performed under different indoor dynamic environments such as placing clutter objects above the chipless RFID tag. Figure 4.5 shows the placing of hand 7 cm above covering the tag adding back reflection to the received signal. Similarly, a copper plate was also placed above the tag at 7 cm, and the received signal was observed using the VNA.

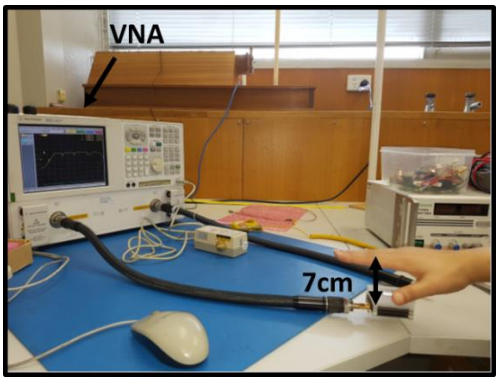

Figure 4.5 - Placing hand on top of the tag at 7 cm distance giving attenuation to the signal received at the VNA

4.3 Results

The measured results of the tag detection are shown in Figure 4.6.

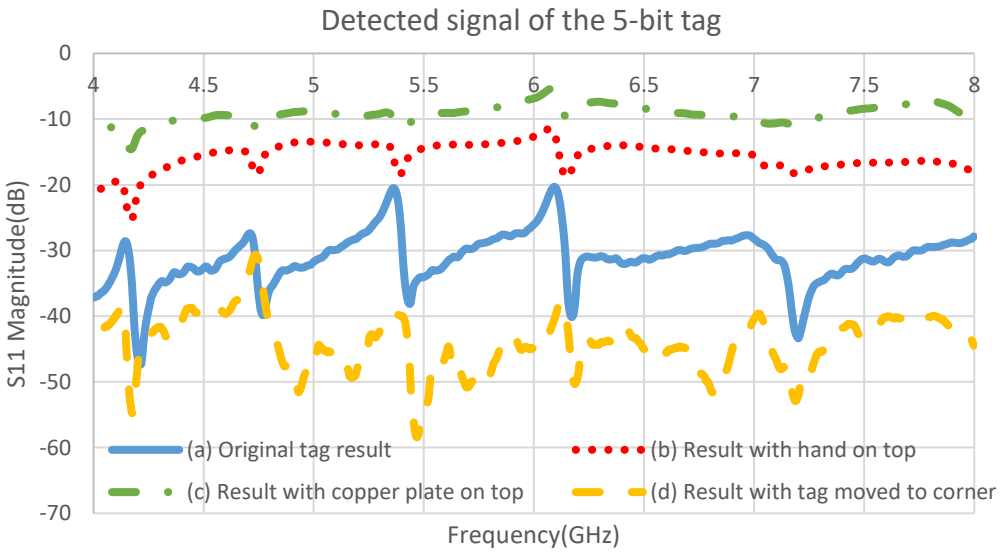

Figure 4.6 - Measured results (a) of the original tag at 1.5 cm above the patch antenna, (b) with hand placed above the tag at a distance of 7 cm, (c) with copper plate placed on top of the tag at a distance of 7 cm, (d) by placing the tag at the corner of the patch antenna.

It shows the received signals from the reader before applying the algorithm. In the original signal with the tag, we can identify the 5-bit resonances from the received signal itself. But when the hand, the copper plate is placed on top of the tag we can see that the received signal has increased in magnitude and has been shifted up. Also, peaks are not distinguishable at a glance. When the tag is placed in the corner of the antenna which implies the tag is moved out of the beamwidth of the antenna, we can again see a distortion in the signal as well as shifting the signal down in magnitude.

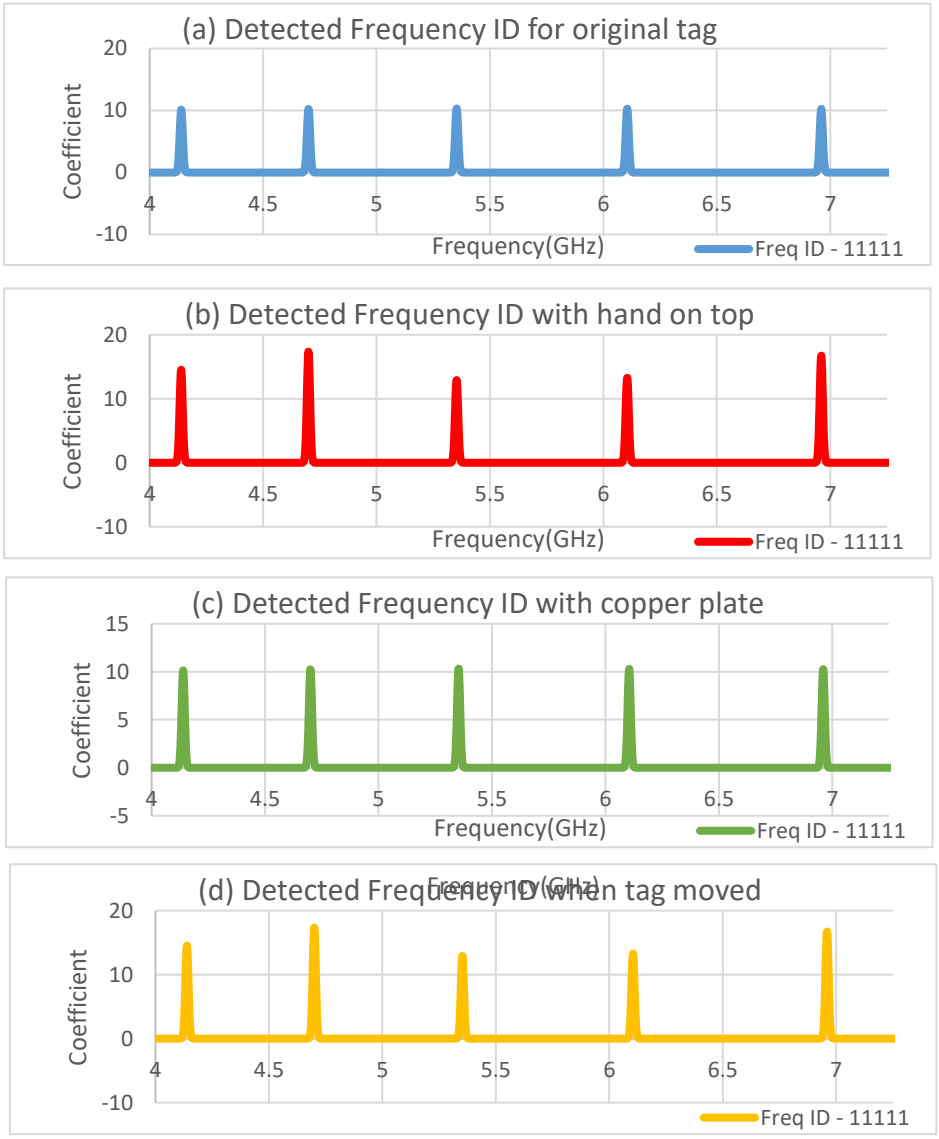

Figure 4.7 – Wavelet coefficients of the detected signals after applying the developed algorithm. (a) Original tag detection (b) Hand on top of tag (c) Copper plate on top of tag (d) Tag moved to the corner of antenna

4.4 Analysis

The detected signal after applying the wavelet decomposition detection algorithm is analysed in this section. The data is then interpreted to the end user. The results obtained after applying the developed wavelet-based detection algorithm is given in Figure 4.7.

The coefficients obtained are analysed in Table 4.1. The coefficients of the original tag are set to 10 which is taken as the threshold value of detection for the original tag with bits '11111'. A 'condition band' is set for the maximum and minimum detectable coefficient bands. For the chipless RFID tag used in this experiment, the 'condition band' is set between ±8, which gives +18 as the maximum value of detection as bit '1' and +2 as the minimum level of detection as bit '1'. If the coefficient is below or above these values, it will detect its ID as a bit '0'.

Table 4.1 – Wavelet coefficients for (a) Original tag detection – when the antenna is loaded with tag only (b) Hand on top of tag – when the hand is placed at 5cm distance above the tag (c) Copper plate on top of tag - when a copper plate of dimensions 10 × 10 × 0.2 mm is placed at 5 cm distance above the tag (d) Tag moved to the corner of antenna - when the tag is placed in the corner of the antenna

Resonance Freq. (GHz)	Original tag detection (Coefficient value)	Hand on top of tag	Copper plate on top of tag	Tag moved to corner of antenna
4.15	10.14	14.53	10.15	14.53
4.70	10.25	17.35	10.25	17.35
5.37	10.32	12.88	10.32	12.88
6.10	10.29	13.26	10.29	13.26
6.95	10.27	16.72	10.27	16.72

When the hand is placed, we can see that the coefficients are varying, and the maximum coefficient reaches 17.35. When the copper plate is placed, it reaches a maximum value of 10.32 and the tag moved

to the corner of the antenna gives a coefficient of 17.35. According to these results, the frequency ID of the tag is detectable as ‘11111' under all the applied conditions.

The frequency domain reader developed in MMARS lab uses the same patch antenna design for detection and is working in the frequency range of 4 – 7.5 GHz. Therefore, future direction of this research will be the implementation of the novel detection algorithm in firmware.

4.5 Conclusions

According to these results, it can be seen that a hand or conductive material (Cu) placed in the close vicinity of the tag (less than 10 cm) will have an effect on the magnitude of the tag measurement. Still applying the novel detection algorithm, the tag can be identified even if the conductive material is placed covering the tag. Also, when the tag is moved around the surface area covered by the antenna, the tag can be detected using this detection algorithm. Since the experiment was conducted by placing the clutter only on one side of the tag, more experiments should be performed by varying the position, size, material, etc. to conclude the probability of error due to the different material surrounding the tag.

An advantage of this detection algorithm is that it could detect up to a minimum of 1 dB magnitude variation with added noise. The adaptability of the wavelet is another advantage of this algorithm as it can be applied for any type of tag in the time domain or the frequency domain and could cover the required frequency range. Also, the detected bit resolution is high, which leaves room for the applications with higher number of bits in future.

When compared with other algorithms this has the most adaptability to any kind of chipless RFID system. Comparing the number of bits of a tag, the presented algorithm can be applied for higher number of bits whereas algorithms developed by Kalansuriya et al. [18], Rezaiesarlak et al. [20] and Divarathna et al. [27] are implemented for low number of bits due to their mathematical complexity. As the width of the wavelet used in the detection is only 10 MHz, with a guard band of another 10 MHz a 20-bit tag can be easily detected in the given frequency range of 4-8 GHz.

The algorithm can be adapted into a wider bandwidth of frequencies and can be applied for any other chipless tag design in the time or the frequency domain.

Most of the developed detection algorithms in this research area are tested only for simulation results or for measured results using a vector network analyser. Presently the algorithm has been programmed into the microcontroller of the chipless RFID reader [3] developed at MMARS Laboratory. Therefore, this tag detection algorithm can be used further to investigate the robustness of the chipless RFID reader system under a dynamic environment. A further study and comparison of the detection error rate applying this algorithm will be performed based on results. It can be concluded that the simplicity of this algorithm allows it to be implemented in firmware and can be further fine-tuned to give robust detection of the tag in a real environment of chipless RFID tag detection.

5 Chipless RFID tag detection with stepped movement using improved adaptive wavelet-based detection algorithm

5.1 Introduction

Chipless Radio Frequency Identification (RFID) technology is a new domain in RFID systems. It is currently at the stage of research and initial application. The chipless RFID technology can be widely applied in many areas including item level tagging and tracking, infrastructure monitoring, health monitoring and sensing, protecting food & drug counterfeiting, airline luggage tracking, animal identification, environment monitoring and inventory control [1]. This research presents a new aspect of the chipless RFID tag detection that is detecting and identification of the tag while it is in motion. Many item level tagging (e.g. product manufacturing, postal, baggage handling) applications will be using conveyor belts which will be on the move and the tagged items will need to be detected on the move. Moreover, animal identification and environment monitoring will also need their targets to be detected accurately while in motion.

The literature on chipped RFID tags shows the importance and demonstrates the localisation capability of moving tags [24]. The moving chipless RFID tag detection is therefore a novel approach which will help to complete the chipless RFID system and will give a broader marketing aspect to its applications. A number of detection techniques have been applied to achieve an accurate result of its tag ID. The basic detection technique is based on comparing the received data with threshold values obtained by calibration. It is therefore a basic approach and it does not possess the flexibility and adaptability required in the detection process to address errors due to a dynamic environment [1].

Moving average technique is a simple de-noising technique which removes noises by acting as a low pass filter. An 11-point moving average filtering has been successfully implemented on a low-cost mid-range microcontroller having low processing power capabilities, and a smoothened waveform is resulted after using this filtering technique [17]. A drawback of this detection method is that, the false

peaks and nulls cannot be eliminated in dynamic environment. Hilbert transform (HT) is a complex analytical signal processing technique [18]. This technique has been used to reconstruct the frequency signatures of the chipless tags. It has been experimentally proven that HT provides the extraction of the amplitude and phase functions of the frequency signature. Because of its complexity it is not practically applicable to the system.

The signal space representation of chipless RFID tags uses an efficient mathematical model to decode information in a chipless RFID tag [18]. The frequency signatures are represented by a matrix which is composed of orthonormal column vectors and a singular value matrix. The constellation of signal points are plotted with a basis function. It can be seen that as the number of bits increase this method will face limitations. Matrix pencil method (MPM) and Short time matrix principle method (STMPM) are two more detection techniques that have been applied for chipless RFID systems [23]. These two techniques are applied in the time domain and are mentioned as accurate detection techniques in extracting the carrier to noise ratio (CNR) of the response. Detection is performed by extracting the poles and residues from the backscattered signal using the Matrix Pencil Algorithm. A Maximum Likelihood (ML) based tag detection technique and Trellis decoding technique has been developed where detection error rate is compared with the bit to bit detection [27]. It has been found that ML detection has the best performance. It also reports that the computational complexity is higher in ML detection technique than Trellis detection technique. A notch detection algorithm using the energy detection has also been developed but has not been implemented in hardware [28].

All the above mentioned detection methods are performed on stationary tags but not much work can be found in literature performed on moving clipless RFID tags. Many of these algorithms are also highly complexed in implementing in the chipless RFID reader and face limitation in the number of bits that can be detected.

The main aim of this chapter is to apply the adaptive wavelet based detection algorithm on results obtained by the Vector Network Analyzer (VNA) to confirm the robust detection of a chipless RFID tag in motion. So that, it can be implemented and tested in hardware for a real-time chipless RFID system with tag on the move in planned future research.

This chapter is organised as follows. Section 2 presents the working principle of a chipless RFID system, the behaviour of a tag in motion, the reader antenna used in the experiment and the experimental setup. Section 3 presents the improved adaptive wavelet-based detection algorithm that has been used in detecting the tags in motion. Section 4 produces the measurement results and analysis of the results in a statistical point of view. Section 5 concludes this paper with future directions.

5.2 Chipless RFID system

5.2.1 Working principle of a chipless RFID tag

Figure 5.1 illustrates the operating principle of a backscattering chipless RFID tag. The chipless RFID reader interrogates the chipless RFID tag with an ultra-wide band (UWB) signal. The tag returns a backscattering signal of a very low amplitude with a data stream which is the identification data. A chipless RFID system is comprised of a chipless RFID tag reader and a chipless RFID tag as shown in the figure. The reader is complex microwave transceiver electronics. It comprises as an antenna and RF section, a digital section that controls the RF section that processes the backscattered signal from the tag, and a power supply unit to energise the digital RF sections.

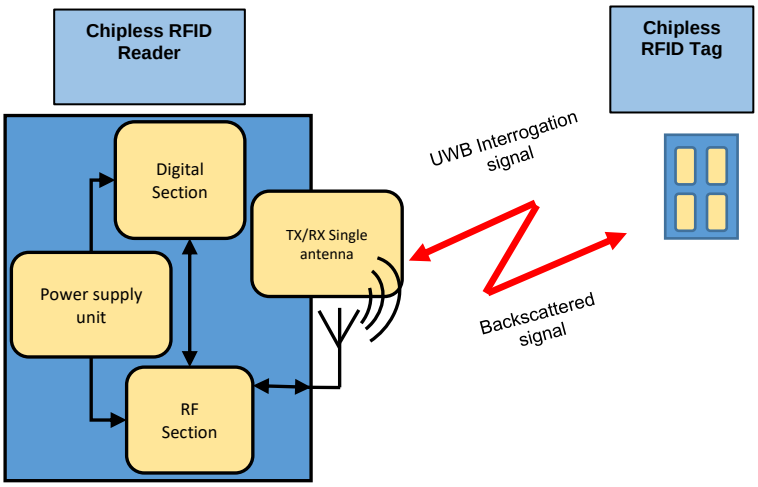

Figure 5.1 – Chipless RFID system with reader and tag

5.2.2 Chipless RFID tag in motion

In real time movement the tagged object can be moved in different directions as shown in Figure 5.2. A tagged object that is moving in horizontal motion is considered in these experiments. The geometrical and system parameters are considered in relative to a translational motion. The top view of the tagged object in horizontal motion under the influence of the 3 dB beamwidth of the reader antenna is illustrated in Figure 5.3.

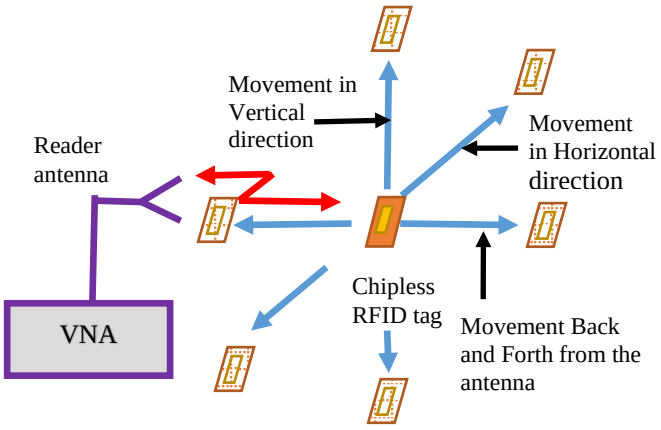

Figure 5.2 - Moving chipless RFID tag detection

The chipless tag on the object follows a straight line motion in direction ±*d*, of the object. The origin of the spatial coordinate ($d = 0$) is assumed to be coincident at minimum distance R_{min} from the reader antenna's phase center.

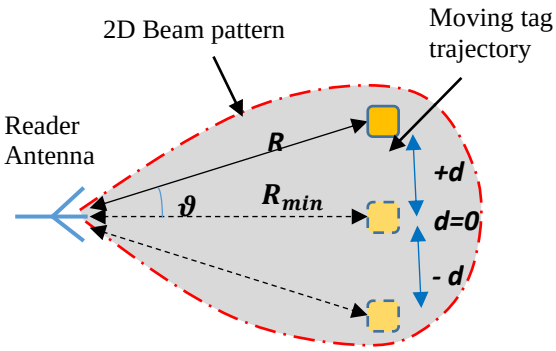

Figure 5.3 - Top view of the moving tag in reader antennas radiation pattern (zone)

where R_{min} - Minimum distance from reader to tag

R- Direct distance from reader to tag

±*d* - The horizontal distance from mid position

The direct distance (R) and phase angle (θ) can be given by,

$$R = \sqrt{d^2 + R_{min}^2} \tag{5.1}$$

$$\theta = \tan^{-1}\frac{d}{R_{min}} \tag{5.2}$$

The perpendicular distance between the reader antenna and the tag is kept constant at a given distance. The instantaneous measurements of the magnitude and the phase of the backscattered signal of the tag is measured at different positions using a VNA.

5.2.3 Reader antenna

A horn antenna is used as the reader antenna which shows an operational bandwidth of 7-14 GHz bandwidth. The measured radiation patterns of the horn antenna are at 8, 10 and 12 GHz shown in Figure 5.5. The half power beamwidth (HPBW) of the horn antenna is calculated as 40^0. The reflection loss (S11 in dB) vs frequency of the wideband horn antenna measured with a VNA from 8-12 GHz is shown in Figure 5.5. The 3 dB beamwidth of 40° and the minimum read distance of 30 cm provide a 3 dB look angle linear width of ±D = 30 cm × tan 20° = 10.9 cm.

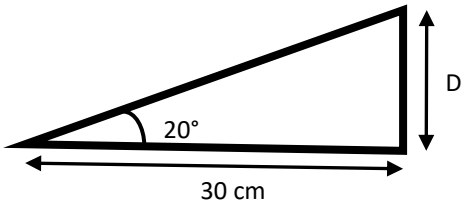

Figure 5.4 – 3 dB look angle

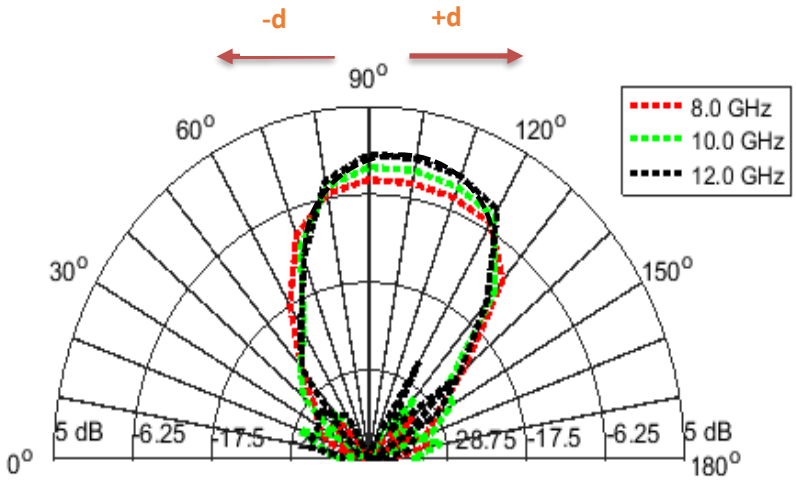

Figure 5.5 - Radiation pattern of the antenna measured in lab

The S11 in dB vs frequency of the antenna includes the background signal comprising of the cable/connector losses and the additive noise from the surrounding environment. The tag loaded S11 in dB measurement is obtained after subtracting the stored background signal which performs a vector subtraction in the VNA.

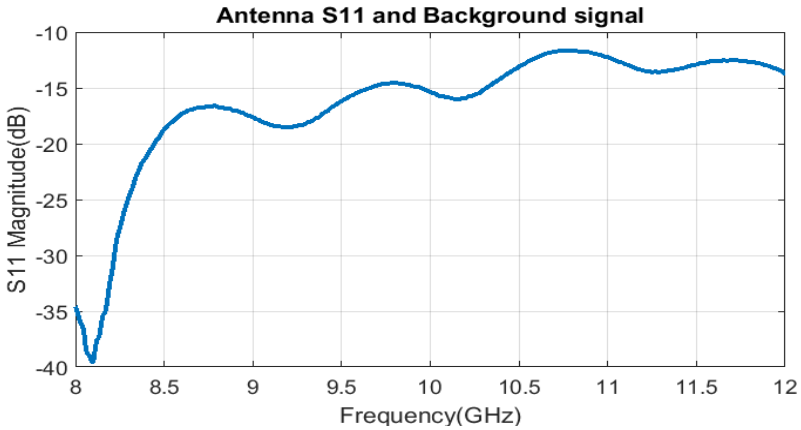

Figure 5.6 – S11 of the horn antenna used in experiment between 8-12GHz

5.2.4 Chipless RFID tag

A 4-bit rectangular patch resonant tag as shown in Figure 5.7 is used with the horn antenna in the experiment. The background subtracted S11 of the chipless RFID tag at d = 0 mm which is at its minimum distance (R_{min}) is shown in Figure 5.8. These are considered as the reference plots for the comparison with movement. According to Figure 5.8 the 4-bit resonant frequencies are 8.4, 9.4, 10.5 and 11.6 GHz respectively.

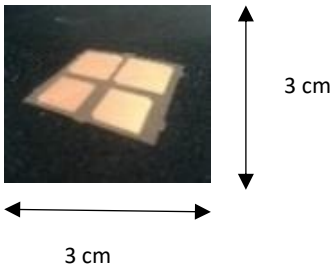

Figure 5.7 - Taconic 4-bit patch resonant tag

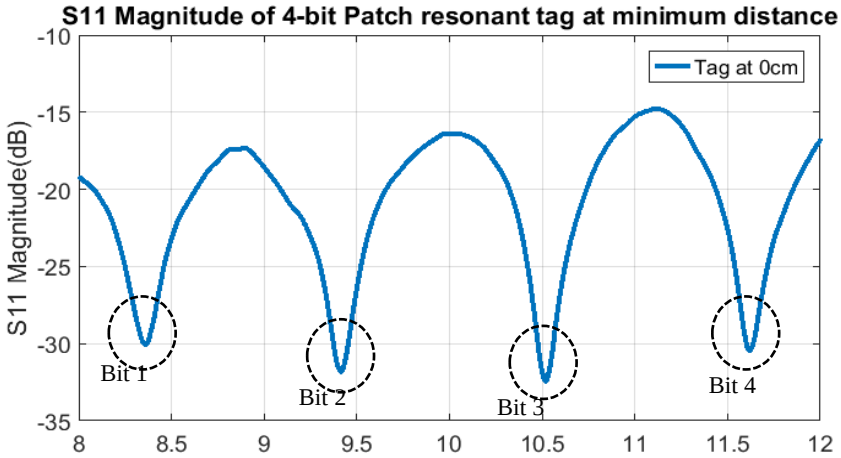

Figure 5.8 – S11 (dB) magnitude of the 4-bit patch resonant tag at its minimum distance. The resonant frequencies are located at 8.4, 9.4, 10.5 and 11.6 GHz

5.2.5 Experimental setup

The experimental set up for the horn antenna and the patch resonant tag in the MMARS lab environment is shown in Figure 5.9. The experiment is performed using the patch resonant tag on a moving jig and the horn antenna. The tag is placed 30 cm away from the phase centre of the antenna and is displaced within the HPBW of the antenna. The displacement of the tag is in 5 mm steps in positive and negative directions from the reference point at d = 0 mm. The frequency is varied between 8 – 12 GHz in this instance.

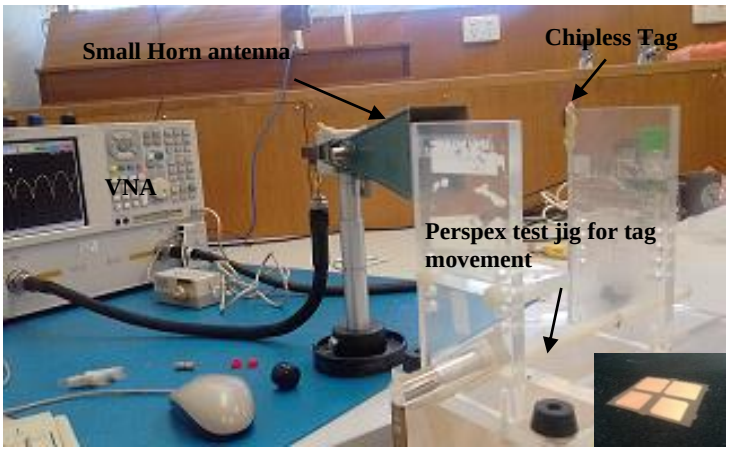

Figure 5.9– Experimental setup using horn antenna, 4-bit Taconic chipless RFID tag and VNA

The flowchart given in Figure 5.10 shows the procedure of the moving tag experiment. First the VNA is calibrated and then the horn antenna which is used as the reader antenna is connected. The S11 parameter which gives the background only data without the tag is then saved on the VNA. Next the tag is loaded and the S11 parameter data are collected at the different positions. In this experiment the tag is placed at 30 cm away from the phase centre of the antenna which is taken as the reference point. The tag is moved by varying the distance and all data are collected for post processing. Using the experimental model, the tag is moved in step motion. When using chipless RFID reader the capturing of data while the tag in motion will depend on the sampling time. Depending on the speed of the movement the number of capturing positions will differ. If it is very fast movement, we could capture only the data at few positions. But at lower speed the reader (VNA) will be able to capture data at several positions. So, the performed experiment was done at a low speed of 0.5 ms^{-1} where the recorded results are still visible from the VNA while in motion. The measured results with step movement will be equivalent to the results set that will be getting using the reader. In this experiment the distance is varied from +7 cm to -7 cm and the step size is 0.5 cm. Therefore, analysis of 30 data sets are shown in this work. In the following section the detection algorithm of the moving tag is presented.

5.3 Improved adaptive wavelet-based detection algorithm

The hypothesis of this work is that the adaptive wavelet-based detection algorithm detects the frequency ID of a chipless RFID tag while in motion. The algorithm has been tested and implemented in hardware [14]. The theory of an adaptive wavelet transform approach that has been applied on the detected signals is presented in this section.

Fourier Transform only gives what frequency components exist in a signal where the time and frequency information cannot be seen at the same time. Therefore time-frequency representation of the signal is useful for the detection of output signals. In equation 5.3, it shows the definition of continuous wavelet transform.

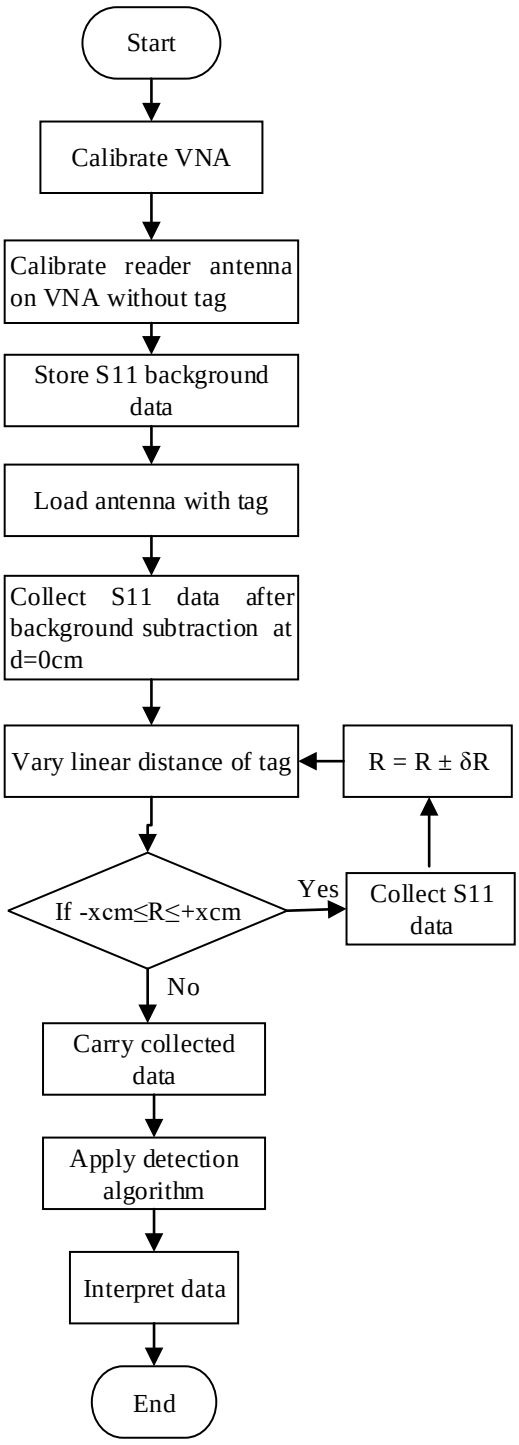

Figure 5.10 – Flowchart of the procedure for the moving tag experiment

$$CWT\ {}_{x}^{\psi}(\tau,\ s) = \Psi_{x}^{\psi}(\tau,\ s) = \frac{1}{\sqrt{|s|}} \int x(t).\ \psi^{*}\left(\frac{t-\tau}{s}\right) dt \tag{5.3}$$

where, CWT – Function of the Transformed signal, Ψ – Function of the Mother wavelet
x (t) – Signal,τ – Translation and s – Scaling

As seen in the above equation, the transformed signal is a function of two variables, tau (τ) and s, the translation and scale parameters, respectively. The translation is the location of the window as the window is shifted through the signal and the scale gives detailed information of the hidden pattern. $\psi(t)$ is the transforming function and is called the mother wavelet. The mother wavelet is a prototype for generating the other window functions. The different mother wavelets such as Morlet, Haar, Daubeshis and Symlet available in Matlab platform were tested against the tag response to detect the correct identification. Figure 5.11 gives a visualization of the continuous wavelet transform algorithm. In this example, a Morlet wavelet is considered as the mother wavelet *ψ(t)* and it is integrated with the original backscattered signal *x(t)*. The wavelet simply acts as a matching filter and calculates a coefficient which shows the correlation between the two signals. Here, in the first window of its last figure, it shows C = 0.0102. If the two signals are closely matched it would give a value close to 1. The wavelet is moved through the whole signal continuously in its integration till the end of the signal.

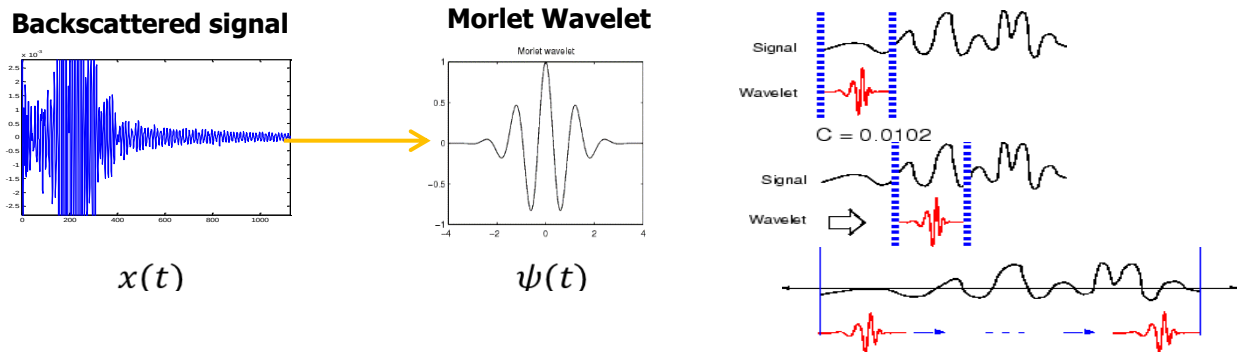

Figure 5.11 - Integration of morlet wavelet with the backscattered signal

The results show that it misleads the detection when there are spurious peaks in the signal due to added noise. A novel wavelet design was proposed to overcome this drawback taking into account the variations occurred due to the tag motion. Further detection conditions for decoding the ID was defined using the experimental results under different environments.

The mother wavelet is based on the Morlet wavelet which is a modulated Gaussian function and is given by equation 5.4.

$$f(x) = a \times e^{\frac{-(x-b)^2}{2c^2}} \quad (5.4)$$

where *a* is the height, *b* is the position and *c* is the width of the wavelet. The values *a*, *b* and *c* are adjusted to maximise the detection.

The wavelet design is shown in Figure 5.12. The width of the wavelet is adaptive according to the number of bits in the tag. In Figure 5.13, the width of the wavelet has been taken as 250 MHz giving a wider bandwidth to the wavelet. Further for the detection of the results this has been changed to 100 MHz giving better resolution of the detected bits. This is an advantage of this algorithm as higher number of bits can be detected with better resolution. This allows the algorithm to be applied for the detection of chipless RFID tags with more than 20-bits within a frequency range of 4 GHz. The amplitude variation is allowed within a predefined prediction band and for the decoding of the ID the wavelet coefficient should fall within the confident band as shown in Figure 5.13 to determine it as a bit '1'. Figure 5.14 shows the detection conditions set for the decoding of the ID and the analysis is given in Section V. The algorithm is adaptive to any frequency range in the UWB range frequencies.

The detected signal is compared with the mother wavelet, and a coefficient is defined to represent how closely it is correlated with each part of the signal to the wavelet.

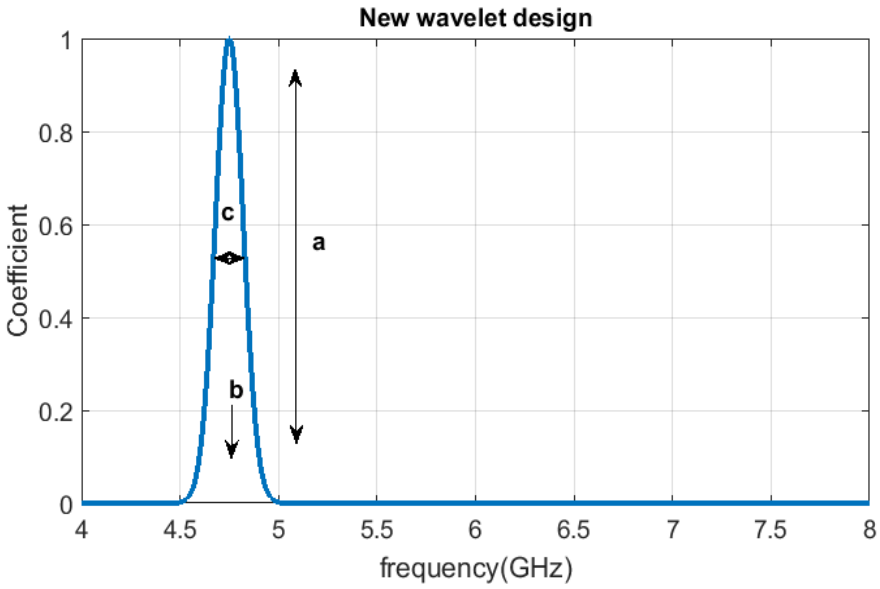

Figure 5.12– Adaptive mother wavelet

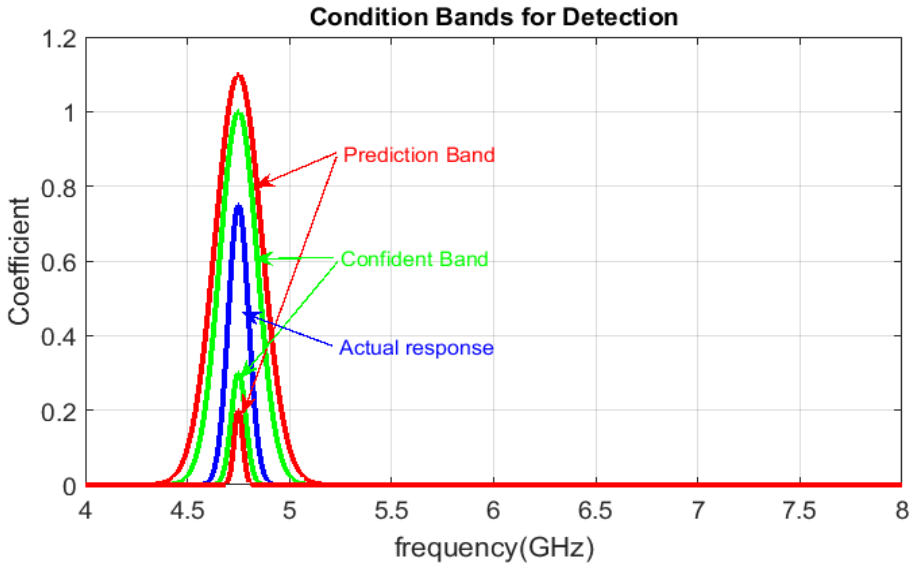

Figure 5.13 - Condition band set for the decoding of the frequency ID

The wavelet is shifted until it covers the whole signal spectrum. The reference level coefficient (r) is defined after performing the experiment for the tag with the data bit '1111' number of times under different environmental changes. By the variation in the detected signal under different circumstances, a minimum (x) and a maximum (y) coefficient is set giving rise to a condition (confident) band for detection. A general scenario of this condition bands is shown in Figure 5.13.

The flowchart given in Figure 5.14, shows the steps of the developed algorithm and how it is applied to the received signal. The S11 measured results are loaded into Matlab. A baseline removal is performed to the data to bring the nulls or peaks to the zero level. Then the mother wavelet is defined according to the tag's original resonant frequencies. Next the wavelet is integrated with the resulting signal, this eliminates unwanted peaks or nulls of the signal and detects the presence of the desired nulls or peaks at the correct frequency. By changing the height of the mother wavelet to negative and positive this algorithm can be adapted to different types of chipless RFID tags which recognised its tag ID as nulls or peaks. The peak or null positions are detected by scanning the detected signal for maxima or minima. The detected values are saved for decoding the tag ID. The frequency ID is then determined by checking against the 'condition band' values. If the stored coefficient value falls within the 'condition band', it is determined as a Bit '1' or if it is out of the band it is determined as a Bit '0'. Finally, the detected frequency ID is displayed.

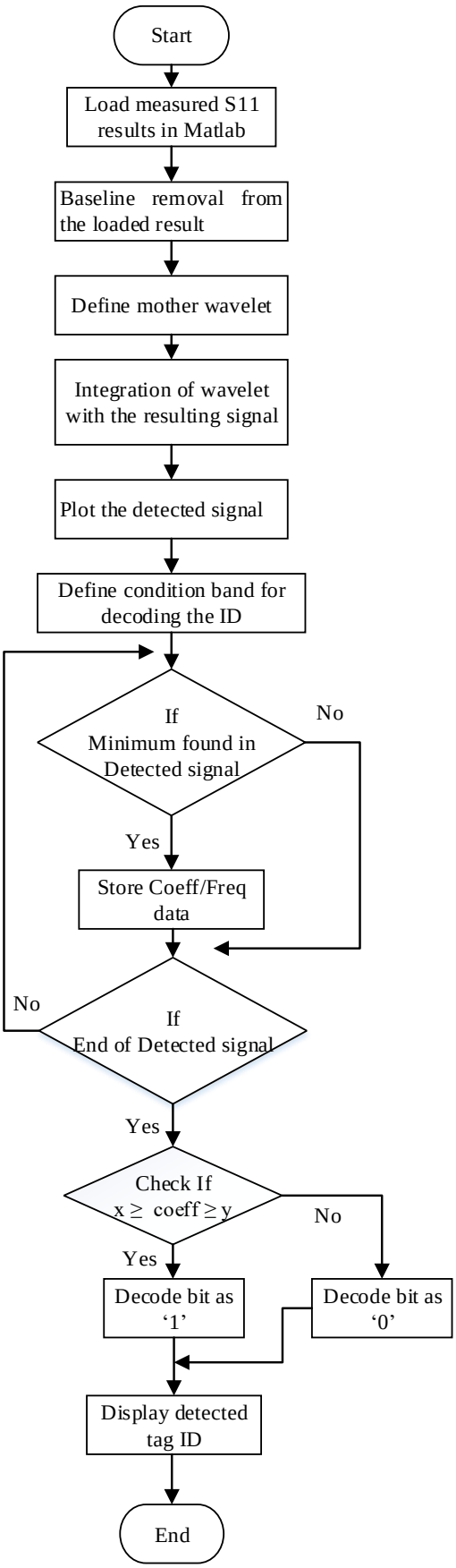

Figure 5.14 – Flowchart for detection

5.4 Measurement results and analysis

By performing the experiment explained in Section 5.3 the measured data were stored using the VNA. The data is processed in Matlab using the procedure as shown in the flowchart in Figure 5.14. The plotted results in Matlab are shown in Figure 5.15 and 5.16. This shows the variation in the magnitude of S_{11} while the chipless RFID tag is in motion. The results obtained in Figure 5.15 are while the tag is moved in the positive direction (+d cm) from 0 to +7 cm in 0.5 cm steps. In this direction the amplitude gradually changes, and a small frequency shift is also visible. In Figure 5.16 the tag is moved in the negative direction (-d cm) from 0 cm mid position to -7 cm in 0.5 cm steps. The magnitude variation is more significant in this direction and beyond -3 cm the resonances are highly disturbed and not visible.

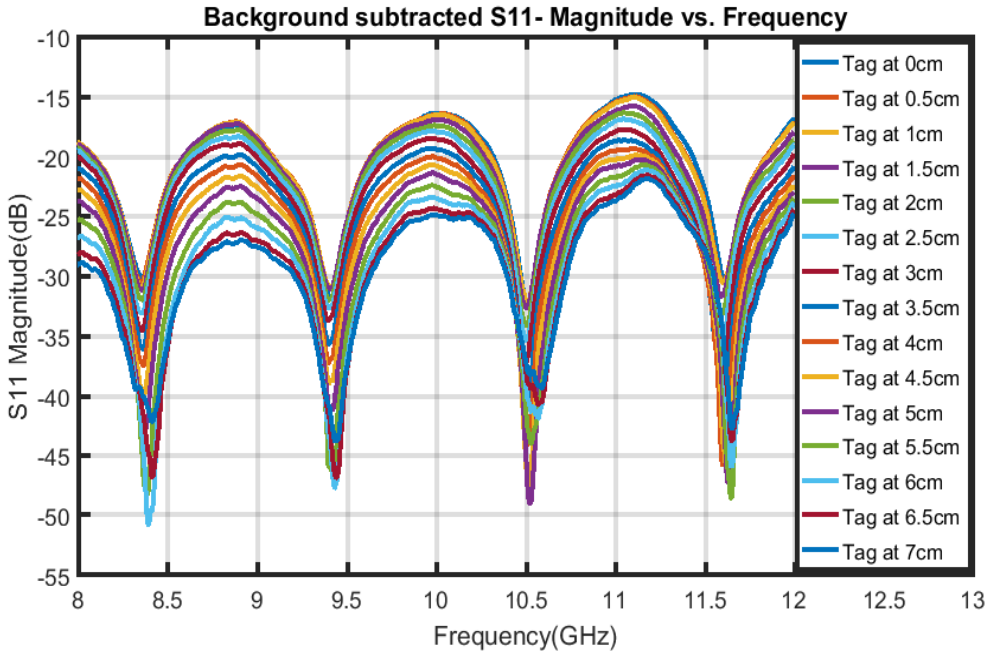

Figure 5.15 - Background subtracted S11 Magnitude (in dB) vs. Frequency (in GHz) while the tag is moved in the positive direction (+d) from 0cm mid position to +7 cm by varying the distance in 0.5 cm steps

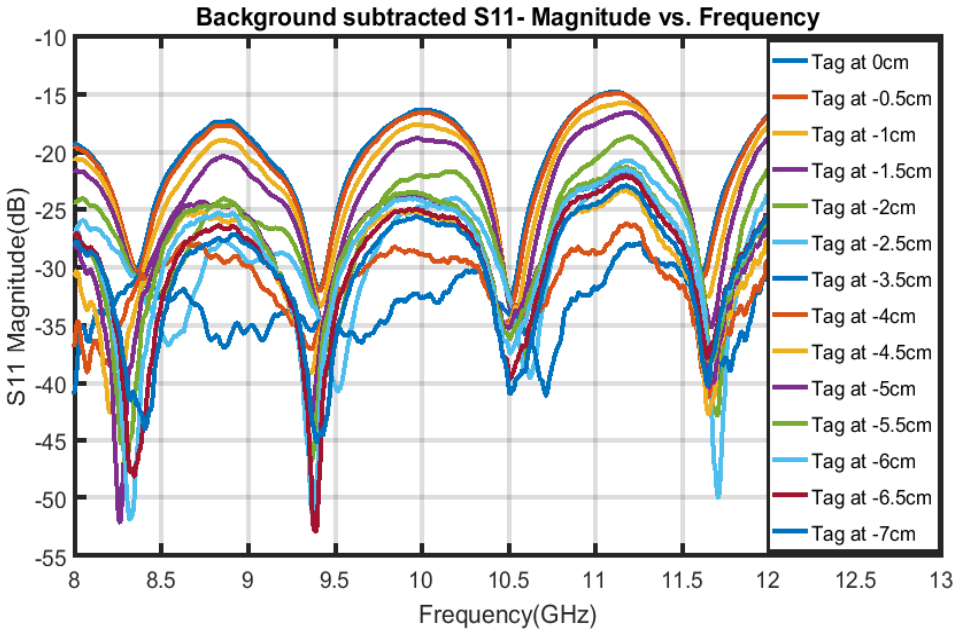

Figure 5.16 - Background subtracted S11 Magnitude (in dB) vs. Frequency (in GHz) while the tag is moved in the negative direction (-d) from 0cm mid position to -7cm by varying the distance in 0.5cm steps

The magnitude variation and the frequency shifts at each position from -7 to +7 cm are plotted in Figures 5.15 and 5.16. In Figure 5.17 it can be seen that the magnitude variation ranges from 1 to -21 dB. The variation in the positive direction is similar for all 4 bits. But the variation is more significant when it passes +5 cm position, which is when the tag moves out of the beamwidth of the antenna. In the negative direction the higher frequency bits show less variation compared to Bit 1.

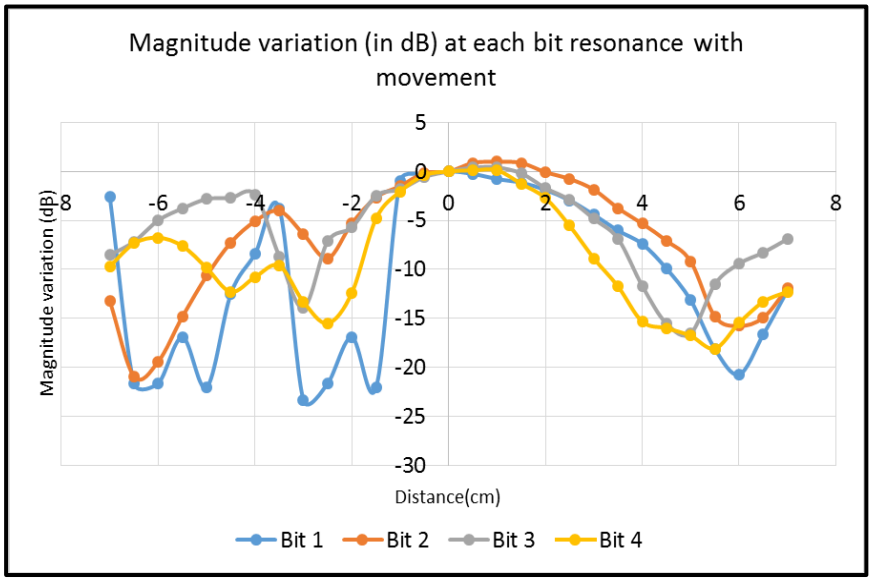

Figure 5.17 – Magnitude variation at each bit resonance with movement in dB relative to the result when the tag is in mid position at d=0cm

In the negative direction the variations occur at a closer distance of -3.5 cm. Since the beam pattern of the horn antenna is not symmetric around d = 0 cm the variation in the measured S11 results is also not symmetric in both positive and negative directions. According to the results the signal starts getting distorted when the tag moves partly or completely out of the antennas radiation pattern.

The frequency shift in GHz at each bit resonance with movement is shown in Figure 5.18. In the positive direction the frequency shift ranges between -50 and +75 MHz. In the negative direction it varies between -200 and +200 MHz. Compared to the magnitude variation the variation in frequency is negligible. The variation in both magnitude and frequency are plotted in Figure 5.19 at each bit resonance. The amplitude varies from 20- 25 dB as shown in the figure. This may be due to the interference and cluttered environment as shown in the experimental set up in Figure 5.8. The edge diffraction from the 2nd perplex jig and nearby reflecting surface may be the cause of the asymmetric results. Note the jig is not adjusted for better and symmetric results to test the robustness of the proposed detection algorithm.

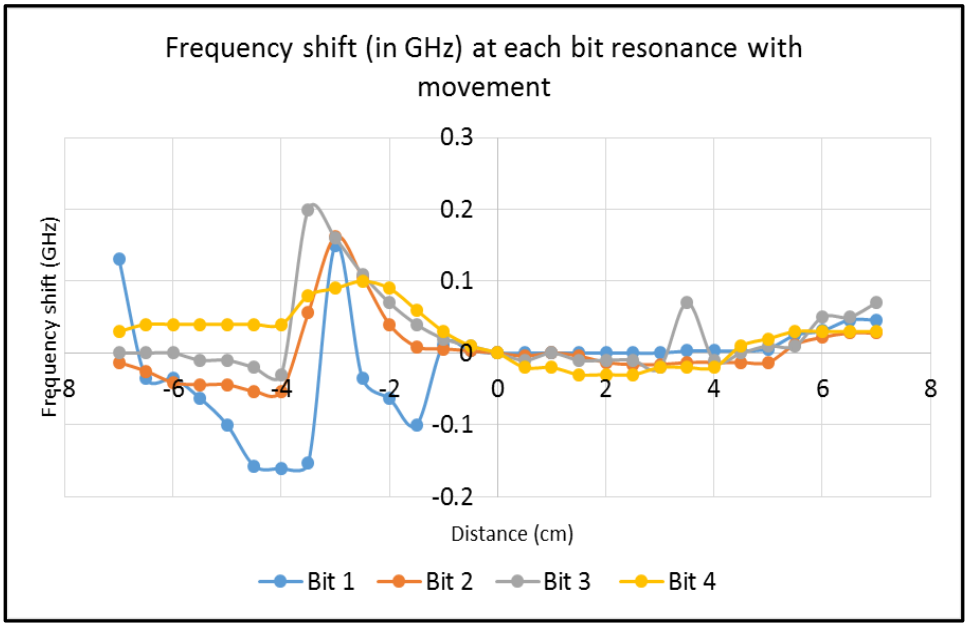

Figure 5.18 – Frequency shift at each bit resonance with movement of the tag in both positive and negative directions

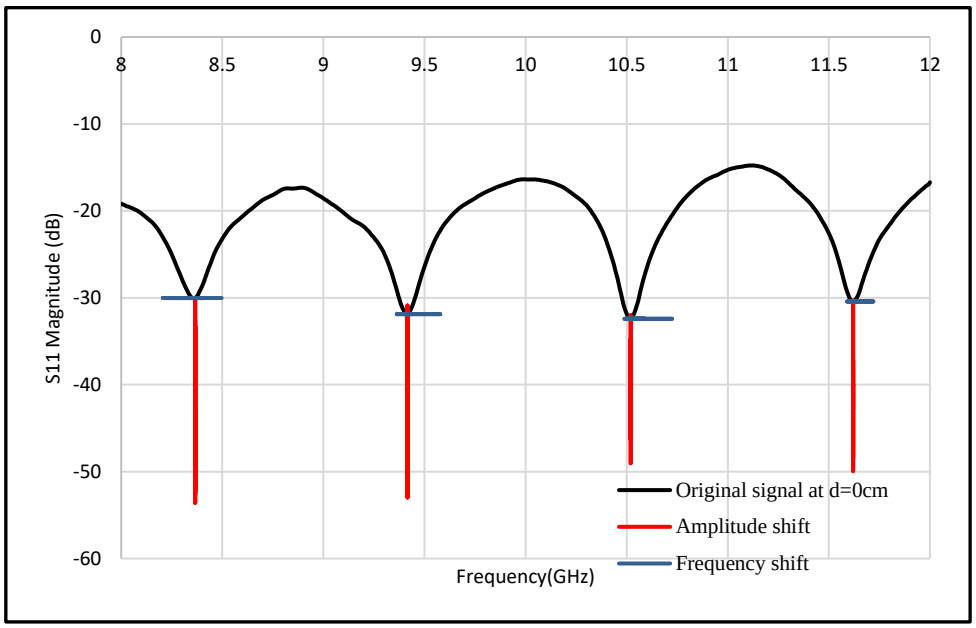

Figure 5.19 - The variation in both amplitude and frequency at each bit resonance in both positive and negative directions

The detection algorithm is applied on the results obtained. Figures 5.20, 5.21 and 5.22 show the detected signals after applying the adaptive wavelet detection algorithm at d = 0, +7 and -7 cm respectively. The variation in its coefficient from the reference level after detection can be seen in Figures 5.18 and 5.19 at the further most positions at +7 and -7 cm. The decoding of the frequency ID is performed using the predefined condition band for the wavelet.

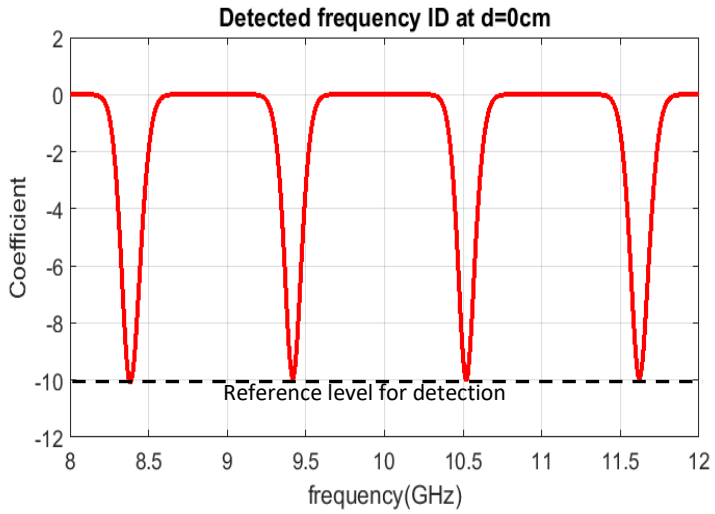

Figure 5.20 - Detected frequency ID at 0cm

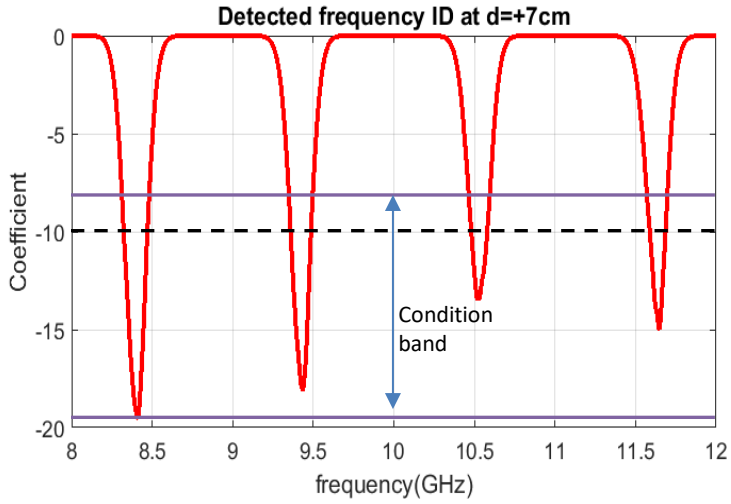

Figure 5.21 – Detected frequency ID at +7cm

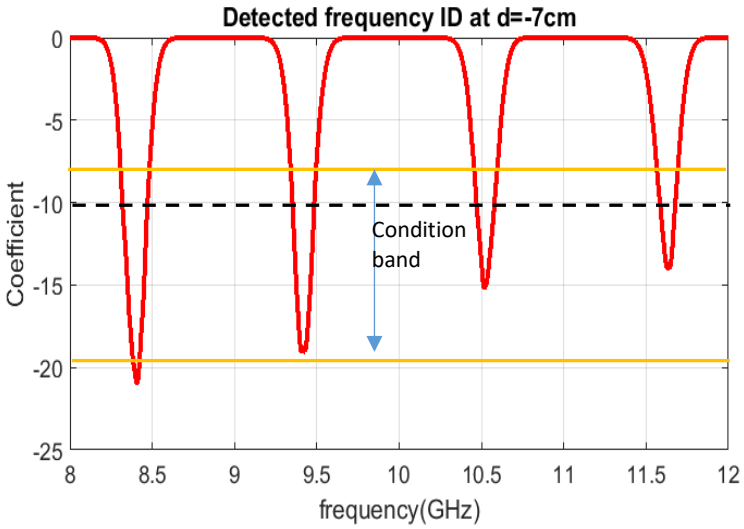

Figure 5.22 – Detected frequency ID at -7cm

As shown in Figure 5.20 for the tag in its best position (at d = 0 cm) the detected signal has been set to a reference level coefficient of -10 for all the bits. Based on previous experimental results with movement and different environmental conditions the condition band is set between -20 and -8 as marked in Figures 5.21 and 5.22. Therefore, the coefficient values lying between the condition band is decoded as Bit '1' and the coefficients out of the range are considered as Bit '0'. The frequency ID detected for the tag at d = 0 cm is '1111', for the tag at d = +7 cm is '1111' and for the tag at d = -7 cm is '0111'. A one-bit error is occurred when the tag is at -7 cm. The detected Frequency ID and the coefficient variation from the reference level -10 is shown in Table 5.1.

Table 5.1 – Detected tag ID and wavelet Coefficients

Distance	Bit1-var	Bit2-var	Bit3-var	Bit4-var	Freq. ID
-7	-10.87	-9.04	-9.08	-4.02	0111
-6.5	-11.78	-13.97	-4.38	-2.91	0011
-6	-9.68	-10.23	-11.14	-2.5	1001
-5.5	-4.78	-5.85	-7.52	-2.87	1111
-5	-3.09	-5.04	-1.65	-3.8	1111
-4.5	-1.78	-1.75	-1.73	-4.88	1111
-4	-0.91	-1.43	-2.47	-4.39	1111
-3.5	-1.54	-2.03	-2.09	-3.35	1111
-3	-2.4	-3.09	-0.76	-2.62	1111
-2.5	-2.65	-3.35	-0.53	-1.77	1111
-2	-2.43	-3.14	-0.87	-1.58	1111
-1.5	-1.52	-1.96	-1.01	-1.02	1111
-1	-1.1	-1.13	-0.97	-0.7	1111
-0.5	-0.48	-0.17	-0.35	-0.2	1111
0	0	0	0	0	1111
0.5	-0.01	0.56	0.15	0.13	1111
1	-0.35	0.67	0.22	0.06	1111
1.5	-0.67	0.57	0.01	-0.38	1111
2	-1.15	-0.04	-0.87	-1.08	1111
2.5	-1.84	-0.49	-1.58	-2.33	1111
3	-2.82	-1.13	-2.66	-3.85	1111
3.5	-4.12	-2.54	-5.17	-5.62	1111
4	-5.02	-3.64	-7.04	-7.69	1111
4.5	-6.92	-4.99	-9.47	-8.07	1111
5	-9.54	-6.71	-10	-8.37	1111
5.5	-14.05	-10.59	-6.85	-7.96	0111
6	-16.17	-10.92	-5.23	-6.57	0011
6.5	-12.74	-10.11	-4.13	-5.52	0011
7	-9.41	-8.12	-3.45	-3.51	1111

The accuracy of the tag ID detection is higher between -5 cm to +5 cm. The detectability can be reduced in the further ends of the beamwidth due to less radiation power of the antenna resulting less accuracy. As seen from Table 5.1, at the distance of -7 cm the Bit-1 coefficient variation is -10.87. This is beyond the minimum level of detection of the condition band. Therefore, it is detected as bit '0'. At the distance of +6.5 cm the Bit-1 and Bit-2 coefficient variations are -12.74 and -10.11 respectively. Both values are out of the condition band and are detected as bit '0's.

According to the above results Figure 5.23 shows the variation in its calculated wavelet coefficients for Bit 2. The coefficient values vary from 1 to -17 as shown in the figure. The mean and the standard deviations are calculated for the results and are plotted in Figure 5.24. The dashed lines show one standard deviation around its mean. This shows that 80% of the data can be detected without any error using this algorithm even while the tag is in motion.

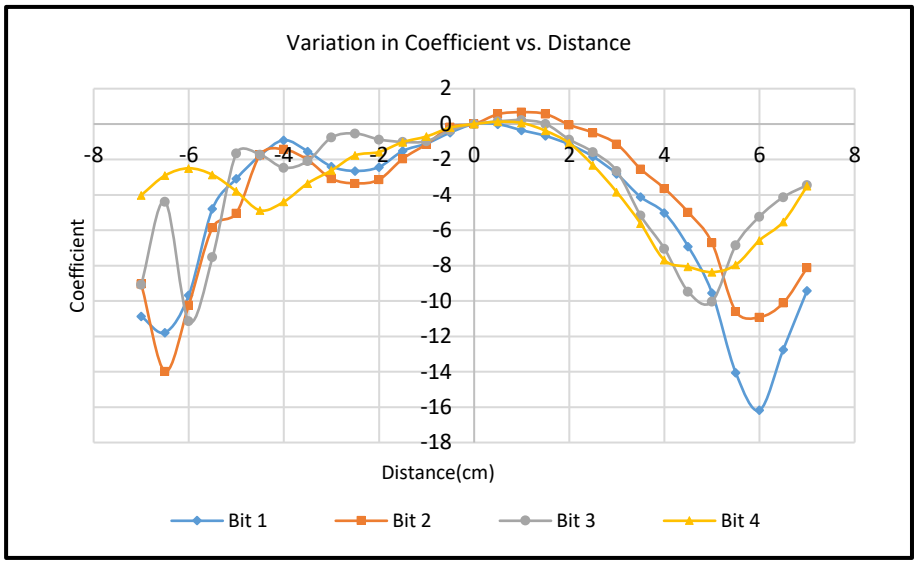

Figure 5.23 – Variation in calculated wavelet coefficient for each bit resonance with distance

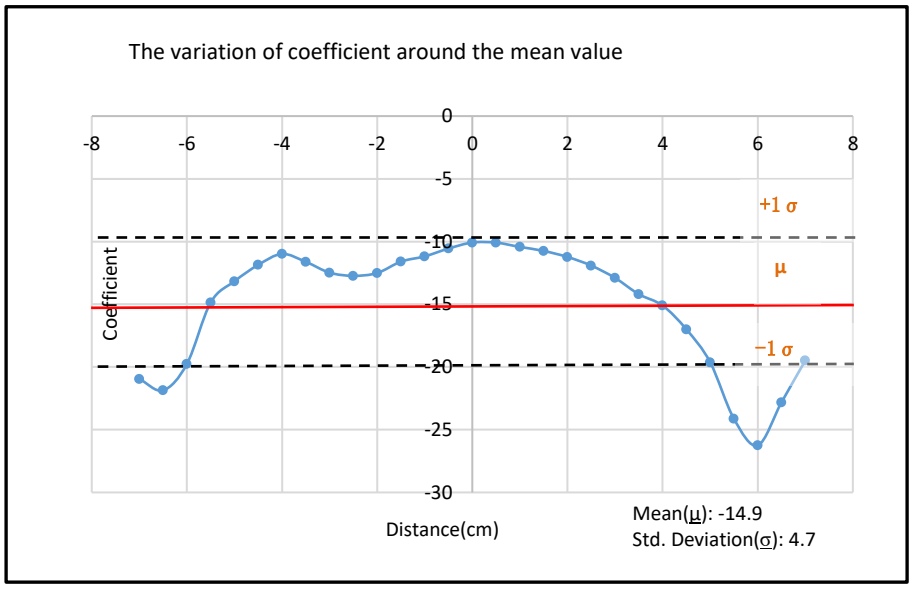

Figure 5.24 – The variation of coefficient for bit 2. The mean value is shown by the red solid line and one standard deviation around the mean value is shown by the black dashed lines

The Detection Error Rate (DER) is given by,

$$DER = 1 - throughput \tag{5.5}$$

$$throughput = \frac{N_S}{N_T} \tag{5.6}$$

where N_s is the number of successful tag detections and N_T is the total number of tag readings.

Therefore, the DER calculated for the above results is 0.207 where the throughput is 0.793. For repeated experiments of the same it shows a DER of 20% when given as a percentage.

5.5 Conclusion

This chapter has revealed an approach and method to detect the movement of a chipless RFID tag on the move. It gives an exposure to the parameters that are affected by a chipless RFID tag in stepped motion and gives an estimation to the robustness of its tag ID using the adaptive wavelet-based detection algorithm.

The S11 magnitude shifts at the relevant resonant frequencies are as expected within the half power beam width of the antenna and is not detectable as it moves out from the antenna aperture. The confident band set in the detection algorithm using the results for a moving chipless RFID tag proves that the correct frequency ID can be detected successfully around a percentage of 80%. Also, this leads to a research pathway for the improvement of the reading range which is essential as the variation in magnitude and phase increases as it moves beyond the beamwidth of the given antenna. The experiments also confirm that the frequencies stay mostly unperturbed thus giving the ability to detect the tag ID without much difficulty.

In this experiment stepped motion was considered since the VNA cannot capture the data while it is in motion. But the number of data captures analysed in this experiment will be equal to the number of data sets captured by the chipless RFID reader in a real time movement scenario. Therefore, the results of this experiment will be equivalent to results expected from the system. The detection algorithm has been implemented only for a single antenna chipless RFID reader. For the robust detection of tags in motion, future directions of this research are to test the detection algorithm with an array antenna and a chipless RFID reader which is under development. Also, further development to the system can introduce error correction techniques to correct any bit errors after detection. This will open the research pathway to many practical applications with tagged objects to be tracked in movement.

6 Implementation of detection algorithm for single antenna reader system

6.1 Introduction

In this chapter, the detection algorithm is implemented in a single antenna reader system. The function of a single antenna chipless RFID reader system is highlighted in Section 2 of this chapter. The block diagram of the single reader architecture used in this research work is shown in Figure 6.1 [3]. It consists of the transmitter (TX), directional couplers, receiver (RX), TX/RX antenna and the digital signal processing (DSP) unit. The chipless RFID reader interrogates the chipless tag by sweeping the frequency spectrum at a given sampling rate. The developed detection algorithm has been implemented in the microcontroller to detect the tag ID which determines the bits in logics "1" and "0". The calibration of the reader can be performed at the start of the measurements or in between each reading which eliminates the influences of the environment. After the tag ID has been decoded it is sent to a display screen on the DSP unit and/ or via RS-232 to the host computer application. There is no need of human interaction for the reader to interrogate the tag. At any time, the user can choose to save the tag data received by the reader in a specified database/server.

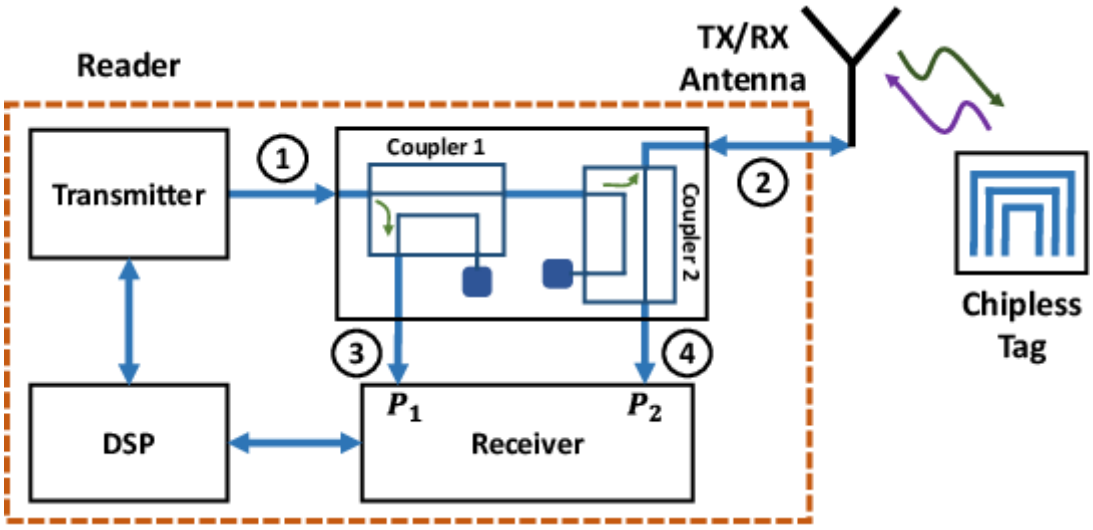

Figure 6.1 – Block diagram of the single-antenna chipless RFID front end [3]

As shown in Figure 6.2, an aperture coupled micro-strip patch antenna (ACMPA) [7] is used as the 'TX/RX' antenna of the system. In Section 3 it presents 3 different patch antennas and comparing the return loss the antenna which has its best performance within the reading range is selected for the experiments. A 9-bit encoded copper tag [8] as well as the printed flexible version of the same tag are tested using this reader system.

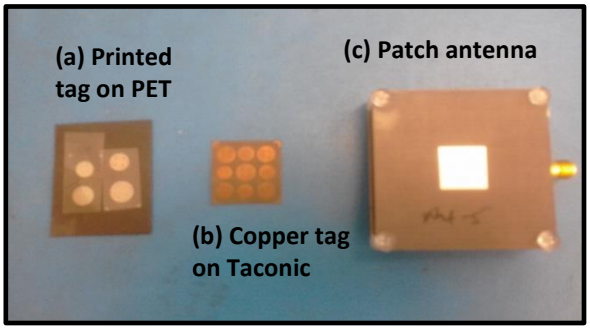

Figure 6.2 – (a) 4- bit printed tag on flexible material PET,
(b) 9 – bit Copper tag, (c) ACMPA

The PIC32MZ microcontroller is used as the programming device in the digital section of the reader which provides a complete range of programming and diagnostic features that can increase the flexibility of the reader application and is presented in Section 2. The implementation of the developed detection algorithm is presented in Section 3 of this chapter. The detected signals are analysed and compared with the results obtained by the vector network analyser (VNA). By applying the detection algorithm, the tag ID's are decoded, and the detectability of the tags is discussed. As the research aim is to apply the developed algorithm in real time application, a clutter characterization is presented in Section 4. It is further tested in the CST simulation environment and the new detection algorithm is applied for detection of the tag. After getting a clear understanding of the problems that can be encountered due to clutter and movement with distance from the results, the testing for the detection of tags using the reader is presented in Section 7. A comparison of the results obtained by the VNA and the reader shows that the chipless RFID tags presented in this work can be correctly and robustly detected by the new generation chipless RFID reader designed and developed in the MMARS laboratory.

6.2 Reader architecture

Reading of the chipless RFID tag requires either a frequency domain measurement, measurement of the amplitude or the phase of the transmission coefficient of the tag that can be used for decoding data. In many of the experiments carried out in the laboratory, a VNA has been used for this purpose. Since the VNA is not a conventional reading technique and is an expensive piece of equipment, three generations of chipless RFID tag readers are reported in [12] by MMARS laboratory at Monash University.

The reader extracts the scattered signal and decodes the tag ID. This is an ongoing challenge as the detection procedure for a chipless RFID tag has more complexities compared to a conventional RFID tag. A new generation single antenna desktop reader has been designed and used in this research work, under Australian Research Council (ARC) Linkage Project LP #130101044. Figure 6.3 shows the block diagram of the reader. The TX and the RX blocks of the RF section consists of an oscillator (VCO), band pass filters (BPF1 and BPF2), power amplifier (PA1), low noise amplifier (LNA1), antenna (TX/RX antenna) and directional couplers (COUP1 and COUP2).

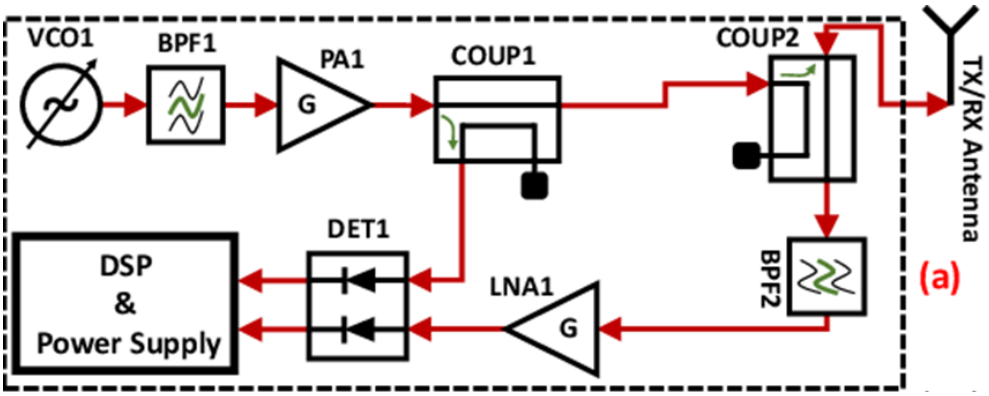

Figure 6.3 – Detailed block diagram of the chipless RFID reader [3]

The PIC microcontroller used in the digital section of the developed desktop reader is shown in the block diagram shown in Figure 6.4. The features and interfaces which are presented by this PIC microcontroller could be enumerated as UART, I2C, SPI, Internal ADC, WDT, USB OTG, SQI, Ethernet, CAN and ISP.

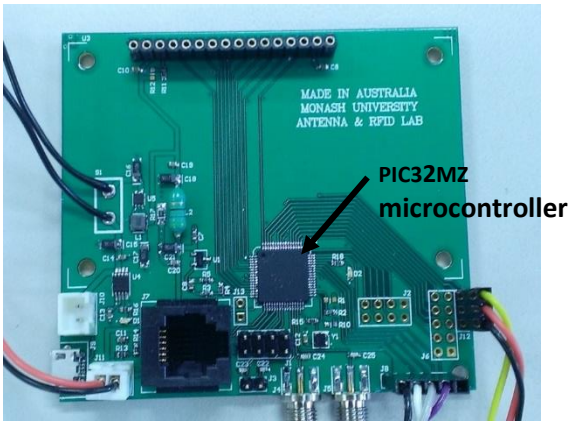

Figure 6.4- Digital Section of the Desktop Reader with PIC32MZ microcontroller

PIC32MZ device provides a complete range of programming and diagnostic features and to achieve this an ICD3 serial programmer proposed by Microchip for PIC devices is used as shown in Figure 6.5.

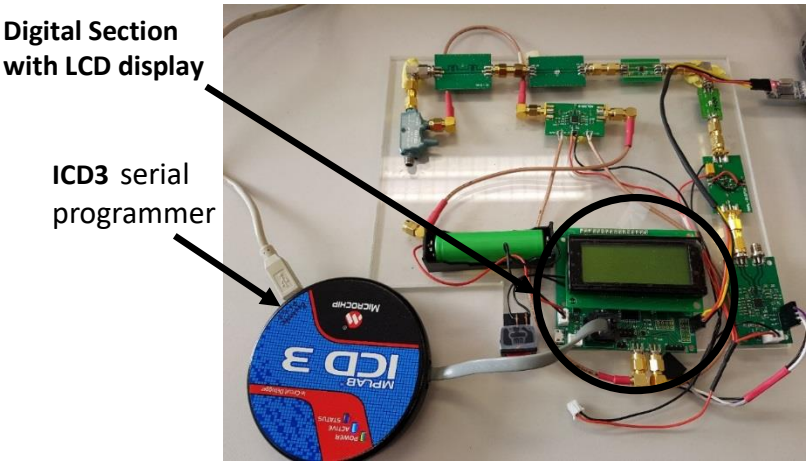

Figure 6.5- ICD3 serial programmer used to program PIC microcontroller

Also, a 4 x 20 character LCD has been selected to demonstrate the extracted information for user. The LCD has an 8-bit parallel data interface and it uses a single 3.3 V supply voltage for both power source and backlight. A 16-pin IDC header was used for providing required supplies for LCD and making physical connection between PIC32 and LCD.

MPLAB X IDE is a software program that runs on a PC (Windows, Mac OS, Linux) to develop applications for Microchip microcontrollers and digital signal controllers. It is called an Integrated Development Environment (IDE), because it provides a single integrated "environment" to develop

code for embedded microcontrollers. MPLAB X IDE is based on the open source NetBeans IDE from Oracle. A code format standard is set up to be used within the editor. Visual C has been used to program the microcontroller in this case. The programming environment is shown in Figure 6.5.

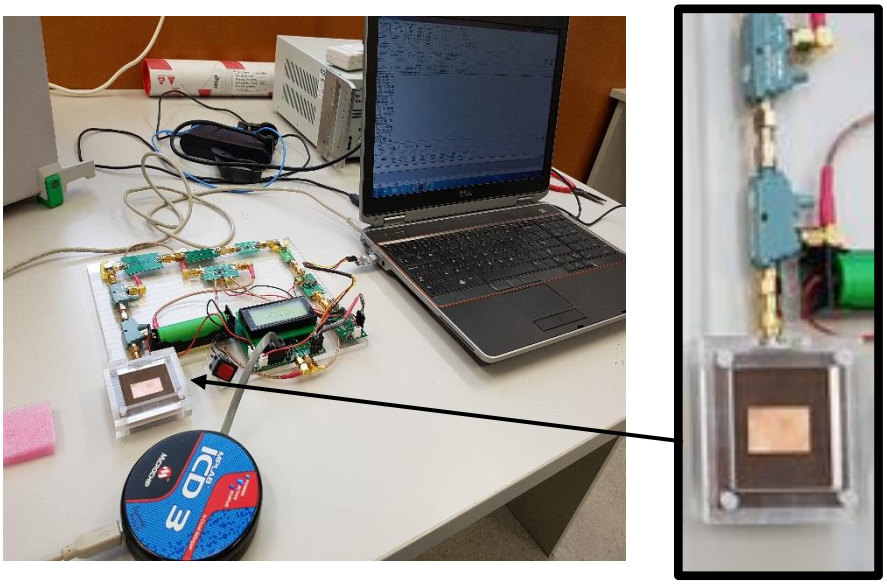

Figure 6.6 - Using MPLAB X IDE software to program the pic microcontroller, the inset figure on the left shows the single reader antenna

To capture the gain of transmitted and received analog signals and provide them to next stages for further processing, the built-in ADC module of PIC32 has been utilized. It acts as the interface between the RF section and the digital section of the reader. To maintain simultaneous data gathering, both transmitted and received signals were captured at the same time making benefit from internal Sample & Hold circuits and then converted one after another to digital data. The built-in pipeline ADC has the ability of converting 48 different sources with a 10-bit resolution in the range of $-V_{REF}$ to $+V_{REF}$ reference voltages.

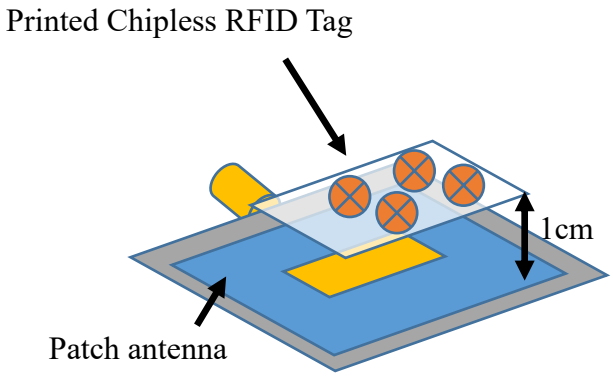

Figure 6.7 - Patch antenna loaded with the printed tag at 1cm

As shown in Figure 6.7 the tag is held 1 cm above the patch antenna and the received signal is processed in order to obtain the tag ID.

6.3 Implementation of the detection algorithm in the microcontroller

6.3.1 Implementation of the detection algorithm

Moving forward in the implementation of the detection algorithm in the microcontroller the modified program in MPLAB X IDE has been downloaded and executed successfully.

A terminal emulation program called 'Terminal' is used as the debugging tool. It is a simple serial port (COM) and can be used for monitoring all kinds of Serial Port (UART) communications between PC and other Micro Controller Units (MCU). Figure 6.8 shows the testing set up and the captured data through the terminal which is used to plot the output signal for debugging. In the real time application, the output/ tag ID will be displayed on the LCD screen on the board itself.

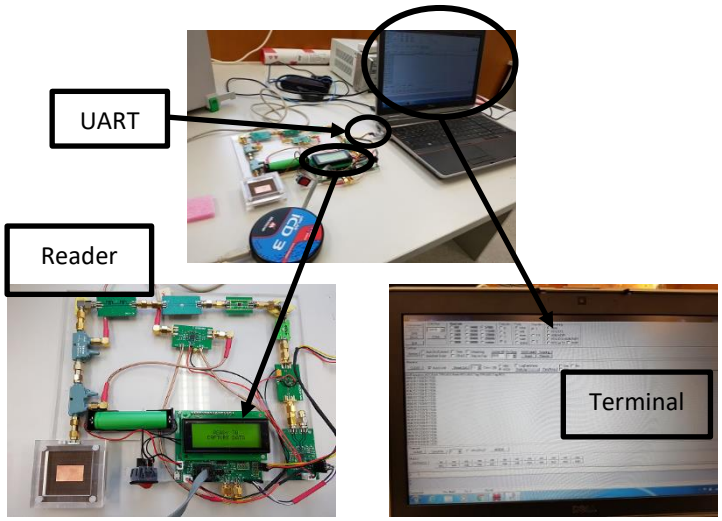

Figure 6.8 - Testing setup

6.3.2 Testing patch antennas and detection of copper tags using VNA

Three patch antennas as shown in Figure 6.9, Ant 3 - *big patch antenna*, Ant 2 - *patch antenna 2* and Ant 1 – *patch antenna 1* were tested using the VNA to choose the best antenna for the test and two tags 'Tag 1 – *AM05* ' and 'Tag 2 – *a41*' were also tested using the selected antenna as shown in Figure 6.10.

The results for antennas and tag ID using VNA were plotted using Matlab as shown in Figure 6.11.

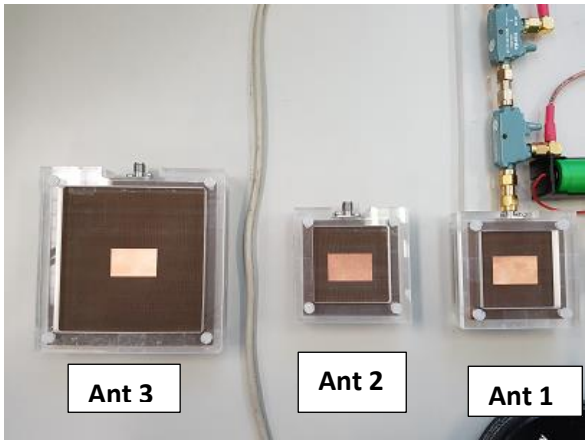

Figure 6.9 – patch antennas used for testing

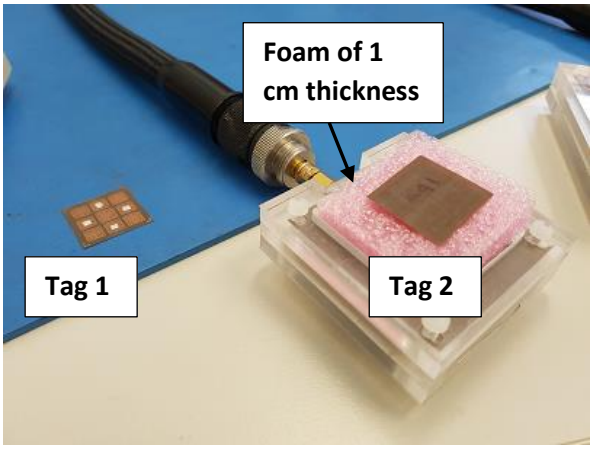

Figure 6.10 – Tags tested for detection

The reading range of the designed chipless RFID reader is in the frequency range of 4 – 8 GHz. Therefore, looking at the results in Figure 6.11, Ant 2 (patch antenna 2) has the best performance within the range. The responses of Ant 1 and 3 have several notches within the frequency band of detection which is a disadvantage for tag detection. Patch antenna 2 is used for the experiments performed in the next sections. The tag is placed on a piece of foam of thickness 1 cm on top of the patch as shown in Figure 6.10. The background subtracted S11 magnitude (dB) vs frequency (GHz) data are collected and stored in the VNA. The saved data are then processed in Matlab and the tag responses are shown in Figure 6.12. The detected signals after applying the algorithm are shown in Figure 6.13

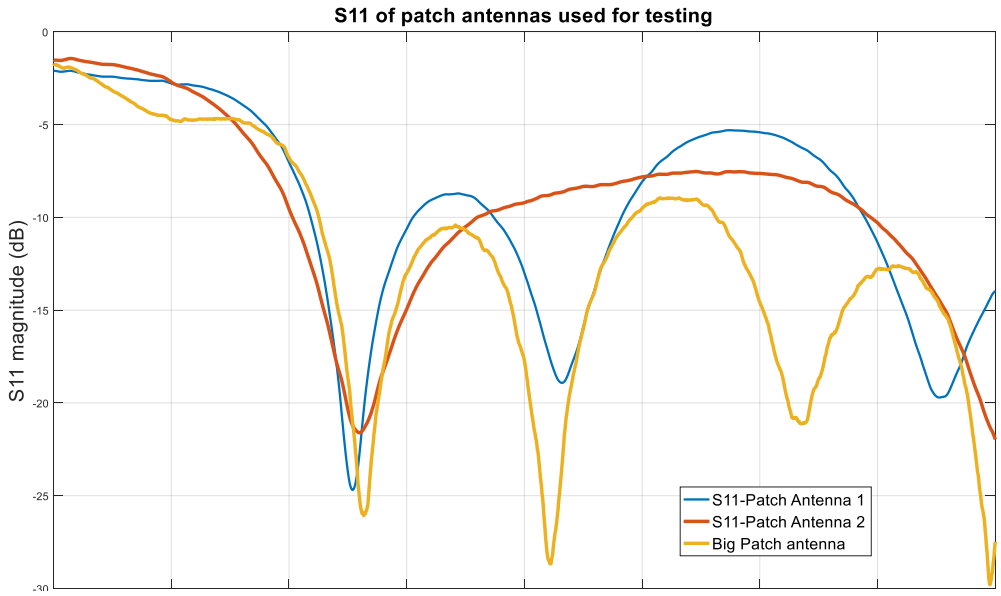

Figure 6.11- S11 magnitude (dB) vs frequency comparison of patch antennas used for testing

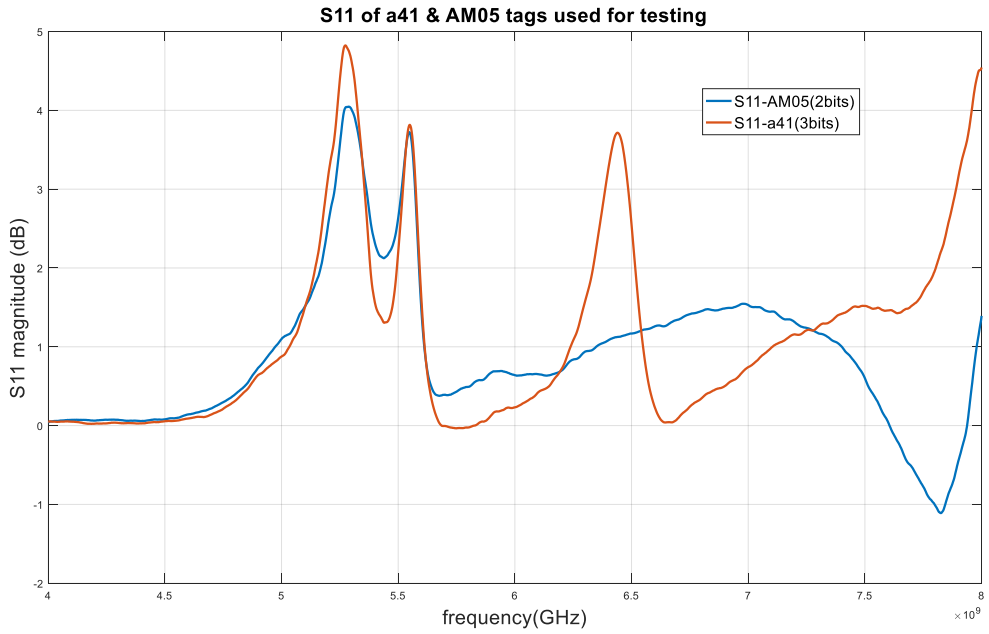

Figure 6.12 - Tag responses of Tag 1 -'AM05' and Tag 2 – 'a41' using VNA

According to Figure 6.13 the threshold level for detection is set to 0.2. The condition band for decoding bit '1' and bit '0' is set as between 0.1 – 0.5 of the coefficients. Therefore, Tag 1 ID is decoded as '111' and Tag2 ID is decoded as '111'. From these results it can be seen that only 3 bits of the 9-bit copper tag is encoded between the frequency range of 4 – 8 GHz.

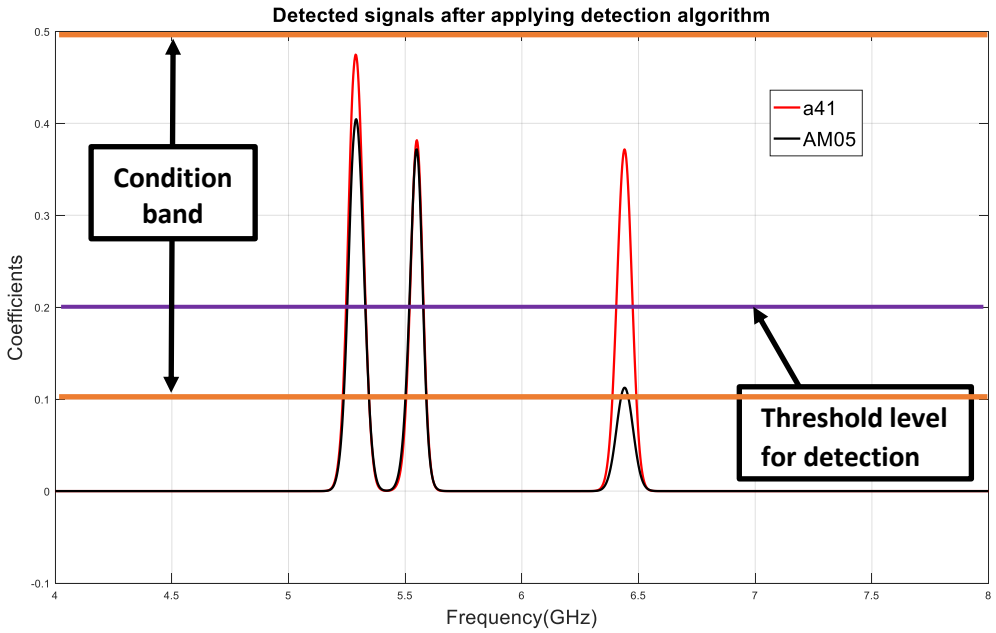

Figure 6.13– Detected tag ID using the implemented algorithm

6.3.3 Characterization of clutter and detection of printed tag using VNA

Ant 2 (Patch antenna 2) was used for the following experiments. S11 of the patch antenna is shown in Figure 6.14. According to the plot S11 magnitude is below -7.5dB from 5GHz to 8GHz. The printed 4-bit tag was loaded on the patch antenna as shown in Figure 6.15 and the result of the received signal obtained using the VNA is shown in Figure 6.16.

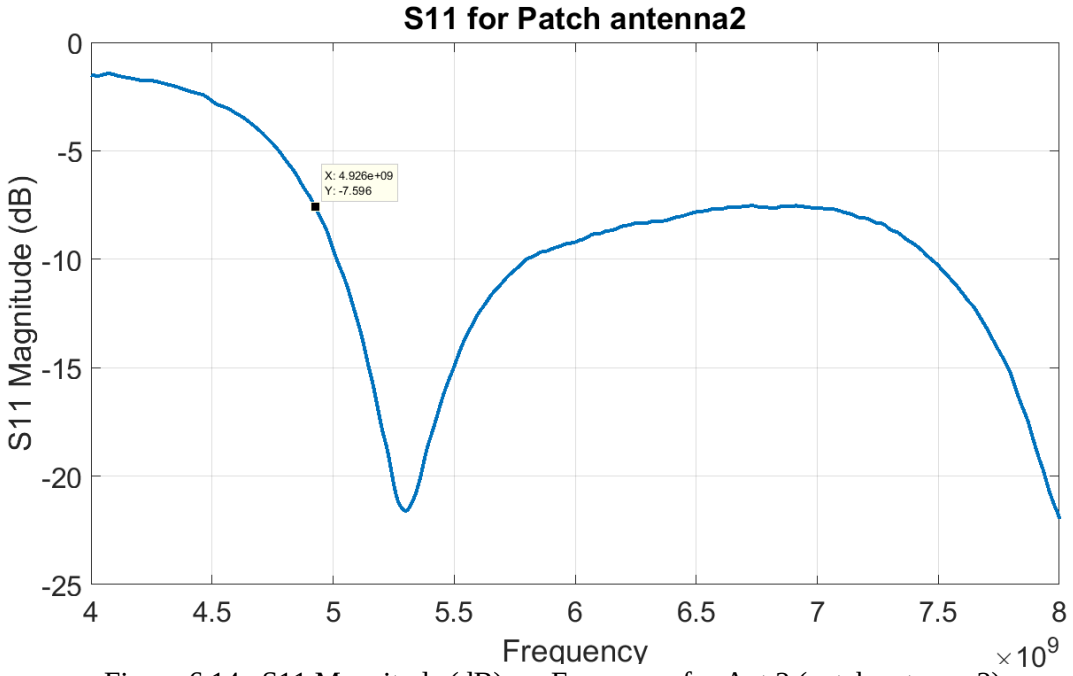

Figure 6.14– S11 Magnitude (dB) vs. Frequency for Ant 2 (patch antenna 2)

According to the results shown in Figure 6.16 only 3 bits can be detected as the first bit occurs below 4 GHz. According to the measured results the 3 bits are located at 4.908, 5.752 and 6.752 GHz, respectively.

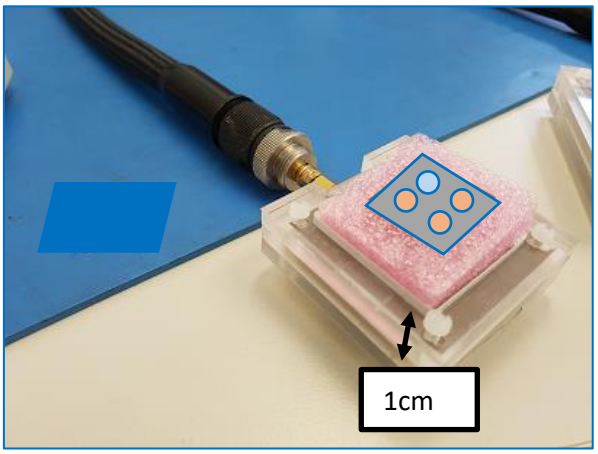

Figure 6.15 – Patch antenna loaded with the printed tag at 1cm

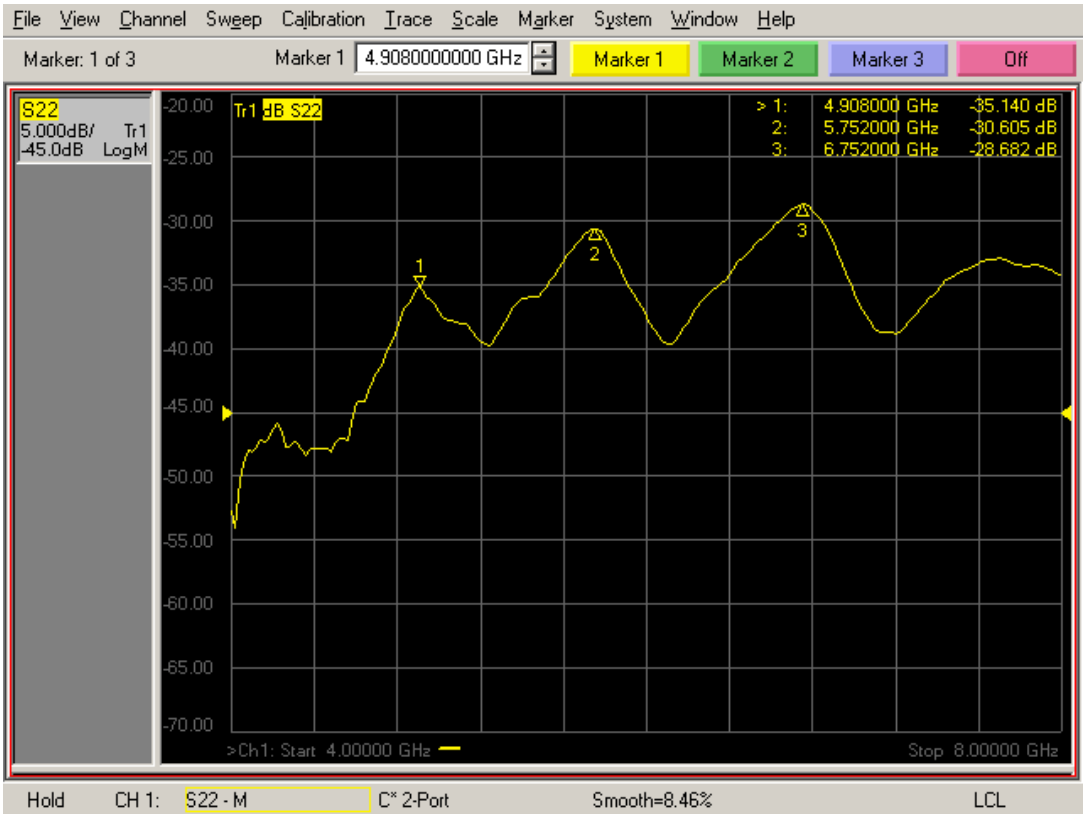

Figure 6.16 – Measured result for printed tag using VNA without any clutter object

Then the measured results were analysed using Matlab. The detection algorithm was applied to decode the frequency ID of the original tag as shown in Figure 6.17.

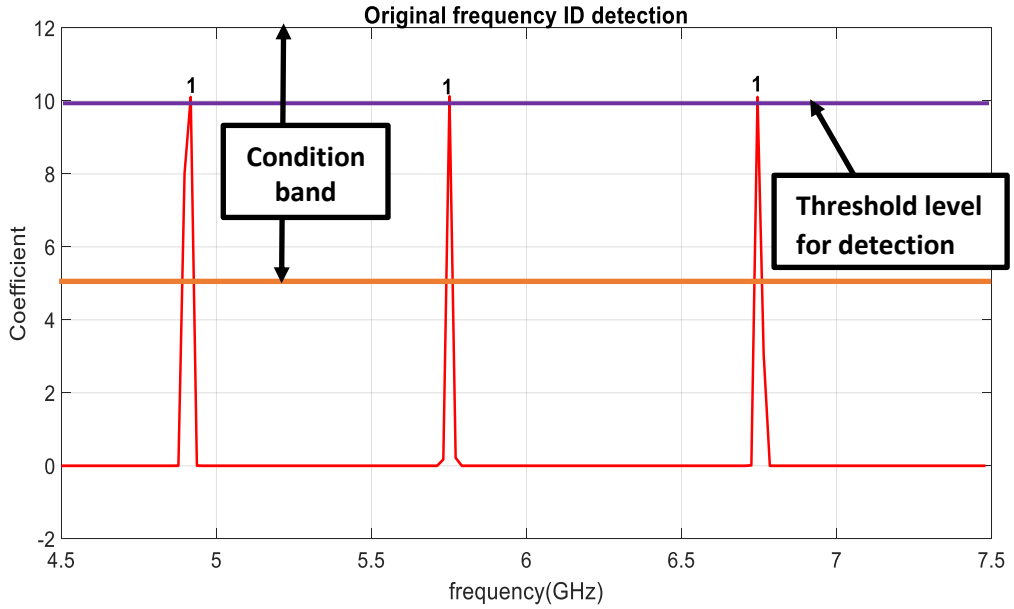

Figure 6.17 – Detection of the frequency ID without any clutter object

The detection coefficient is at 10 for the original frequency ID and the experimental results with clutter will be compared with this detection level. A condition band of ±5 is allowed for the coefficient variation due to clutter or movement. Also ±0.25 GHz guard band is allowed for the frequency shift due to any clutter or movement. These condition band was predefined based on the simulation and experimental results obtained previously for movement and clutter.

Four types of clutter were tested with the above printed tag, positioned at 1cm above the patch antenna as shown in Figure 6.18. Namely copper plate (square), wooden block, plastic container, hand with Gold ring and Hand only. The measurements were taken using the Agilent VNA while the clutter object was placed at a distance (*d cm*) from the chipless RFID tag by the side. The distance *(d cm)* was changed from 1 to 10 cm.

6.3.3.1 Tag with Wooden block

The first experiment was with the wooden block of dimensions 18 x 9 x 2 cm placed at different distances *(d cm)* as shown in Figure 6.18 varying from 1 to 10cm.

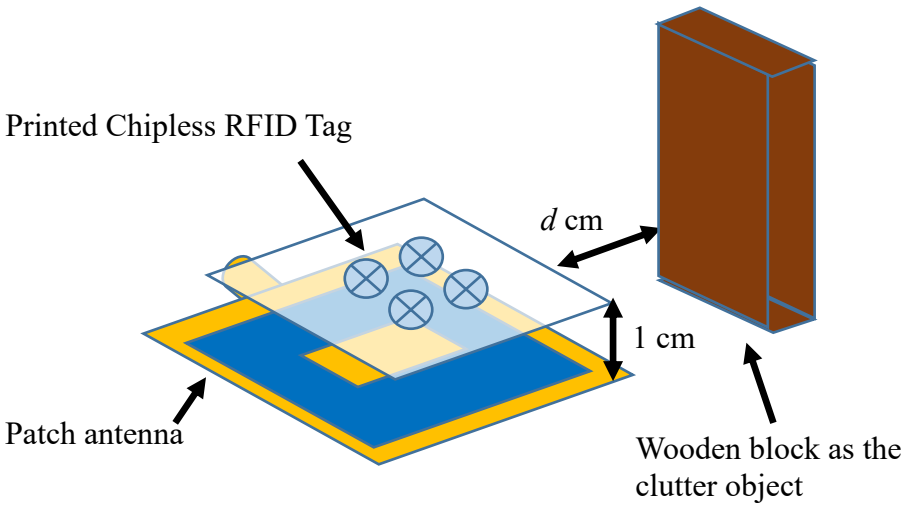

Figure 6.18 - Tag with wooden block placed at different positions

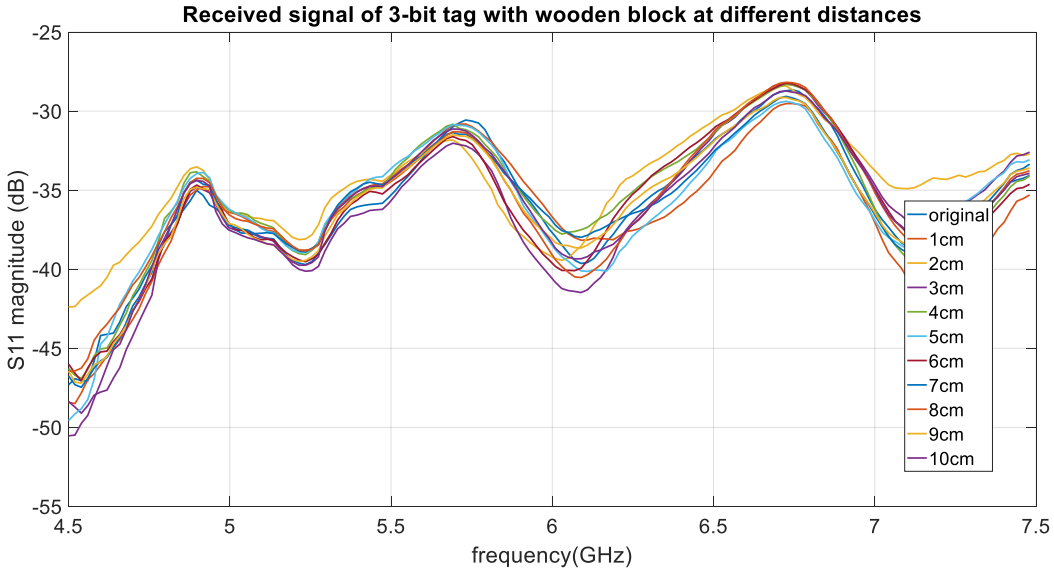

Figure 6.19 – Received signal of tag with wooden block at different distances

By the measured results as seen in Figure 6.19 it can be seen that the magnitude of the S11 does not vary significantly with the displacement of the wooden block. The first blue curve shows the original results without any clutter for comparison. The detected Frequency ID is shown in Figure 6.20 after applying the detection algorithm.

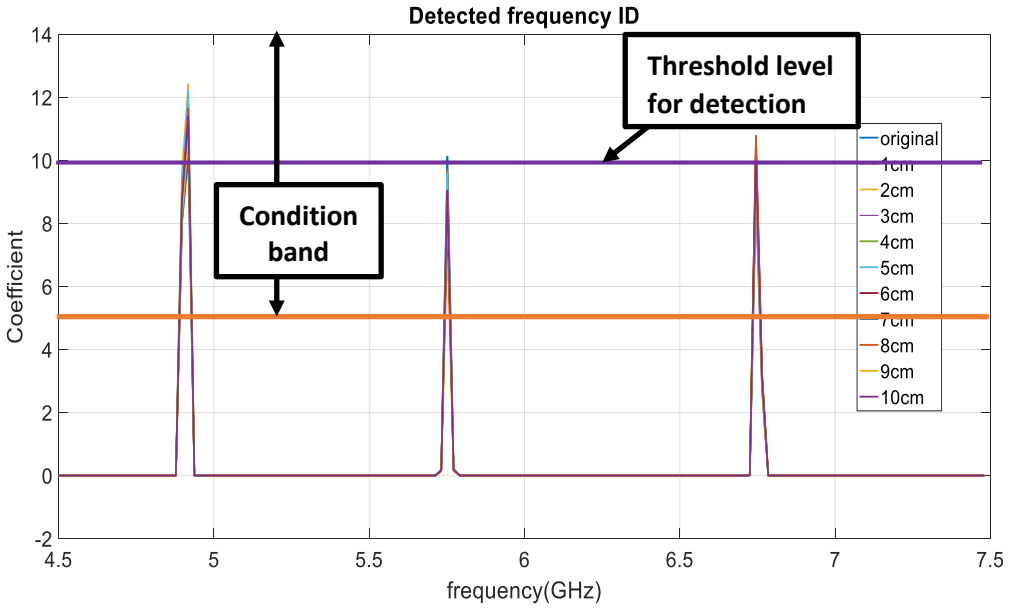

Figure 6.20 – Detected frequency ID while the wooden block is at different distances from the tag

6.3.3.2 Tag with Cu plate

A rectangular copper plate having dimensions of 23 x 17 x 0.1 cm was kept near the tag as shown in Figure 6.21 starting at 1 cm away from the tag and was moved up to 10 cm. The Cu plate was supported by a plastic stand and the background measurement was taken with the stand before fixing the Cu plate to the stand and was subtracted when taking measurements. The detection algorithm was applied to decode the frequency ID. The results are shown in Figures 6.22 and 6.23.

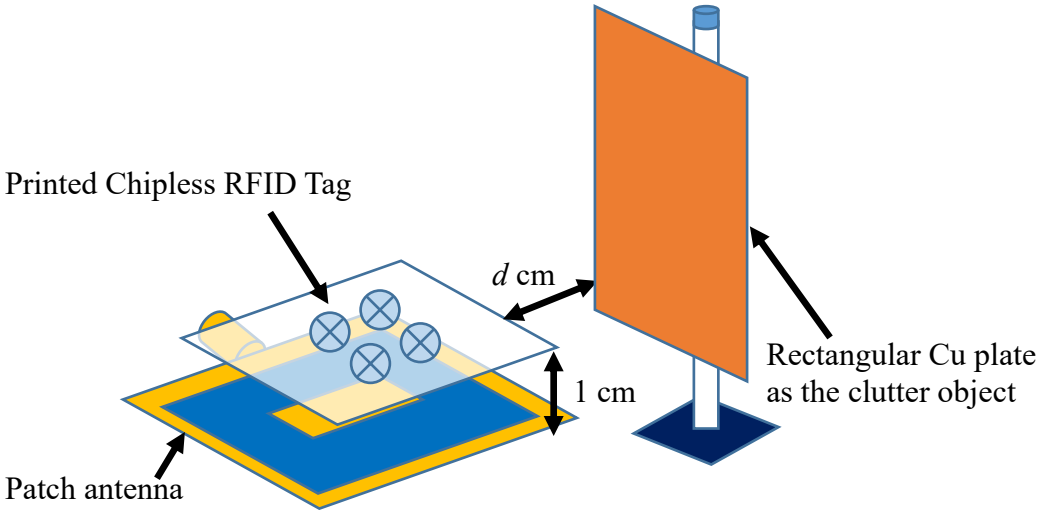

Figure 6.21- Tag with rectangular Cu plate placed at different positions

According to the received signal it can be seen that the S11 magnitude is increasing when the Cu plate is near to the tag. Also looking at the received signal the resonant frequencies cannot be identified. The resulting coefficients after applying the detection algorithm is shown in Figure 6.23.

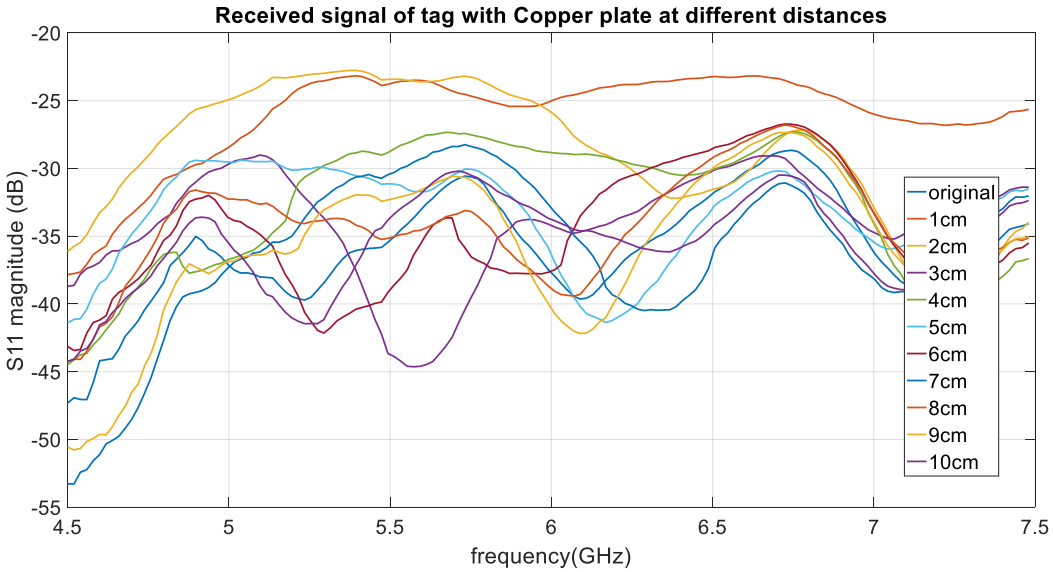

Figure 6.22 – Received signal of tag with copper plate at different distances

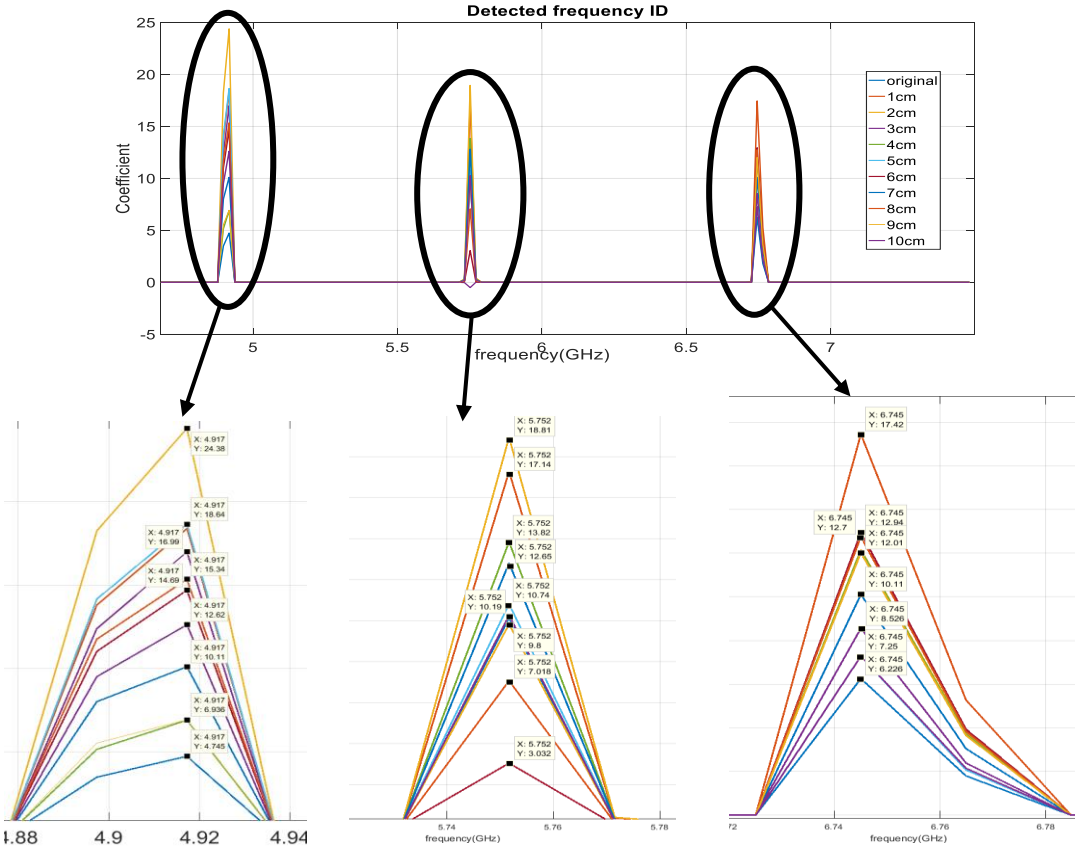

Figure 6.23– Detected frequency ID with copper plate at different distances from tag

According to enlarged figure for the 1st, 2nd and 3rd bit results the coefficients vary from 3 to 25. So, the coefficients detected in the range of 5 to 15 fall into the condition band and are detected as '1' while the other coefficients beyond this range are detected as a bit '0'. The detection algorithm will detect bit 1 as '0' when the copper plate is at 1 and 2 cm positions.

6.3.3.3 Tag with gold ring in hand

The next experiment was placing hand with gold (Au) ring at *d cm* from tag as shown in Figure 6.24. Where the hand is moved from 1 to 10cm away from the tag. This type of clutter was selected as the application of the desktop reader will be using handheld tagged items moving across the antenna and it is expected to detect the tag in such clutter environment.

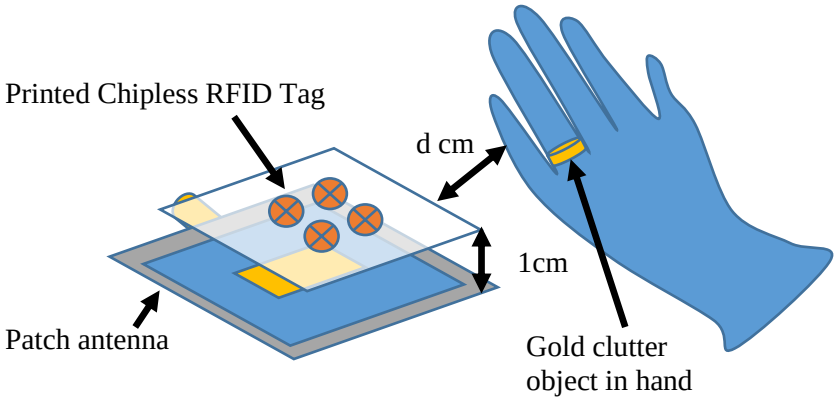

Figure 6.24 – Tag with hand with gold ring at different positions

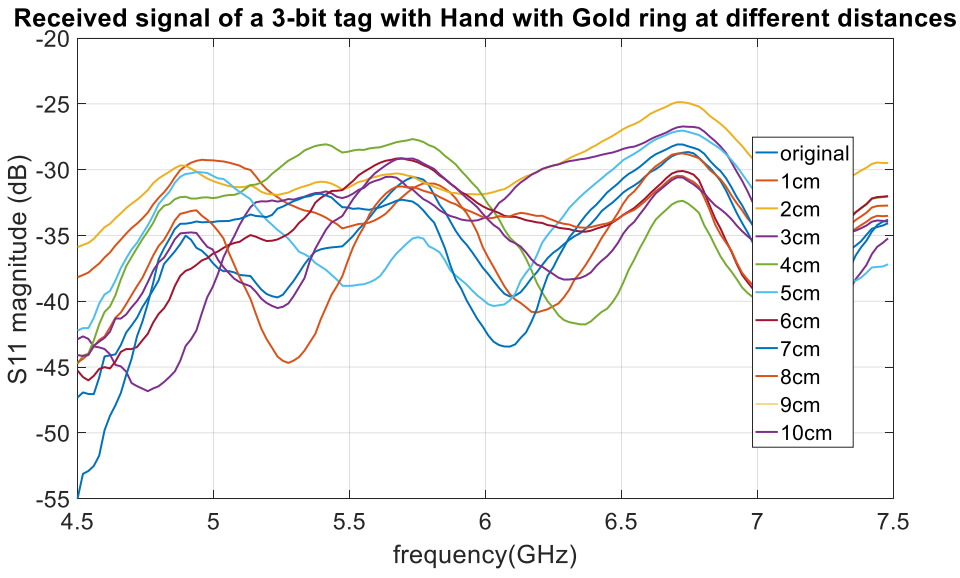

Figure 6.25 – Received signal with hand with gold ring placed near tag at different distances

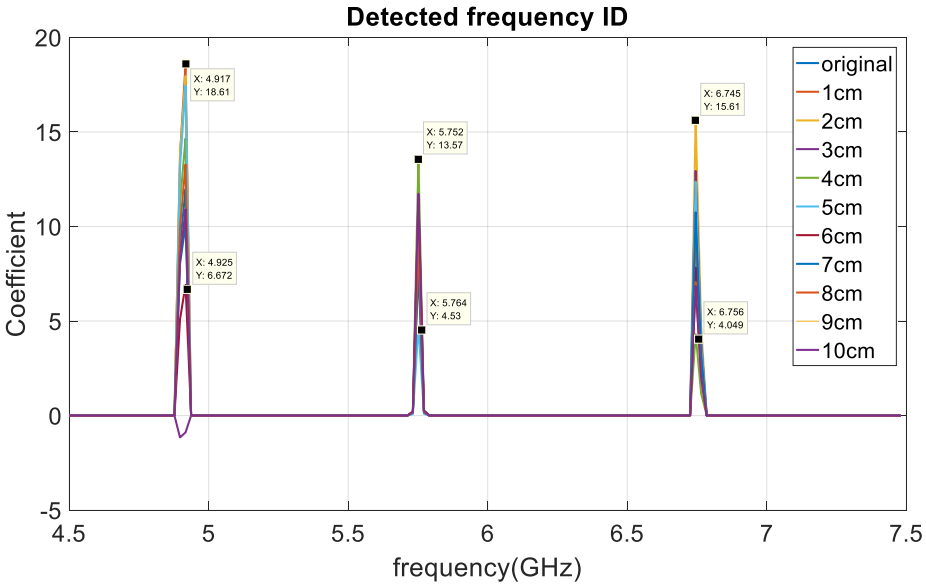

Figure 6.26 – Detected frequency ID for tag with hand with gold ring placed as clutter object

According to the results in Figure 6.25 the peaks are not clear when the hand is in near distance. After applying the detection algorithm as shown in Figure 6.26 almost all bits can be recognized at all distances. Similar experiments were performed with plastic container, hand etc. The received signals were tested by applying the detection algorithm.

According to these results it can be seen that a conductive material (Cu, Au) placed in the close vicinity of the tag (less than 10cm) will have an effect on the magnitude of the tag measurement. Still applying the detection algorithm, the tag can be identified even if the conductive material is placed around 3cm distance from the tag. When semi conductive material and insulators such as wood and plastic are placed in the close proximity of the tag the effect is less and the detection is not affected. Since the experiment was conducted by placing the clutter only in one side of the tag more experiments should be performed by varying the position, size, material etc. to conclude the probability of error due to different material surrounding the tag.

6.4 Simulation of clutters and detection in CST

6.4.1 Simulated results for a 4-bit circular tag using single aperture coupled antenna

The 4-bit circular tag shown in Figure 6.27 has been used in the CST simulation with the single aperture coupled antenna shown in Figure 6.28. The tag RCS is shown in Figure 6.29 and the simulation results when the tag is placed at 2cm away from the antenna is given in Figure 6.30.

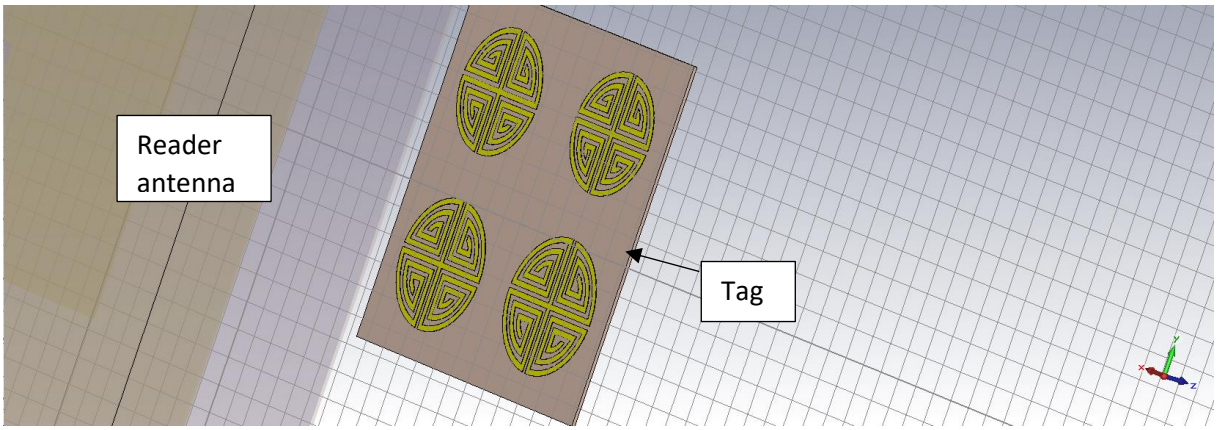

Figure 6.27 – 4-bit circular tag used for simulation

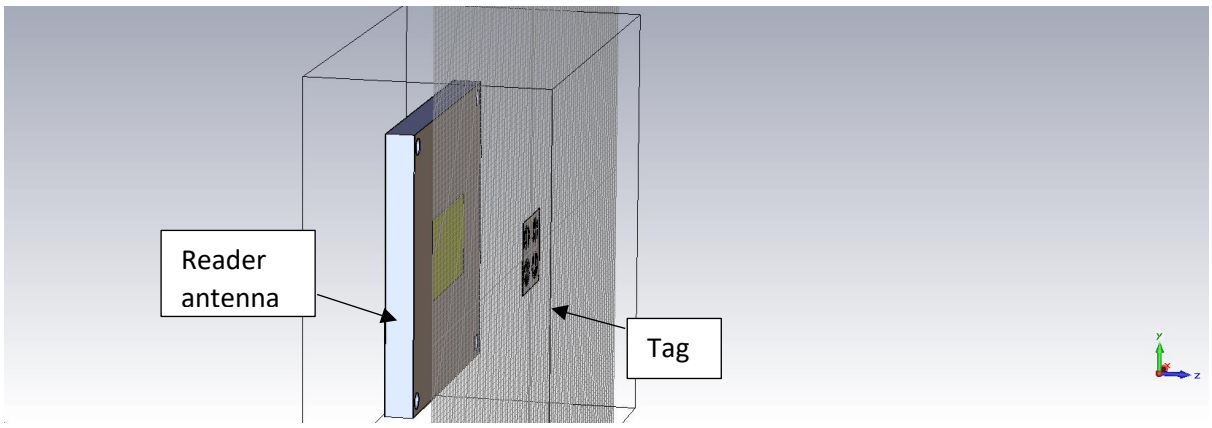

Figure 6.28 – CST simulation with patch antenna

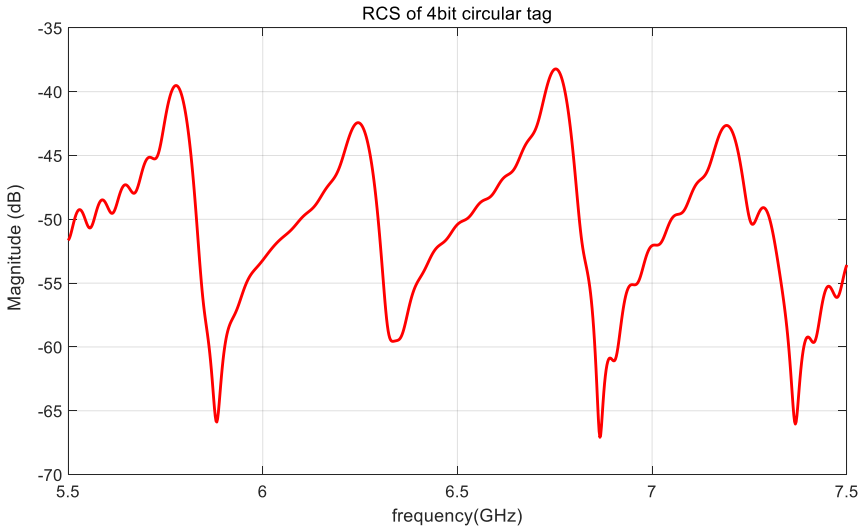

Figure 6.29 – RCS of the 4-bit circular tag

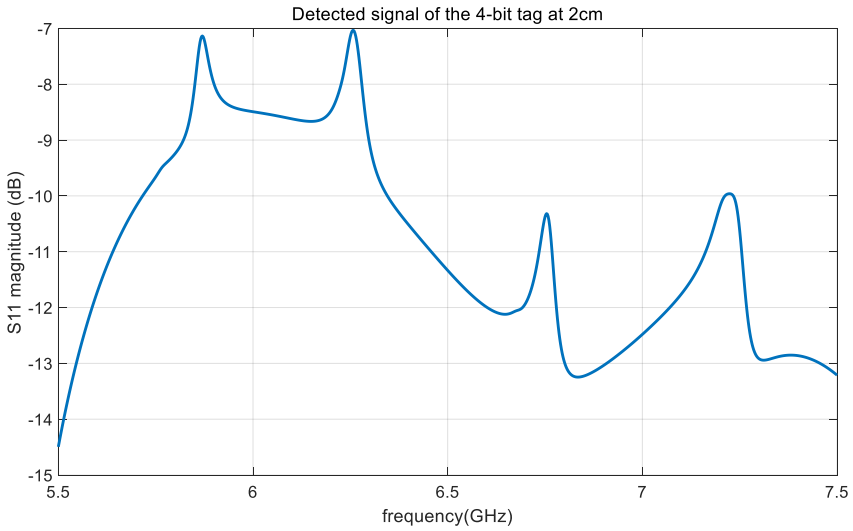

Figure 6.30 – Detected signal of the 4-bit tag at 2cm from the antenna

6.4.2 Detection of the simulated results using new detection algorithm

The detection algorithm is based on the new wavelet as presented in Chapter 4. Figure 6.31 shows the wavelet used to convolve with the output signal of the chipless RFID tag. It is based on the Gaussian function, which is given by,

$$f(x) = a \times e^{\frac{-(x-b)^2}{2c^2}} \qquad (6.1)$$

where a is the height, b is the position and c is the width of the wavelet. The values of a, b and c has been adjusted in order to maximise the detection.

When measuring a large number of peaks, it is often effective to subtract an estimated baseline from the data. Therefore, in applying the new detection algorithm the baseline removal has been added as an improvement and robust detection. In this algorithm the estimate is constructed by fitting a low-order polynomial, to the data only where it appears to contain no peaks. Then the resulting curve fit result is subtracted from the data. The difference then contains mostly the peak data. The wavelet transform is performed on the resulting peak data to distinguish the exact peaks.

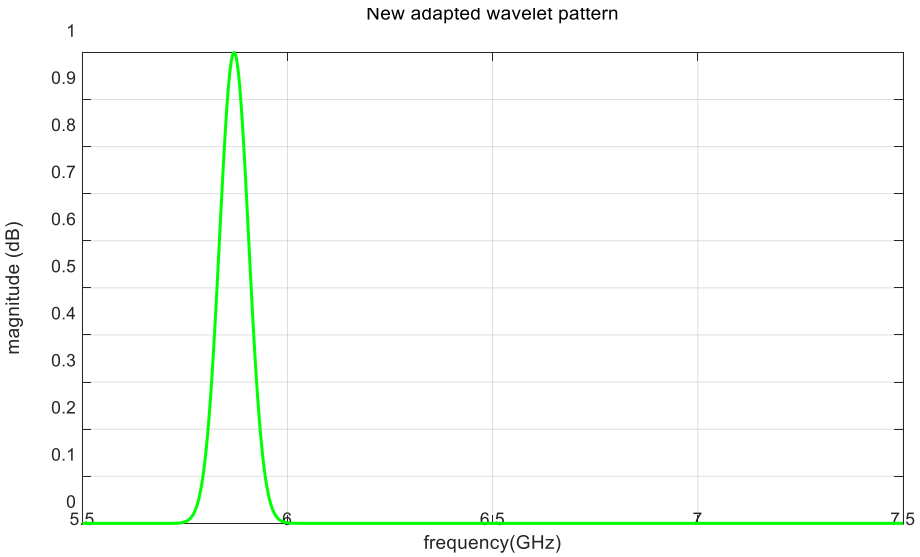

Figure 6.31 – New adopted wavelet pattern

The signal detected after the baseline removal is shown in Figure 6.32.

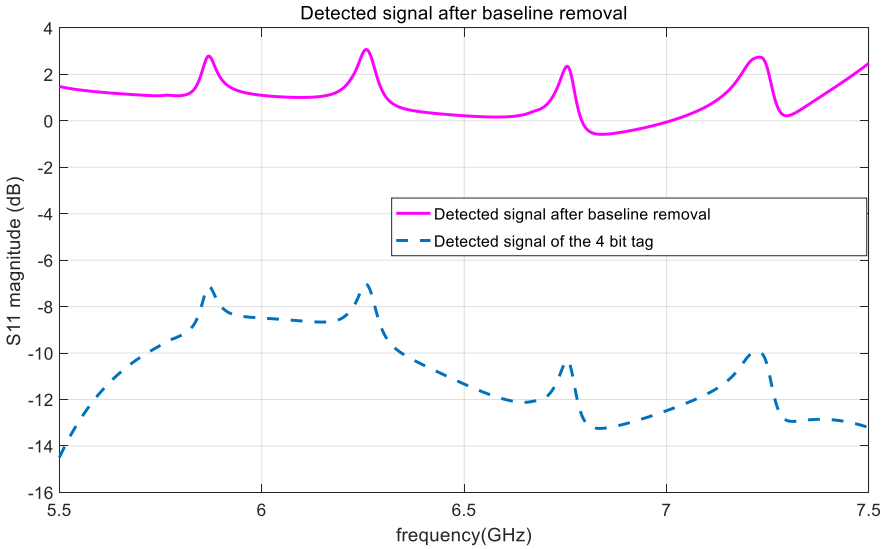

Figure 6.32 - Detected after the baseline removal

The detected signal after wavelet transform is shown in Figure 6.33.

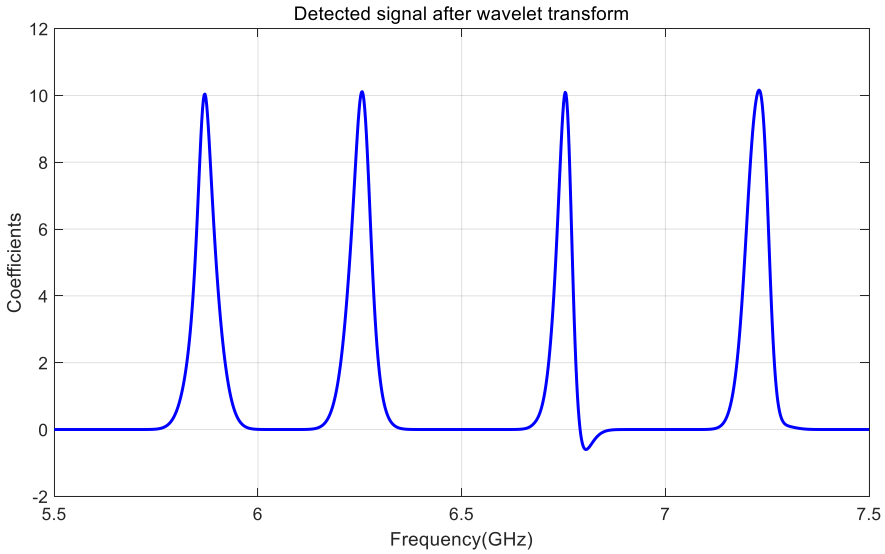

Figure 6.33 - Detected signal after wavelet transform

The frequency ID is generated by comparing the coefficient. For the above signal which gives '1111' the output is given as,

Freq ID = 1 1 1 1

Location = 5.870 6.256 6.754 7.230 GHz

Coefficient = 10.04 10.11 10.09 10.16

6.4.3 Introducing clutter in CST simulation environment

The practical environment of the tag detection was simulated in CST using 4-bit tag (copper) and patch antenna (working within 5.5GHz – 7.5GHz). Clutter was introduced as a block of material placed close to the tag. The simulation setup is shown in Figure 6.34.

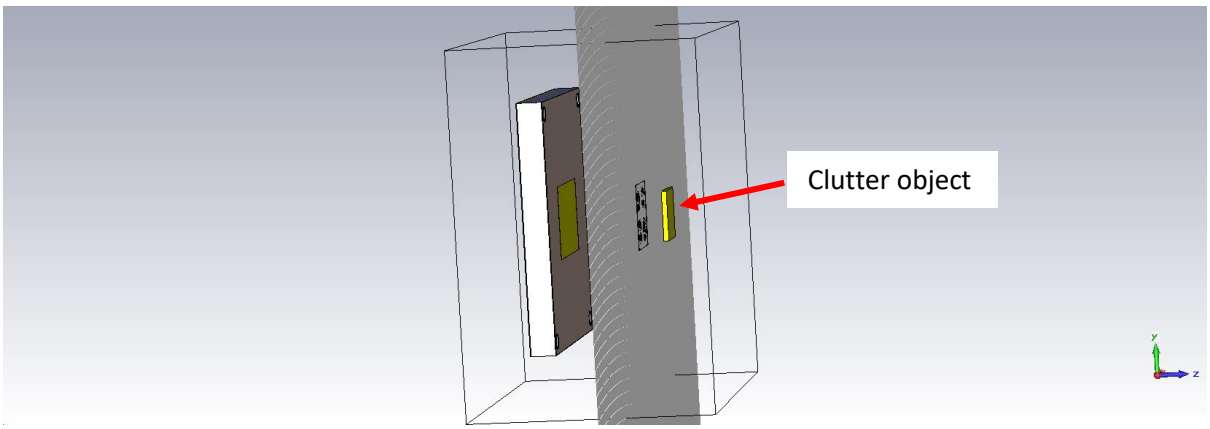

Figure 6.34 –Simulation setup in CST with clutter object

The simulation was done for several material while the clutter object was in a stationary position. Table 6.1 gives the details of the dimensions of the clutter objects and the information related to distance from antenna and tag. Figure 6.35 shows the simulation results for different clutter.

Table 6.1 – Details of the dimensions of the clutter object and the distance from tag and antenna

Clutter Object	Dimensions of Object	Distance from tag	Distance of tag from Antenna
Metal block	20x20x2mm	10mm	20mm
Wooden block	20x20x2mm	10mm	20mm
Gold block	10x10x1mm	5mm	20mm
Bio Tissue/Bone	10x10x1mm	5mm	20mm
Paper	10x10x1mm	5mm	20mm

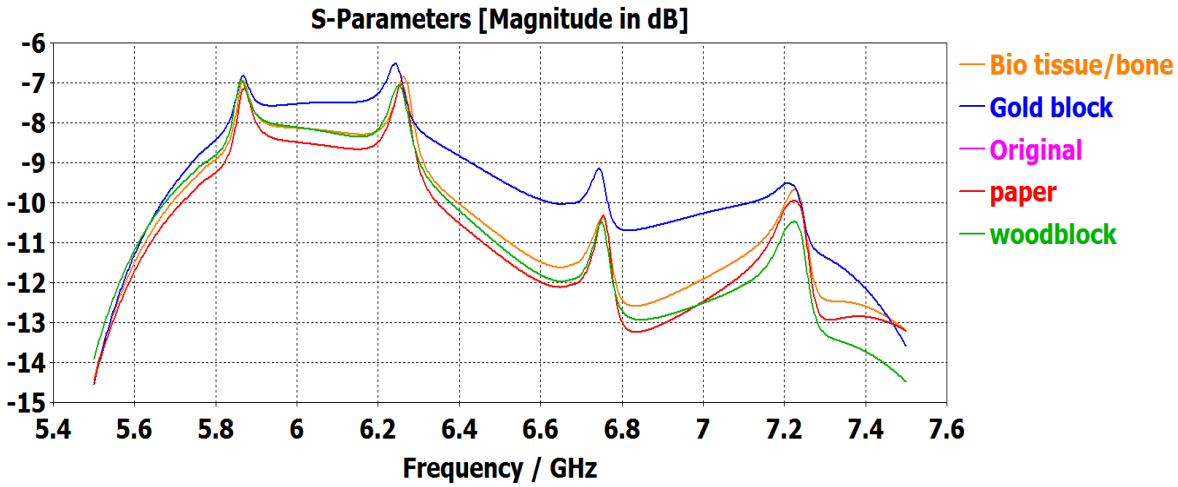

Figure 6.35 – S11 Magnitude (dB) vs. Frequency (GHz) for tag detection with clutter objects placed at very near distance

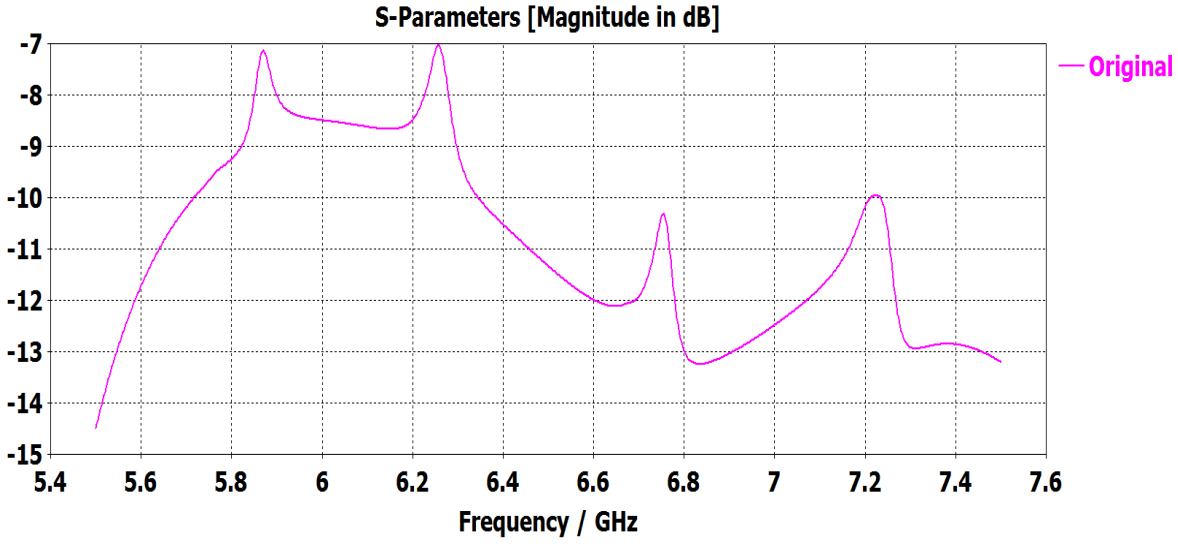

Figure 6.36 – S11 Magnitude (dB) vs. Frequency (GHz) without any clutter

Figure 6.37 shows the outputs obtained by placing copper object and bio tissue (representing human body) close to the tag. The upper part of the figure shows the residual plots with the original signal. Table 6.2 shows the material properties of the different objects placed near the tag in the CST simulation environment.

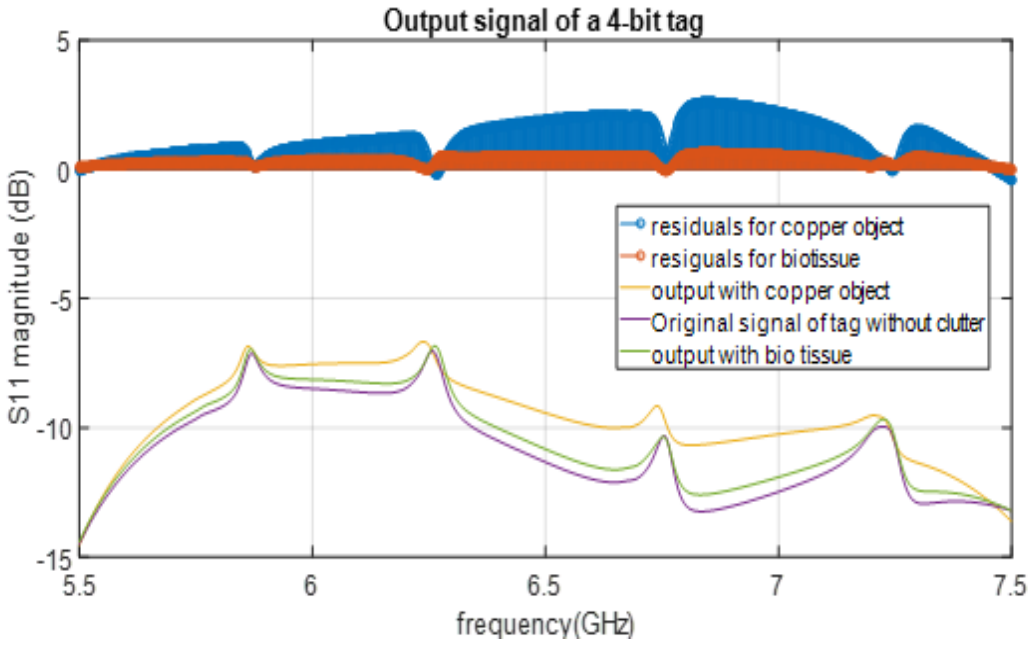

Figure 6.37- Outputs obtained by placing copper object and bio tissue

Table 6.2 – Clutter object position and the its material properties

Clutter Object	**Dimensions of Object**	**Distance from tag**	**Distance of tag from Antenna**	**The 4 peaks can be identified?**	**Material Properties**					
Metal block	10x10x1 mm	5mm	20mm	yes	Type = Lossy metal	μ = 1	El. cond. = 5.8e+007 [S/m]	ρ = 8930 [kg/m^3]		
Bio Tissue/ Bone	10x10x1 mm	5mm	20mm	yes	Heat cap. = 1.3 [kJ/K/kg]	μ = 1	Therm.cond. = 0.41 [W/K/m]	ρ = 1850 [kg/m^3]	Diffusivity = 1.70478 e-007 [m^2/s]	Blood flow = 3400 [W/K/m^3]

Applying the detection algorithm, the outputs have been achieved as given in Figure 6.38.

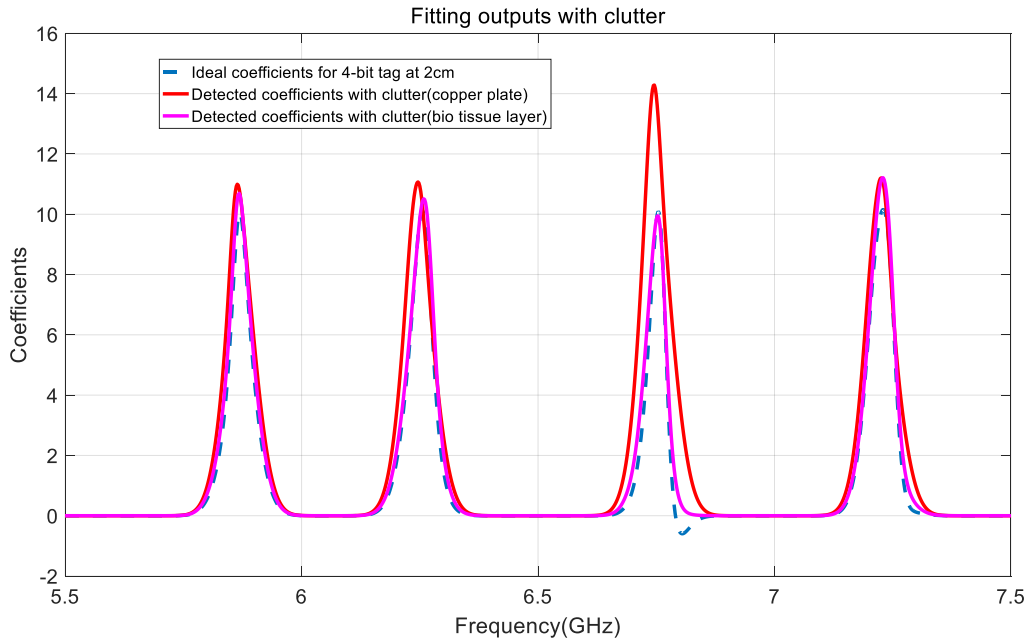

Figure 6.38– Detected frequency IDs from the cluttered signals

Output:

FreqID_1 = 1 1 1 1

Coeff_1 = 10.04 10.11 10.32 10.16

FreqID_2 = 1 1 1 1

Coeff_2 = 10.99 11.07 14.61 11.20

FreqID_3 = 1 1 1 1

Coeff_3 = 10.69 10.51 10.17 11.20

The Frequency ID is based on the coefficient obtained using the algorithm.

6.5 New detection algorithm for the detection of printed tags using VNA

6.5.1 Application of printed chipless RFID tags

The single antenna reader is developed to apply for the detection of a tagged bank note. A tagged banknote that is moving in translational motion is being detected by a reader on the desktop. The problem is to find whether the tag ID can be detected accurately while moving. The placement of the reader and the bank note movement is shown in Figure 6.39. The printed tags used for the detection are shown in Figure 6.40.

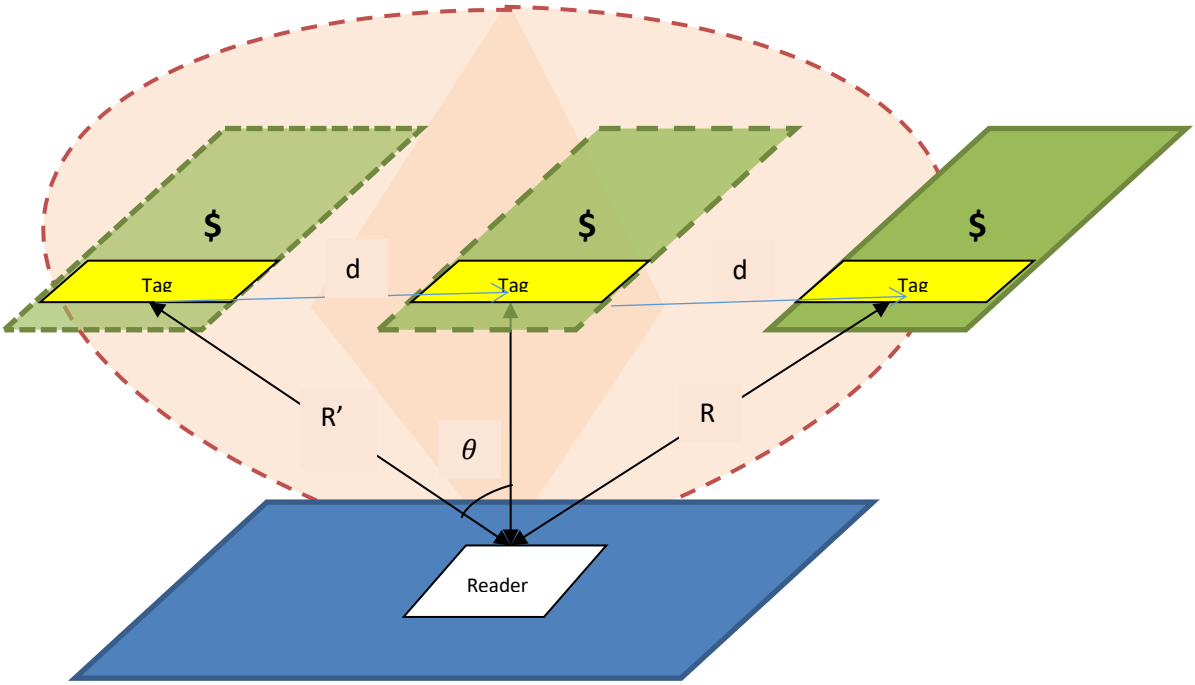

Figure 6.39 – Banknote reader set up

R- Minimum distance from reader to tag

R'- Direct distance from reader to tag

d- The horizontal distance from tag to mid position

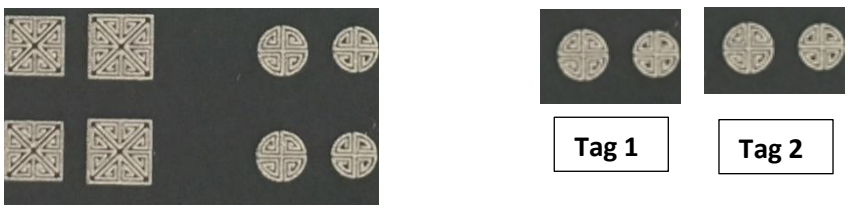

Figure 6.40 – Printed tags on PET

6.5.2 New detection algorithm on measured results using VNA

(i) The 2-bit printed tags Tag1-‘404_SC4_R2_6_bd_1_2’ and Tag2-404_SC4_R2_6_bd_3_4’ as shown in Figure 6.40 has been measured using the ACMPA and VNA. Each tag consists of 2 bits and when placed together it can be combined as a 4-bit tag. The measured results are plotted using Matlab as shown in Figure 6.41 which shows the 4-bit resonances.

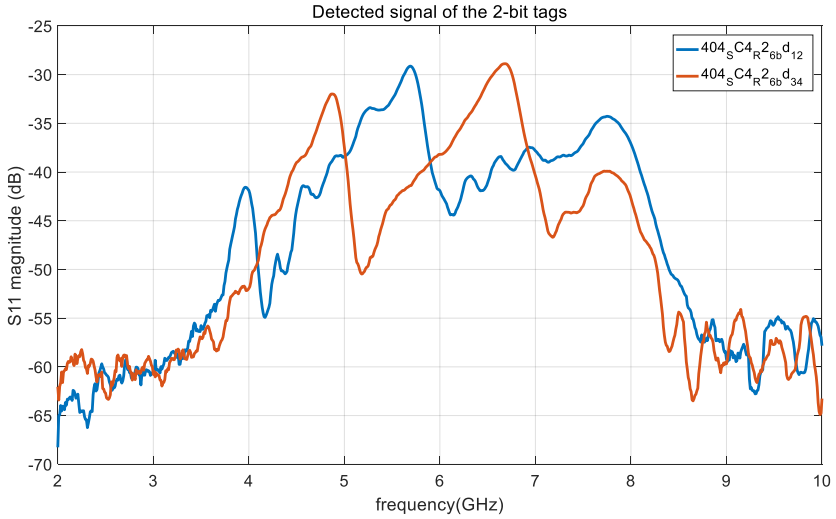

Figure 6.41 – Measured results of the two 2-bit tags using the ACMPA used for banknote project

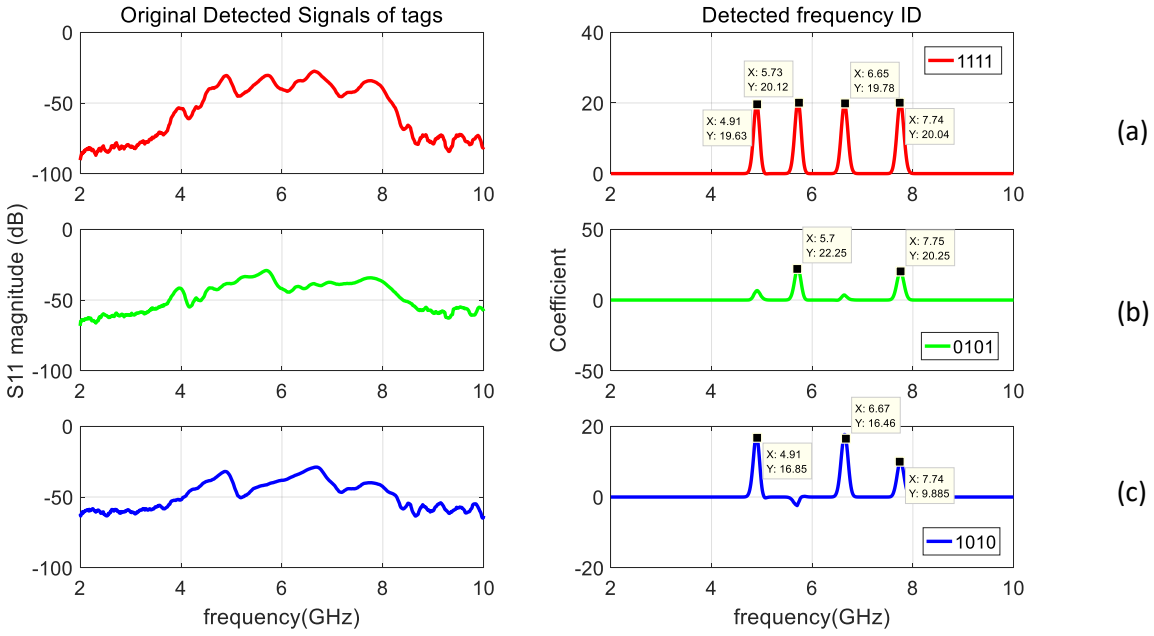

Figure 6.42 – Applying detection algorithm on measured results for printed tags (a) Detected signal of 4-bit tag giving the threshold coefficients (b) Detection of Tag 1 giving tag ID ‘0101’ (c) Detection of Tag 2 giving tag ID ‘1010’

The results after applying the detection algorithm is shown in Figure 6.42. Different tag IDs have been measured and applying the detection algorithm it can be seen that the correct tag ID of each instant can be detected successfully. As a 4-bit tag can have 16 combinations of Tag IDs, the algorithm should be robust to detect all combinations accurately. From this experiment it verifies that bit '1' and '0' can be detected correctly for any bit combination.

Output:

FreqID_1 = 1 1 1 1 FreqID_2 = 0 1 0 1 FreqID_3 = 1 0 1 0

Coeff_1 = 20.09 20.44 20.07 20.41 Coeff_2 = 0 22.71 0 20.25 Coeff_3 = 17.45 0 17.68 0

(ii) The printed tag 'SC4_RC2_bc4' has been measured using the horn antenna and VNA. The measured results and the detected result are shown in Figure 6.43.

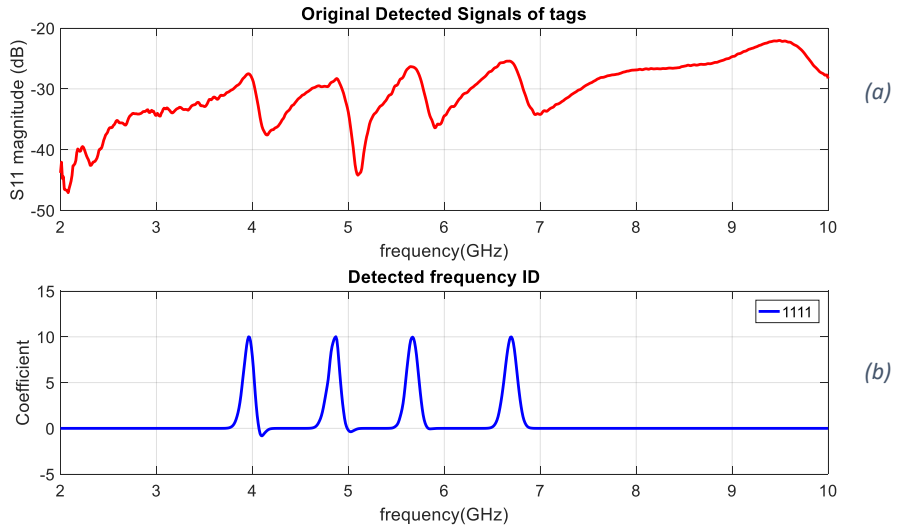

Figure 6.43 - (a) The measured result of 'SC4_RC2_bc4' using Horn antenna (b) Detected signal using the detection algorithm giving the output as '1111'

The printed tags are measured using the horn antenna used in Chapter 3. This test was performed to further clarify the detection of the tags using various antennas. It shows the same results as measured using the patch antenna. Therefore, the results can be proved correct and it opens the door to move forward in testing using the chipless RFID reader.

6.6 Applying the detection algorithm for tag at different distances

The printed tag on PET was tested for its RF performance using the VNA and was presented in the above section 6.5.2. This experiment presents the maximum reading distance of the patch antenna using the VNA. By increasing the distance of the tag from 1.5cm to 8.5cm the data was stored in the VNA. The stored data was then saved and transferred for post processing using Matlab. Figure 6.44 shows the obtained results for the tag placed at different distances.

By the results shown in Figure 6.44 the S11 magnitude has decreased from a maximum of -25 dB to -55 dB when the tag is moved away from the antenna. Beyond 5cm the signal is further distorted, and the signal is very weak.

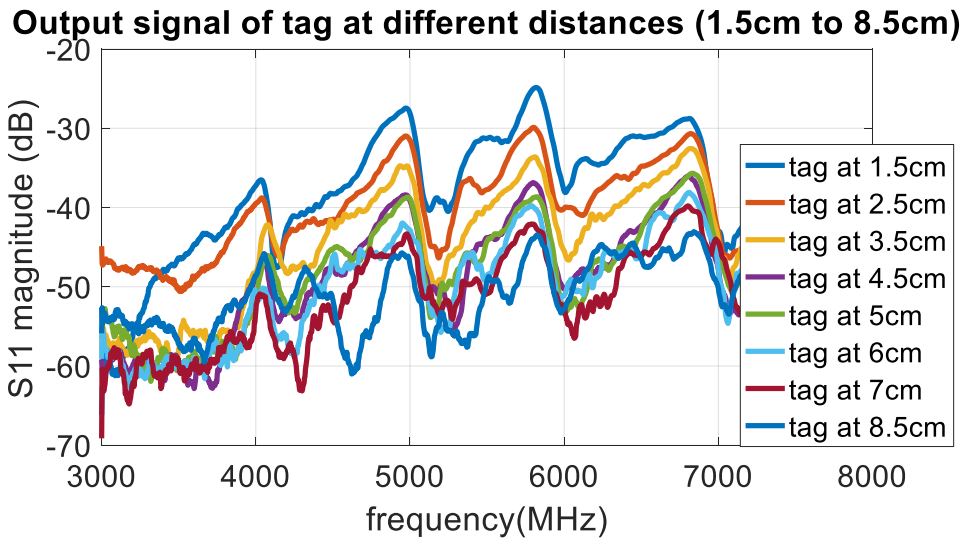

Figure 6.44– Received signal using VNA for the printed tag at different distances

The detection algorithm was applied to the above results and Figures 6.45 to 6.46 shows the detected spectrum coefficients of the tag. Up to 5 cm the 4-bit tag can be identified correctly. When the tag is at 6 cm as in Figure 6.45 the detected frequency ID is '0111', where the first bit coefficient is below the condition band to be identified as a bit '1'. In Figure 6.46., when the tag is at 7 cm again one bit is in error as it detects the frequency ID as '0111'. At a distance of 8.5cm there are 2-bit errors.

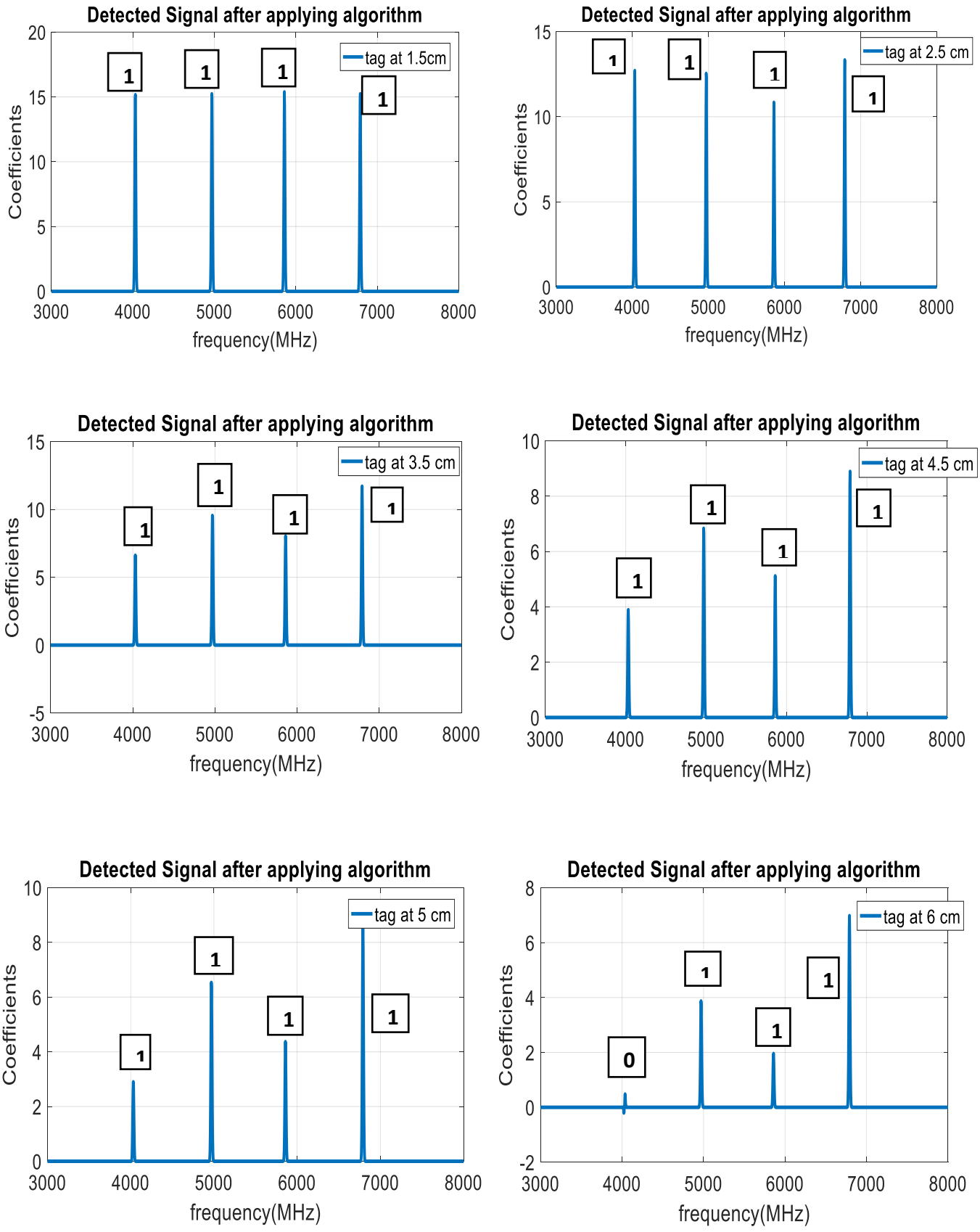

Figure 6.45 – Detected tag IDs after applying the detection algorithm for tag at 1.5 cm above the patch antenna to 6 cm above patch antenna

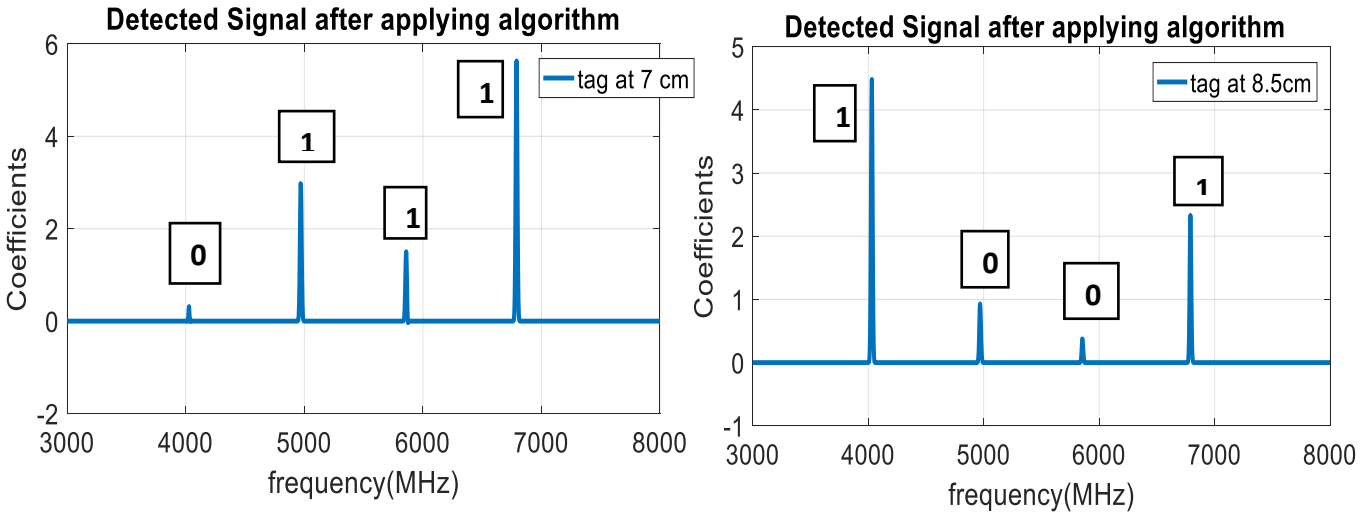

Figure 6.46 – Detected tag IDs after applying the detection algorithm for tag at 7 cm above the patch antenna to 8.5 cm above patch antenna

From these results it can be seen that the algorithm detects the correct tag ID when the received signal is at least above -40dB. If the tag RCS is higher than -40dB the tag resonances can be detected. The main aim of this experiment is to apply the adaptive wavelet-based detection algorithm in hardware for a chipless RFID system. The tag is placed within the half power beam width (HPBW) of the antenna. Signal processing using Matlab validate the received signals obtained to the original data of the tag using the proposed algorithm.

6.6 Comparison of VNA results and chipless RFID reader results

6.6.1 Experimental results using VNA for printed tag (3 bits)

The experimental set up for the tag test using the VNA is shown in Figure 6.47. The results obtained for the printed tag (on PET) using the vector network analyser is shown in Figure 6.48.

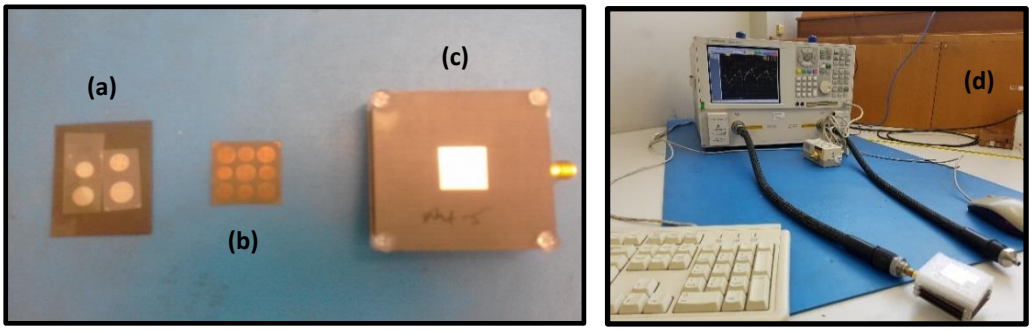

Figure 6.47– (a) Printed tag on PET flexible material (b) Copper tag on Taconic (c) Patch antenna (d) Experimental setup for printed tag test using VNA

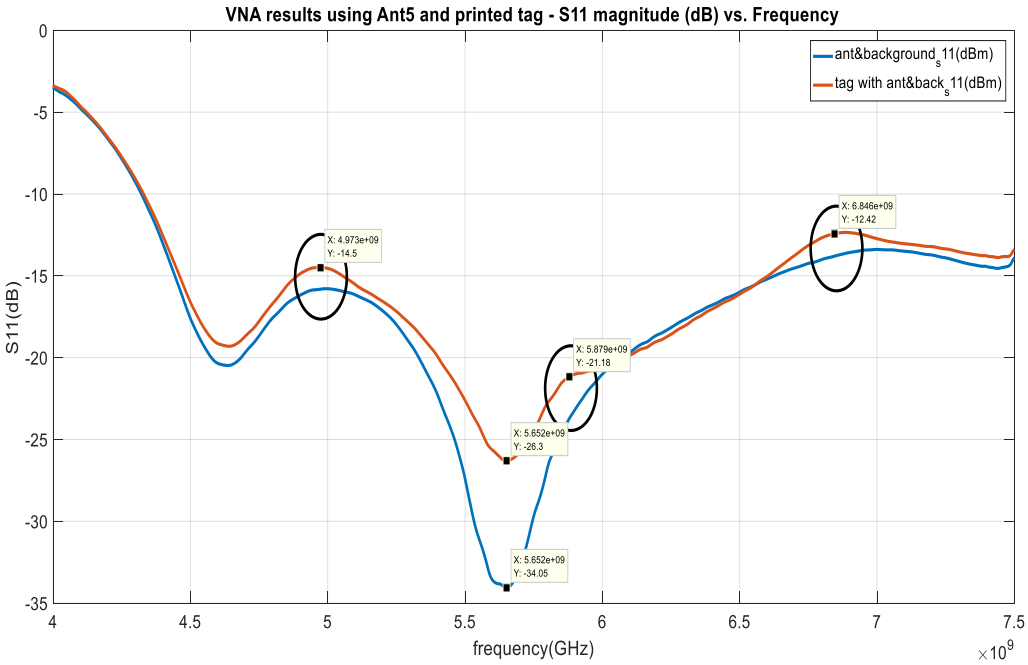

Figure 6.48 – (a) The blue line plot is the VNA s11 result for the antenna only. The foam was also placed in order to get the complete background data before placing the tag. (b) The red line plot is the s11 result when the tag was placed above the antenna on the foam where the foam has a thickness of 1cm.

As seen in Figure 6.48 the minimum variation in the tag result seen in VNA is around 1dB. The detection algorithm is applied to both signals in Figure 6.49. In the present modular reader, the tag identification is performed only using the magnitude, therefore when implementing the algorithm in the reader the minimum variation is considered.

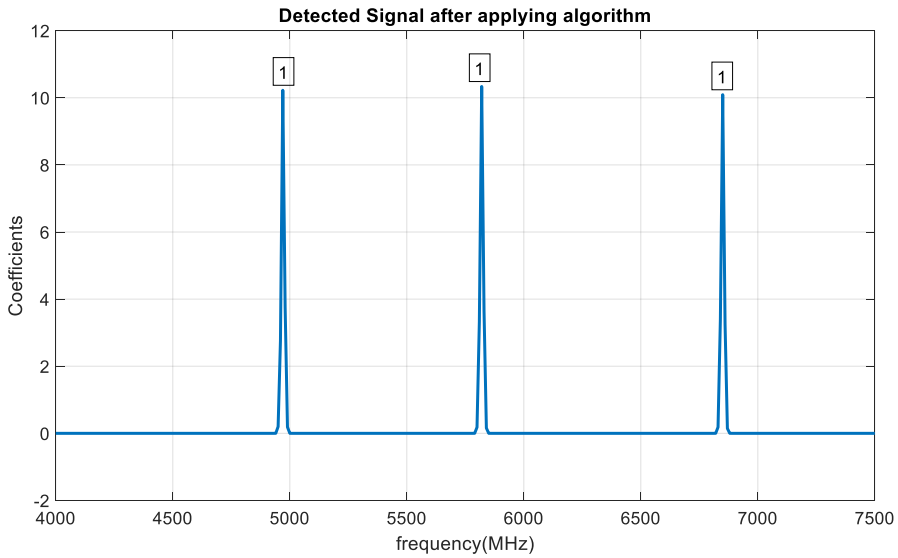

Figure 6.49 – Detected signal after applying the algorithm

The adopted wavelet has 3 parameters that can be changed its position, height and the width. Depending on the strength of the signal obtained by the reader these parameter values are adopted at the preliminary calibration so that the smaller variation can be amplified to get the correct ID. Once the preliminary calibration is done, the tag is tested using the modular reader. The results obtained from the reader are presented in the next section.

6.6.2 Experimental results using Modular reader for printed tag (3 bits)

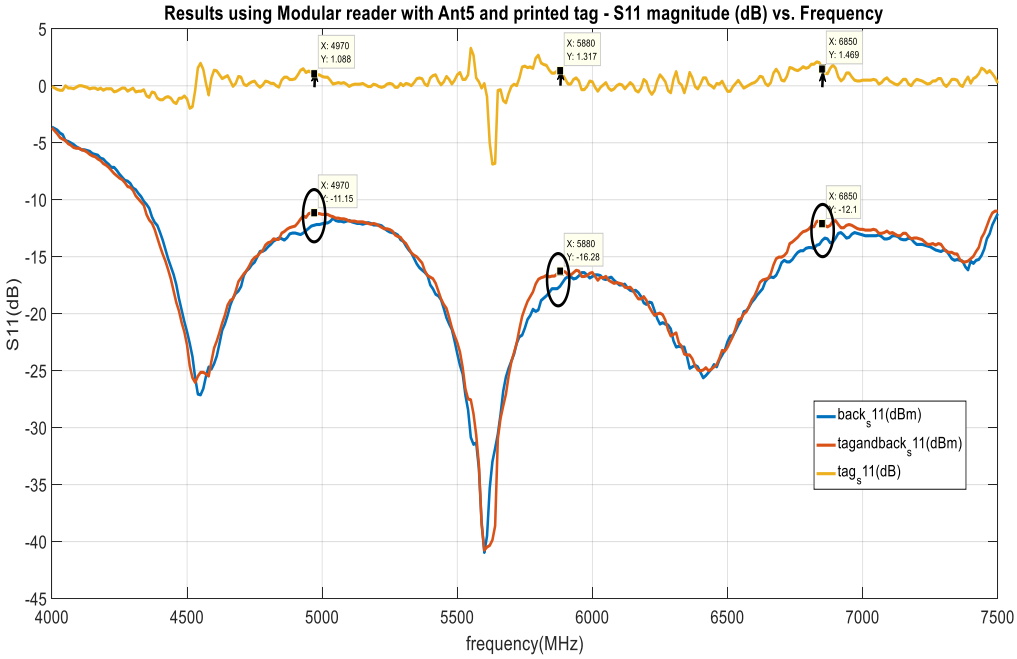

Figure 6.50 – (a) The blue line plot shows the s11 result when the tag is placed above the antenna using vector subtraction (b) The red line plot shows the s11 result for the tag by looking only at the magnitude subtraction these plots are obtained using Matlab with saved VNA data

As seen in Figure 6.50 the tag data is now embedded in noise and attenuations from the background and the system. The algorithm used filters unwanted peaks and retrieves the relevant peaks for tag identification. The binary decoding is also performed in the algorithm and the output on the screen is as shown below:

Peak magnitude (coefficient) = 10.8806 10.6417 10.8167

Peak location at (MHz) = 4970 5820 6850

Tag_ID = 111

The peak magnitude corresponds to the wavelet coefficient obtained from the transform. In the preliminary calibration the threshold coefficient is set to 10 when all bits are present which is tag ID '111'. When the tag is being read due to the surrounding environment the coefficient values are expected to change. After repeating the testing of tag for 100 times the condition band for detection was defined. Therefore the minimum coefficient and the maximum coefficient where the peak magnitude value is detected as bit '1' is set as 5 and 15. If the coefficient is below 5 it is identified as bit '0' and also if it is above 15 it is identified as bit '0'. This condition band should be further tested under different environments.

6.6.3 Experiment using VNA with copper tag (5 bits)

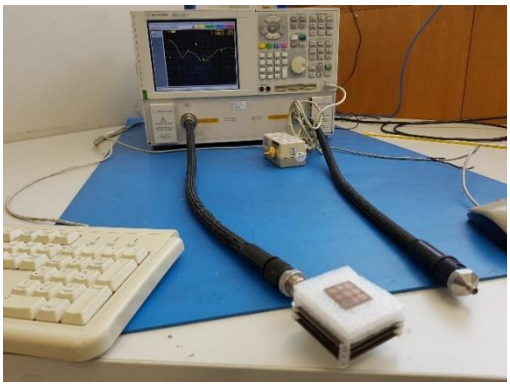

Figure 6.52 – Experimental setup for copper tag test using VNA

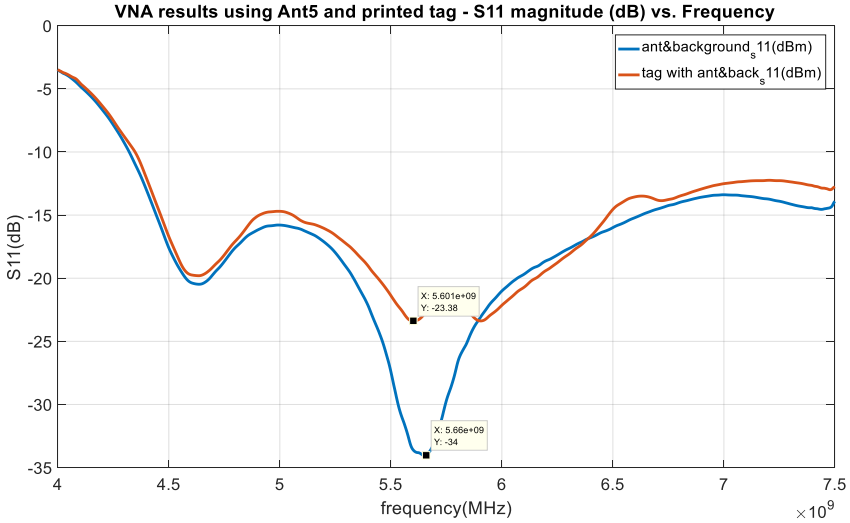

Figure 6.51 - (a) The blue line plot is the VNA s11 result for the antenna only. The foam was also placed in order to get the complete background data before placing the tag. (b) The red line plot is the s11 result when the tag was placed above the antenna on the foam where the foam has a thickness of 1cm.

6.6.4 Experiment using modular reader with copper tag (5 bits)

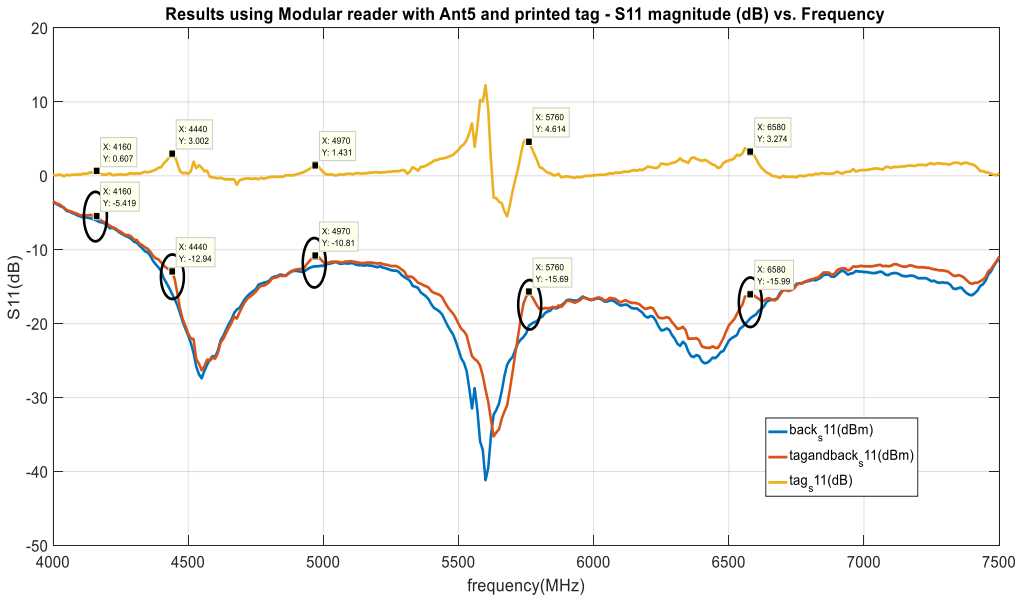

Figure 6.53 - Detection using the modular reader. (a) The blue line plot shows the background data (antenna + foam + noise). (b) The red line plot shows the received signal from the system when the tag was placed above the antenna on the foam. (c) The yellow line plot shows the subtraction of the signals (a) & (b) which gives the tag data to which the detection algorithm is applied to retrieve the tag ID

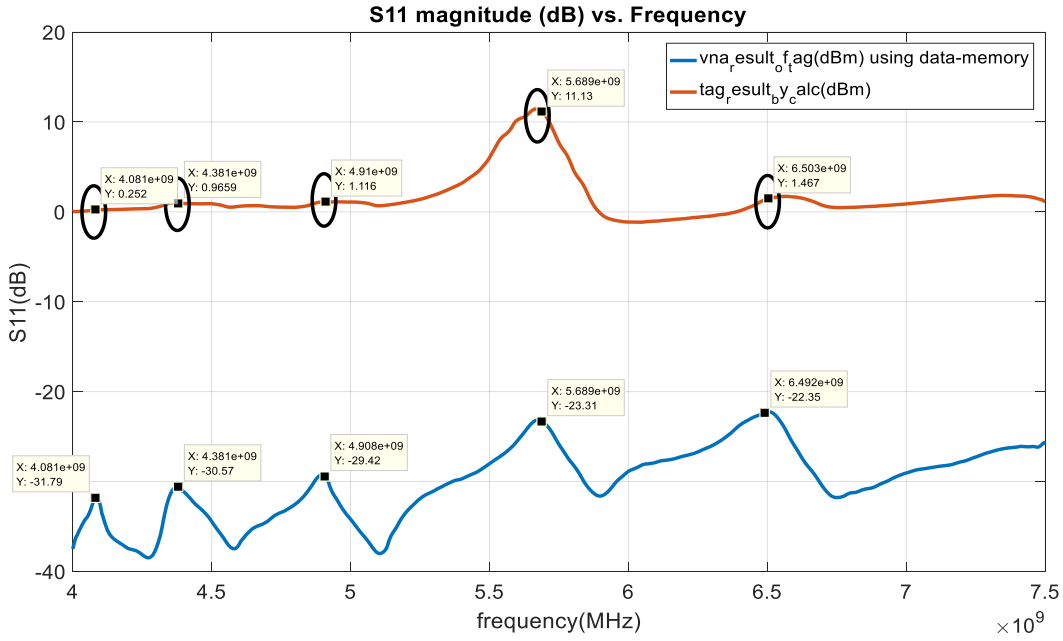

Figure 6.54 - (a) The blue line plot is the VNA s11 result. (b) The red line plot is the s11 result when the tag was placed above the antenna on the foam where the foam has a thickness of 1cm.

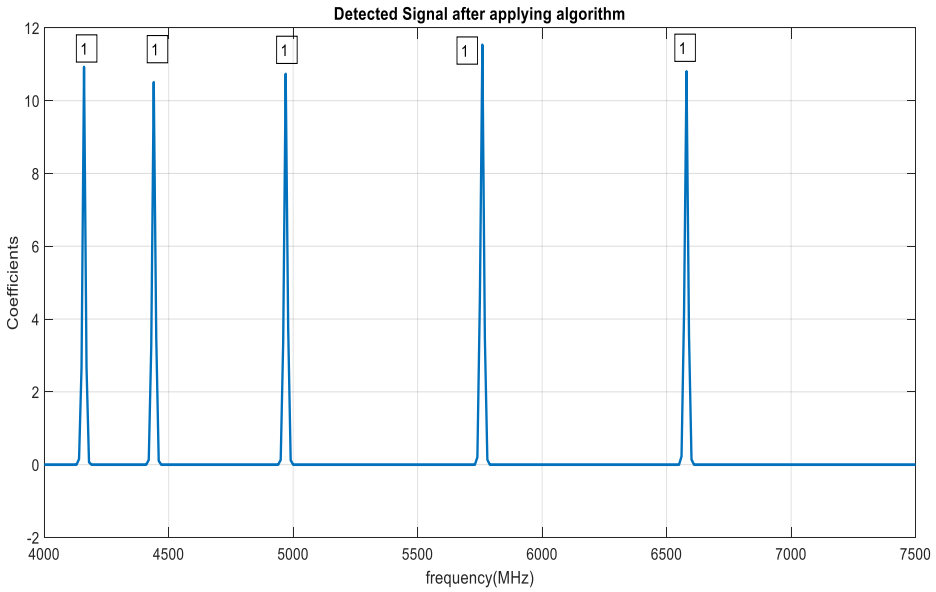

Figure 6.55 - Detected tag ID after applying detection algorithm.

The above results show that the printed tag as well as the copper tag is detectable using the modular reader. Comparing the results of section 6.6 it can be concluded that the modular reader gives the same performance in detecting the frequency IDs of chipless RFID tags when placed 1 – 2 cm above the reader antenna.

6.7 Conclusion

This chapter presented an approach and method to detect the ID of a chipless RFID tag using a single antenna reader. It explains the operation of the reader and how the pic-microcontroller is programmed with the detection algorithm.

Two types of tags have been tested, a printed tag which is flexible and will be in high demand for commercialization and a copper tag which has more durability. Both tags can be detected using the single antenna reader by applying the adaptive wavelet-based detection algorithm and gives robust detection of a static tag. By the characterization of clutter and detection presented in section 4 it shows that the received backscattered signal changes depending on the type of clutter around the tag. Mainly for conductive material like copper and gold the variation is high. This is expected as there is high reflection of electromagnetic radiation from conductive material and this effect the low power backscattered signal and raises its S11 magnitude (dB) level. In the experiment where the tag is held

by hand, the results show a variation. The results presented using CST simulation gives similar results and can be concluded that the electrical conductivity (El. cond), permeability (μ), resistivity (ρ) of the clutter environment effects the detection of a chipless RFID tag. By applying the new detection algorithm to tags under these clutter environment has shown that still the tag ID can be decoded under these circumstances.

The main aim of this research work has been the implementation of the detection algorithm in the developed single antenna reader. This has been successfully completed and tested and compared with the VNA results in section 6. The next goal is to improve the reading distance of the reader in order to detect tags on the move. As presented in this chapter the maximum reading range of this desktop reader is 5 cm above the reader antenna. Therefore, an array antenna is designed and integrated in the MMARS laboratory and the reader is further improved to detect tagged objects in motion and is presented in Chapter 8.

7 Detection error rate and sensitivity analysis of a chipless RFID system

7.1 Introduction

The signals backscattered from a chipless RFID tag are very weak when they reach the front end of an RFID reader. They are affected by both path-loss and fading introduced by the wireless channel between the tag and the reader. The signals received at the reader in a chipless RFID system are not digitally modulated and do not have provisions for forward error correction mechanisms like in a chipped RFID system. Therefore, the RFID reader completely relies on an analog and passive variation of parameters in the received signal such as amplitude, phase and time of arrival to decode information bits encoded by the tag [1]. These errors manifest as a form of noise that attenuates and shifts the resonance frequencies from there intended locations.

Many de-noising models use white Gaussian noise as its noise, but through experiment it can be seen that white noise is not applicable for a chipless RFID system. In Section 2 of this chapter coloured noise is introduced to determine the detection error rate of a moving chipless RFID tag and is compared with the probability of detection from the experimental results.

The sensitivity of the chipless RFID system is an important aspect to be looked at before commercialization as a product. Section 3 presents a repeatability and reproducibility study (Gage R & R) proposed to evaluate the robustness of the detector (reader) developed by MMARS Laboratory of Monash University for the process of reading the chipless RFID tags. In this study several operators perform the test to ensure the repeatability and the reproducibility of the system. It will help to investigate the detector variability compared to the process variability. For this study 4 appraisers were selected who has a minimum knowledge of the system and process and 20 sample tags were used for the measurements. The results of this research work prove that the chipless RFID reader system is ready for production.

This analysis performed on the detection error rate and the sensitivity of the reader builds confidence on the robustness of the new detection algorithm and the reliability of the reader after the implementation of the algorithm in a single antenna reader system. Further improvement to the reader and the detection algorithm for applications with real time movement in chipless RFID tags are presented in chapter 8 and 9.

7.2 Detection error rate Analysis using coloured noise

In this section first the coloured noise is defined followed by the factors that affect the backscattering signal of a moving tag.

7.2.1 Coloured noise

The power spectral density of a coloured noise process can be given by equation (7.1) [xx].

$$S(f) = \frac{L(f)}{|f|^{\alpha}} \qquad (7.1)$$

where α is a real number in the interval [-2, 2] and $L(f)$ is a positive slowly varying or constant function. If α > 0, $S(f)$ goes to infinity as the frequency, f, approaches 0. If α < 0, the process is anti-persistent and exhibits negative correlation between increments.

Due to the movement of the tag as explained in Chapter 3, the resultant signal shows some attenuation in magnitude and frequency shift. The causes for these variations can be due to clutter, interference, fading, Doppler Effect, moving away from a reader antenna's radiation pattern or due to the field in which the tag is placed in near (Reactive / Fresnel) / far field. These effects can range from an increase in error rate to a total loss of the tag data. In the following section the experimental set up of a moving chipless RFID tag in front of two reader antennas and their received signals are presented.

7.2.2 Experimental design and results

Two horn antennas are used in this experiment and the S21 parameter measurement of the vertical movement of a tag is observed using the Vector Network Analyser (VNA) as shown in Figure 7.1. A

hexagonal tag is used for the experiment. The tag is having 18-bits in the frequency range of 3-10 GHz. The 3-bits between 4-6 GHz are only focused in this experiment as shown in Figure 7.2. 4 – 6 GHz frequency range is selected as the horn antennas effectively works only in the frequency band. The horizontal distance between the tag and the horn antenna is first set to 15 cm. At 15 cm the tag is moved vertically between a distance of 0 - 30 cm and the S21 parameter in dB is saved in VNA at each 3cm interval. The experiment is repeated at 20, 25, 30 and 35cm distances from the antennas.

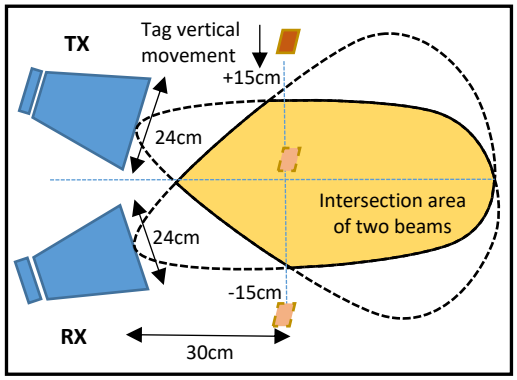

Figure 7.1 – Experimental set up using two horn antennas and hexagonal tag to measure S21 of the vertical movement of the tag

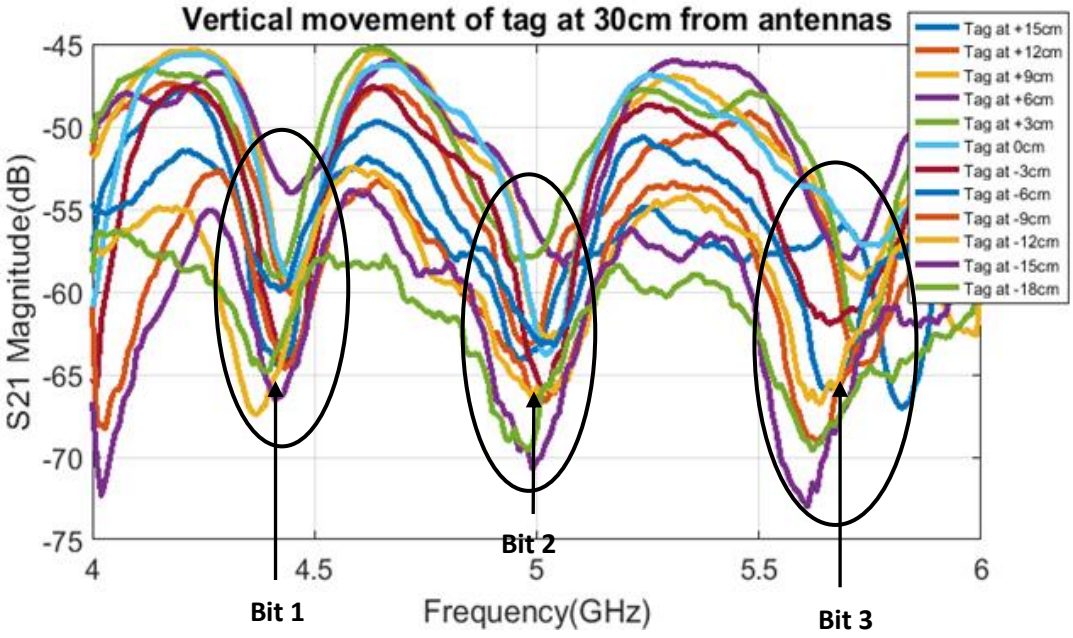

Figure 7.2 - Vertical movement of tag at 30cm from horn antenna set up

The results of the measured data when the tag is at 30 cm distance from the antenna is given in Figure 7.2. According to the results it can be seen that the amplitude and the frequency varies when tag is in vertical movement. From the above results the root mean square error (RMSE) is calculated for the amplitude variation in dB at the specific resonance frequency points. The 3 bits are namely at 4.41, 5, 5.7 GHz. The RMSE values are calculated using equation 7.2 given below.

$$RMSE = [\sum(fi - f0i)^2 / N]^{1/2} \quad (7.2)$$

where, fi – bit frequency

$f0i$ – bit frequency when tag is at 0 cm

It is repeated for the tags at different distances. Table 7.1 shows the results of the RMSE and it can be seen that the value of RMSE increases as the tag moves away from the mid position.

Table 7.1 - RMSE amplitude variation in dB at the specific resonance frequencies points

Freq. (GHz)	RMSE at 15cm	RMSE at 20cm	RMSE at 25cm	RMSE at 30cm	RMSE at 35cm
4.41	7.48	10.21	13.68	18.58	20.22
5	8.46	7.86	10.47	17.82	19.10
5.7	6.46	4.66	7.96	14.05	18.19

7.2.3 Analysis of results

7.2.3.1 Analysis of experimental results

The adaptive wavelet detection algorithm for chipless RFID has been applied and the detection error rate (DER) is then calculated based on the results at different distances using equations (7.3) and (7.4).

$$DER = 1 - throughput \quad (9.3)$$

where, $$throughput = \frac{N_S}{N_T} \quad (9.4)$$

where N_s is the number of successful tag detections and N_T is the total number of tag readings.

Table 7.2 – Change in probability of detection and detection error rate with increased distance from 15 cm to 30 cm.

Distance from antenna in cm	Probability of Detection	Detection Error Rate
15	0.75	0.25
20	0.83	0.17
25	0.92	0.08
30	1.00	0.00

7.2.3.2 Analysis of simulation results using Matlab

Using the VNA it is not possible to configure it for moving tag reading as it cannot capture the data while in motion. Therefore, the above experimental analysis of stepped motion with static reading is not sufficient to come to the conclusion of the detection error rate of a tag in motion. To calculate the detection error rate a higher number of data set is analysed. This has been performed in simulation using Matlab. The S21 parameter data are loaded in Matlab and are used as the tag response in the simulations. As explained in Section I, noise addition is done using coloured noise replacing AWGN which is used in previous research work. The value for α is chosen as 2 which adds 6 dB attenuation to the signal which is the closest to the attenuation shown in real time results. A data set of 10^4 is generated for the analysis. The detection error rate at different distances obtained by simulation are shown in Table 7.3.

Table 7.3 – Detection error rate and Signal to Noise ratio at different distances in simulation

Distance from antenna in cm	Signal to Noise Ratio (SNR)	Detection Error Rate
15	3.96	0.20
20	4.04	0.09
25	6.98	0.00
30	10.61	0.00

From the above results the detection error rate is minimum at 25 cm and 30 cm and closely matches with the experimental results. This shows that when the tag is not within the range of the intersection of the radiation patterns of the antennas the tag has a lower probability of detection.

7.3 Sensitivity analysis using gage R & R study

7.3.1 Sample preparation

The original sample tag selected for the test is shown in Figure 7.3. Each of the tags has 9 resonators and gives 3 different Frequency Signatures (FS). The relevant resonators giving same resonant frequency are marked as FS1, FS2 and FS3 in Figure 7.3 and Figure 7.4.

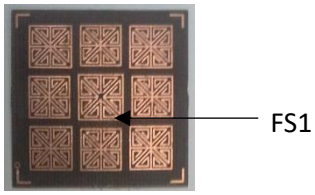

Figure 7.3 - Original sample tag used for test, the marked resonator gives frequency signature FS1

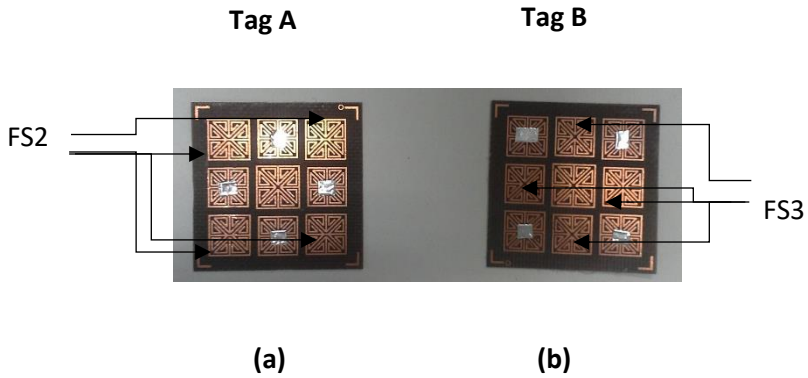

Figure 7.4 – The relevant resonators are shorted to obtain required tag frequency (a) 4 resonators giving frequency signature FS2 for Tag A (b) 4 resonators giving frequency signature FS3 for Tag B

By shorting the relevant resonators as shown in Figure 7.4 (a) and (b), two different tags were obtained which are Tag A giving FS1, FS2 and Tag B giving FS1, FS3. For Tag C in Figure 7.5 (a), all resonators were shorted except the middle resonator giving FS1 only. The Tag D shown in Figure 9.5 (b) is a reflector with no resonators present.

Figure 7.5- (a) Tag C having only one frequency signature FS1 (b) Reflector used for Tag D

20 Samples were selected, and the tag response was measured using the VNA. According to the correct measured data using the VNA the samples were randomly numbered and categorized into 4 groups as given in Table 7.4.

Table 7.4 - Grouping of samples for test (Tag A – 5 samples, Tag B – 5 samples, Tag C- 5 samples, Reflector – 5 samples)

Group	Tag ID	Sample Number	Frequency Signature
1	A	4,8,10,17,19	FS2, FS1
2	B	2,3,6,13,20	FS3, FS1
3	C	1,7,9,12,16	FS1
4	D/ Reflector	5,11,14,15,18	None

The rectangular shaped samples were then covered and numbered as shown in Figure 7.6. An arrow sign was printed on one side for alignment with the reader antenna.

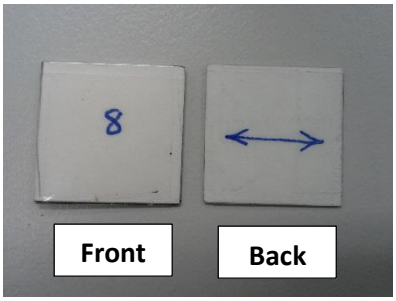

Figure 7.6– Sample used for Gage R&R test

7.3.2 Detector and test preparation

The modular reader setup shown in Figure 6.6 has been used for the R & R test. The reader setup includes the digital control section, various RF modules (frequency synthesizer, RF amplifier, low pass filter, directional coupler, frequency doubler and RF detector), a battery (to supply power to the reader system), 1 single polarized aperture coupled microstrip antenna and an LCD display (to display the outcome/result).

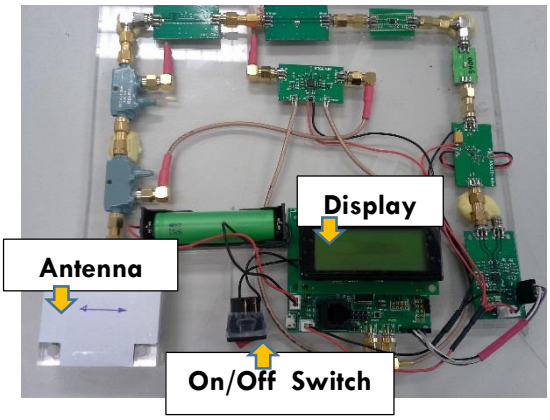

Figure 7.7- Modular Detector designed by MMARS team to be evaluated by the gage R&R test.

The selected samples were tested using the detector. The sample tags were placed on the reader antenna in alignment with the arrow marked on the antenna as shown in Figure 7.7 during the detection. The results were displayed on the LCD display shown in Figure 7.7.

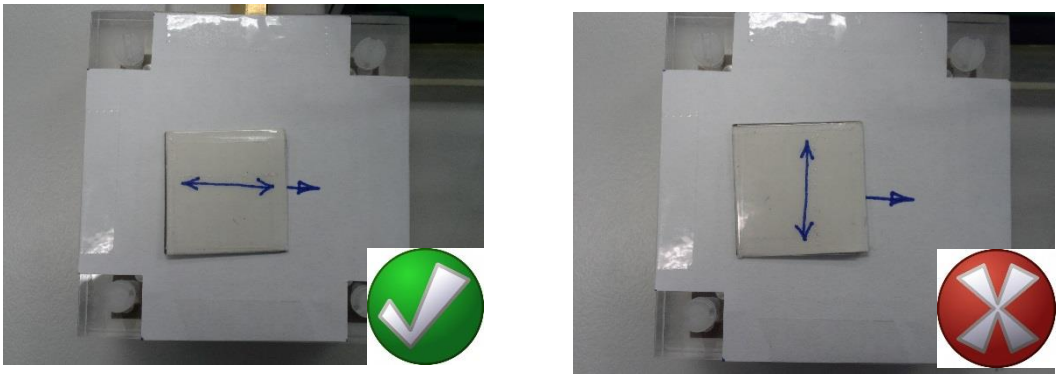

Figure 7.8- Correct placement of sample tags on reader antenna

The reader was re-calibrated using the on/off switch in between the tests.

To perform the test, 4 appraisers were chosen who did not prepare the samples and had minimum knowledge of the system. Each person had to use the detector 20 times in succession to read the 20 samples. 4 people in total performed the test, using the detector 80 times giving 80 results for the statistical analysis. Statistical analysis using 'Kappa' statistics can be found in the Appendix A.

7.3.3 Results and analysis

Results of the test is given in Table 7.5 below.

Table 7.5 – Results of Gage R&R Test performed in MMARS Lab

Sample #	Correct Tag ID	Appraiser 1	Appraiser 2	Appraiser 3	Appraiser 4
1	Tag C	C	C	C	C
2	Tag B	B	B	B	B
3	Tag B	B	B	B	B
4	Tag A	A	A	A	A
5	Reflector	R	R	R	R
6	Tag B	B	B	B	B
7	Tag C	C	C	C	C
8	Tag A	A	A	A	A
9	Tag C	C	C	C	C
10	Tag A	A	A	A	A
11	Reflector	R	R	R	R
12	Tag C	C	C	C	C
13	Tag B	B	B	B	B
14	Reflector	R	R	R	R
15	Reflector	R	R	R	R
16	Tag C	C	C	C	C
17	Tag A	A	A	A	A
18	Reflector	R	R	R	R
19	Tag A	C	A	A	C
20	Tag B	B	B	B	B

7.4 Conclusion

This chapter presents an approach and method to model the noise for a chipless RFID tag in movement. It gives an exposure to the parameters that are affected by a moving chipless RFID tag and gives an estimation to the robustness of its tag ID detection while in stepped movement. These results show that the selected noise closely match with the effect on the tag response due to movement. It shows that the antenna radiation pattern has a larger effect when the tag is in movement as it can be within or completely out of the antenna's vicinity. Therefore, more than its clutter environment or the distance from the antenna the fact that the tag is within the beam is important for the channel modelling of a chipless RFID tag in movement.

The sensitivity analysis using gage R&R study presented above shows the measurement system is adequate in producing reliable results with 95% agreement between appraisers and an overall 95% of samples measured by all appraisers matching known standards. Appraiser 1 and 4 both achieved 95% agreement by matching 19 out of 20 samples with confidence intervals ranging between 75.13 – 99.87%. Appraiser 2 and 3 matched 100% of samples to standards with a 95% confidence interval range of 86.09 – 100%. The high Kappa Statistics indicate the consistency and correctness of appraiser ratings is within acceptable limits.

This study has proven that the percentage process variation is less than 10% and hence the measurements using the detector is acceptable. It has proven the ability of an operator to consistently repeat the same measurement using the same reader (gage), under the same conditions and its ability, to be used by multiple operators, to consistently reproduce the same measurement of the same part, under the same conditions.

The detection error rate as well as the sensitivity of the reader system can be further developed by incorporating complex signal processing algorithms in the detection procedure. This will improve the reliability of the developed chipless RFID system to above 95% and make this technology suitable for commercial applications.

8 Application of detection algorithm for moving tag detection with improved reading range using array antenna

8.1 Introduction

This chapter is the heart of the thesis where the developed detection algorithm is further improved for the moving tag detection with improved reading range using array antenna. The single antenna reader hardware is also modified for better performance. Chipless RFID readers widely use two antennas for the interrogation of the tag and reception of the response, making them heavy and bulky. Also, the strong self-jamming leakage signal degrades the sensitivity of the reader and compromises the maximum reading range of the system [4]. MMARS Laboratory has proposed a single antenna chipless RFID reader enabled with a self-interference compensation unit (vector modulator unit) and an enhanced signal generation technique to address the above constraints [3].

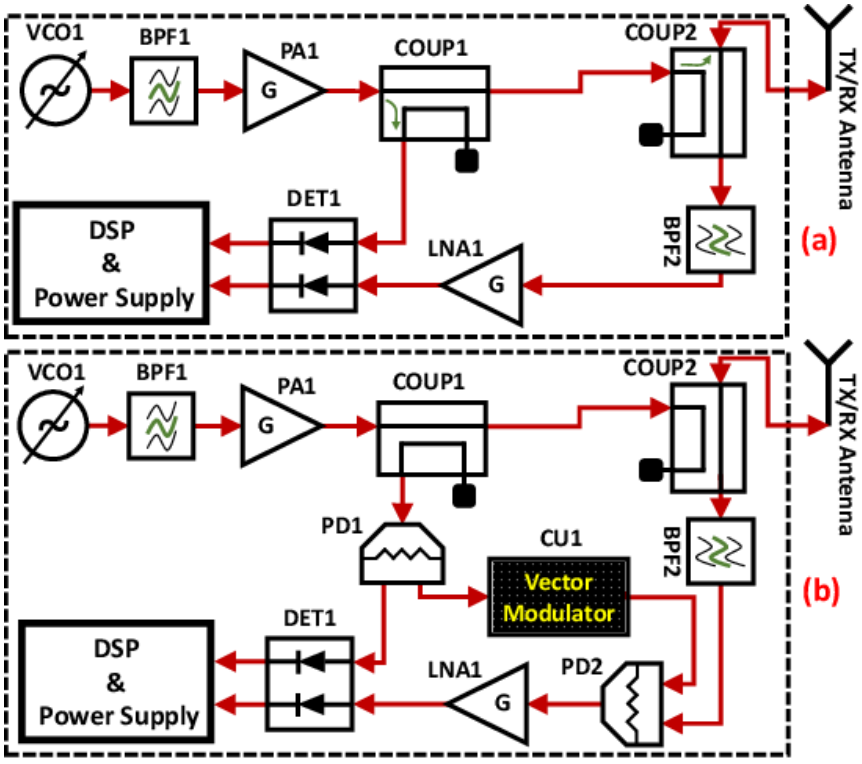

Figure 8.1 - Block diagram of a single antenna scalar chipless RFID reader: (a) Conventional architecture, (b) Enabled with vector modulator unit [3]

The proposed solution holds great promise for commercial adoption of this technology. Figure 8.1 shows a comparison of the two new generation single antenna readers and it shows the modified components of the RF section of the reader in Figure 8.1 (b). The microprocessor and the digital signal processing unit (DSP) remains the same. This modification has been able to minimize the noise level in the transmitted and received signal giving provision for better detection.

The 4 x 4 dual polarized aperture coupled stacked microstrip patch antenna (DPACMPA) designed and fabricated in the MMARS Laboratory of Monash University is shown in Figure 8.2 (a). The single element antenna configuration is shown in Figure 8.2 (b).

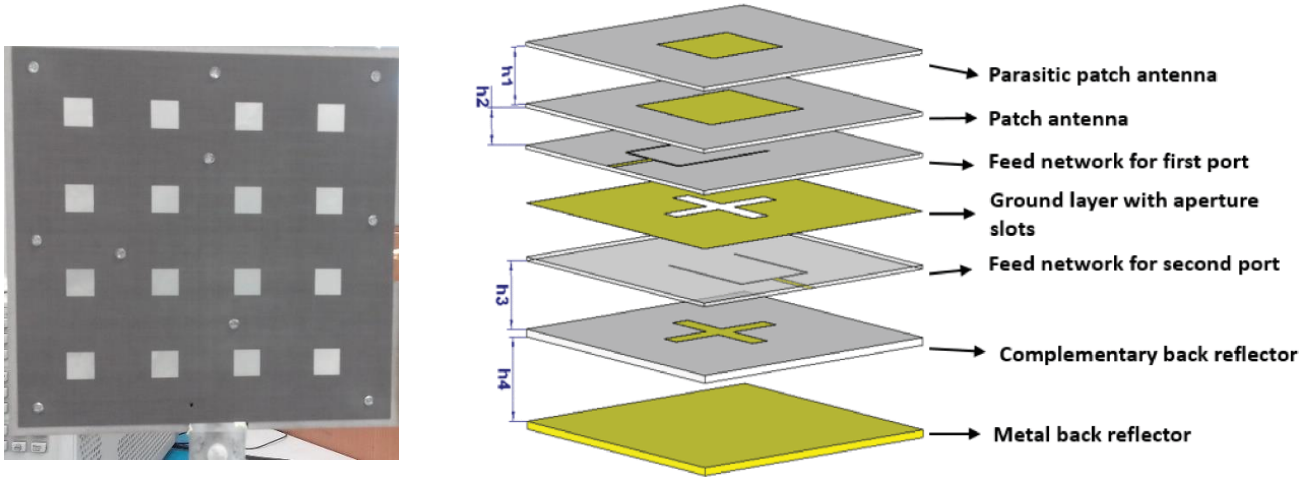

Figure 8.2 – (a) 4 x 4 patch array antenna with improved reading range (b) single patch antenna structure [4]

It has a frequency bandwidth of 4.2 to 7.1 GHz and has been chosen for the chipless RFID system to simplify the implementation of the reader and chipless RFID tag fabrication. The antenna is capable of detecting a multi-bit chipless RFID tag for high ranges above 8 meters using a commercial VNA as a reader with a transmit power of −10 dBm. Compared with the conventional chipless RFID systems with the maximal reading range of a few centimetres, the proposed antenna has achieved a much longer reading range [4]. The return loss of the array antenna is shown in Figure 8.3.

Apart from the improved vector modulator reader (VMR) and the array antenna the VNA and a commercial horn antenna is also used for the experiments performed and presented in this chapter. 4 types of chipless tags namely (i) Hexagonal copper tag, (ii) 4-bit circular patch tag, (iii) circular ring

tag and (iv) 4-bit rectangular patch tag are used in the different sections of this chapter. In Section 2, an analysis on the number of data sets captured by the reader depending on the antenna beamwidth covering a given area is presented. Also, experimental results are given for the detection of a chipless RFID tag in vertical movement using the horn antenna and the hexagonal tag using VNA as the reader.

This research work is delivered for the development of a smart trolley project and the main goal is to detect a tagged item while it is dropped into the shopping trolley and while it is removed from the shopping trolley. Therefore, the tags need to be fixed onto the items as well as can be covered by a material for protection. CST simulation in Section 2 shows the effect of covering the tag with materials for tags with and without the ground plane. In Section 3 and 4, a wide range of experiments are presented in order to find the effect of attaching the tag to different items using the VNA and the VMR as the reader. The results have proved successful detection of tags in vertical movement using the VMR reader. This research work expands into Chapter 9, where the real-time testing is presented inside a shopping trolley.

8.2 Detection of chipless RFID tag in movement

8.2.1 Analysis on the number of data sets captured by reader depending on the antenna beamwidth covering the shopping trolley

In this task the number of data sets that can be captured by the reader while the tag is dropping vertically is studied. The antenna aperture is varied considering it is designed for single or two antenna reader. Figure 8.3 shows the parameters related to S21 measurement for a vertical tag in movement.

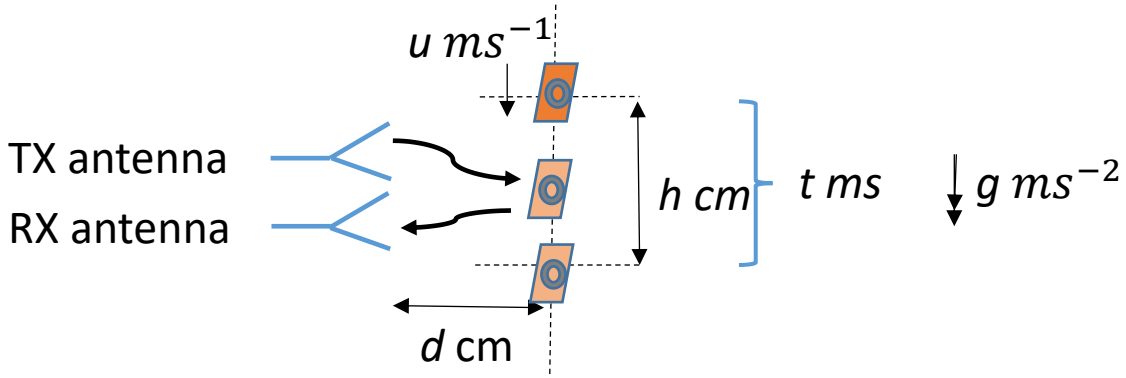

Figure 8.3 – Data capturing while the chipless tag is in vertical movement

As seen in Figure 8.3 when the tag is dropping it will pass through a vertical distance of h which is approximately same as the height of the aperture of the transmitting and receiving antennas. Within this region the tag should be detected by the reader. The time taken by the reader to transmit the signal to hit the target and get the reflected signal back from the tag and process the data need to be calculated in order to see how many data captures can be done while the tag passes this region. Also, the time that the tag is within the h region needs to be calculated. This time depends on the initial velocity of the tag which controls the speed of the dropping and also the vertical distance it is directly in front of the beam of the antenna.

The parameters are defined as follows:

$g -$ gravitational acceleration
$h -$ vertical distance of dropping within beamwidth
$t -$ time taken for the dropping
$u -$ initial velocity

Writing the equation for motion in vertical direction,

$$h = ut + \frac{1}{2}gt^2 \tag{8.1}$$

gives, $t = \sqrt{2h/g}$ when u = 0

If the time taken to process one data set is (single frequency sweep) t_s, the number of data captures C during the dropping is given by,

$$C = \frac{t}{t_s} \tag{8.2}$$

Based on equations (8.1) and (8.2) for different h values C has been calculated in Table 8.1. Here it is calculated for free dropping with $u=0\ ms^{-1}$ and $g = 9.8 ms^{-2}$.

For the reader if the frequency sweep is 2 GHz and the sampling frequency is 10 MHz, there will be 200 points generated. Assuming the PLL time and signal processing time as 100 µs the time taken for a single frequency sweep can be calculated to be 20 ms.

Table 8.1 – Calculation of data captures during the free dropping of the tag

h (cm)	*t (ms)*	t_s *(ms)*	C
10	143	20	7
20	202	20	10
30	247	20	12
40	286	20	14
50	319	20	16

8.2.2 Experiment with two big horn antennas and hexagonal tag, S21 measurement using VNA

The two big horn antennas are used to experiment the S21 measurement of the vertical movement of a tag using the VNA as shown in Figure 8.4. The two horn antennas are connected to port 1 and port 2 of the VNA and one antenna acts as the transmitter and the other as the receiver. S21 parameter (dB) vs. frequency is measured and the data is stored in the VNA. Two antennas are used in this experiment to get the maximum beamwidth to maximise the dropping distance.

Figure 8.4 – (a) The experimental setup with two big horn antennas (0-18GHz) for S21 measurement using VNA (b) The hexagonal tag of 18-bits working in the range of 3-10GHz

The hexagonal tag is used for this experiment having 18-bits in the frequency range of 3-10 GHz. The 4-bits between 4-6 GHz are only focused in this experiment as shown in Figure 8.5. Important parameters related to the horn antenna, tag and VNA are given in Table 8.2.

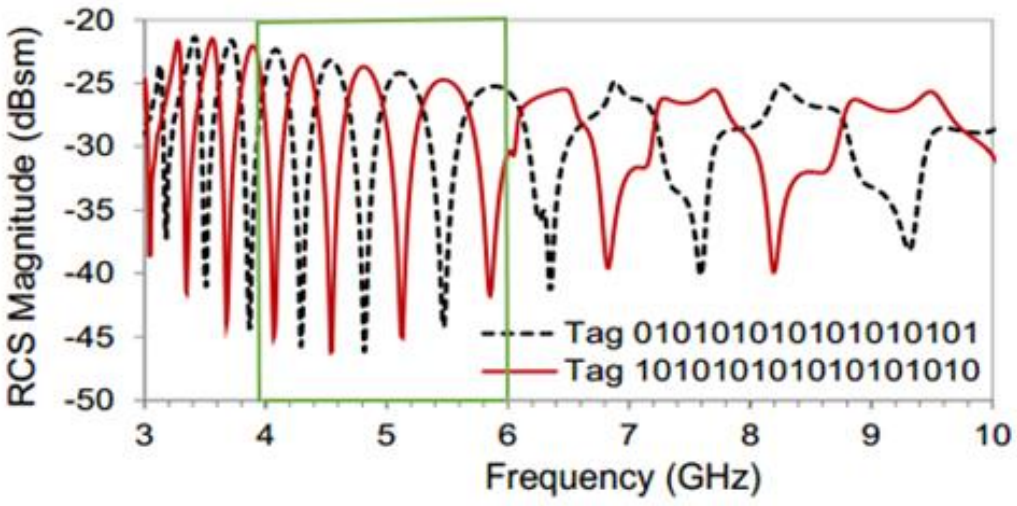

Figure 8.5 - RCS of the hexagonal tag with 18-bits. CST simulation results for two different tag IDs as shown in dotted black line and red line plot. The highlighted bits from 4-6GHz is focused in this experiment.

Table 8.2 - Important parameters related to the tag, horn antenna and VNA used in the experiment

Parameters	**Value and Item**
Total bits encoded in a tag	3 bits
Types of Antenna	Horn Antennas
Area of Antenna	24 x 14 cm square
Resonance Frequencies	[4.41, 5, 5.7] GHz
Experimental Distance (Horizontal)	[15, 20, 25, 30, 35] cm
Experimental Distance (Vertical)	[3-30]cm at every 3cm interval
Power IF Bandwidth	-15dBm 35kHz
Analysis Bandwidth	2 GHz

The horizontal distance between the tag and the horn antenna is first set to 15 cm. At 15 cm the tag is moved vertically between a distance of 0 - 30 cm and the S21 output is saved in VNA at each 3 cm interval. The experiment is repeated at 20, 25, 30 and 35 cm distances from the antenna. The results of the measured data are given in Figures 8.6, 8.7, 8.8 and 8.9. According to the results it can be seen that the amplitude and the frequency varies when tag is in vertical movement.

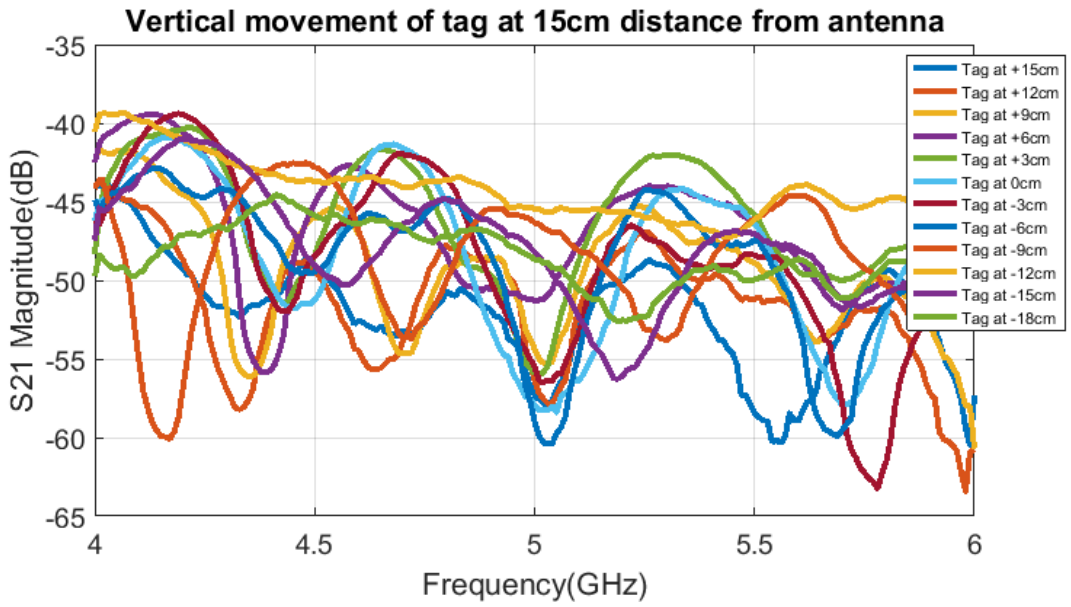

Figure 8.6 – Vertical movement of tag at 15 cm from Horn antenna set up

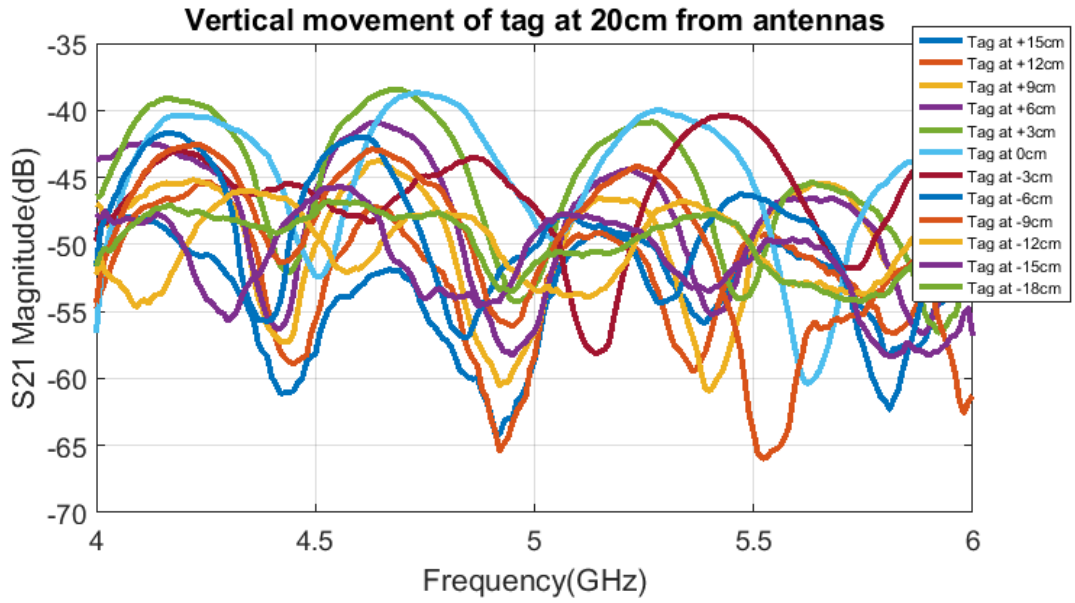

Figure 8.7- Vertical movement of tag at 20 cm from Horn antenna set up

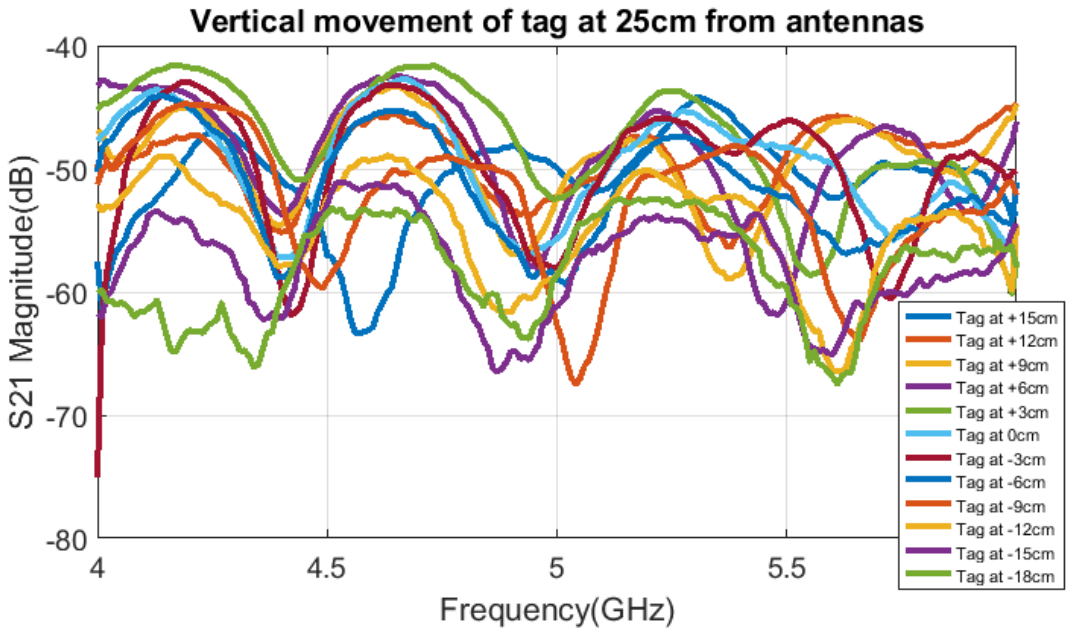

Figure 8.8 - Vertical movement of tag at 25 cm from Horn antenna set up

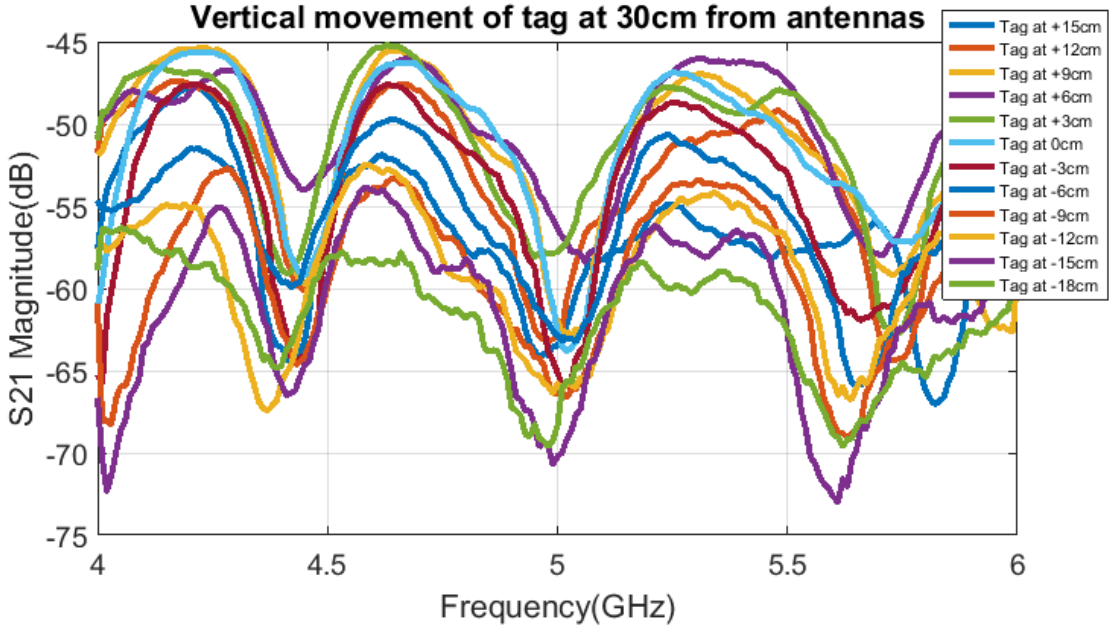

Figure 8.9 - Vertical movement of tag at 30 cm from Horn antenna set up

For the results at 20 cm and 30 cm applying the detection algorithm the variation in its coefficients is shown in Table 8.3 and 8.4. The confident band for detection is set between -3.5 and -16 so that the probability of detection is more than 80%.

Table 8.3 - Wavelet coefficient and detected tag ID when the tag is at 20cm

Vertical distance from center (cm)	Coefficients	Detected Tag ID
+15	-10.9845 -5.8872 -7.7926	111
+12	-9.8248 -5.2422 -7.6015	111
+9	-9.0474 -5.4137 -3.9096	111
+6	-7.9702 -5.5491 -4.4660	111
+3	-6.4291 -4.5110 -3.9718	111
0	-4.0790 -3.7250 -6.9877	111
-3	-3.0470 -3.5640 -7.1397	011
-6	-5.6761 -3.6020 -7.7870	111
-9	-5.9612 -4.5310 -9.3146	111
-12	-3.6910 -5.4875 -8.1882	111
-15	-4.3910 -3.4200 -7.5654	101
-18	-4.7110 -4.4600 -8.5155	111

Table 8.4 - Wavelet coefficient and detected tag ID when the tag is at 30cm

Vertical distance from center (cm)	Coefficients	Detected Tag ID
+15	-12.5352 -8.9658 -9.7999	111
+12	-10.3865 -8.1907 -13.9715	111
+9	-10.2195 -9.5976 -11.2083	111
+6	-7.3674 -7.4810 -10.7001	111
+3	-9.4932 -6.9699 -13.1561	111
0	-9.9922 -9.9288 -9.8497	111
-3	-12.6315 -10.7495 -12.4231	111
-6	-10.2624 -9.6877 -14.0705	111
-9	-12.7294 -10.9902 -14.2927	111
-12	-11.7572 -10.8572 -13.5651	111
-15	-13.1921 -12.0475 -15.1482	111
-18	-11.3519 -10.8069 -15.4234	111

According to the above results the probability of detection (P_D) is 83.33% when the tag is at 20 cm from the antenna set up and is 100% when the tag is at 30 cm.

These results show that if the antenna aperture is around 30 cm and if the chipless RFID reader can read 12 sets of data, up to 30 cm distance the correct tag ID of the hexagonal taconic tag can be detected.

8.2.3 Passive microwave circuit design and simulation for moving tag

A ring resonator tag is designed for the purpose of simulations for different application scenarios and testing in signal processing. This 4-bit tag gives 4 frequency resonances between 3.5 and 5.5 GHz range as shown in Figure 8.10. By changing the line widths which changes the gap widths the position of the 4 bits can be changed.

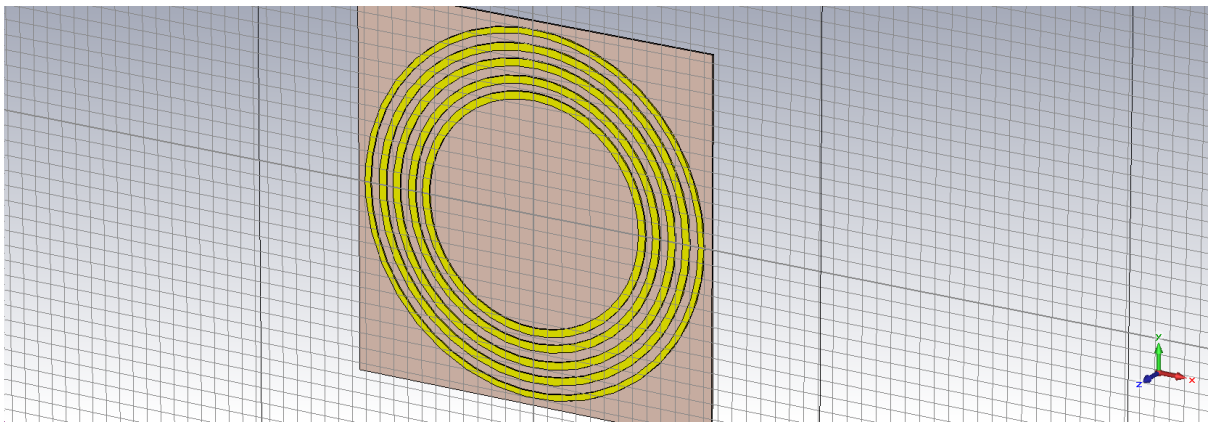

Figure 8.10– 4-bit circular ring tag

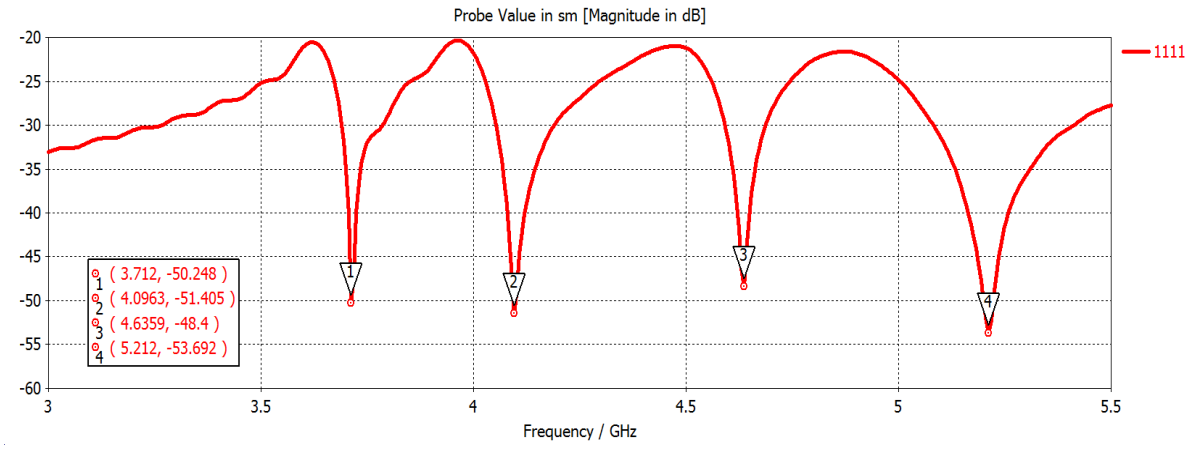

Figure 8.11– 4-bit tag response when the line widths are 0.4, 0.5, 0.5, 0.5, 0.4 mm respectively giving frequency signature at 3.7 GHz, 4.1 GHz, 4.6 GHz and 5.2 GHz

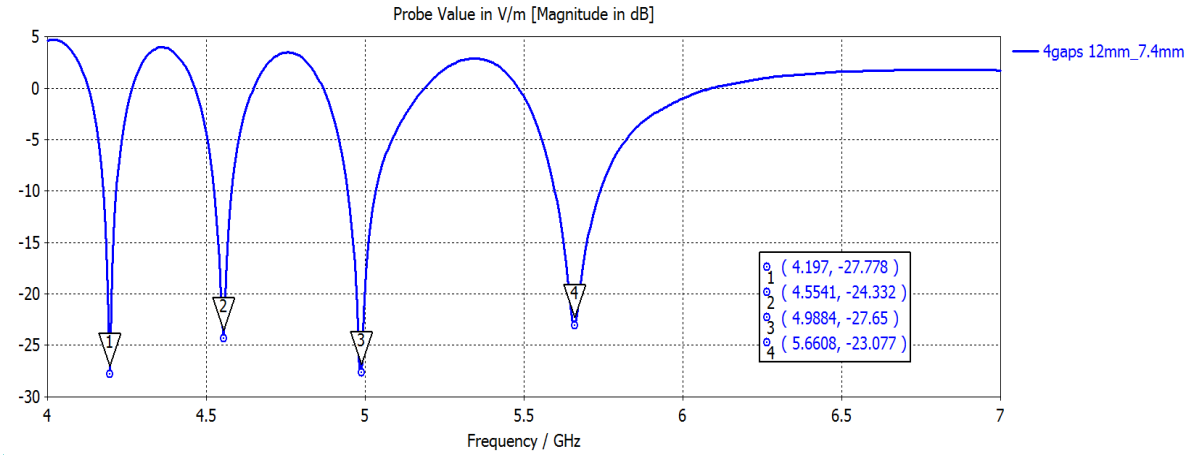

Figure 8.12 – 4-bit tag response when the line widths are reduced from 12 to 7.4 mm giving 4 bits within 4 to 7 GHz range.

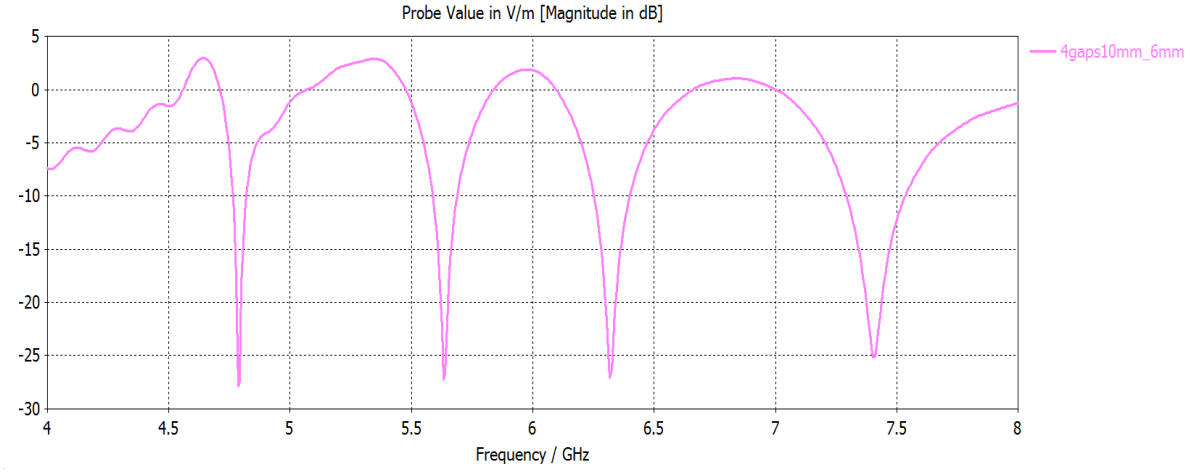

Figure 8.13 - 4-bit tag response when the line widths are reduced from 10 to 6 mm giving 4 bits within 4 to 8 GHz range.

In Figure 8.11 the resonances are between 3.5 to 5.5 GHz. The line widths are 0.4, 0.5, 0.5, 0.5 and 0.4 mm giving equal gap widths. In Figure 8.12 the resonances are between 4 to 7 GHz and in Figure 8.13 the resonances are between 4 to 8 GHz. The frequency range of the chipless RFID reader is also between 4 to 8 GHz which is used in these simulations to compare the measured outputs.

By introducing a stub between the gaps allows generating the different tag IDs 0101, 1011, 1101 etc. Figure 8.15 shows the different tag IDs with the introduces stubs.

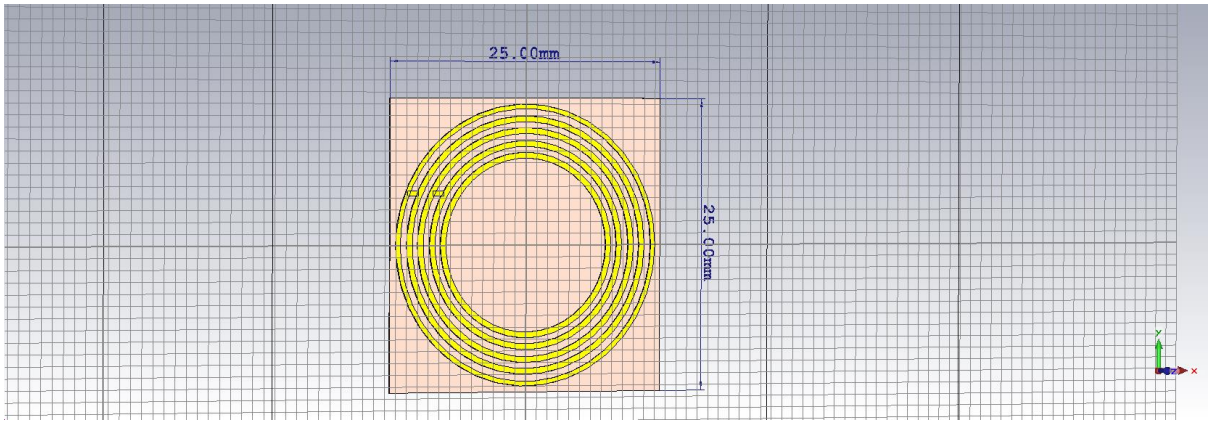

Figure 8.14– 4-bit circular ring tag with stubs to generate different tag IDs

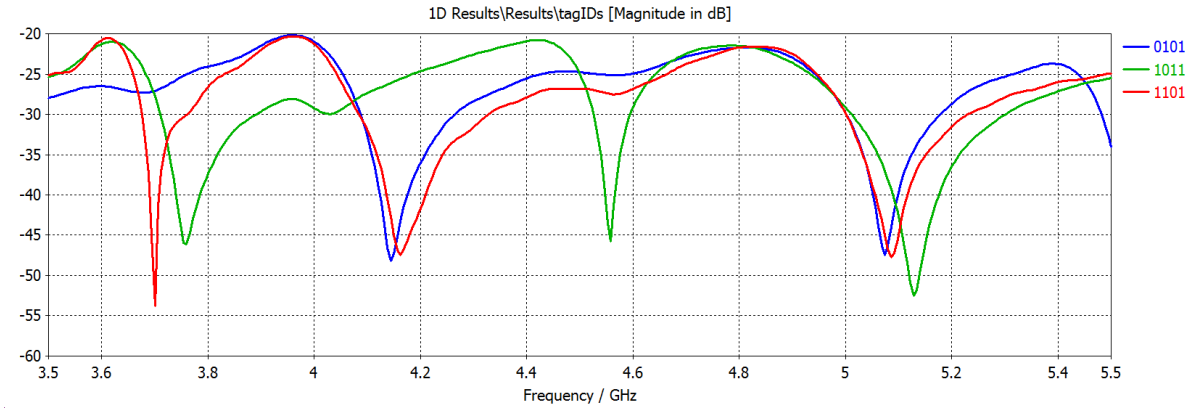

Figure 8.15 – The different tag ID responses 0101, 1011 and 1101

8.2.4 Simulation of a chipless RFID tag covered with a material layer

The final application of this reader with an array antenna is to detect tagged items dropping into a smart trolley. So, the tag is to be covered with a thin material to give protection. The objective of this simulation is to obtain the correct tag ID while the tag is covered with a material of thickness less than 500µm. Two tag designs have been tested with and without ground plane.

8.2.4.1 Simulation with a circular ring tag without ground plane

A circular ring tag design is used in this simulation which gives 4-bit resonances. The tag design and its simulated results is shown in Figures 8.16 and 8.17.

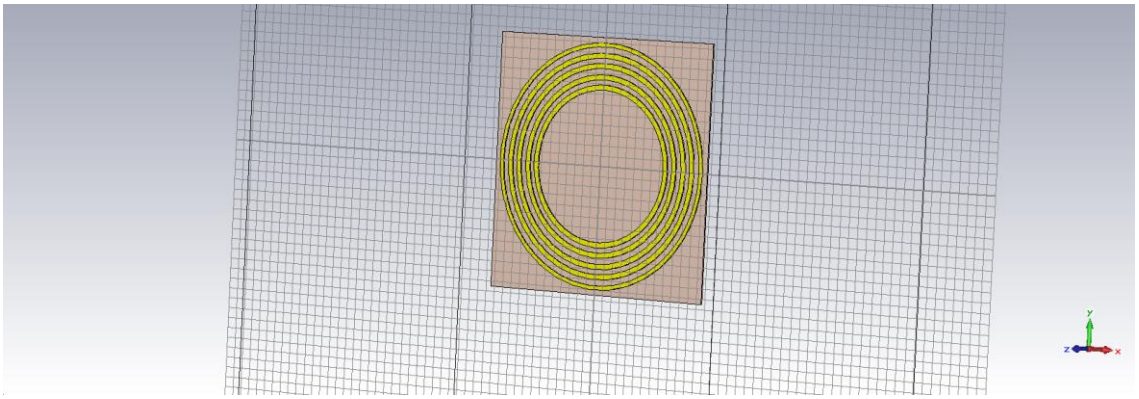

Figure 8.16 – 4-bit circular ring tag

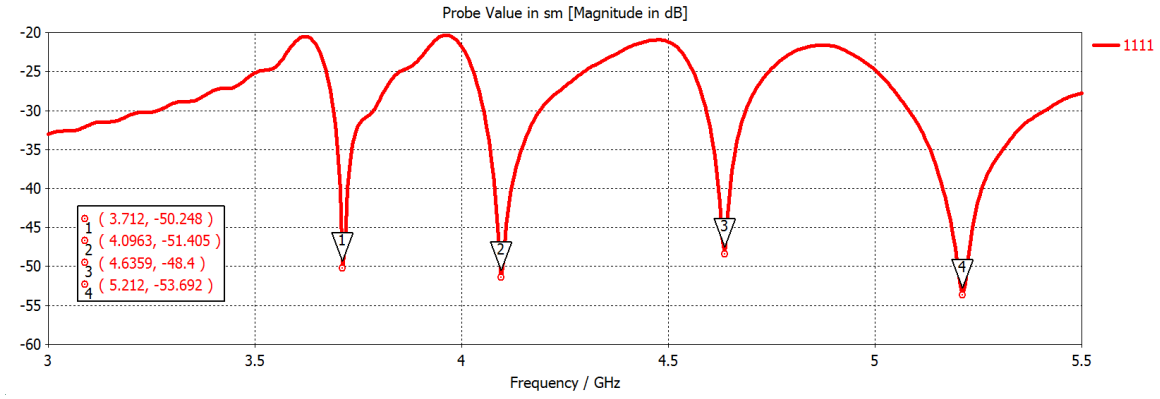

Figure 8.17 – RCS of the 4-bit circular ring tag

The tag is then covered by a layer of material and is tested whether the correct frequency signature is retrievable. Paper and BOPP has been used as the material as shown in Figures 8.18 and 8.20 and the results are shown in Figures 8.19, 8.21 and 8.22. The thickness of the layer has been varied from 1 to 100 µm in 20 µm steps and from 100 to 500 µm in 100 µm steps.

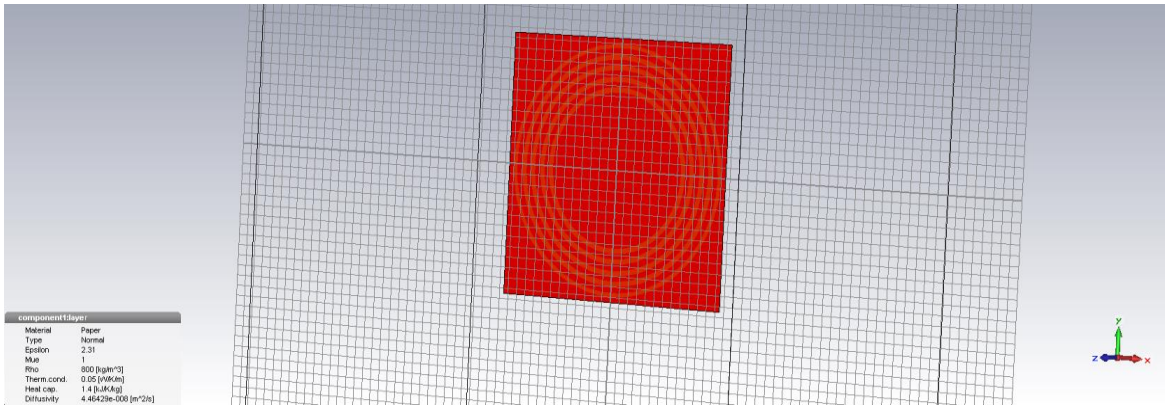

Figure 8.18 – Tag covered with paper layer

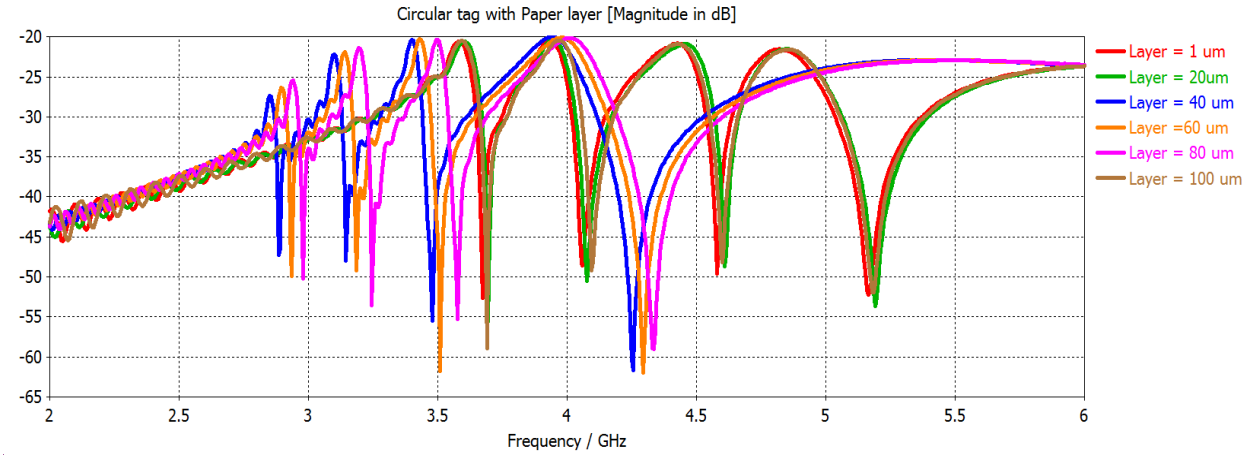

Figure 8.19 – Simulation result when the paper thickness is varied from 1 to 100 µm

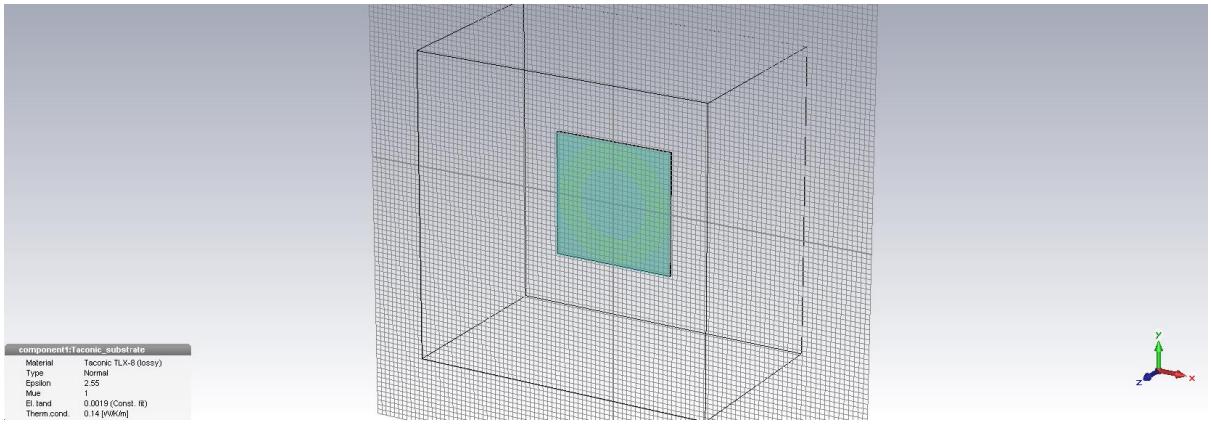

Figure 8.20 – Tag covered with BOPP layer

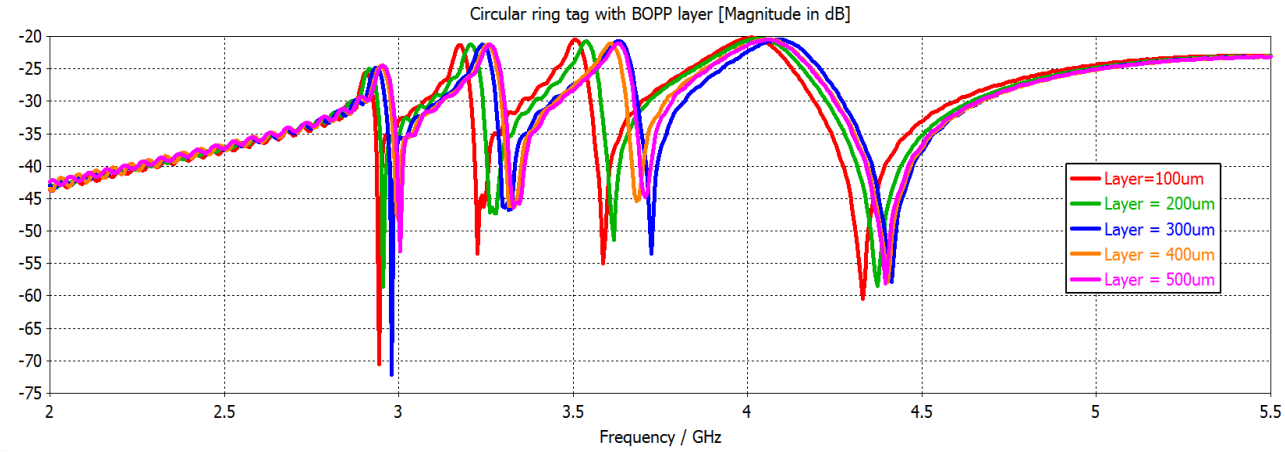

Figure 8.21– Simulation result when BOPP layer thickness is varied from 100 to 500 µm

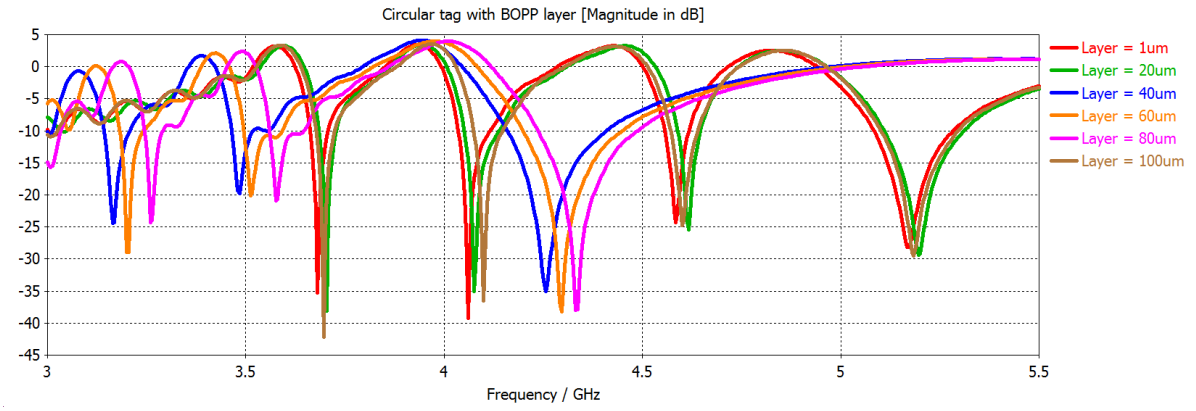

Figure 8.22 - Simulation result when BOPP layer thickness is varied from 1µm to 100µm

According to the results in both cases though the 4 bits are visible a frequency shift is observed. When the layer is 1, 20 and 100 µm the frequency shift is negligible, but when its 40, 60 and 80 µm the resonances have moved towards 3GHz which is approximately a 0.7 GHz shift.

8.2.4.2 Simulation with a rectangular patch tag with ground plane

A 4- bit rectangular patch tag with ground plane is used in this simulation as shown in Figure 8.23.

The tag is simulated with a BOPP and a paper layer on top with varying its thickness. The RCS of the tag is shown in Figure 8.24 and the application of a material layer and their results are presented in Figures 8.25 to 8.27.

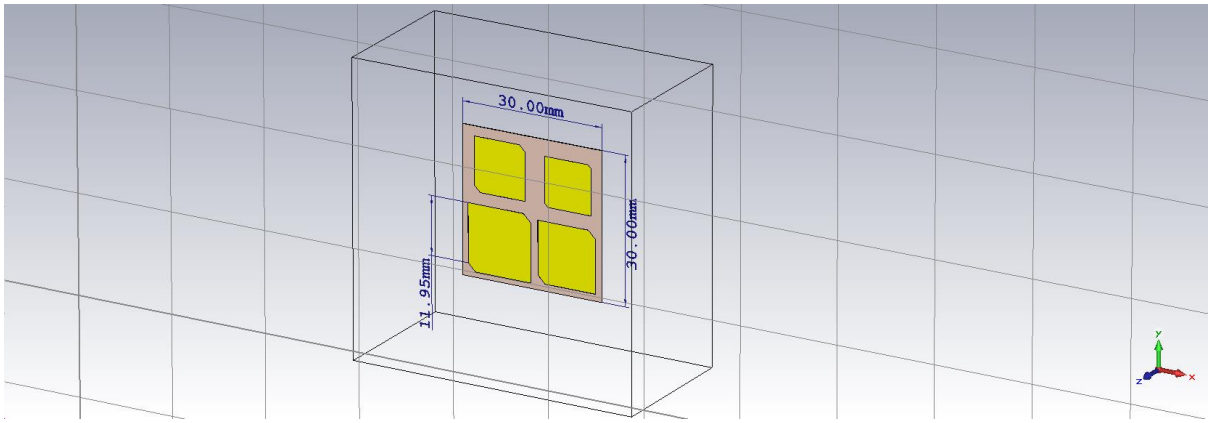

Figure 8.23 – 4-bit square patch tag with ground plane

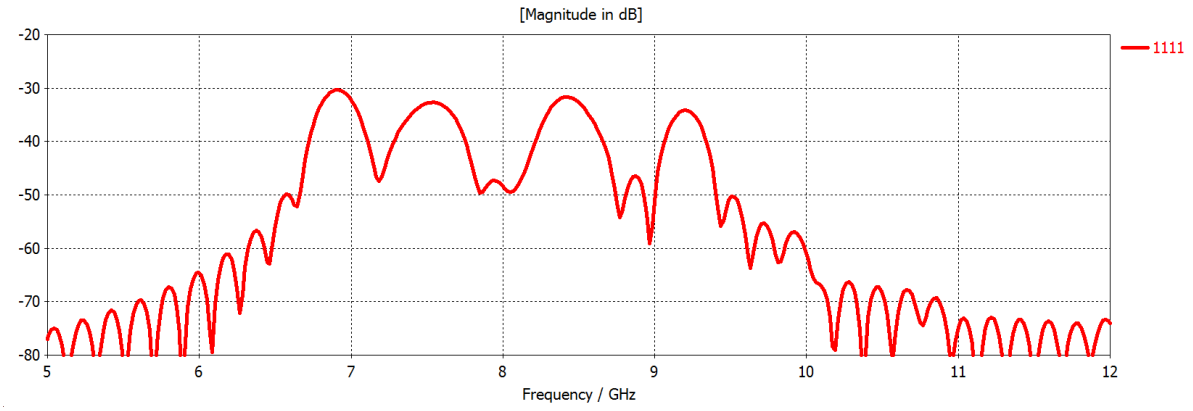

Figure 8.24– Square patch tag RCS

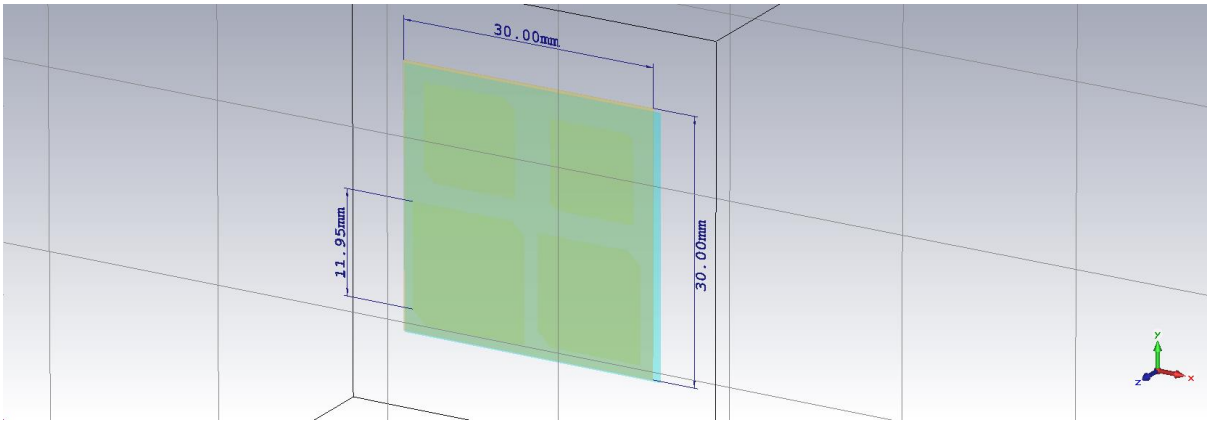

Figure 8.25 – Square patch tag with BOPP layer

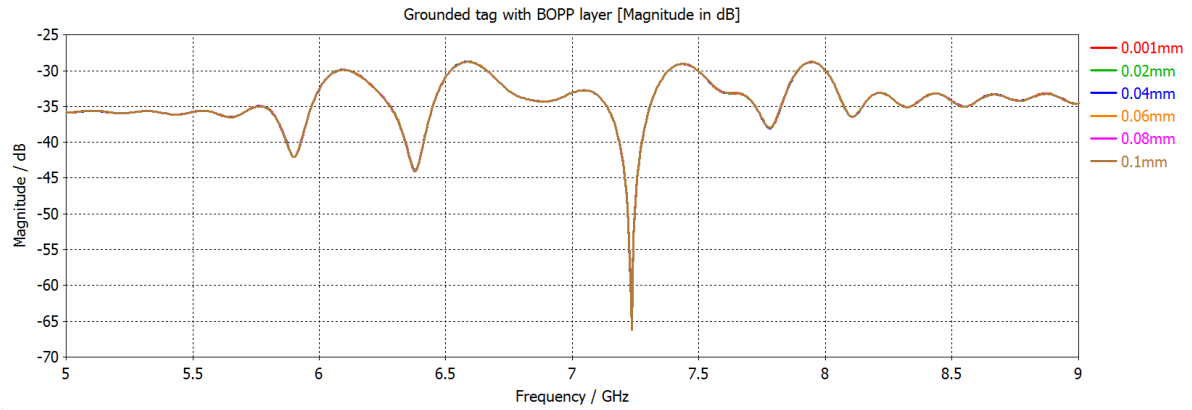

Figure 8.26 - Simulation results when BOPP layer thickness is varied from 1 to 100 µm

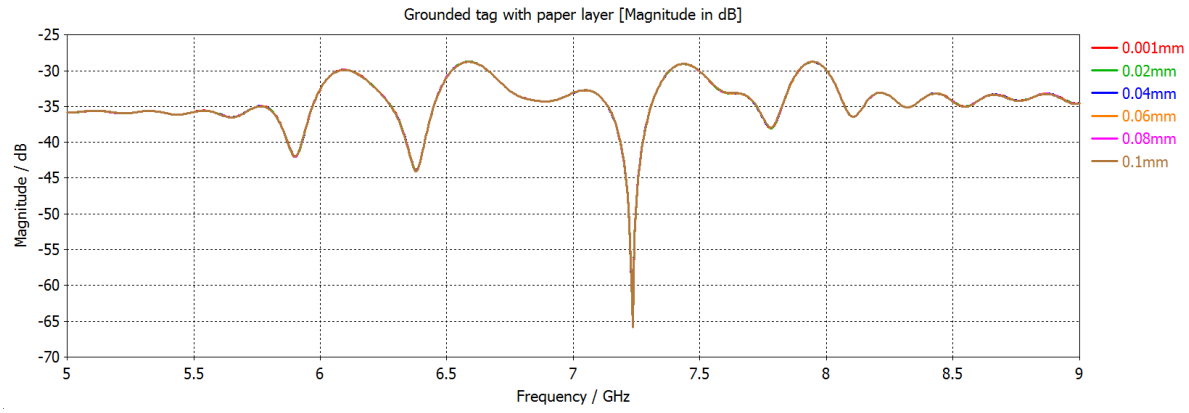

Figure 8.27 – Simulation results when paper layer thickness is varied from 1µm to 100µm

According to the results in Figures 8.26 and 8.27 it can be seen that for a tag with a ground plane even after placing a layer of material in front of the tag the frequencies does not shift and stays stable. When a ground plane is added to the tag it acts as a reflector and reduces the distribution of the reflected signal in other directions as well as the absorption by objects or medium behind the tag. This increases the reflected signal power. This concludes that by adding a ground plane can increase the received signal power as well as keep the backscattered signal stable even when a material layer covers the tag for its protection.

8.2.5 Doppler Effect while reading the tag in vertical movement

For the application of this reader in a smart shopping trolley the tag needs to be read while the item is dropped inside the shopping trolley. This requires an analysis of Doppler Effect as the tag will be read while it is on the move. In this experiment, the movement of hand in front of the target is considered. From the Doppler analysis perspective this is considered as micro-Doppler. For example, if we swing our hand towards a smart trolley, i.e. we are moving our hand towards the antenna inside the trolley, it will give us a positive Doppler. Likewise, if we move our hand away, it will be a negative Doppler. These micro-Doppler's analysis can provide the valuable information for the proper identification of the tag IDs attached on the Item. The experimental parameters are presented in Table.

Table 8.5. Experimental Parameters and Setup

Parameters	Value and Item
Types of Devices	VNA, Horn Antenna
Types of Antenna	Horn Antenna
Area of Antenna	24 x 14 cm square
Power Level	0dBm, -15dBm
Constant Frequency	4 GHz
Sweep time	5 sec
Number of Data Points	201
Distance between Object & Rx	Approximately 15 cm
IF Bandwidth	35 KHz

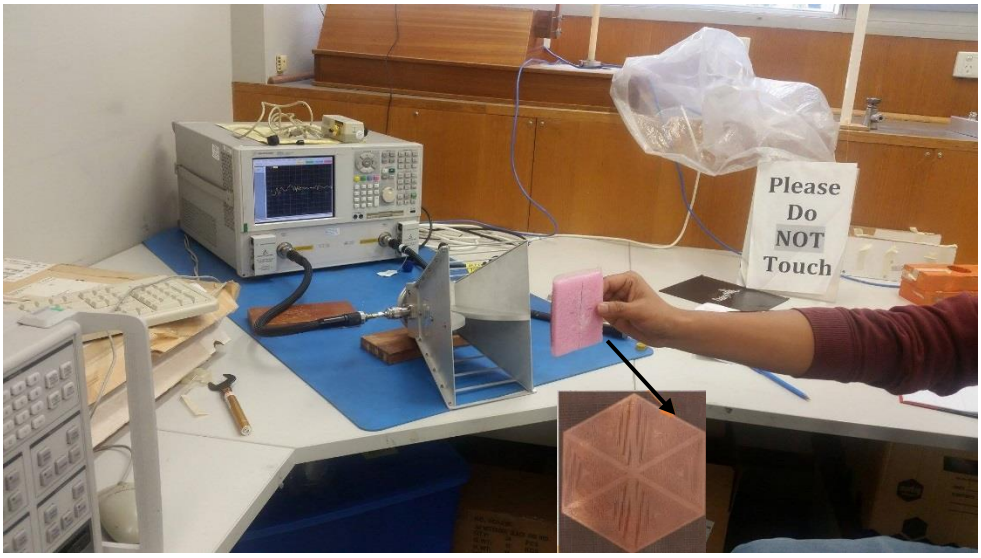

Figure 8.28 - Experimental Setup to measure the Doppler effects

In Table 8.6, the Doppler spread with respect to coherence time is analysed. The coherence time is the time duration over which there will be no variation of impulse response, which means signal have similar response at different times or impulse response is invariant. The comparison of coherence time

based on maximum Doppler is shown in Table 8.6. The coherence time for free fall, hand ideal case, hand fast motion and hand slow motion is 32ms, 681ms, 23ms, and 341ms respectively. As the coherence time is inversely proportional to maximum Doppler, with the increase in Doppler coherence time decreases and vice versa. The hand ideal case and hand slow motion have a more coherence time compared to free fall and fast motion which means the ideal case and slow motion have a more stable impulse response which holds a longer duration and suffers less variations whereas, free fall and fast motion suffer maximum variation with shorter duration of coherence time.

Table 8.6- Analysis of Doppler spread

Motion	Carrier Frequency	Speed	Maximum Doppler	Coherence Time
Free fall	4 GHz	2.35 m/s	31.33 Hz	32ms
Hand Ideal Case	4 GHz	1.1013m/s	1.4684	681ms
Hand Fast Motion	4 GHz	3.23 m/s	43.06 Hz	23ms
Hand Slow Motion	4 GHz	0.22 m/s	2.93 Hz	341ms

The above results show how the micro Doppler effects the tag motion towards the antenna in horizontal movement. But, in chapter 9 for the real time dropping of an item into the shopping trolley only the vertical movement is considered. Therefore, Doppler Effect will be negligible in the vertical direction hence the frequency shift that might occur is not due to Doppler Effect.

8.3 Detection with different items held in hand with the tag

To find the effect of having wearables in hand while dropping the tagged item into the trolley the hexagonal tag is been used in this experiment and the S11 results are recorded using big horn antenna and vector network analyser. The 3bit resonances in the frequency range of 4-6 GHz are studied in this experiment. First the tag is held in hand in a dropping position as shown in Figure 8.29. The observed result and the decoded tag ID after applying the detection algorithm is shown in Figures 8.30 and 8.31.

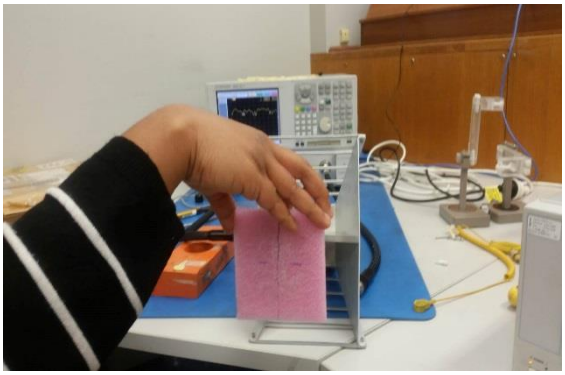

Figure 8.29 – Hexagonal tag held with Right hand in dropping position

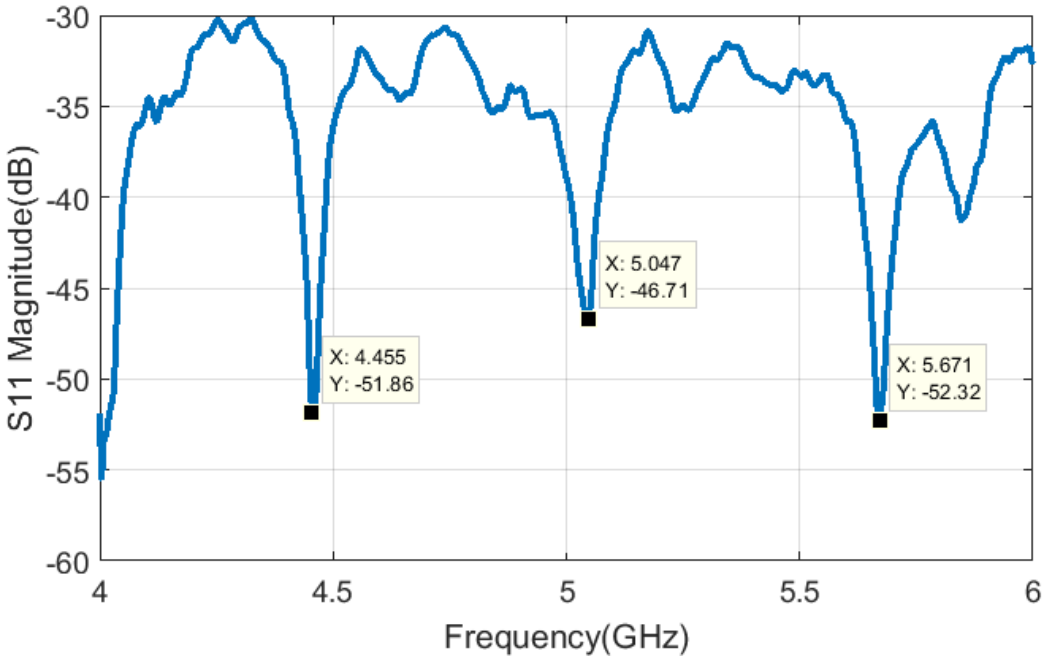

Figure 8.30– Hexagonal tag result from 4-6 GHz (3- bits)

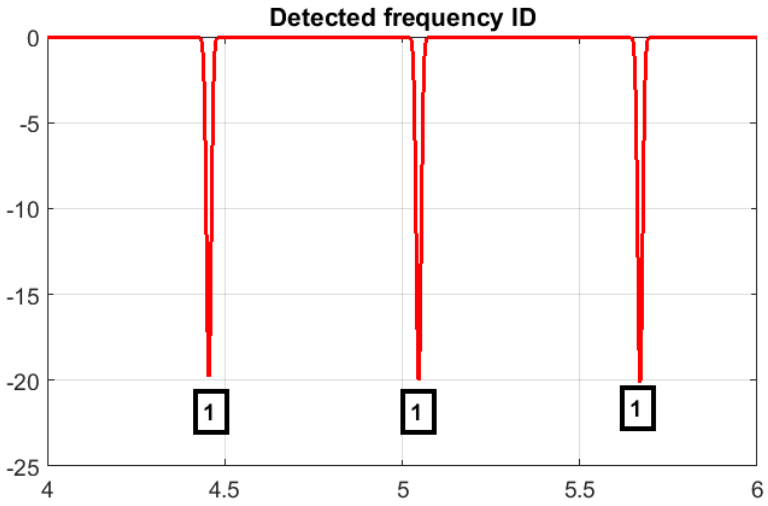

Figure 8.31– Hexagonal tag result from 4-6 GHz (3- bits)

In Figure 8.32 it shows the possibility of having a ring and a key in hand when handling the tagged item. The response is shown in Figure 8.33. It can be seen that the 2nd bit at 5.1 GHz has been distorted due to the objects in hand. But by applying the detection algorithm the correct tag ID can be still detected as shown in Figure 8.34. When the hand has a watch and all other items as before the response is shown in Figure 8.35. As the 3bit resonances are still significant the tag ID is still detectable.

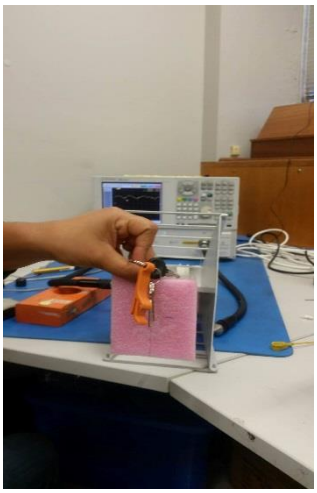

Figure 8.32 – Hand with ring and key tag

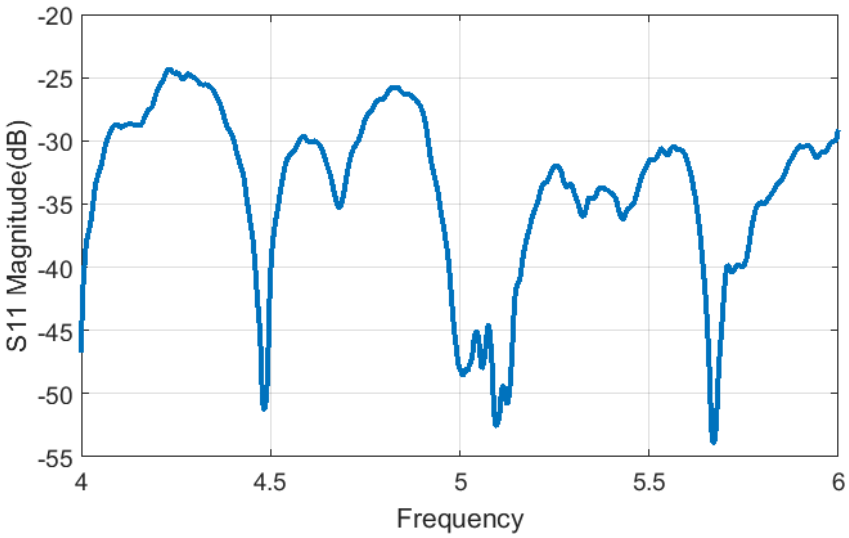

Figure 8.33– S11 magnitude vs. frequency hand with ring and keys

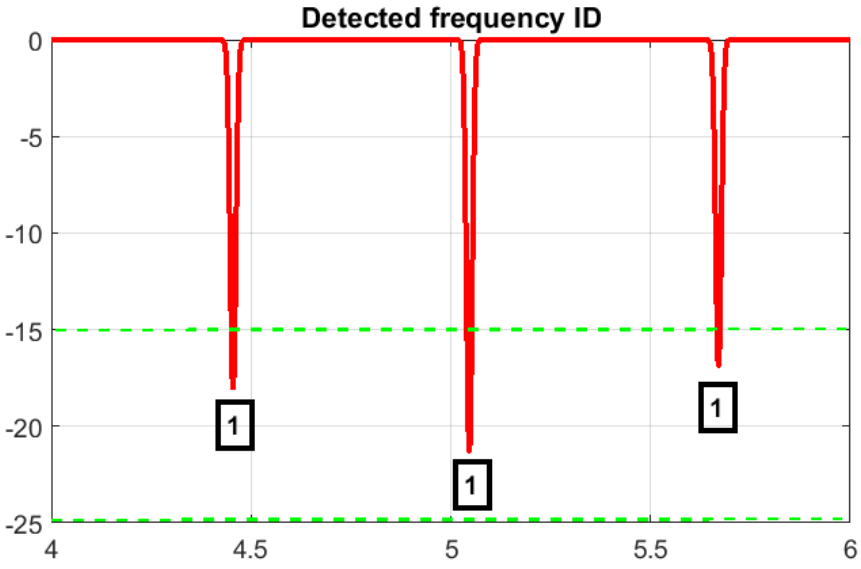

Figure 8.34– Hand with Ring, Keys, Watch and Tag

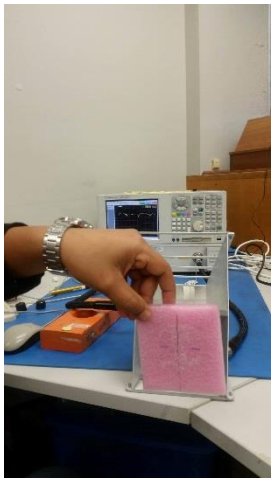

(a)

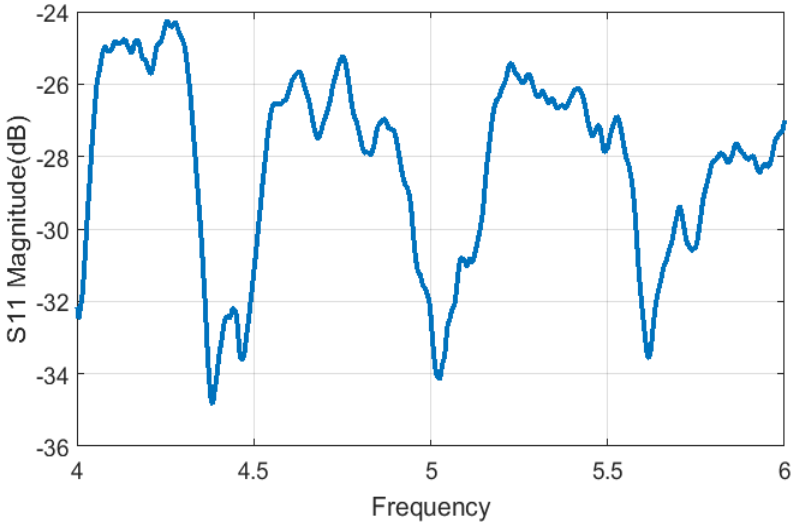

(b)

Figure 8.35– (a) Hand with Ring, Keys, Watch and Tag (b) S11 magnitude vs. frequency results

These experiments with items held in hand with tag gives an idea whether the tag can be detected with the chipless RFID reader in a similar environment. Also, the big horn antenna is used for this experiment as it gives an aperture similar to the array antenna which is used in the real application.

8.4 Effect of attaching the tag to different materials

The material properties of the tagged objects have profound impacts on tag detection. The materials can seriously affect the backscattered signal from the tag, hence detection. In this section the effect of different materials such as dielectric, conducting solid and liquid material contents are subjects of investigation.

The 4-bit circular tag with ground plane has been used in this testing along with the 4x4 patch array as the reader antenna. The chipless tag has been fixed to different items a coke can, a water bottle and a cereal box. The tag response has been detected using the Vector Network Analyser (VNA) as shown in Figure 8.36. Here the VNA is considered as the RFID reader in this case as before. The reader antenna has a 50 Ω output port and is connected with the VNA input port P1. The measured data is in the form of the return loss (S11 in dB) vs frequency.

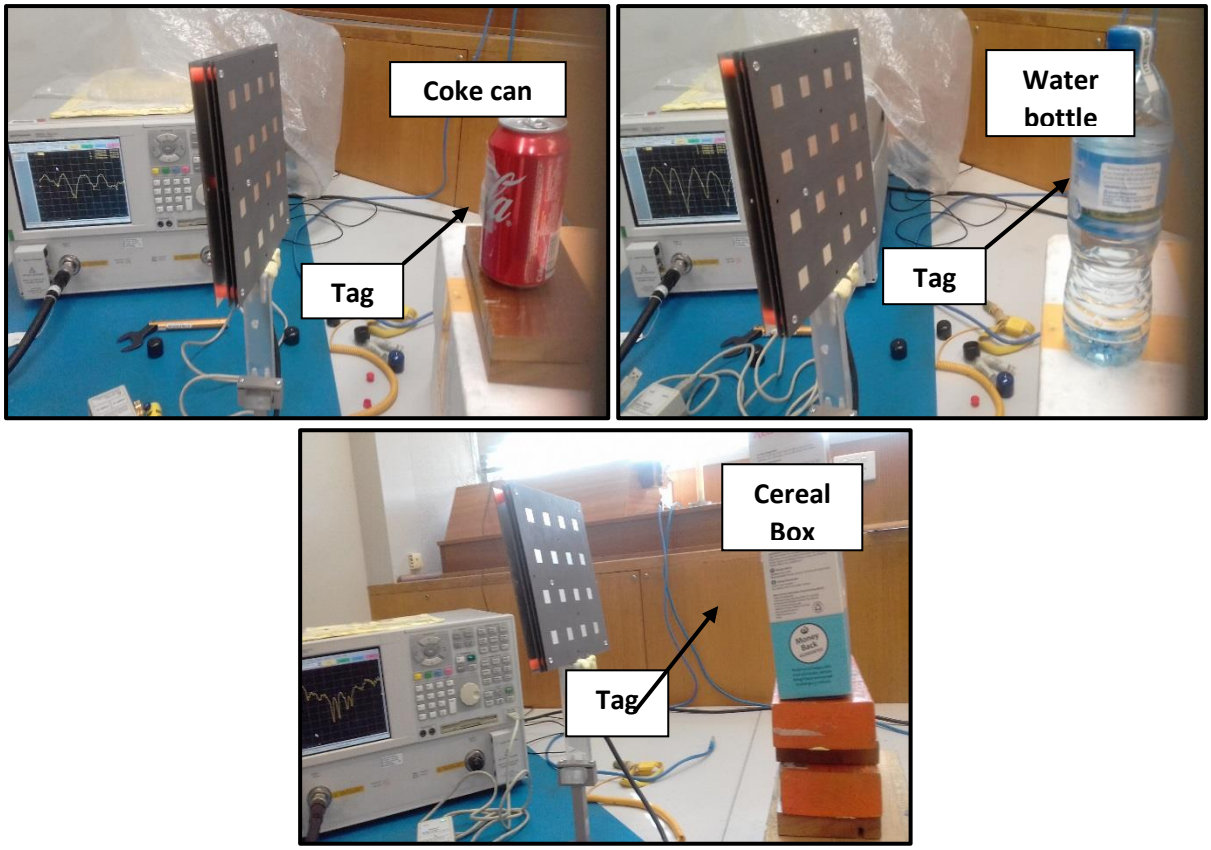

Figure 8.36 - Detection of chipless RFID tag attached to different items coke can, water bottle and cereal box using 4x4 patch array antenna.

The experiments performed earlier with chipless RFID tags without ground plane was not able to detect the tag when it was attached to metallic objects such as the coke can as there was reflection from the metal. Also, a tag on any bottle containing liquid was also not detectable. But using a grounded tag enables the tag to be detected with less distortion and attenuation. In the above experiment the tagged item is placed 20 cm away from the antenna and is still detectable. The tag responses measured from the VNA are shown in Figure 8.37. The transmitted power through the port 1 of the VNA was -10 dBm (10 μW). As it can be seen from the tag responses from various attached items the tag is still detectable. From the results in Figure 8.37, the result of the tag on coke can and water bottle shows around 10 dB raised S11 magnitude which shows the effect of reflection from the metal and plastic surfaces of the items. The hand on side of tag has also changed the S11 magnitude level and some bit resonances show more distortion. The tag result on the cereal box shows the highest level of distortion to the received signal. In all curves a frequency shift of around 250 MHz around the original bit resonance is noticeable.

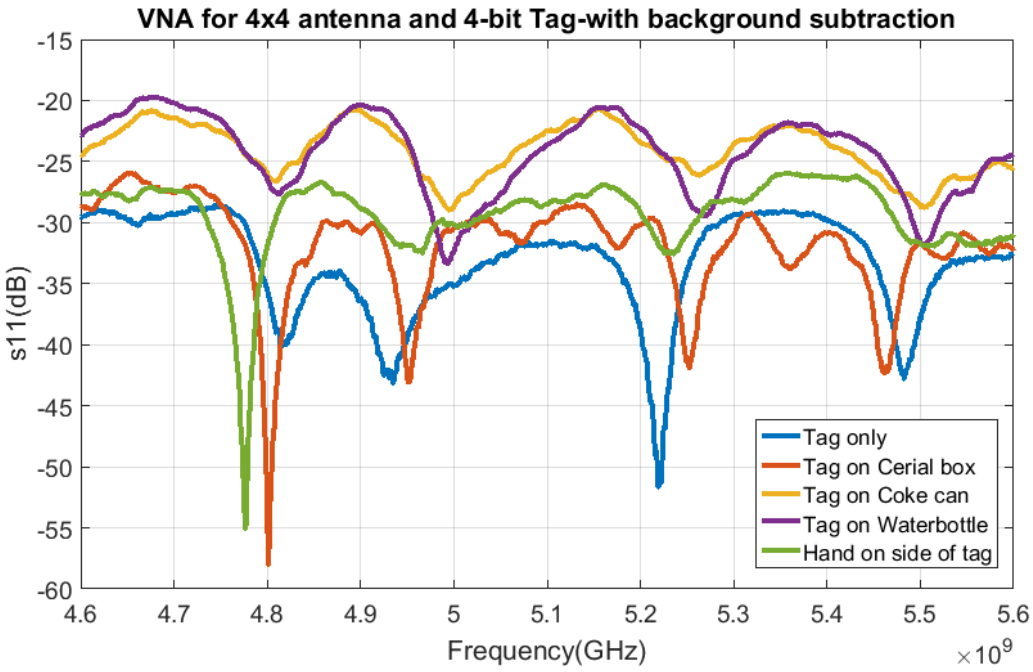

Figure 8.37 - Detection of chipless RFID tag attached to different items coke can, water bottle and cereal box using 4x4 patch array antenna.

The 4 x 4 patch array antenna was tested with the previous single antenna reader. A 4-bit circular patch resonator tag was used for this experiment. The tag was freely dropped in front of the antenna at a distance of 10 cm. The test showed that the tag data can be read while the tag is in motion. The tag ID detection algorithm was tested on the results. After successful detection of the tag with materials with the VNA as the reader and the 4 x 4 element patch antenna as the reader antenna, the state-of-the-art in-house developed vector modulator based chipless RFID tag reader is used to do the confidence test.

8.5 Detection of tag on different items using Vector Modular Reader

8.5.1 Detection of different tag IDs using 4 x 4 array antenna with VMR

The RF section of the chipless RFID reader to be used with the array antenna is a modified version of the previous reader that has been used in Chapter 5. The main difference is the inclusion of a vector modulator which reduces the feedback using vector subtraction. It also gives both magnitude and phase data which are used in the generation of the detected tag signal. Also, it has been improved to reduce the noise within the hardware.

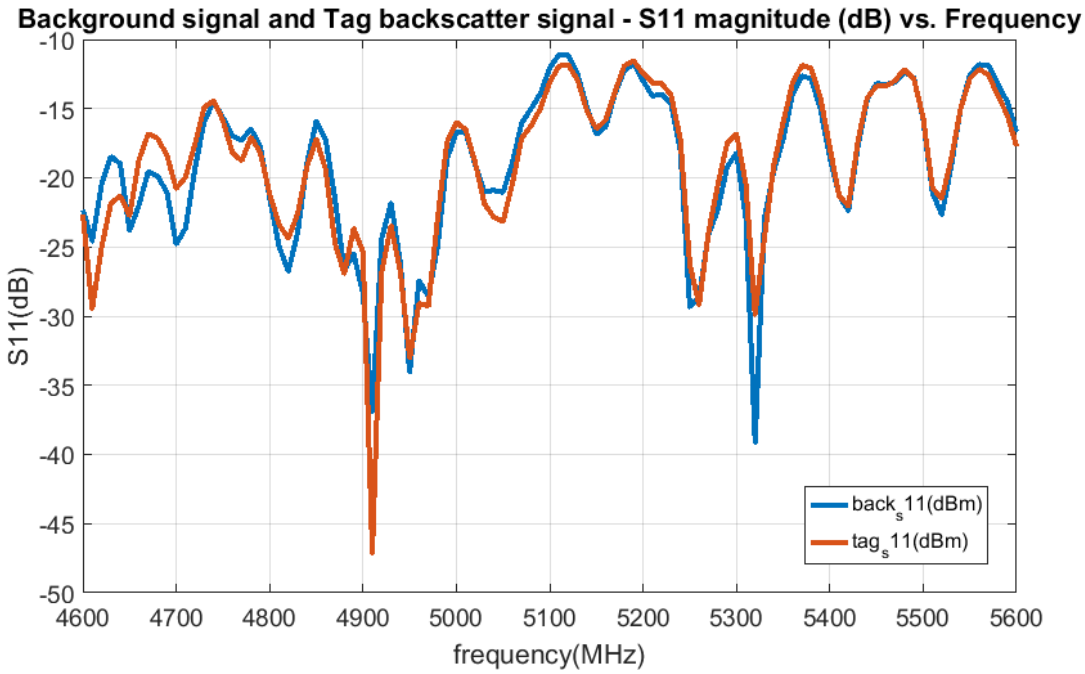

Figure 8.38 – The background signal and the backscatter signal without any tag

In the previous section, the 4-bit circular tags with ground plane attached on different items (coke can, water bottle, cereal box) were tested and analysed. Also, the 4-by-4 array antenna was placed 20 cm away from the tags to measure the backscattered tag signal using VNA and the modular reader in the previous section. This measurement set up with the new vector modular reader hardware is shown in Figures 8.38 to 8.41. Firstly, a single patch antenna has been used for this measurement and the tag has been held by hand at a distance of 15-20 cm in front of the antenna. In the experiment first the reader system is calibrated without a tag. This technique is called the background subtraction to remove the environmental effect of the system. This is a one-time process. Figure 8.38 shows the S11 (dB) vs frequency data for the background subtraction without any tag in front of the reader antenna. Then a 4-bit tag of ID 1100 is placed, and data is acquired as shown in Figure 8.39. As can be seen the data is detectable but full of noise. Then the de-noising algorithm is used to read the tag and clear tag ID is obtained as shown in Figure 8.40.

This shows the improved measurements with the new vector modular reader using magnitude and phase data. Further experiments are performed with the 4 x 4 array antenna and the new reader for the movement of the tag and are presented in the next Chapter.

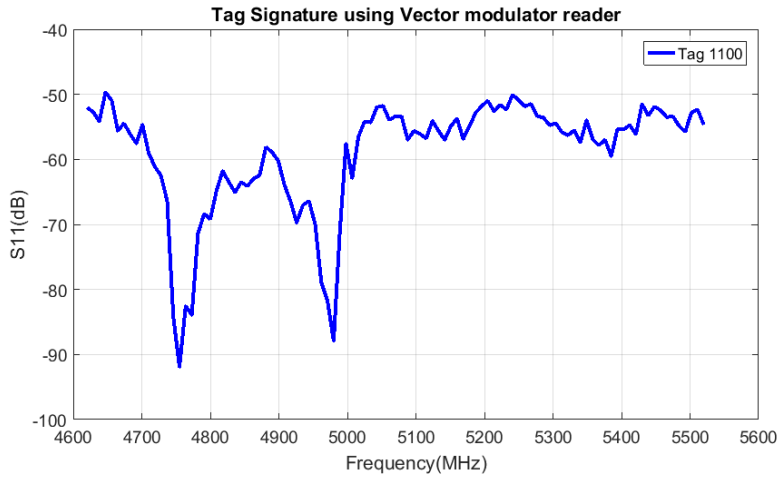

Figure 8.39 – Tag signature measured using vector modulator reader for Tag - 1100

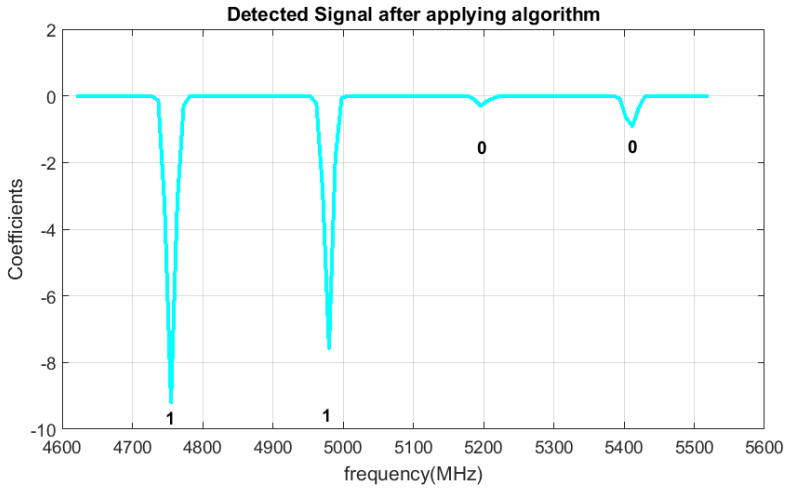

Figure 8.40 – Detected ID – 1100 after applying the detection algorithm

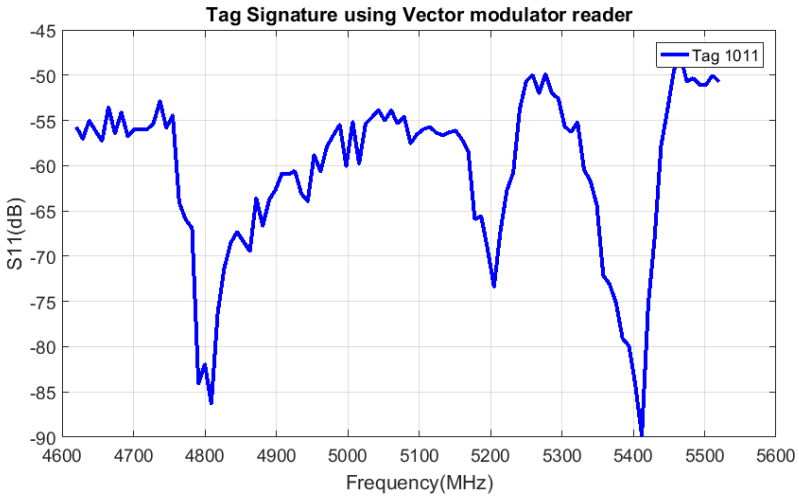

Figure 8.41 - Tag signature measured using vector modulator reader for Tag - 1011

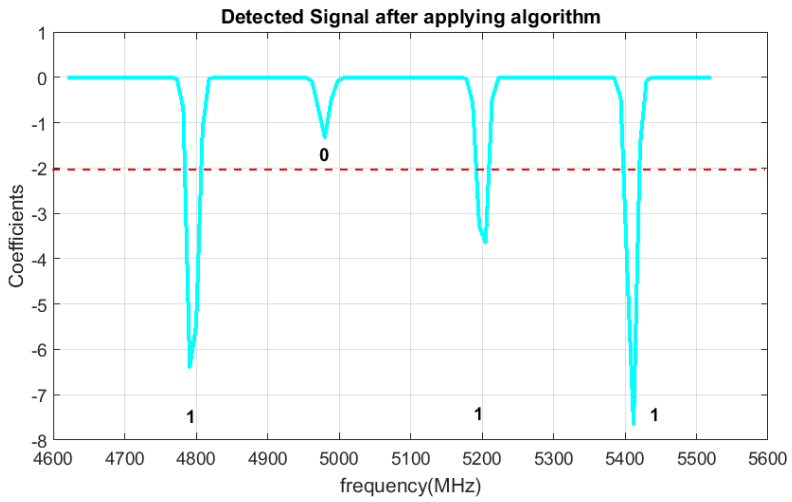

Figure 8.42 - Detected ID – 1011 after applying the detection algorithm

In Figure 8.39 and 8.40 it shows the detection of tag ID 1100 and in Figure 8.41 and 8.42 it shows the detection of tag ID 1011. In both cases when applying the detection algorithm, the threshold level is taken as -2. So, it can be seen that from the results the tag ID can be retrieved correctly.

8.5.2 Detection of Tagged Items using Single patch antenna with VMR

This section is an important and challenging part of the research as it moves into the practical application of a chipless RFID. The tag is attached to different items namely, a coke can, a cereal box, a milk carton, a book and a metal plate. These are some of the most critical items where the tag detection could be affected due to its outer material as well as the content of the item. A 4-bit circular patch tag is used for these experiments as shown in Figure 8.43. The different combinations of the tag ID are fabricated by short circuiting the relevant circular patch. Tag 1111 has been tested on these items. As the first approach the single patch antenna has been used for the experiment. The experiments are done with variety of objects at different distances to estimate the effect of objects in terms of size, material, and reading distances. We also try with calibration with background subtraction, but with objects to see how the presence of objects affects the results.

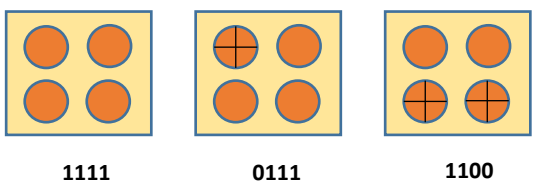

Figure 8.43 – 4-bit circular patch copper tag design with ground plane

8.5.2.1 Results for coke can

The first experiment is with the coke can, which is made of metal and filled with liquid. Tag 1111 is fixed onto the coke can. The coke can only placed at 5, 10, 15 cm in front of the antenna and the S11-parameter is measured using the vector modulator reader. In Figure 8.44 only the coke can is placed in front of the antenna. It is displaced from 5 to 15 cm.

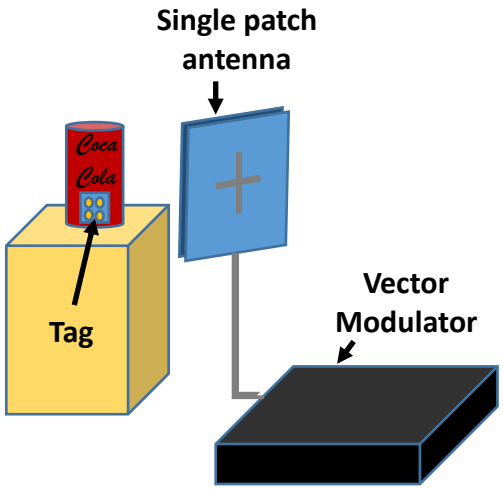

Figure 8.44 – Coke can as the tagged item

At 5 cm the S11gives a stable flat signal around -20 dB. When the coke can is moved to 10cm then the signal gets weaker and noisier. When it is at 15cm distance as shown by the yellow curve it moves further down to -35 dB level. At the shortest distance 5 cm the reflection is high and is around -20 dB. When it is moved further the level drops to about -35 dB. It is observed that when the object is close to the patch and in line the result is almost flat, but when it is moved further the variation increases with distance. This gives rise to the fact that when the object is covering the beam of the antenna and at a near distance, the result is better and when it further down the reflections from the surrounding is added as the beam is open to a larger area. Figure 8.45 shows the results when the coke can is placed in front of the antenna at the given distances without attaching the tag. It shows a -20 dB magnitude level when it is at 5 cm and when it is at a longer distance it drops to -35 dB.

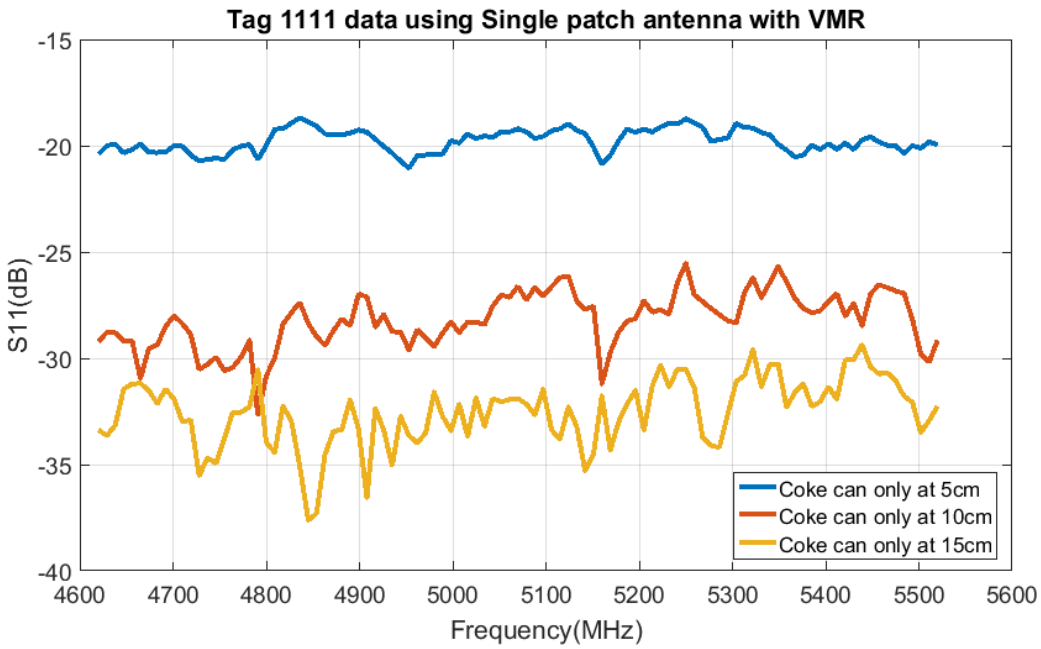

Figure 8.45 – Coke can without the tag placed at 5, 10 and 15 cm

In Figure 8.46 the tag is attached to the coke can and placed in front of the antenna. As previously done only for the coke can the distance is varied from 5cm to 15cm. At 5cm and 10cm the tag resonances are clearly visible. But when it is moved further the signal is distorted and results with many ambiguous resonances. When a tagged item is at a close distance, as can be seen from the Figure 8.46, it is easy to detect the signature at 5 cm. However, when the coke can move away the antenna, at 15 cm and beyond, the beamwidth of the antenna becomes bigger, so the reflected signals is not only from the tag, but also from the coke can surfaces. Additionally, the signal power received is inversely proportional to R^4 where R is the distance. Thus, the signal power drop dramatically when increasing the distances. At 15 cm and beyond it is very difficult to detect the tag signature and drops below the dynamic range of the reader. Figure 8.47 gives a comparison of the results obtained with the tag attached to the coke can. The blue curve shows the tag only result at 10cm. The orange curve shows the result when the calibration is first performed with the coke can and then the tag is attached and read from the reader. The yellow curve shows the result of tag attached to the coke can at 10cm and the purple curve shows the result when the background is subtracted from the previous result after the detection.

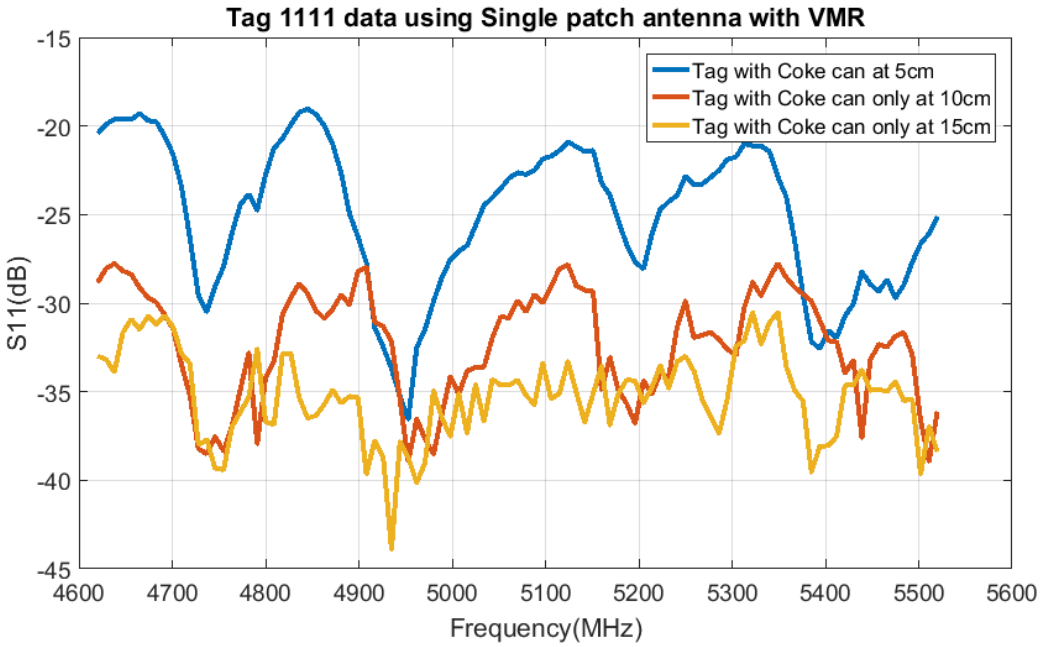

Figure 8.46 – Coke can with tag ID 1111 at 5, 10 and 15 cm

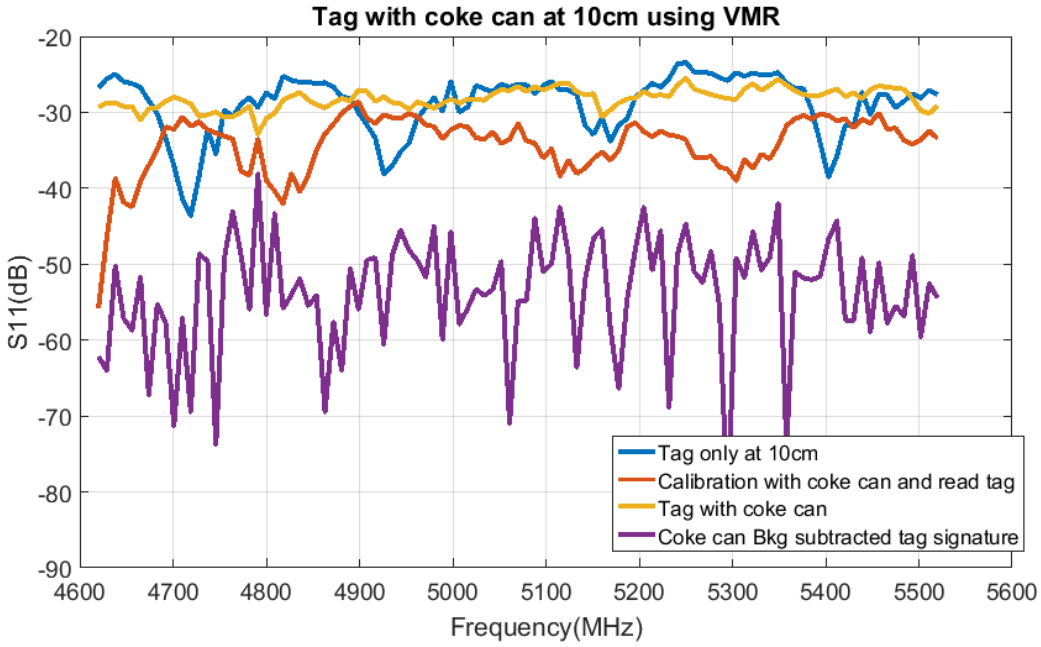

Figure 8.47 – Comparison of Results with tag attached to Coke can

From this comparison of the reflected signals from the tag only and coke can with tag, we can see that the reflected signal is shifted left about 100 MHz to a lower frequency when the calibration is performed with the object before the reading of the tag. We can handle this problem by applying an appropriate technique as long as the pattern of the tag signature at receiver does not change. But when the

background of the item is stored and later subtracted from the reading with the tagged item it does not show the correct expected result. Thus, it gives the understanding that the instantaneous result changes each time. By applying the detection algorithm for the above results, the correct tag ID of the tag can be detected up to the distance of 10cm. After 15 cm due to the heavy distortion few bits can be detected correctly but sometimes causes false detection.

8.5.2.2 Results for Cereal box

The tag is attached to the cereal box in this experiment. It is moved from 10 cm to 30 cm. First only the cereal box is placed in front of the antenna. As seen from Figure 8.48 the backscattered signal of the cereal box is highly distorted. Therefore, the detection of a tag attached to this item is very challenging.

Unlike the coke can without the tag, the cereal box only has very strange reflected signal patterns. The signal at some frequencies are stronger than the others. The effect will cause severe problems compared to a coke can does. We can see it in the next experiment. These variations can be due to the cereal inside and gaps in between where the signals transmit and reflects tremendously. The tag signature is still readable when the item at the close distance, 5 or 10 cm.

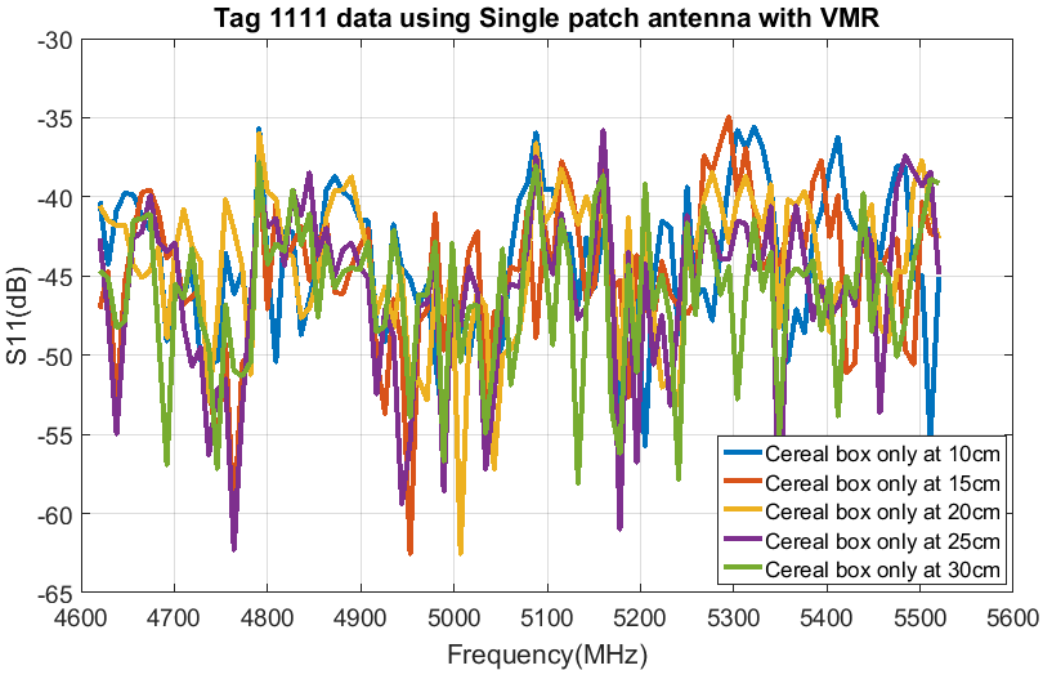

Figure 8.48 – Result with cereal box only

This is because the beam width of antenna is relative to the size of tag, so the signal at the receiver is mainly reflected from the tag. There are no effects of objects. When the distance to antenna are 15 cm and beyond, the signal pattern received is distorted and will be hard to undergo any detection algorithm. This problem may be due to the big size of the object in comparison to the wavelength, so it severely causes fading effect. Figure 8.49 gives the results with the tag attached to the cereal box. It can be seen that up to 10 cm reading distance the tag resonances are clearly visible. But, after 15 cm the response is highly distorted.

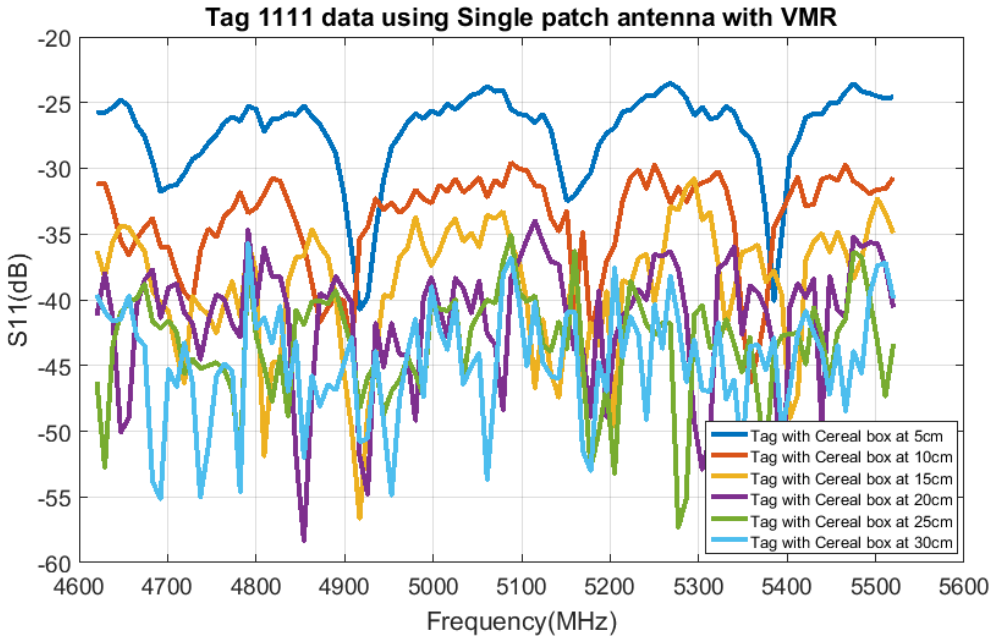

Figure 8.49 – Tag and cereal box result

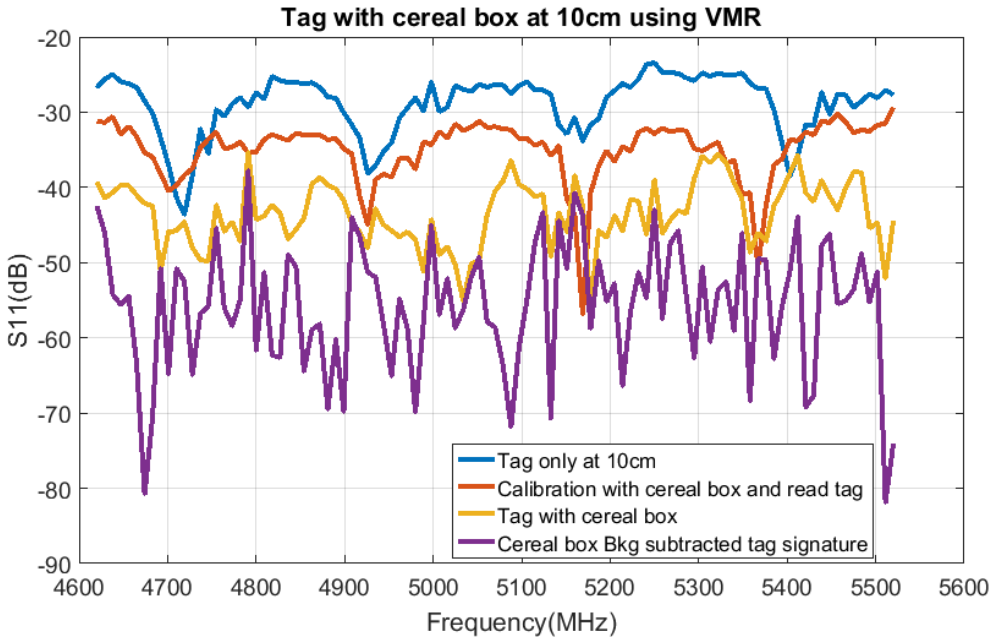

Figure 8.50 – Comparison of results with cereal box

A comparison of results is shown in Figure 8.50. Unlike the frequency shift effect with a coke can, the frequency shifted effect is not really noticeable, though the frequencies change a bit. Figure 8.49 shows the experimental setup used for the detection of tag only.

8.5.2.3 Results for Milk carton

Here, we do the experiment in several ways. First is the tag only. Second, we calibrate when object presented then attach the tag and read the signature. Next is tag with the milk carton without calibration. Finally, read the signature after doing background subtraction. This Figure 8.51 shows the S parameter at antenna when the item is a milk carton without the tag. The signal power decrease when the distances increase.

Figure 8.51 – Tagged milk carton detection using single patch antenna

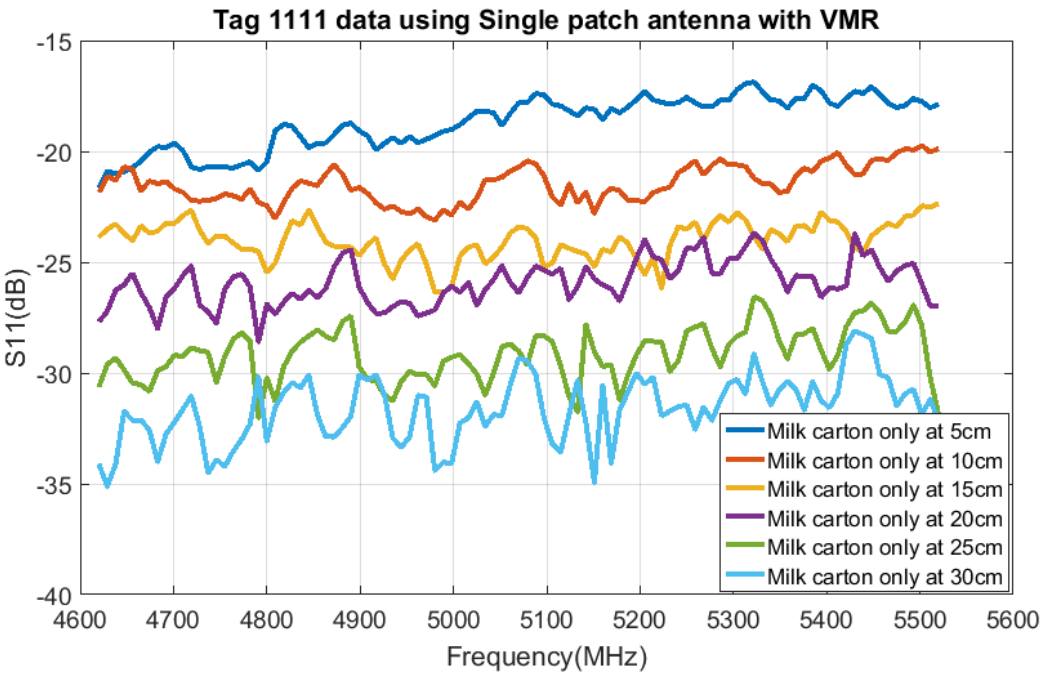

Figure 8.52 – Milk carton only

With this kind of item, the tag signature can be detected at furthest distance at 20 cm. At 20 cm with detection techniques, we can still read the tag ID correctly. But further than 15 cm, it is really difficult to read the tag ID, or the possibility of produce a wrong tag ID is really high, and the result is unreliable. The Figure 8.53 shows that, at 10 cm, we can detect the ID at the conditions tested.

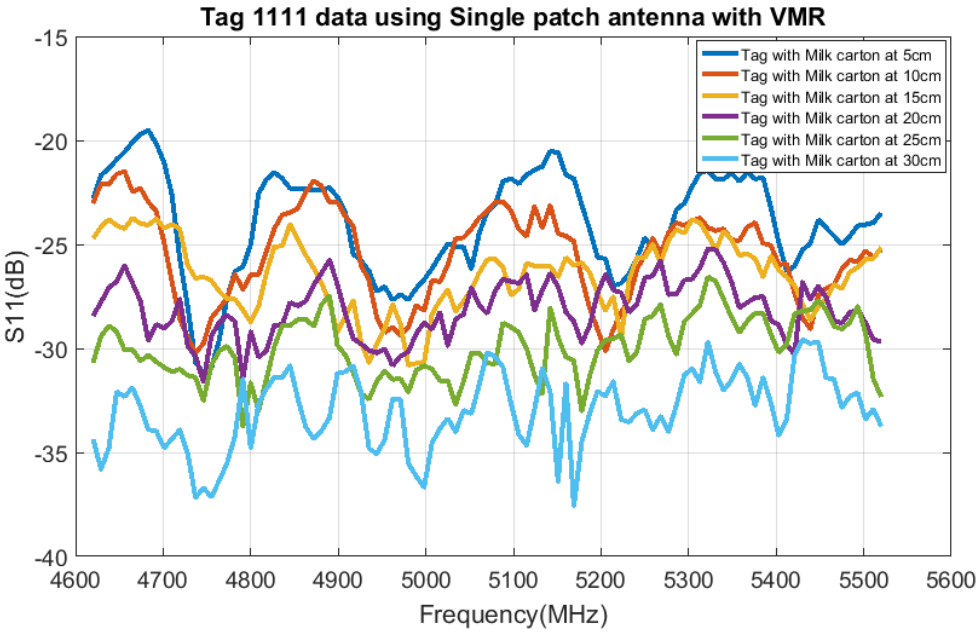

Figure 8.53 – Results of Tag with Milk carton

It shows in Figure 8.54 that the tag can be detected easily up to 20 cm. Compared to the tag on coke can and cereal box, the detection of the tag on the milk carton is extended up to 20 cm.

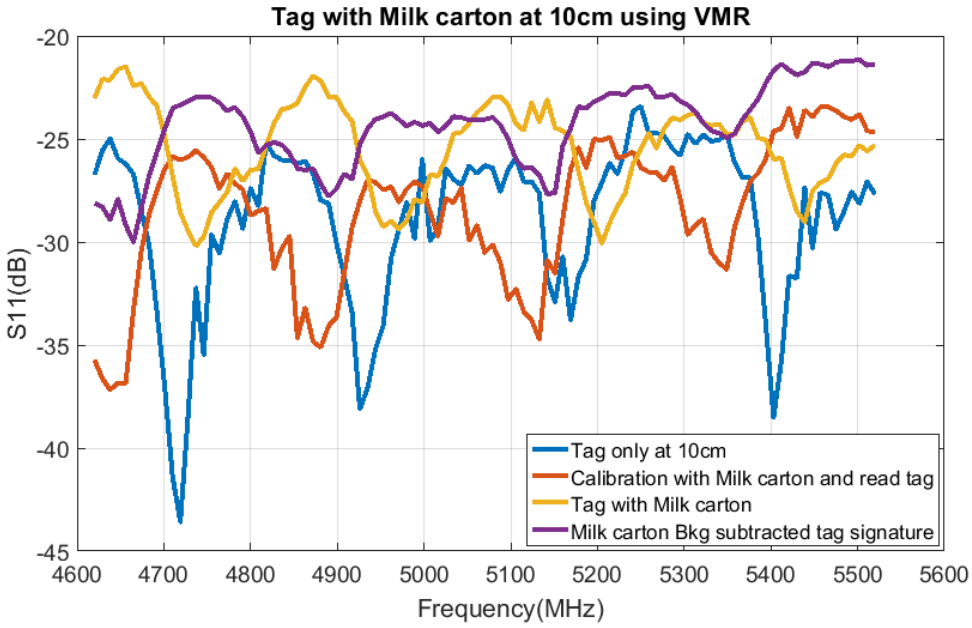

Figure 8.54 – Comparison of results

8.5.2.4 Results for book

The next item tagged is a hard cover journal book. This gives a distorted signal due to the high reflection of the book even from a closer distance. The attached hard cover journal book has a thickness of 1.5 cm. Even at close proximity the received signal is distorted. When the item is dense there is high reflection from the surrounding surfaces which are open to the antenna. This eliminates the tag signal which is with very low power.

8.6 Conclusion

At the beginning of the chapter it presents how many data sets can be captured while the tag is on the move depending on the antenna beamwidth. Experiments are carried out using single horn antenna and two horn antennas giving a larger aperture, hence improving the reading range. A hexagonal tag is used in the experiments which has its tag resonances within the reading range of these horn antennas. Both types of experiments show that the tag ID can be detected applying the developed detection algorithm, but the amplitude variation at different distances are observed.

In section 2, the material effect when the tag is covered by a material is simulated in a CST simulation studio. A circular ring resonator tag and a rectangular patch is tested in these experiments with and without a ground plane. The results presented shows that a grounded tag is more stable even with the tag covered by a material. The analysis on the Doppler Effect concludes that the effect is minimum when the tag is dropped vertically across the antenna. If there is a movement towards or away from the antenna it will cause a micro Doppler Effect. This is not considered in this research work as in chapter 9 this work is extended into the dropping of items into a shopping trolley in a real environment.

Using an array antenna and a single patch antenna it is shown that a 4-bit circular patch tag can be read up to 30 cm. When the tag is attached to items it shows a slight frequency shift but is detectable up to 20 cm. When the tagged item is moved away from the antenna beyond 20 cm the signal is distorted due to reflections from the surface around the tag as well as the surrounding environment. The tag and item were placed in line with the antenna for all of the experiments. The tags used so far in these experiments

were co-polar backscattered tag, hence signal produces noise. In further investigation the cross polar backscattered tag is recommended for tagging items as it mitigates the reflection issue.

9 Smart trolley project using chipless RFID system

9.1 Introduction

The barcode system is no longer the best way to business operation. Customers are tired of waiting in long, slowly moving checkout line in departmental stores, especially, in holidays. With the decrease of prices through efficiencies of technology and large-scale production of semiconductor wireless components, there has been a search for new markets in which semiconductor chips can be used. This has led to the use of RFID technology [16]. The MMARS Laboratory has implemented a UHF RFID based smart trolley which can track products and provide item level information to consumers in real time [34]. Smart Shopping system consists of two sections one is Shopping cart section, and another is Server section. Each RFID tag is attached to respective products and when RFID Reader reads the RFID tag this information is transmitted to a microcontroller (database gets updated from the server continuously controlled by system Admin). The RFID tag number is compared with data available, if it is present in the database then it displays product details like name of the product, cost, and total amount of bill to be paid. As you keep on adding the products into your cart, the total cost is also updated at the same time. The implemented system is shown in Figure 9.1.

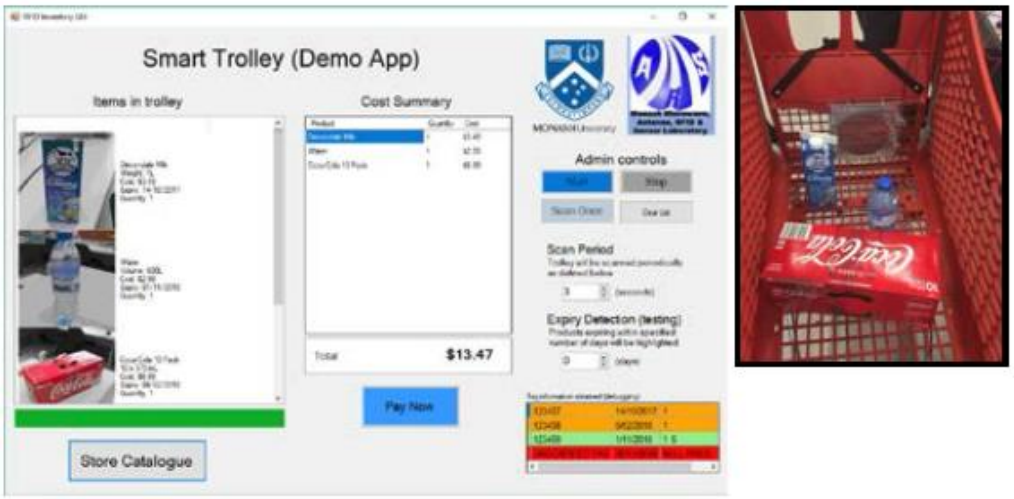

Figure 9.1 – UHF RFID based smart trolley system [34]

The main goal of this project introducing chipless tag is to minimize the cost of tagging items and enhance the shopping experience of customers in shopping malls. As the present barcode scanning sometimes takes several attempts and depends on the orientation of the item, introducing chipless RFID tags is expected to reduce the checkout time while eliminating the time taken to wait in a queue. On dropping each product into the cart, the number of products and its total cost is displayed on to the display unit. The proposed smart trolley with chipless RFID system is shown in Figure 9.2.

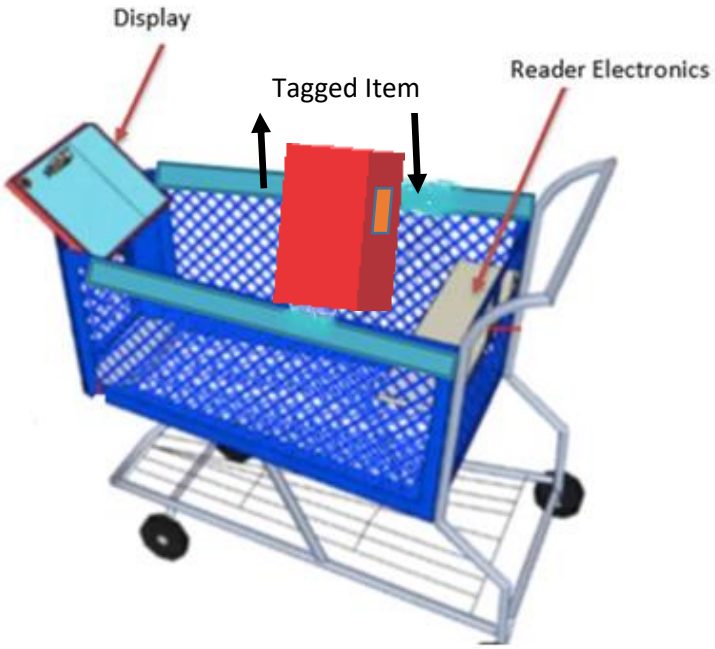

Figure 9.2 – Proposed smart shopping trolley

The smart shopping trolley project objective was based on the detection of different tagged items as they are dropped into the trolley. The items dropped in has to be identified and also if any item is taken out from the trolley it needs to be detected. The reader antenna is fixed in front of the reader electronics at the pushing end of the trolley as shown in Figure 9.3.

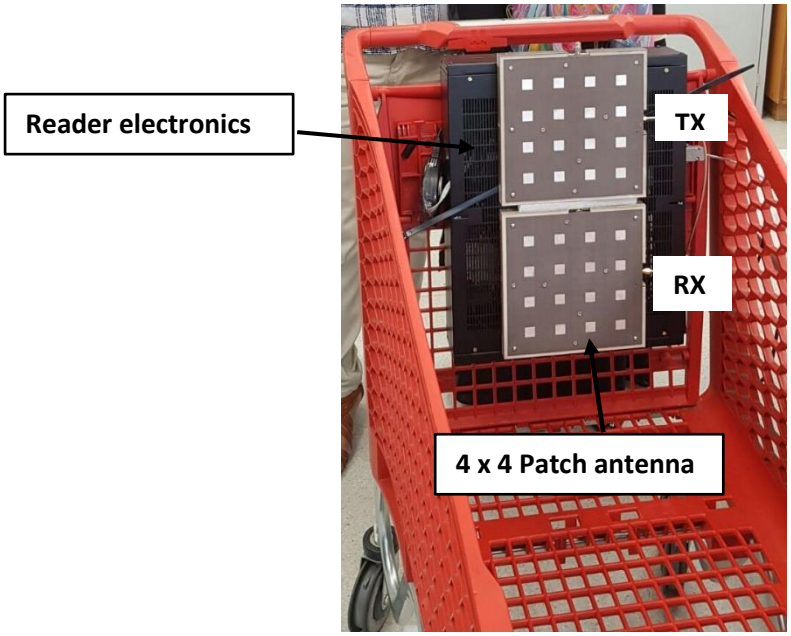

Figure 9.3 – Shopping trolley with VMR and 4 x 4 patch array antennas installed for detection of items

In section 2, individual items are detected on the move. Firstly, the tag detection is tested on materials such as metal, cardboard and plastic. This is to get a picture of the material effect as many items to be detected are metal cans, cardboard boxes or packets and plastic bottles. The next goal of this project is to detect the direction of movement which is presented in section 3. As the customer have the option of dropping in any item as well as taking out the item this has to be addressed. Two 4 x 4 patch array antennas were used in the system for this purpose. By the use of the received signal power strength (RSS) of each antenna the direction of tag movement is has been detected successfully. Finally, as shown in Figure 9.4 the detection of the tag in a dynamic environment is presented.

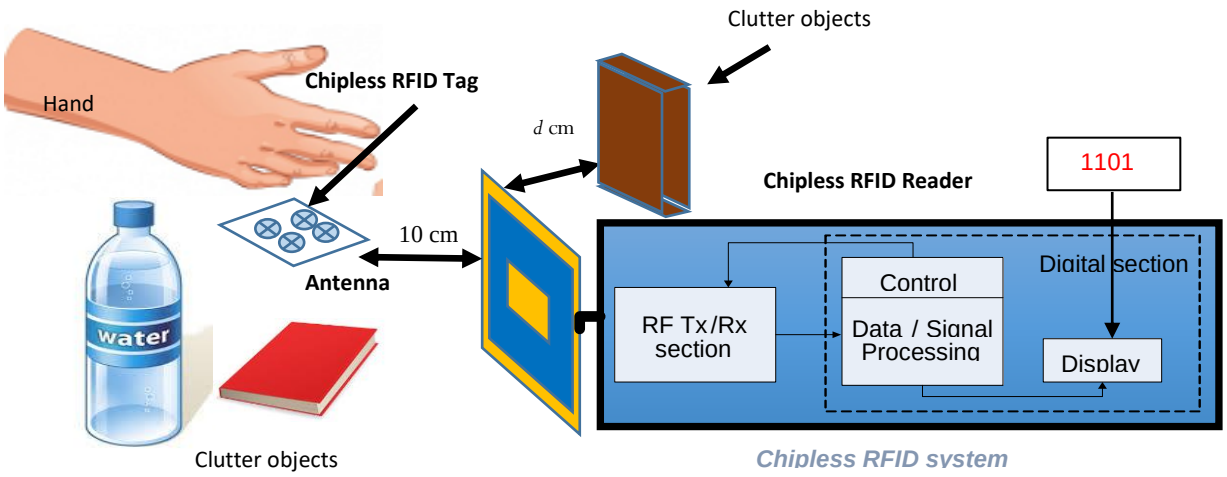

Figure 9.4 – Detection in a dynamic environment

9.2 Individual item detection on the move

The 4x4 array antenna developed has been used with the vector modulator reader (VMR) placed inside a real shopping trolley and the different experiments are performed in a real time environment in this chapter. The same 4-bit circular patch resonant tag introduced in the previous chapter was used in the experiments presented in this chapter. Tag with ID '1000' was attached on different objects in this experiment. In Figure 9.5, the tag is fixed on a pole and placed inside the trolley in front of the antenna for S11 parameter measurements.

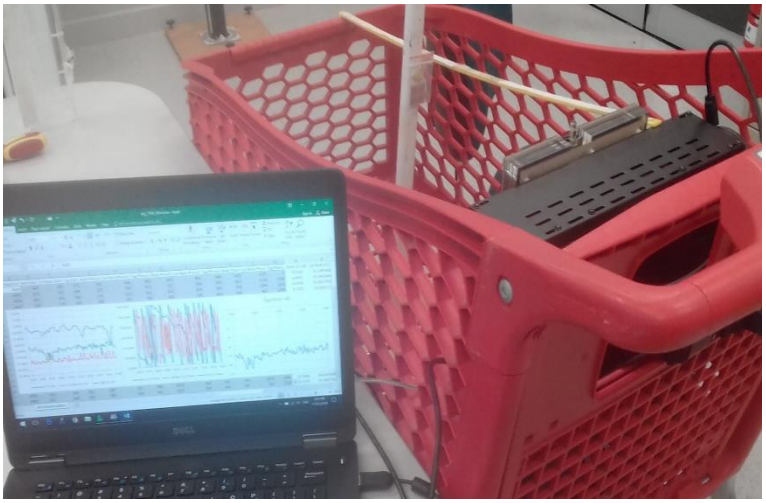

Figure 9.5 – S11 Measurement of tag 1000 in Smart shopping trolley

In Figure 9.6, the Back-S11-dB curve shows the background measurement with the trolley environment. The red curve, Cal-Back-S11-dB shows the measurement after calibration. The pole is set inside the shopping trolley basket for accurate calibration measurement initially and later on it was removed. The green curve shows the S11 measurement when the tag is placed in front of the antennas at a distance of 20 cm on the pole. Hence, Tag-S11-dB is the tag data that contains the ID information. As can be seen, the tag ID can be detected if noise can be removed. Figure 9.7 shows the S11 measurement without any tag which falls onto the same calibration curve level.

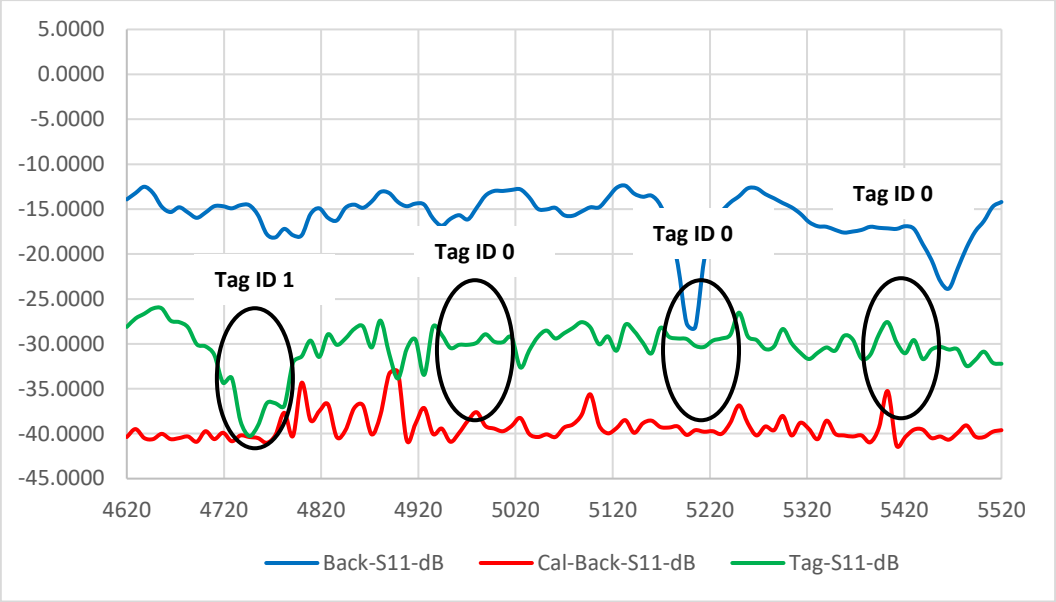

Figure 9.6– Tag 1000 detection with array antenna using VMR

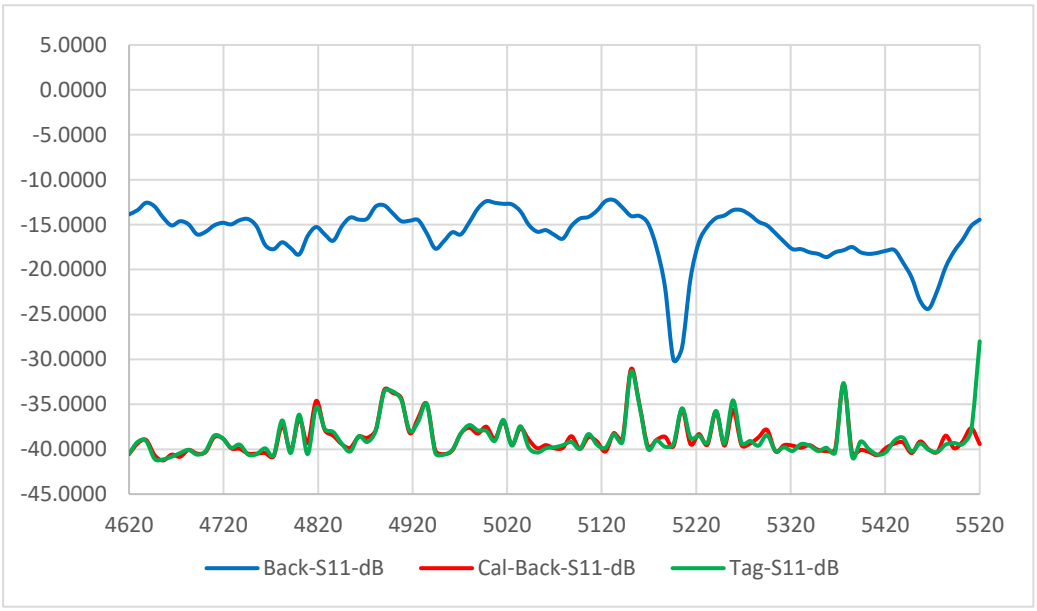

Figure 9.7- Calibration only antenna with environment

As seen from the previous section due to the material and the object size the tag response changes. Therefore, the material effect is first tested in this section.

9.2.1 Calibration of material effects

a. Tag attached to a metal plate

A metal plate was placed in front of the antenna at the same distance of the tag placed in the previous experiment and the result is shown in Figure 9.8. The green curve in the figure shows the increase of the magnitude level and lies between -10 and -15 dB.

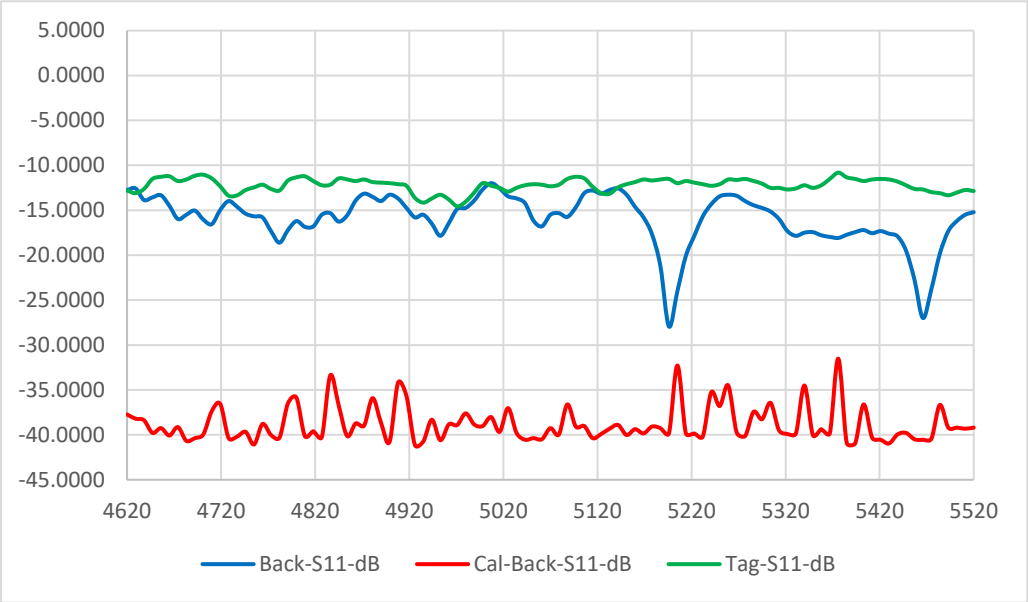

Figure 9.8– Placing metal plate in front of antenna

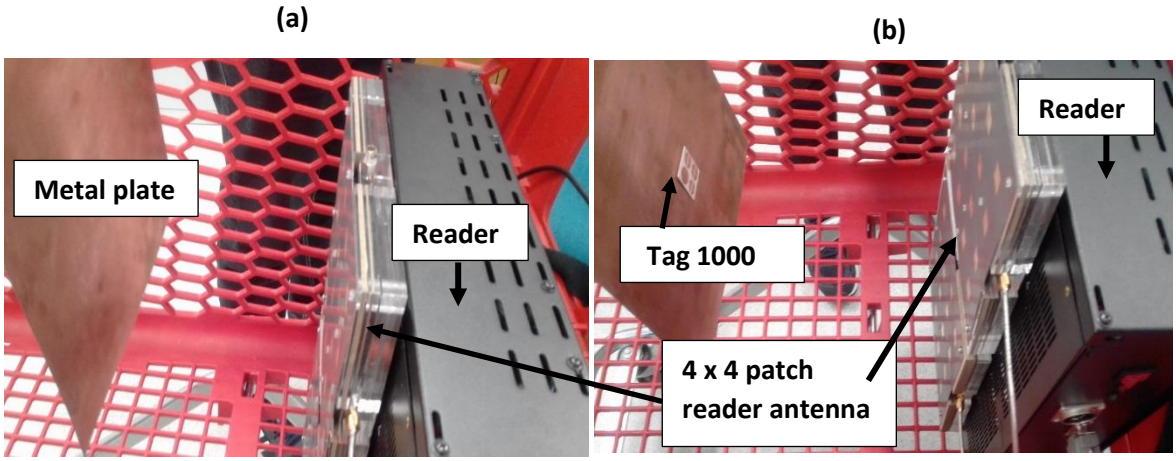

Figure 9.9– (a) Metal plate in front of antenna (b) Metal plate with tag 1000 attached

Figure 9.9 (a) and (b) shows the real practical set up for the experiment with the shopping trolley, reader, array antenna and tagged material.

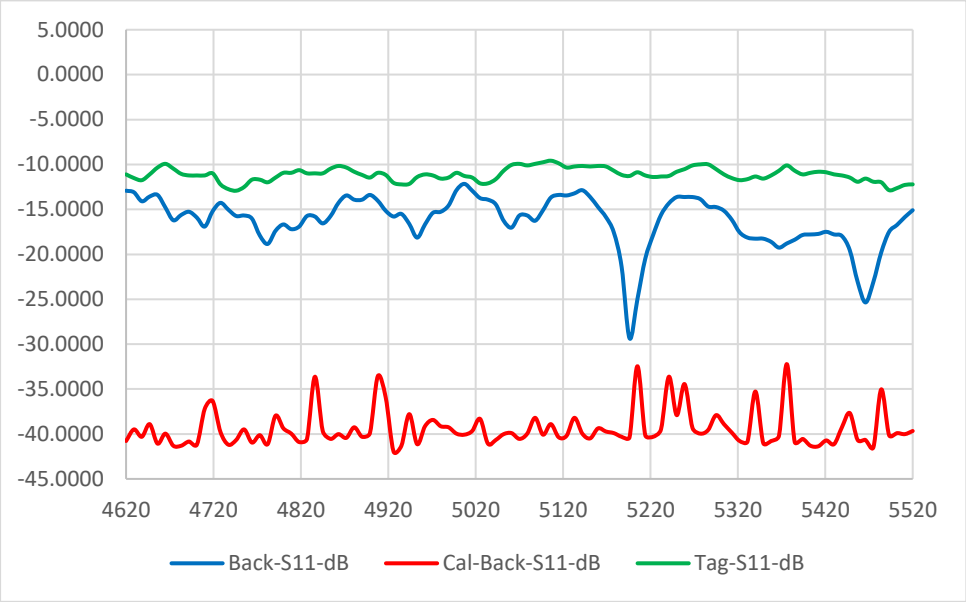

Figure 9.10 – Tag 1000 on metal plate

The tag response is not visible in Figure 9.10. It shows that the reflection of the surrounding area of the tag is higher than the tag backscattering. Therefore, even the circular patch resonant tag is with a ground plane, since the surrounding area falls within the beamwidth of the receiving antenna the reflection signal from the metal is higher than the backscattered signal of the tag. This is a challenge for the detection of tagged metal objects.

b. Tag attached to a thin cardboard

A thin cardboard is attached to see the effect of the materials used for cartons such as cereal and biscuit packets.

Figure 9.11 – Small thin cardboard in front of the antenna

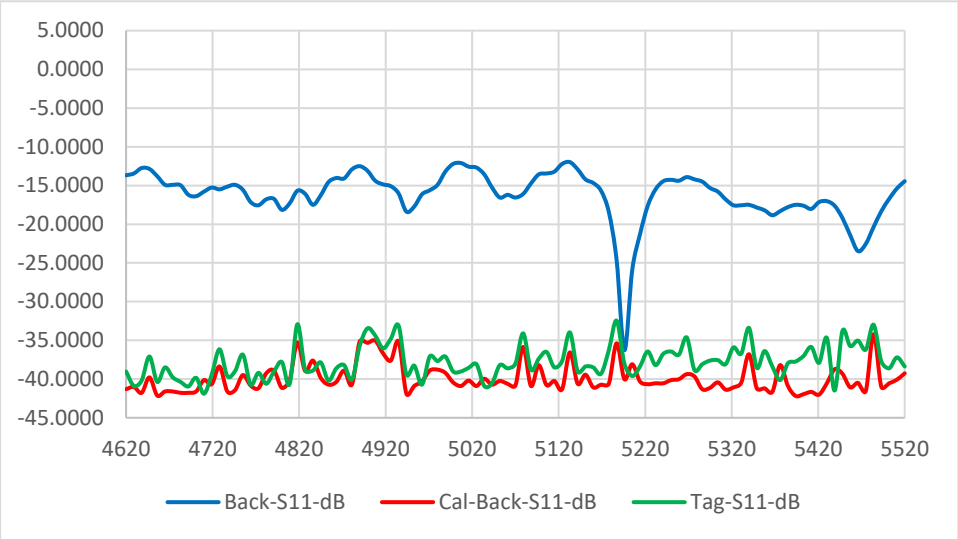

Figure 9.12 – Cardboard only placed in front of array antenna

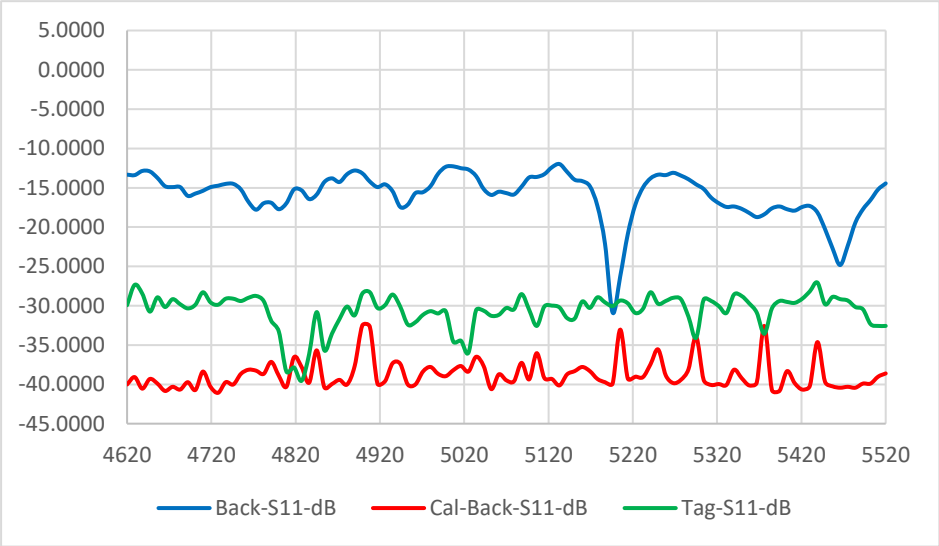

Figure 9.13 - Cardboard with tag 1000 at 30cm

As given in Figure 9.12 and 9.13 the tag 1000 can be detected at a distance of 30 cm. Then another tag of the same ID is also attached to the cardboard. As shown in Figure 9.14 the depth of the 1st bit has increased by approximately 4 dB. This shows that if we have a strip of the same tag, we can improve the detection result.

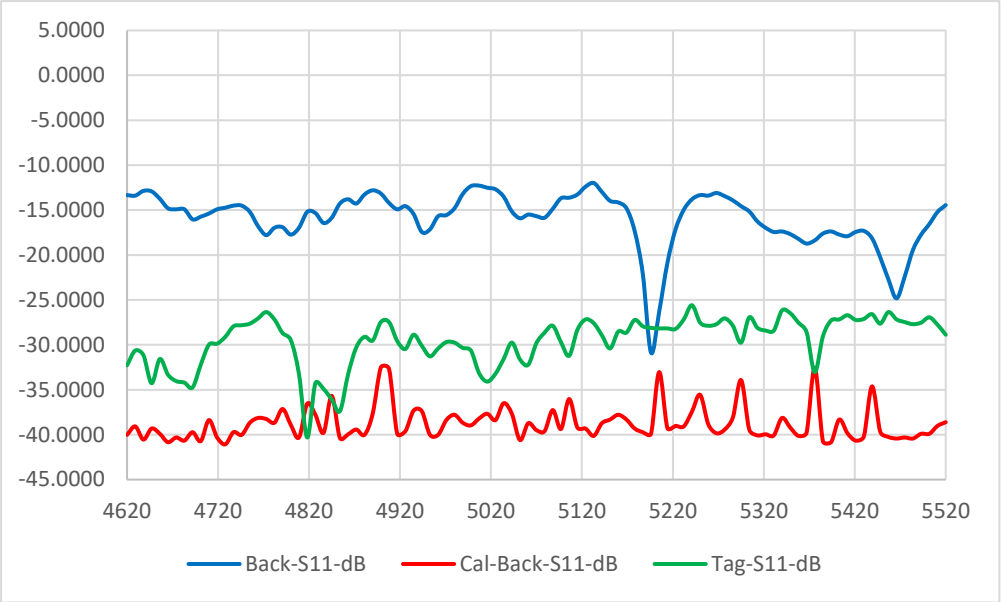

Figure 9.14 – Cardboard with two tags of 1000

c. Several tags of the same tag ID attached to an empty cardboard box

In this experiment a small empty cardboard box is tested with many tags of the same ID. In Figure 9.15 the experimental setup is shown. Figure 9.16 and 9.17 shows the results when 2 tags and 8 tags are attached to the box respectively.

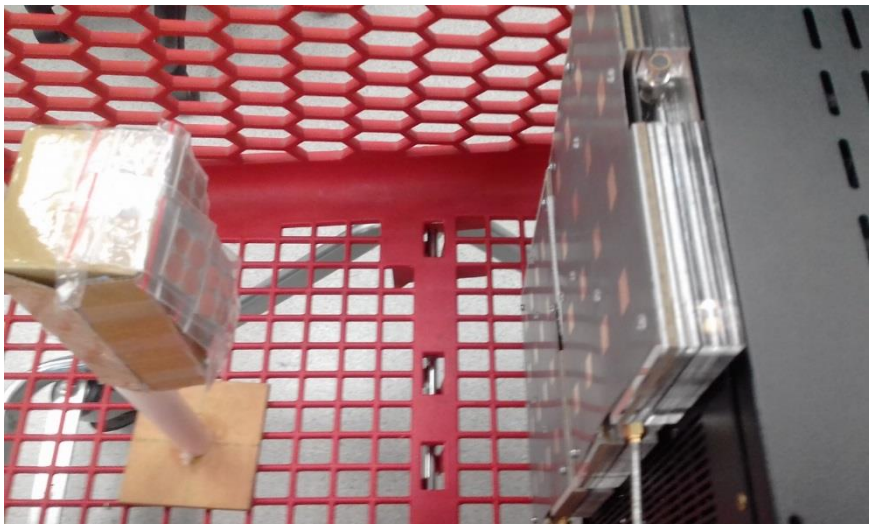

Figure 9.15 – Small cardboard box with tag 1111 attached

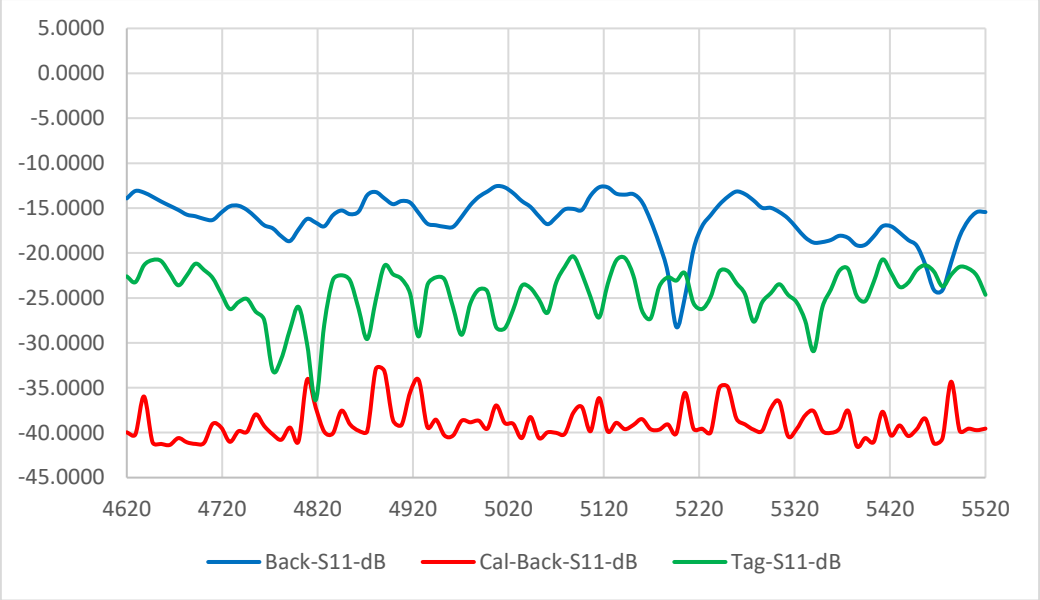

Figure 9.16 – Cardboard box with 2 tags of tag ID 1000

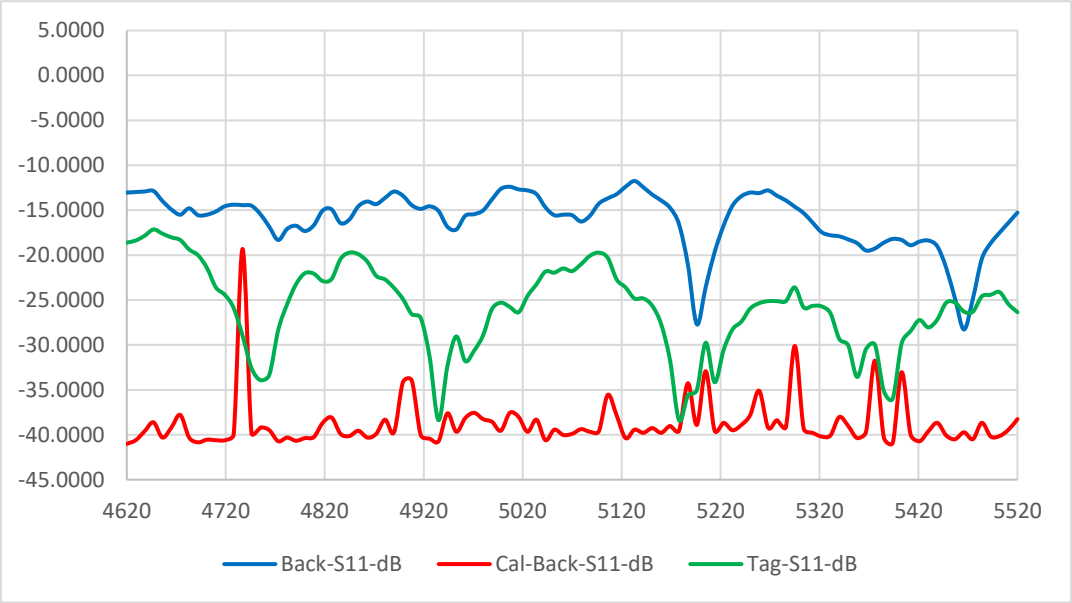

Figure 9.17 – Cardboard box with 8 tags of tag ID 1111

In Figure 9.16, the green curve shows the result of the tag information and the tag ID can be detected after applying the detection algorithm as '1000'. But, the signal shows lot of distortion and can lead to false detection. When multiple tags are attached to the box as shown in Figure 9.15 the received signal shows a big improvement. As seen in Figure 9.17 the 4 bits can be clearly identified even without applying the detection algorithm. This experiment shows that for items which are hard to detect due to

distortion can be detected by tagging them with multiple tag strips of the same ID. It can be concluded that the combined backscattered signal of all tags enhances the performance.

9.2.2 Detection of tagged items

In this section the experimental results of the detection of tagged targeted commercially available items are presented. The results of the items which are hard to detect due to material effects are shown below. First, the S11 parameter measurements are taken by placing the cereal box only. Figure 9.19 shows the corresponding results which shows a signal with lots of notches. Due to the airgap inside the box there are many reflections occurring which results in this output.

Figure 9.18 – Cereal box in front of the system

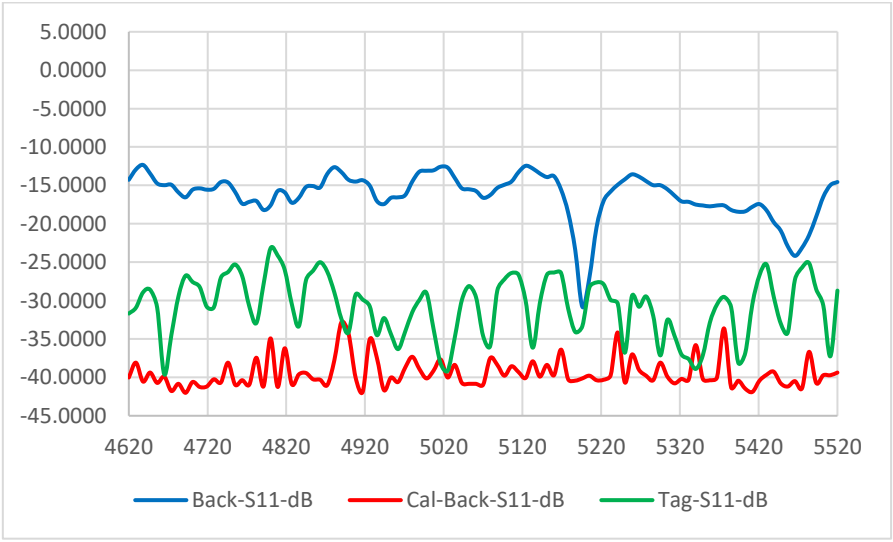

Figure 9.19 – Cereal box only with array antenna

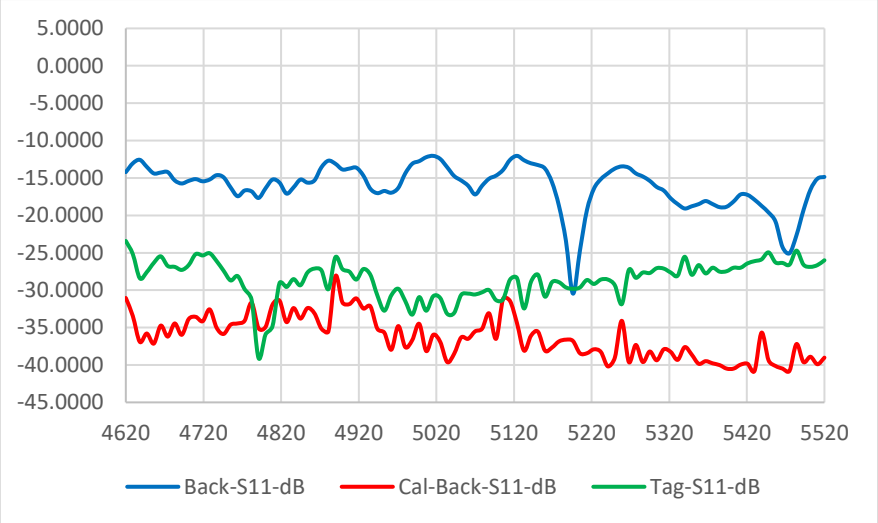

Figure 9.20 – Empty Cereal box with tag 1000

Then the tag 1000 was attached to the cereal box and was dropped into the trolley. This was not able to detect and showed a similar result as in Figure 9.19. Next, the cereal packet was removed from the box and the empty box without cereal was placed for detection. Figure 9.20 shows the result of the empty cereal box with tag 1000 on it, which shows the correct tag ID of '1000' at a distance of 30cm.

The detection of all items were tested with the system as before. The result with the coke can is shown below in Figure 9.21 and 9.22, which shows the final detection after applying the detection algorithm. As shown in the results the condition band is set during the calibration. The background calibration is repeated after one thousand frequency sweeps. This updates the condition band accordingly if there is a change in the surrounding environment. Also, while calculating the 'condition band' for the detection, the minimum and maximum noise levels due to the surrounding environment are stored in separate variables and are eliminated during the process.

In Figure 9.21 it shows the result when no tag was attached to the coke can. After applying the detection algorithm, the bit coefficients of all 4-bit frequencies does not fall into the condition band. Therefore, for this detection the tag ID will be decoded as 'No tag' or '0000'. When tag 1111 is attached to the coke can all 4-bits fall within the 'condition band'. The tag ID is decoded as '1111'.

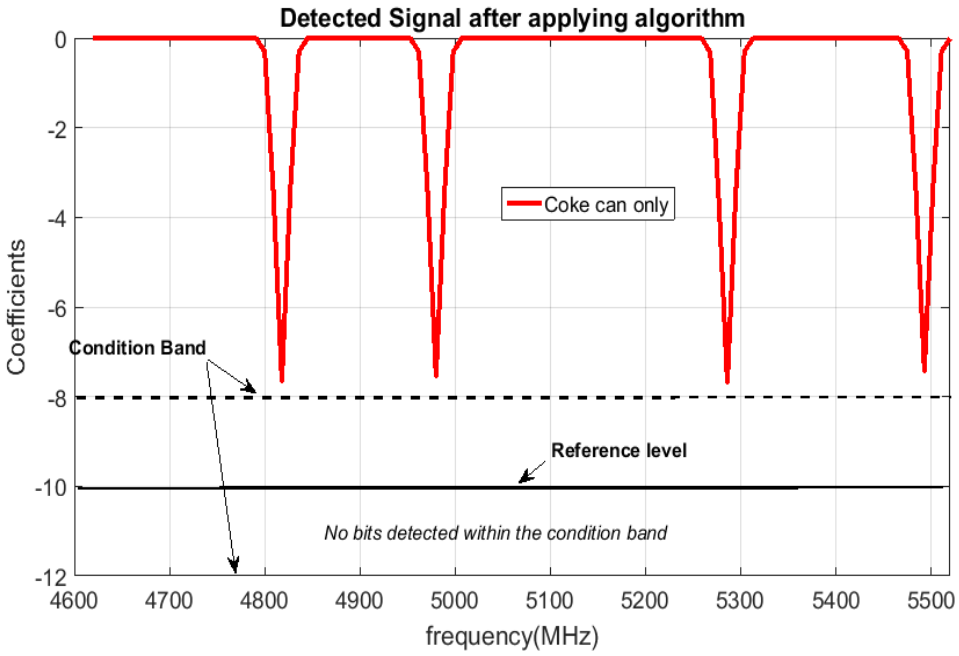

Figure 9.21 – Coke can only detected as 0000

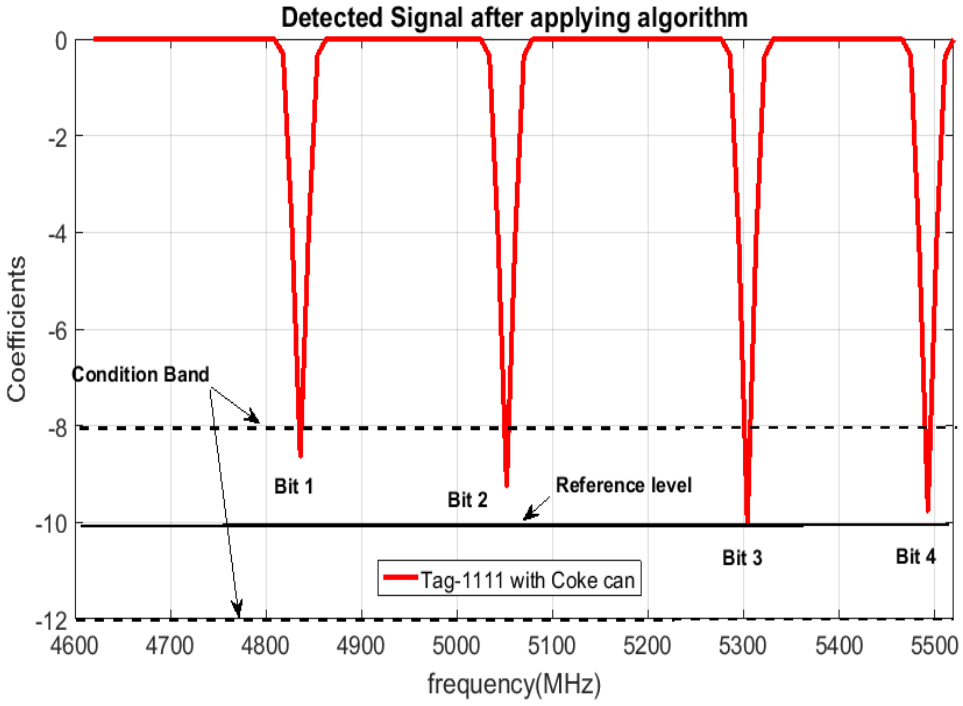

Figure 9.22 - Tag 1111 attached to the coke can detected as 1111

In the next section the detection of the direction of movement is presented. The detailed method of the improved detection algorithm for the final shopping trolley system including the detection of the direction of the movement is given by the flowchart shown in Figure 9.24.

9.3 Tagged object dynamics and direction of movement

The final stage of the smart shopping trolley is to detect the items while it is dropping into the trolley and while the item is taken out from the trolley. Figure 9.23 shows the final setup for the smart shopping trolley project with a user interface which displays the output.

Figure 9.23 - Chipless RFID reader system for Smart Trolley Project

The direction of movement is detected by calculating the received signal power strength (RSS) for Antenna 1 and Antenna 2 at the beginning and during the detections. The parameters P1, P2 were defined which are the initial signal power of Antenna 1 and Antenna 2. They are calculated at the calibration and the parameters R1 and R2 were defined as the received signal power of Antenna 1 and Antenna 2 at a given time. Comparing R1 and R2 in each iteration of the item detection with stored P1 and P2 values the algorithm was updated to detect the direction of the movement of the item with the tag. A separate bit was generated to denote the direction at the beginning of the final decoded tag ID. An item dropping in is denoted as bit '1' and if an item is taken out it is denoted as bit '0'. Therefore, the final decoded result will be given in 5 bits on the display. Figure 9.24 shows how the antennas are selected for the detection of the direction of movement.

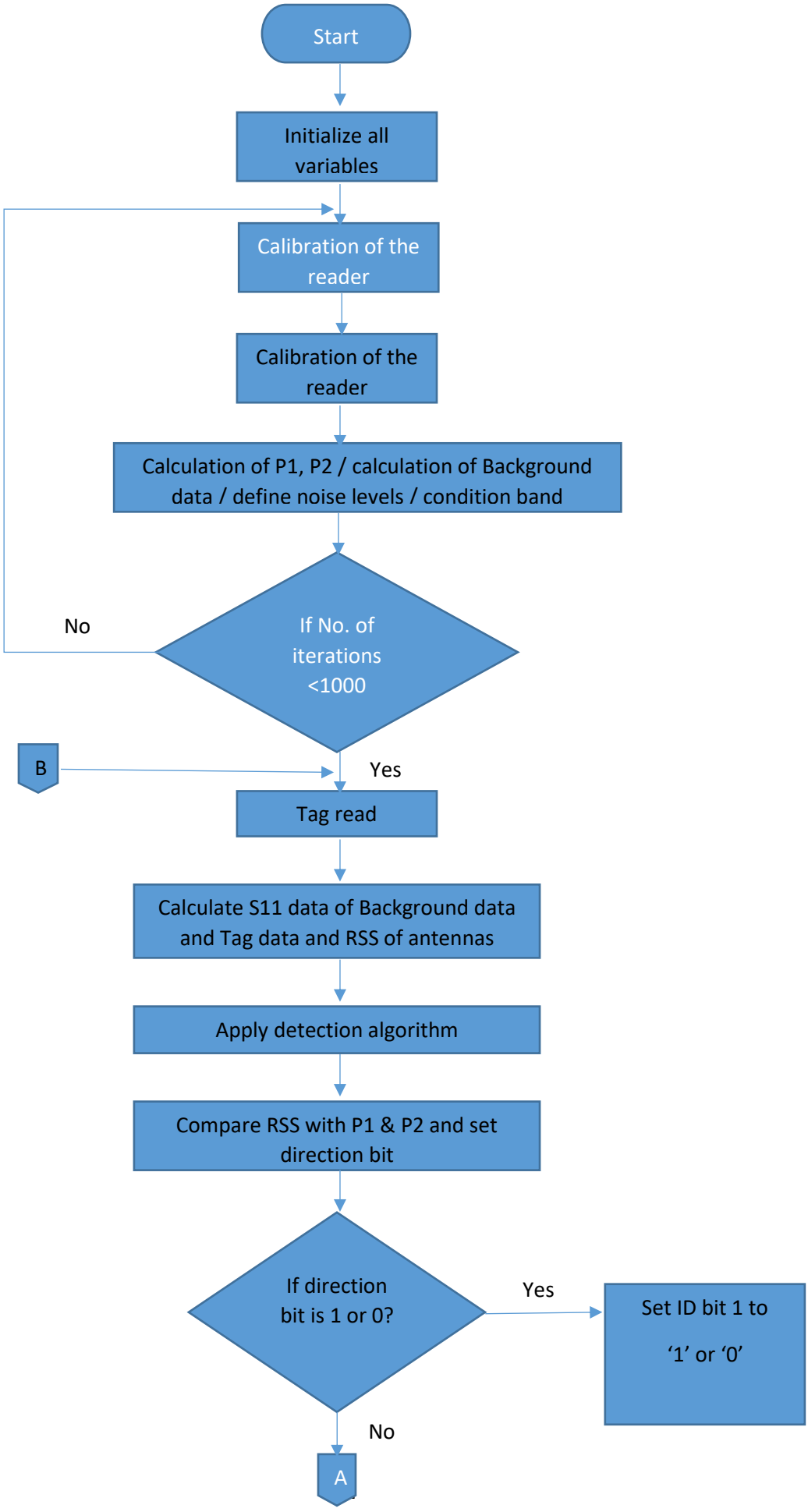
Start
Initialize all variables
Calibration of the reader
Calibration of the reader
Calculation of P1, P2 / calculation of Background data / define noise levels / condition band
If No. of iterations <1000
No
Yes
B
Tag read
Calculate S11 data of Background data and Tag data and RSS of antennas
Apply detection algorithm
Compare RSS with P1 & P2 and set direction bit
If direction bit is 1 or 0?
Yes
Set ID bit 1 to '1' or '0'
No
A

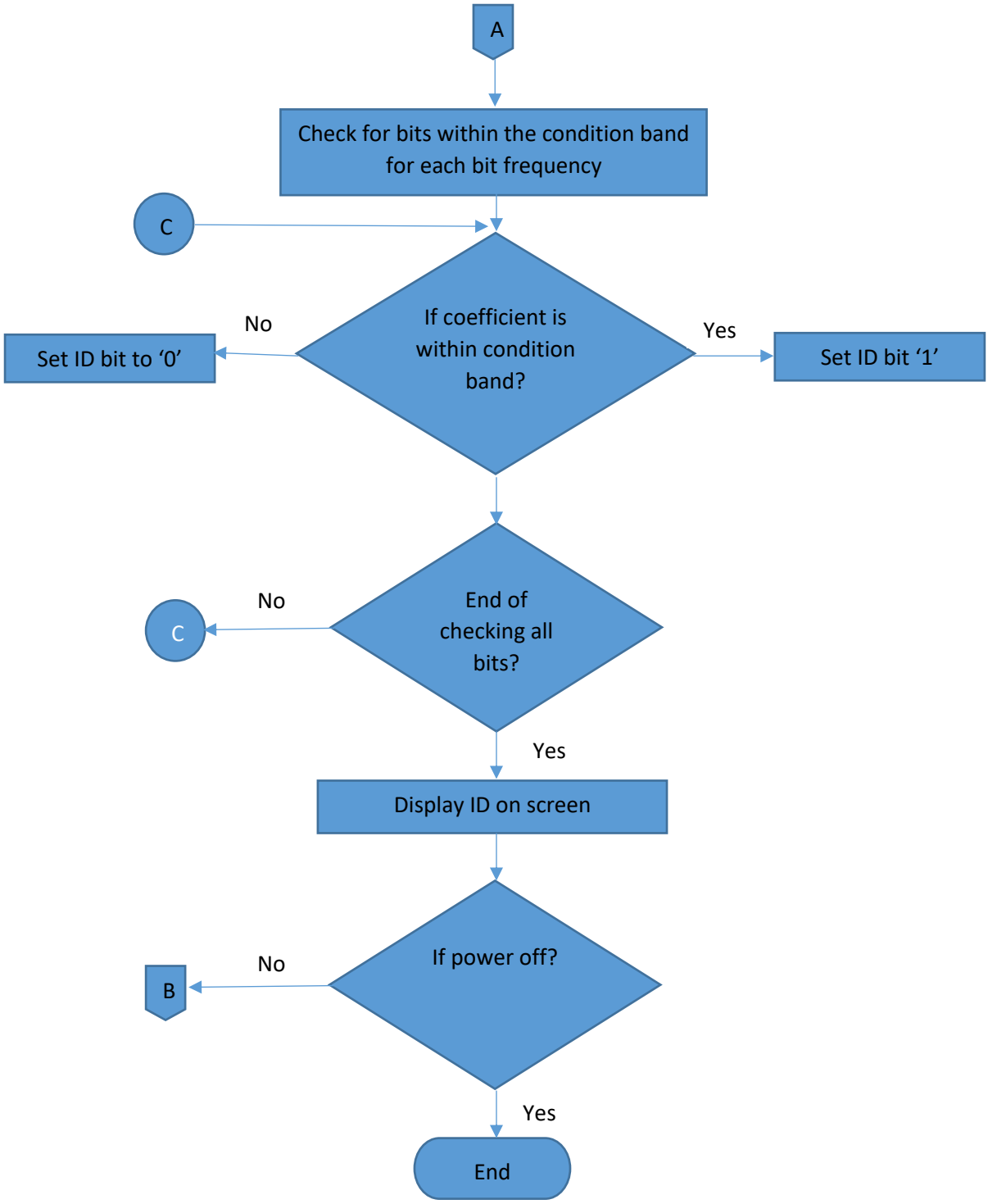

Figure 9.24 - Flowchart for the detection of tagged items in the smart shopping trolley with direction of movement

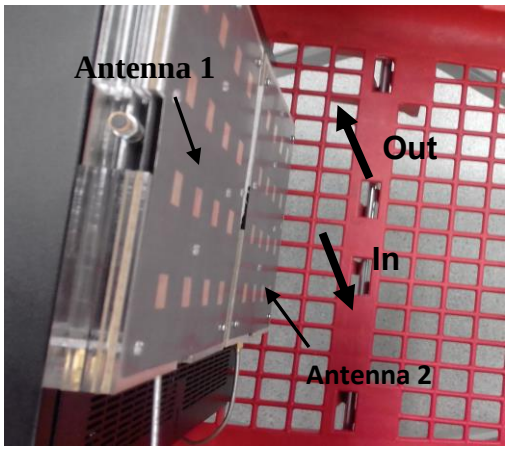

Figure 9.25 – Antenna configuration for the detection of the direction of movement

9.4 Detection of tag in a dynamic environment

Signal collides with other scatterers or tags which give a ‘clutter' signal with interference. Measured results with hand and copper plate placed at 10 cm distance, placing the tag at the corner end of the patch antenna and its original signal in a normal indoor environment using vector modulator reader. The detection with different clutter objects and its results are given in Figure 9.26 and 9.27.

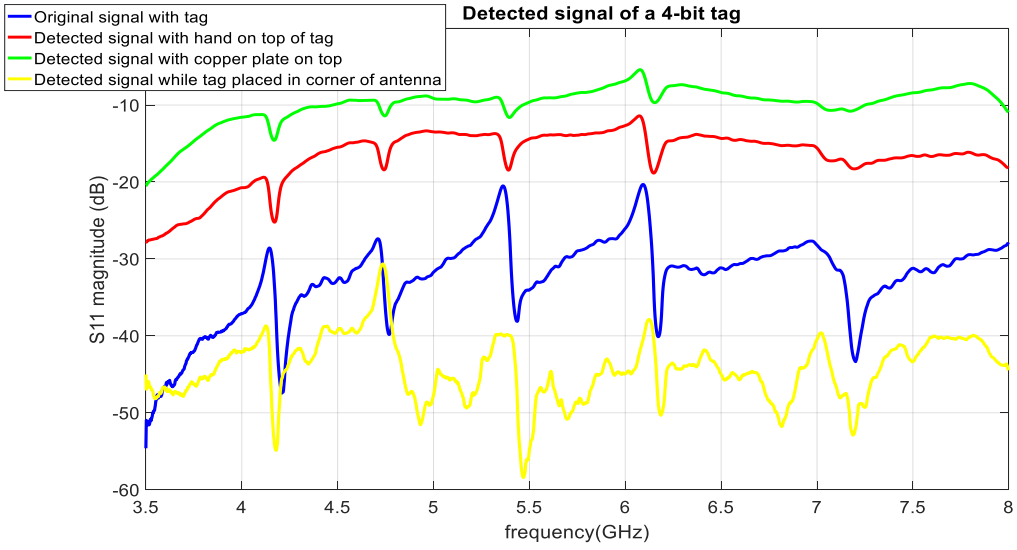

Figure 9.26 - Measured results with clutter

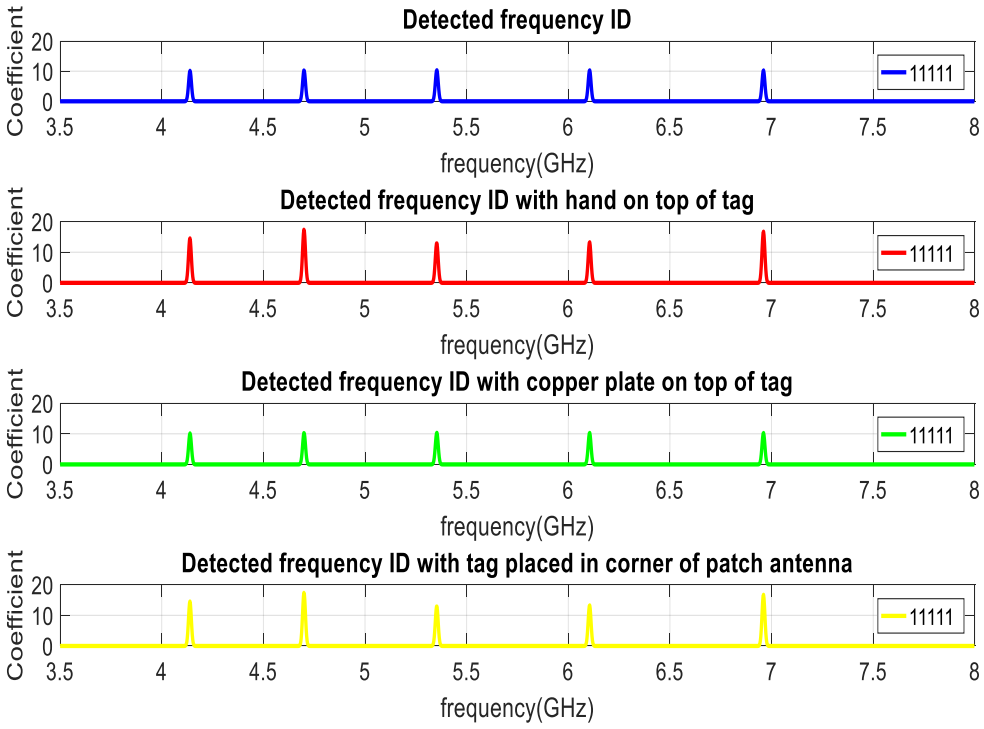

Figure 9.27 - Wavelet coefficients of the detected signals after applying the detection algorithm

The 4-bit printed tag with tag ID '1111' was used with the VMR in this experiment. As the detection algorithm gives an extra bit for the direction of movement the first bit is set as '1' for the entire experiment. As seen in Figure 9.27 the tag at 10 cm distance can be easily detected among the clutter objects. Also, the last result shown by the yellow curve is when the tag is placed not right in front of the antenna, this shows that the tag can be detected when it is not in direct contact with the antenna. But, as proved in previous chapters the tag should be within the beamwidth of the antenna.

9.5 Conclusion

The smart shopping trolley had the most challenging goals to achieve in this research work. The vector modulator reader and the 4 x 4 patch array antenna implementation along with the applied digital signal processing made these goals achievable.

The chapter opens with the testing of tags using the VMR and the results show that the tags are detectable up to a distance of 30 cm. The calibration for material effects gives the conclusion that items

with a metal backgrounds will degrade the low power tag backscattered signal giving rise to the S11 magnitude level. Comparatively cardboard materials as background will have less effect to the detection of the tag. The real application tests with tagged different items gives successful detection on the move up to a distance of 10 to 15 cm. The tagged coke can with a metal background can be still detected up to a distance of 10 cm. On the other hand, the cereal box containing cereal creates a highly distorted signal and it is hard to detect the tag at 10 cm. This can be overcome by tagging more than one tag on the cereal box as it has been proved in this section that the combined tag effect enhances the performance detection. This fulfils the goal of the detection of different tagged items on the move.

The direction of movement of the tagged item is successfully detected using the received signal power strength of the TX and RX antennas. The only drawback in the system was that the detection could not be covered for the full area of the shopping trolley. The length of the shopping trolley was 40 cm and the detection were possible only to a distance of 15 cm for all items. Since the patch array antenna has the ability to detect to a far more distance, by improving the tag into a cross polar tag as concluded in the previous chapter it is believed that this issue also could be overcome.

10 Conclusion

A brief summary of the research background, initial objectives set for addressing the research gaps, and tasks accomplished in the previous chapters to achieve the thesis aims are discussed hereby. This research work is part of the project funded by the Australian Research Council's Linkage Project Grant # LP130101044, titled, "Discreet Reading of Printable Multi-bit Chipless RFID Tags on Polymer Banknotes". The proposed research aims to evaluate the robust performance of chipless RFID systems by addressing (i) moving tag detection, (ii) developing robust detection algorithms (iii) Implementation of the algorithm in firmware, (iv) Investigation into the robustness of the algorithm in dynamic environment and finally, (v) the reduction of false negatives and false positives. This research has filled the gaps in the contemporary knowledge of moving chipless tag detection, for a single antenna and an array antenna of the chipless RFID reader. This research will contribute to making chipless RFID commercially viable for applications with movement such as conveyor belt applications, handheld motion of tagged objects and animal monitoring.

10.1 Fulfilling the goals of the thesis

The main goal of the thesis is to develop advanced yet computationally feasible tag detection technique for the chipless RFID system with tag movement. The technique is capable of improving the tag reading accuracy, reading range and the data bit capacity. In this section, how the goals are fulfilled in the many chapters of the thesis are presented. Chapter 4 presented signal processing techniques using adaptive wavelet-based detection algorithm [2] for successfully detecting the tag ID of a moving tag. The adaptive wavelet-based detection algorithm was used on results obtained by the Vector Network Analyzer (VNA) to confirm the robust detection of a chipless RFID tag in motion. So that, it can be implemented and tested in hardware for a real-time chipless RFID system with tag on the move.

The detection of a chipless RFID tag in stepped motion is proposed in Chapter 5. The performance is evaluated through experiment and measurement using vector network analyzer. The post processing of

the measured results is performed using Matlab. A novel adaptive wavelet-based detection algorithm is used for the decoding of the tag ID [2]. An error analysis is conducted on the experimental results to study the variation of magnitude and frequency due to the movement of a chipless RFID tag. As far as the tag signature has not been disappeared from the reading range it has the same confidence level for the detection of its tag ID. This opens a new avenue towards developing detection algorithms and decoding techniques when the chipless RFID tag is in motion. It also opens the doors for the localization of moving chipless RFID tags and prediction of the tagged objects moving trajectory modelling in the future.

This algorithm has been applied for a single antenna reader system using a single patch antenna [3] in Chapter 6, as well as a vector modulator reader system using an array antenna in Chapter 8. In both applications it has been shown that the encoded tag data bits were identified successfully.

This reveals a novel approach and method to detect the movement of a chipless RFID tag. It gives an exposure to the parameters that are affected by a chipless RFID tag in stepped motion and gives an estimation to the robustness of its tag ID using the adaptive wavelet-based detection algorithm [2].

The S11 magnitude shifts at the relevant resonant frequencies are as expected within the half power beamwidth of the antenna and is not detectable as it moves out from the antenna aperture. The confident band set in the detection algorithm using the results for a moving chipless RFID tag proves that the correct frequency ID can be detected successfully around a percentage of 80%. Also, this leads to a research pathway for the improvement of the reading range which is essential as the variation in magnitude and phase increases as it moves beyond the beamwidth of the given antenna. The experiments also confirm that the frequencies stay mostly unperturbed thus giving the ability to detect the tag ID without much difficulty.

In this experiment stepped motion was considered since the VNA cannot capture the data while it is in motion. But the number of data captures analyzed in this experiment will be equal to the number of data sets captured by the chipless RFID reader in a real time movement scenario. Therefore, the results of this experiment will be equivalent to results expected from the system. The detection algorithm has been implemented for a single antenna chipless RFID reader. Also, further development to the system

can introduce error correction techniques to correct any bit errors after detection. This will open the research pathway to many practical applications with tagged objects to be tracked in movement.

Once the detection was satisfactory the chipless RFID reader system has been tested for its reliability and repeatability. By the performance of a sensitivity analysis on the parameters of variability of a chipless RFID system giving rise to false negatives and false positives during fabrication and printing the algorithm has been improved to reduce the errors of the system. Thus, the developed algorithm for moving tag detection is brood to the stage of commercial reality. The research has brought the following original contributions in the field:

1. A novel empirical model approach is presented to detect a moving tag [32].
2. A novel detection algorithm is developed using an adaptive wavelet-based algorithm to detect a moving tag in an improved reading range [2].
3. Implementation of the developed algorithm in a real time system [29].
4. A sensitivity analysis of the reader system is conducted to reduce false negatives and false positives [33].
5. Tracking the direction of the moving chipless RFID tags using two antenna system in a smart shopping trolley.

The thesis generates two Q1 Journal publications, one invited research chapter, one open access journal paper by invitation and three conference papers.

10.2 Limitations of the proposed system

The final goal of the proposed system, as part of the smart shopping trolley project was to detect identical items dropped into the trolley and detect if any of them are taken out of the trolley. This could not be satisfied as multiple tag detection was not applied in the system. Also, it was proposed in this project to detect item dropping from any point of the trolley. But as the array antenna developed did not cover the complete area of the trolley this was not satisfied. But the main goal in this research work was the robust detection of the tag while it is in movement, which was successfully satisfied as we could detect the tagged items while they were in the movement of dropping into the trolley.

However, the performance of the proposed tag detection method could be limited by few factors. One of the main factors is the fabrication defects such as the dielectric constant of the substrate and the precision of the line widths. Due to these inaccuracies in tag design, two tags with the same tag data bits could have slight frequency shifts in their tag responses. These imperfections could affect the successful tag detection rate. In addition, when the tags are fabricated on paper the resonance level is less, compared to that on substrates. Also, the material and density of the items caused distortion which was not able to be removed using the proposed algorithm.

The tag should generate high backscattered signal hence a high radar cross section (RCS) tag design is the prime for a successful RFID system design. Next, the tag must be low cost and directly printed on substrate materials. High conductivity ink and low loss laminates are used for fabrication of the tag. MMARS Laboratory perfected various printing techniques such as screen printing, flexography and gravure printing techniques for best tag performance. In addition to the above, a low loss thin dielectric coating on the printed chipless RFID sensors as a protective measure can be used. However, the substrate material needs to be examined in order to make them more sensitive in UWB microwave frequency.

In the chipless RFID sensor [1], we do not need any power supply as they are fully passive. Usually a reader sends energy to the sensor. Therefore, it is the power of the reader that needs to be extended. Usually, a rechargeable battery or a power supply is connected with the main power supply is used for the reader. Since a chipless RFID sensor is a fully passive printable device. Therefore, the lifetime of the sensor depends on the application of the chipless RFID tag.

If a chipless RFID tag is used for item tagging as discussed in Chapter 9 then it will have a long lifetime unless it is damaged or scratched. If it is applied in cash notes as an identification, it will be covered with a protective flexible material, hence will have log lifetime. But, if the notes are crumpled there can be difficulties in identification. For tags on big items such as in luggage tracking or conveyor belt applications it will be more suitable as it will not suffer from crumpling and will have a longer lifetime.

10.3 Future improvements and applications

A cross polar tag is proposed to overcome many problems and drawbacks in detecting different tagged items in the smart trolley project. The same algorithm can be used for a cross polar tag and since the tag RCS will be in a different polarization it could be easily detected with a noise free signal. Therefore, with a new design of a cross polar tag this project can be completed successfully. In the era of information communication technology (ICT), everything is going to be wireless. The emerging internet of things (IoT) needs trillions of very low cost on demand wireless sensor nodes each year. Therefore, the sensor should be low cost, disposable, compact and environmentally friendly like optical barcodes. Therefore, the technology will solve the vision for IoT in mass deployment. Also as mentioned in Chapter 10, Section 3, a cross polar tag would overcome many problems in detecting a noise free scatter signal giving the correct tag ID. Therefore, the main challenge will be designing a cross polar tag to meet all the frequency requirements. Printing material and ink chosen for the tags will be the next challenge. In Monash Microwave, Antenna, RFID and Sensor (MMARS) Laboratory the author's team designed tags and printed on various substrate materials with conducting inks. The reader antenna also needs to be miniaturized which will lower the cost of the reader.

The whole system comprises a reader and a chipless tag. The tag is fully printable object like a barcode. Therefore, the system miniaturisation comes from the compact reader design. The reader consists of an antenna, a UWB transceiver electronics and the digital section. The antenna needs to be miniaturised and will face the challenge of reading the same distance if the gain is too low. Also, while miniaturising it need to still be a dual polarised antenna to read a cross polar tag. The reader can be miniaturised and all components designed on a single board. At Monash Microwave, Antenna, and RFID (MMARS) laboratory we developed a handheld reader like an optical barcode scanner.

The proposed detection algorithm can be applied to many other applications such as conveyor belt applications and medical imaging. Hyper parallel optical coherence tomography (HP-OCT) is an emerging technology in optometry. A problem faced in retinal image registration of obtained human

eye images is in the movement of the on fast images. The proposed detection algorithm is a novel approach in solving this issue.

This study explores through the important phases of a chipless RFID system with tag movement which still needs development and the findings can be incorporated to improve the robustness and the reliability of the chipless RFID system to make this technology suitable for commercial applications.

Appendix A

Attribute Agreement Analysis:

Each Appraiser vs Standard

Assessment Agreement

Appraiser	# Inspected	# Matched	Percent	95% CI
1	20	19	95.00	(75.13, 99.87)
2	20	20	100.00	(86.09, 100.00)
3	20	20	100.00	(86.09, 100.00)
4	20	19	95.00	(75.13, 99.87)

Matched: Appraiser's assessment across trials agrees with the known standard.

Fleiss' Kappa Statistics

Appraiser	Response	Kappa	SE Kappa	Z	P(vs > 0)
1	Reflector	1.00000	0.223607	4.47214	0.0000
	Tag A	0.85663	0.223607	3.83097	0.0001
	Tag B	1.00000	0.223607	4.47214	0.0000
	Tag C	0.87461	0.223607	3.91137	0.0000
	Overall	0.93322	0.129316	7.21663	0.0000
2	Reflector	1.00000	0.223607	4.47214	0.0000
	Tag A	1.00000	0.223607	4.47214	0.0000
	Tag B	1.00000	0.223607	4.47214	0.0000
	Tag C	1.00000	0.223607	4.47214	0.0000
	Overall	1.00000	0.129099	7.74597	0.0000
3	Reflector	1.00000	0.223607	4.47214	0.0000
	Tag A	1.00000	0.223607	4.47214	0.0000
	Tag B	1.00000	0.223607	4.47214	0.0000
	Tag C	1.00000	0.223607	4.47214	0.0000
	Overall	1.00000	0.129099	7.74597	0.0000
4	Reflector	1.00000	0.223607	4.47214	0.0000
	Tag A	0.85663	0.223607	3.83097	0.0001
	Tag B	1.00000	0.223607	4.47214	0.0000
	Tag C	0.87461	0.223607	3.91137	0.0000
	Overall	0.93322	0.129316	7.21663	0.0000

Between Appraisers

Assessment Agreement

# Inspected	# Matched	Percent	95% CI
20	19	95.00	(75.13, 99.87)

Matched: All appraisers' assessments agree with each other.

Fleiss' Kappa Statistics

Response	Kappa	SE Kappa	Z	P(vs > 0)
Reflector	1.00000	0.0912871	10.9545	0.0000
Tag A	0.90442	0.0912871	9.9074	0.0000
Tag B	1.00000	0.0912871	10.9545	0.0000
Tag C	0.91641	0.0912871	10.0387	0.0000
Overall	0.95548	0.0527928	18.0987	0.0000

All Appraisers vs Standard

Assessment Agreement

# Inspected	# Matched	Percent	95% CI
20	19	**95.00**	(75.13, 99.87)

Matched: All appraisers' assessments agree with the known standard.

Fleiss' Kappa Statistics

Response	**Kappa**	SE Kappa	Z	P(vs > 0)
Reflector	1.00000	0.111803	8.9443	0.0000
Tag A	0.92832	0.111803	8.3031	0.0000
Tag B	1.00000	0.111803	8.9443	0.0000
Tag C	0.93730	0.111803	8.3835	0.0000
Overall	0.96661	0.064604	14.9621	0.0000

* NOTE * Single trial within each appraiser. No percentage of assessment agreement within appraiser is plotted.

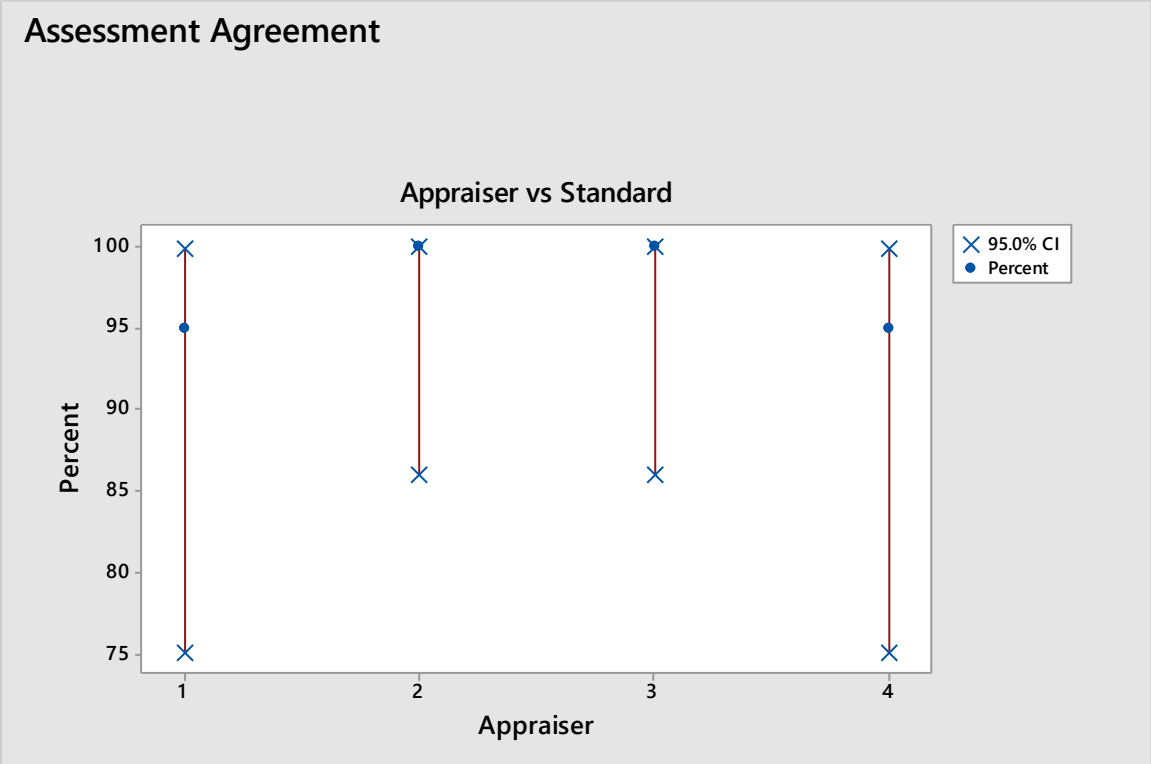

REFERENCES

[1] S. Preradovic, and N. C. Karmakar, “Chipless RFID: Bar code of the future,” *IEEE Microwave Magazine,* vol. 11, no. 7, pp. 87-97, 2010.

[2] M.A.Bibile and N.C. Karmakar, “A novel- adaptive wavelet based detection for chipless RFID system”, *Fourth International Conference on Signal and Image Processing (*SIGL), Geneva, Switzerland, Mar. 25 – 26, 2017. and *Computer Science Conference Proceedings in Computer Science & Information Technology (CS & IT) series*, Geneva, Switzerland, Mar. 25 – 26, 2017.

[3] M. Forouzandeh and N.C. Karmakar, "Towards the Improvement of Frequency-domain Chipless RFID Readers", *IEEE Wireless Power Transfer Conference (WPTC),* 2018

[4] F. Babaeian and N.C. Karmakar, "A High Gain Dual Polarized Ultra-Wideband Array of Antenna for Chipless RFID Applications", *IEEE Access*, 2018

[5] M. A. Islam, and N. C. Karmakar, “A novel compact printable dual-polarized chipless RFID system,” *IEEE Transactions on Microwave Theory and Techniques,* vol. 60, no. 7, pp. 2142-2151, 2012.

[6] S. Preradovic, and N. C. Karmakar, “Chipless RFID: Bar code of the future,” *IEEE Microwave Magazine,* vol. 11, no. 7, pp. 87-97, 2010.

[7] M. A. Islam, and N. C. Karmakar, “A 4 × 4 dual polarized mm-wave ACMPA array for a universal mm-wave chipless RFID tag reader,” *IEEE Transactions on Antennas and Propagation,* vol. 63, no. 4, pp. 1633-1640, 2015.

[8] M. S. Bhuiyan, and N. C. Karmakar, “An efficient coplanar retransmission type chipless rfid tag based on dual-band mcsrr,” *Progress In Electromagnetics Research C,* vol. 54, pp. 133-141, 2014.

[9] S. Preradovic, and N. C. Karmakar, “Design of chipless RFID tag for operation on flexible laminates,” *IEEE Antennas and Wireless Propagation Letters,* vol. 9, pp. 207-210, 2010.

[10] I. Balbin, and N. C. Karmakar, “Phase-encoded chipless RFID transponder for large-scale low-cost applications,” *IEEE Microwave and Wireless Components Letters,* vol. 19, no. 8, pp. 509-511, 2009.

[11] M. Sumi, R. Dinesh, C. M. Nijas *et al.*, “High bit encoding chipless RFID tag using multiple E-shaped microstrip resonators,” *Progress In Electromagnetics Research B,* vol. 61, no. 1, pp. 185-196, 2015.

[12] R. V. Koswatta, and N. C. Karmakar, "A novel reader architecture based on UWB chirp signal interrogation for multiresonator-based chipless RFID tag reading," *IEEE Transactions on Microwave Theory and Techniques,* vol. 60, no. 9, pp. 2925-2933, 2012.

[13] S. Hu, Y. Zhou, C. L. Law *et al.*, "Study of a uniplanar monopole antenna for passive chipless UWB-RFID localization system," *IEEE Transactions on Antennas and Propagation,* vol. 58, no. 2, pp. 271-278, 2010.

[14] S. Preradovic, S. M. Roy, and N. C. Karmakar, "RFID system based on fully printable chipless tag for paper-/plastic-ltem tagging," *IEEE Antennas and Propagation Magazine,* vol. 53, no. 5, pp. 15-32, 2011.

[15] M. Zomorrodi, "mm-wave EM-imaging Chipless RFID System", *A thesis submitted for the degree of Doctor of Philosophy at Monash University,* 2015.

[16] http://www.marketsandmarkets.com/MarketReports/chipless-rfid-market-501.html

[17] R. V. Koswatta, and N. C. Karmakar, "Moving Average Filtering Technique for Signal Processing in Digital Section of UWB Chipless RFID Reader," *Proceedings of Asia-Pacific Microwave Conference,* pp. 1304-1307, 2010.

[18] P. Kalansuriya, N. C. Karmakar, and E. Viterbo, "On the detection of chipless RFID through signal space representation," *Annales des Telecommunications/Annals of Telecommunications,* vol. 68, no. 7-8, pp. 437-445, 2013.

[19] A. R. Antonio Lazaro, D. Girbau, R. Villarino, "Chipless UWB RFID Tag Detection Using Continuous Wavelet Transform," *IEEE ANTENNAS AND WIRELESS PROPAGATION LETTERS,* vol. VOL. 10, 2011.

[20] R. Rezaiesarlak, and M. Manteghi, "A space-frequency technique for chipless RFID tag localization," *IEEE Transactions on Antennas and Propagation,* vol. 62, no. 11, pp. 5790-5797, 2014.

[21] R. Rezaiesarlak, and M. Manteghi, "Complex-natural-resonance-based design of chipless RFID tag for high-density data," *IEEE Transactions on Antennas and Propagation,* vol. 62, no. 2, pp. 898-904, 2014.

[22] R. Rezaiesarlak, and M. Manteghi, "A space-time-frequency anticollision algorithm for identifying chipless RFID tags," *IEEE Transactions on Antennas and Propagation,* vol. 62, no. 3, pp. 1425-1432, 2014.

[23] R. Rezaiesarlak, and M. Manteghi, "Short-time matrix pencil method for chipless RFID detection applications," *IEEE Transactions on Antennas and Propagation,* vol. 61, no. 5, pp. 2801-2806, 2013.

[24] R. E. A. Anee, and N. C. Karmakar, "Chipless RFID tag localization," *IEEE Transactions on*

Microwave Theory and Techniques, vol. 61, no. 11, pp. 4008-4017, 2013.

[25] Karmakar N.C., "Tag You're It", *IEEE Microwave Magazine*, July 2016, pp 64-74

[26] Buffi A., Nepa P., Lombardini F., "A Phase-Based Technique for Localization of UHF-RFID Tags Moving on a Conveyor Belt: Performance Analysis and Test-Case Measurements*", IEEE Sensors Journal, Vol 15, No. 1,* January 2015, pp 387-395.

[27] C. Divarathna, N.C. Karmakar, "A Maximum Likelihood Based Tag Detection Technique for MIMO Chipless RFID Systems," *IEEE International Microwave and RF Conference (IMaRC),* 2014.

[28] A. El-Awamry, A. Fawly, M. El-Hadidy, T. Kaiser, "Smart notch detection techniques for robust frequency coded chipless RFID systems", *IEEE Antennas and Propagation (EuCAP),* 2015

[29] M.A.Bibile and N.C. Karmakar, "Moving Chipless RFID Tag detection using Adaptive Wavelet Based Detection Algorithm", *IEEE Transactions on Antennas and Propagation,* 2018

[30] Shuvashis Dey and Nemai C. Karmakar, "Design of novel super wide band antennas close to the small antenna limitation theory", *IEEE MTT-S International Microwave Symposium (IMS2014),* 2014

[31] Meriam Anushani Bibile, Grishma Khadka, Larry M. Arjomondi and Nemai C. Karmakar, "Analysis of Artifacts on Chipless RFID Backscatter Tag Signals for Real World Implementation", *IEEE Access*, 2019

[32] M.A.Bibile and N.C. Karmakar, "Detection performance of a chipless RFID tag in motion", *IEEE International Microwave and RF Conference (IMaRC),* 2016. , Delhi, India, Dec 26 – 29, 2016.

[33] M.A.Bibile and N.C. Karmakar, "Detection Error Rate Analysis using Coloured Noise for Moving Chipless RFID Tag", *IEEE Australian Microwave Sysmposium (AMS),* 2018, Brisbane, Australia, Feb 6-8, 2018

[34] Tharindu Athauda and Nemai Karmakar, "Robust low-cost passive UHF RFID based smart shopping trolley", *IEEE Journal of Radio Frequency Identification,* Volume: 2 , Issue: 3 , Sept. 2018

[35] S. Shrestha, M. Balachandran, M. Agarwal *et al.*, "A chipless RFID sensor system for cyber centric monitoring applications," *IEEE Transactions on Microwave Theory and Techniques,* vol. 57, no. 5, pp. 1303-1309, 2009.

[36] L. Yang, R. Zhang, D. Staiculescu *et al.*, "A novel conformal RFID-enabled module utilizing inkjet-printed antennas and carbon nanotubes for gas-detection applications," *IEEE Antennas and Wireless Propagation Letters,* vol. 8, pp. 653-656, 2009.

[37] M. Bernier, F. Garet, E. Perret *et al.*, "Terahertz encoding approach for secured chipless radio

frequency identification," *Applied Optics,* vol. 50, no. 23, pp. 4648-4655, 2011.

[38] A. T. Blischak, and M. Manteghi, "Embedded singularity chipless RFID tags," *IEEE Transactions on Antennas and Propagation,* vol. 59, no. 11, pp. 3961-3968, 2011.

[39] R. Miesen, R. Ebelt, F. Kirsch *et al.*, "Where is the tag?," *IEEE Microwave Magazine,* vol. 12, no. SUPPL.7, pp. 549-563, 2011.

[40] E. Perret, M. Hamdi, A. Vena *et al.*, "RF and THz identification using a new generation of chipless RFID tags," *Radioengineering,* vol. 20, no. 2, pp. 380-386, 2011.

[41] A. Ramos, A. Lazaro, D. Girbau *et al.*, "Time-domain measurement of time-coded UWB chipless RFID tags," *Progress in Electromagnetics Research,* vol. 116, pp. 313-331, 2011.

[42] B. Shao, Q. Chen, R. Liu *et al.*, "Configurable ink-jet-printed RFID tag on paper substrate for low cost and green applications," *Microwave and Optical Technology Letters,* vol. 53, no. 12, pp. 2781-2786, 2011.

[43] D. Girbau, J. Lorenzo, A. Lazaro *et al.*, "Frequency-coded chipless RFID tag based on dual-band resonators," *IEEE Antennas and Wireless Propagation Letters,* vol. 11, pp. 126-128, 2012.

[44] D. Girbau, Á. Ramos, A. Lazaro *et al.*, "Passive wireless temperature sensor based on time-coded UWB chipless RFID tags," *IEEE Transactions on Microwave Theory and Techniques,* vol. 60, no. 11, pp. 3623-3632, 2012.

[45] F. J. Herraiz-Martínez, F. Paredes, G. Z. Gonzàlez *et al.*, "Printed magnetoinductive-wave (MIW) delay lines for chipless RFID applications," *IEEE Transactions on Antennas and Propagation,* vol. 60, no. 11, pp. 5075-5082, 2012.

[46] P. Kalansuriya, N. C. Karmakar, and E. Viterbo, "On the detection of frequency-spectra-based chipless RFID using UWB impulsed interrogation," *IEEE Transactions on Microwave Theory and Techniques,* vol. 60, no. 12, pp. 4187-4197, 2012.

[47] M. Nair Sreejith, V. A. Shameena, M. Nijas *et al.*, "Novel chipless RF identification technology for on-touch data transfer applications," *Microwave and Optical Technology Letters,* vol. 54, no. 10, pp. 2325-2327, 2012.

[48] C. M. Nijas, R. Dinesh, U. Deepak *et al.*, "Chipless RFID tag using multiple microstrip open stub resonators," *IEEE Transactions on Antennas and Propagation,* vol. 60, no. 9, pp. 4429-4432, 2012.

[49] B. Shao, Q. Chen, R. Liu *et al.*, "Design of fully printable and configurable chipless RFID tag on flexible substrate," *Microwave and Optical Technology Letters,* vol. 54, no. 1, pp. 226-230, 2012.

[50] Y. Shen, and C. L. Law, "A low-cost UWB-RFID system utilizing compact circularly polarized chipless tags," *IEEE Antennas and Wireless Propagation Letters,* vol. 11, pp. 1382-1385, 2012.

[51] A. Vena, E. Perret, and S. Tedjini, "High-capacity chipless RFID tag insensitive to the polarization," *IEEE Transactions on Antennas and Propagation,* vol. 60, no. 10, pp. 4509-4515,

2012.

[52] A. Vena, E. Perret, and S. Tedjini, "Design of compact and auto-compensated single-layer chipless RFID tag," *IEEE Transactions on Microwave Theory and Techniques,* vol. 60, no. 9, pp. 2913-2924, 2012.

[53] A. Vena, E. Perret, and S. Tedjini, "A fully printable Chipless RFID tag with detuning correction technique," *IEEE Microwave and Wireless Components Letters,* vol. 22, no. 4, pp. 209-211, 2012.

[54] N. C. K. Abul K. M. Baki, "IMPROVED METHOD OF NODE AND THRESHOLD SELECTION IN WAVELET PACKET TRANSFORM FOR UWB IMPULSE RADIO SIGNAL DENOISING," *Progress In Electromagnetics Research,* 2013.

[55] H. Aubert, F. Chebila, M. Jatlaoui *et al.*, "Wireless sensing and identification based on radar cross section variability measurement of passive electromagnetic sensors," *Annales des Telecommunications/Annals of Telecommunications,* vol. 68, no. 7-8, pp. 425-435, 2013.

[56] F. Costa, S. Genovesi, and A. Monorchio, "A chipless RFID based on multiresonant high-impedance surfaces," *IEEE Transactions on Microwave Theory and Techniques,* vol. 61, no. 1, pp. 146-153, 2013.

[57] H. El Matbouly, N. Boubekeur, and F. Domingue, "A novel chipless identification tag based on a substrate integrated cavity resonator," *IEEE Microwave and Wireless Components Letters,* vol. 23, no. 1, pp. 52-54, 2013.

[58] M. Hasani, A. Vena, L. Sydanheimo *et al.*, "Implementation of a dual-interrogation-mode embroidered RFID-Enabled strain sensor," *IEEE Antennas and Wireless Propagation Letters,* vol. 12, pp. 1272-1275, 2013.

[59] C. Mandel, B. Kubina, M. Schüßler *et al.*, "Metamaterial-inspired passive chipless radio-frequency identification and wireless sensing," *Annales des Telecommunications/Annals of Telecommunications,* vol. 68, no. 7-8, pp. 385-399, 2013.

[60] E. Md Amin, N. Karmakar, and B. Winther-Jensen, "Polyvinyl-alcohol (PVA)-based RF humidity Sensor in microwave frequency," *Progress In Electromagnetics Research B,* no. 54, pp. 149-166, 2013.

[61] M. Mirzaee, and B. S. Virdee, "Realisation of highly compact planar lowpass filter for UWB RFID applications," *Electronics Letters,* vol. 49, no. 22, pp. 1396-1398, 2013.

[62] R. S. Nair, E. Perret, and S. Tedjini, "Group delay modulation for pulse position coding based on periodically coupled C-sections," *Annales des Telecommunications/Annals of Telecommunications,* vol. 68, no. 7-8, pp. 447-457, 2013.

[63] R. S. Nair, E. Perret, and S. Tedjini, "A temporal multi-frequency encoding technique for chipless RFID based on C-sections," *Progress In Electromagnetics Research B,* no. 49, pp. 107-127, 2013.

[64] R. S. Nair, E. Perret, S. Tedjini *et al.*, "A group-delay-based chipless RFID humidity tag sensor

using silicon nanowires," *IEEE Antennas and Wireless Propagation Letters,* vol. 12, pp. 729-732, 2013.

[65] B. Shao, Y. Amin, Q. Chen *et al.*, "Directly printed packaging-paper-based chipless RFID tag with coplanar LC resonator," *IEEE Antennas and Wireless Propagation Letters,* vol. 12, pp. 325-328, 2013.

[66] B. Shao, Q. Chen, Y. Amin *et al.*, "Chipless RFID tags fabricated by fully printing of metallic inks," *Annales des Telecommunications/Annals of Telecommunications,* vol. 68, no. 7-8, pp. 401-413, 2013.

[67] Y. Shen, C. L. Law, S. Hu *et al.*, "IR-UWB-based chipless RFID system," *Annales des Telecommunications/Annals of Telecommunications,* vol. 68, no. 7-8, pp. 375-383, 2013.

[68] S. Tedjini, N. Karmakar, E. Perret *et al.*, "Hold the chips: Chipless technology, an alternative technique for RFID," *IEEE Microwave Magazine,* vol. 14, no. 5, pp. 56-65, 2013.

[69] A. Vena, A. A. Babar, L. Sydanheimo *et al.*, "A novel near-transparent ask-reconfigurable inkjet-printed chipless RFID tag," *IEEE Antennas and Wireless Propagation Letters,* vol. 12, pp. 753-756, 2013.

[70] A. Vena, E. Perret, and S. Tedjini, "Design rules for chipless RFID tags based on multiple scatterers," *Annales des Telecommunications/Annals of Telecommunications,* vol. 68, no. 7-8, pp. 361-374, 2013.

[71] A. Vena, E. Perret, S. Tedjini *et al.*, "Design of chipless RFID tags printed on paper by flexography," *IEEE Transactions on Antennas and Propagation,* vol. 61, no. 12, pp. 5868-5877, 2013.

[72] A. Vena, E. Perret, and S. Tedjni, "A depolarizing chipless RFID tag for robust detection and its FCC compliant UWB reading system," *IEEE Transactions on Microwave Theory and Techniques,* vol. 61, no. 8, pp. 2982-2994, 2013.

[73] Y. F. Weng, S. W. Cheung, T. I. Yuk *et al.*, "Design of chipless UWB RFID system using A CPW multi-resonator," *IEEE Antennas and Propagation Magazine,* vol. 55, no. 1, pp. 13-31, 2013.

[74] E. M. Amin, M. S. Bhuiyan, N. C. Karmakar *et al.*, "Development of a low cost printable chipless RFID humidity sensor," *IEEE Sensors Journal,* vol. 14, no. 1, pp. 140-149, 2014.

[75] E. M. Amin, J. K. Saha, and N. C. Karmakar, "Smart sensing materials for low-cost chipless RFID sensor," *IEEE Sensors Journal,* vol. 14, no. 7, pp. 2198-2207, 2014.

[76] A. Attaran, R. Rashidzadeh, and R. Muscedere, "Chipless RFID tag using RF MEMS switch," *Electronics Letters,* vol. 50, no. 23, pp. 1720-1722, 2014.

[77] G. A. Casula, G. Montisci, P. Maxia *et al.*, "A narrowband chipless multiresonator tag for UHF RFID," *Journal of Electromagnetic Waves and Applications,* vol. 28, no. 2, pp. 214-227, 2014.

[78] B. S. Cook, R. Vyas, S. Kim *et al.*, "RFID-based sensors for zero-power autonomous wireless sensor networks," *IEEE Sensors Journal,* vol. 14, no. 8, pp. 2419-2431, 2014.

[79] F. Costa, S. Genovesi, and A. Monorchio, "Chipless RFIDs for metallic objects by using cross polarization encoding," *IEEE Transactions on Antennas and Propagation,* vol. 62, no. 8, pp. 4402-4407, 2014.

[80] S. Gupta, G. J. Li, R. C. Roberts *et al.*, "Log-periodic dipole array antenna as chipless RFID tag," *Electronics Letters,* vol. 50, no. 5, pp. 339-341, 2014.

[81] G. Karimi, and S. Majidifar, "A novel chipless RFID tag using spiral resonator to achieve the pentamerous data encoding form," *Journal of Electromagnetic Waves and Applications,* vol. 28, no. 1, pp. 13-27, 2014.

[82] J. Kim, Z. Wang, and W. S. Kim, "Stretchable RFID for wireless strain sensing with silver nano ink," *IEEE Sensors Journal,* vol. 14, no. 12, pp. 4395-4401, 2014.

[83] B. Kubina, C. Mandel, M. Schübler *et al.*, "Dynamic interference suppression for chipless wireless sensors based on an out-of-band channel estimation method," *International Journal of Microwave and Wireless Technologies,* vol. 6, no. 3-4, pp. 353-360, 2014.

[84] J. Lorenzo, D. Girbau, A. Lázaro *et al.*, "Temperature sensor based on frequency-coded chipless RFID tags," *Microwave and Optical Technology Letters,* vol. 56, no. 10, pp. 2411-2415, 2014.

[85] C. Mandel, C. Schuster, B. Kubina *et al.*, "Dual frequency selective multiple access with quasi-chipless/powerless RFID mixer tags," *IEEE Microwave and Wireless Components Letters,* vol. 24, no. 8, pp. 572-574, 2014.

[86] C. M. Nijas, U. Deepak, P. V. Vinesh *et al.*, "Low-cost multiple-bit encoded chipless RFID tag using stepped impedance resonator," *IEEE Transactions on Antennas and Propagation,* vol. 62, no. 9, pp. 4762-4770, 2014.

[87] S. Sauer, and W. J. Fischer, "A passive wireless humidity threshold monitoring sensor principle based on deliquescent salts and a diffusion based irreversible state change," *IEEE Sensors Journal,* vol. 14, no. 4, pp. 971-978, 2014.

[88] M. Sumi, R. Dinesh, C. M. Nijas *et al.*, "Frequency coded chipless RFID tag using spurline resonators," *Radioengineering,* vol. 23, no. 1, pp. 203-208, 2014.

[89] M. Sumi, C. M. Nijas, R. Dinesh *et al.*, "Spectral signature-encoded chipless RFID tag with planar multiresonators," *Journal of Electromagnetic Waves and Applications,* vol. 28, no. 18, pp. 2266-2275, 2014.

[90] A. Aparecida De Castro Alves, F. Jose Arnold, and L. Lorenzo Bravo Roger, "Prediction of the Performance of a Reconfigurable Resonator for RFID Chipeless Tags," *IEEE Latin America Transactions,* vol. 13, no. 3, pp. 623-627, 2015.

[91] C. Feng, W. Zhang, L. Li *et al.*, "Angle-Based Chipless RFID Tag with High Capacity and Insensitivity to Polarization," *IEEE Transactions on Antennas and Propagation,* vol. 63, no. 4, pp. 1789-1797, 2015.

[92] Y. Feng, L. Xie, Q. Chen *et al.*, "Low-cost printed chipless RFID humidity sensor tag for intelligent packaging," *IEEE Sensors Journal,* vol. 15, no. 6, pp. 3201-3208, 2015.

[93] S. Majidifar, A. Ahmadi, O. Sadeghi-Fathabadi *et al.*, “A novel phase coding method in chipless RFID systems,” *AEU - International Journal of Electronics and Communications,* vol. 69, no. 7, pp. 974-980, 2015.

[94] R. Rezaiesarlak, and M. Manteghi, “Design of chipless RFID tags based on Characteristic Mode Theory (CMT),” *IEEE Transactions on Antennas and Propagation,* vol. 63, no. 2, pp. 711-718, 2015.

[95] V. R. Sajitha, C. M. Nijas, T. K. Roshna *et al.*, “Polarization independent chipless RFID tag,” *Microwave and Optical Technology Letters,* vol. 57, no. 8, pp. 1889-1894, 2015.

[96] A. Vena, L. Sydänheimo, M. M. Tentzeris *et al.*, “A fully inkjet-printed wireless and chipless sensor for CO2 and temperature detection,” *IEEE Sensors Journal,* vol. 15, no. 1, pp. 89-99, 2015.

[97] E.W.T. Ngai, Karen K.L. Moon, Frederick J. Riggins, Candace Y. Yi," RFID research: An academic literature review (1995–2005) and future research directions", science direct Int. J. Production Economics 112 (2008) 510–520